Spring 2011

Analysis of Arabidopsis thaliana Protein Phosphatase 2A C subunit expression

Megan M. Thompson
University of New Hampshire, Durham

ANALYSIS OF ARABIDOPSIS THALIANA PROTEIN PHOSPHATASE 2A C SUBUNIT EXPRESSION

BY

MEGAN M THOMPSON
B.S., Messiah College, 2007

THESIS

Submitted to the University of New Hampshire
in Partial Fulfillment of
the Requirements for the Degree of

Master of Science
in
Genetics

May, 2011

ProQuest LLC
789 East Eisenhower Parkway
P.O. Box 1346
Ann Arbor, MI 48106-1346

This thesis has been examined and approved.

Estelle M. Hrabak

Thesis Director, Estelle M. Hrabak
Associate Professor of Genetics

Richard H. Cote

Richard H. Cote
Professor of Biochemistry, Molecular and Cellular Biology

Kevin Culligan

Kevin Culligan
Research Assistant Professor of Biochemistry, Molecular and Cellular Biology

C V Givan

Curtis V. Givan
Professor of Plant Biochemistry

May 9, 2011

Date

DEDICATION

To my family, friends, teachers, and mentors who have provided me with the necessary skills to make this research and thesis possible.

ACKNOWLEDGEMENTS

I would like to thank Enhua Wang for providing the background research which helped inspire the original interest in this project, the dedicated Rechab Towne and Whitney Hunter whose research was included as a part of this project, Ben Orcheski and Nick Beauchemin for help with DNA extraction and Real-Time PCR, my committee members, and especially Chuck Walker for the use of his microscope.

TABLE OF CONTENTS

LIST OF FIGURES

LIST OF TABELS

ABSTRACT

ANALYSIS OF ARABIDOPSIS THALIANA PROTEIN PHOSPHATASE 2A C SUBUNIT EXPRESSION

by

Megan M Thompson

University of New Hampshire, May, 2011

Estelle M. Hrabak

Reversible protein phosphorylation is required for presumably most biological pathways. One of the major enzymes involved in eukaryotic dephosphorylation is Protein Phosphatase 2A (PP2A). PP2A is composed of three subunits: A (scaffolding), B (regulatory), and C (catalytic). Our lab is interested in determining the function of the five C subunits (C1, C2, C3, C4 and C5) in *Arabidopsis thaliana.* We have identified a Na^+-induced altered root growth phenotype in *c4* mutant plants. The goal of this project was to determine expression of the five *C* subunit genes throughout the life cycle of Arabidopsis with emphasis on correlating the location of *C4* subunit expression to the known root phenotype. *C4* gene expression was observed in the roots and expression was not changed in the presence of additional NaCl or mannitol. Expression of all C subunits was ubiquitous and similar throughout the Arabidopsis life cycle with the highest expression in the root tips.

CHAPTER I

INTRODUCTION

One striking difference between animals and plants is that plants are not mobile. When faced with undesirable conditions, most animals will seek out a more comfortable location. Plants, on the other hand, are sessile and must be able to readily adapt to a myriad of stresses such as excessive or insufficient water, changes in light intensity, pathogen attack, and soil contaminants such as salts or heavy metals. Survival requires the regulation of molecular pathways to produce appropriate responses to stimuli. The stimuli can be inter- or intra-cellular and result in regulation of signaling pathways. Signal transduction pathways typically involve protein-protein interactions and/or protein modifications.

Coordinated modifications of proteins are required to properly regulate signaling networks (Yang, 2005). Protein modifications include sulfation, ADP-ribosylation, biotinylation, methylation, ubiquitination, and phosphorylation. The most common and ubiquitous form of protein modification is the addition and removal of a charged phosphate moiety by reversible phosphorylation. Reversible phosphorylation requires the antagonistic action of both protein kinases and phosphatases (Hunter, 1995). All living organisms, from the smallest and simplest bacterium to the larger and more complex animals and plants, regulate protein function through phosphorylation (Cozzone, 1997; Moorhead et al., 2009). In eukaryotes, protein phosphorylation most commonly occurs at the hydroxyl group on serine, threonine and tyrosine residues (Luan, 2003). In humans, phosphorylation occurs on serine and threonine approximately 86.4% and 11.8% of the

time, respectively, while about 1.8% of phosphorylations occur on tyrosine (Olsen et al., 2006). The presence of a charged phosphate moiety may cause allosteric changes in protein conformation that either block or expose an enzyme's active site to its substrates, target proteins to a specific cellular location, encourage or inhibit protein-protein interaction, or have other regulatory effects (Luan, 2003).

Since the discovery of protein phosphorylation in the mid 1900's, it has become apparent that these reactions are critical for all aspects of growth and development (Cohen, 2002). Many individual phosphatases and kinases are required for survival and their absence is detrimental to the cell (MacKeigan et al., 2005). Reversible phosphorylation allows the essential fine tuning of multiple cell signaling networks. Proteins regulated by phosphorylation are often enzymes involved in fundamental cellular processes, such as metabolic pathways, transcription, cell cycle regulation, and stress responses, but phosphorylation also occurs on structural proteins like tubulin or regulatory proteins such as transcription factors. The exact number of phosphorylatable proteins is unknown, but in humans the current estimate is that 30% of proteins (approximately 10,000 proteins) might undergo phosphorylation at 25,000 or more phosphorylation sites (Cohen, 2000; Olsen et al., 2006; Lemeer and Heck, 2009). Many proteins contain multiple phosphorylation sites which can be targeted by different kinases and phosphatases.

In the human genome, there are 650 known or putative protein kinases and 222 protein phosphatases, representing approximately 3-4% of the protein coding genes (Bernards, 2005). In plants, the *Arabidopsis thaliana* genome contains approximately 1000 protein kinase and 112 protein phosphatase catalytic subunits (Wang et al., 2009).

In general, there are more protein kinase than protein phosphatase catalytic subunits (Dombradi et al., 2002). Many protein phosphatases are further regulated by the interaction of regulatory subunits to form multi-subunit holoenzymes.

Due to the importance of protein phosphorylation, considerable research has been published on this process. However, much of this research has been focused on kinases including identifying substrates and phosphorylation motifs. Even though the importance of dephosphorylation is recognized, our current understanding of protein phosphatases is still limited compared to kinases (Luan, 2003; Pais et al., 2009b).

Protein phosphatases can be classified based upon amino acid sequence similarity or whether dephosphorylation occurs specifically at serine/threonine or tyrosine residues or both (Luan, 2003; Moorhead, 2007). Sequence classification is more accurate than residue specificity because some phosphatases have dual specificity and dephosphorylate all three amino acids. Based on sequence classification, two families of protein phosphatases which typically act on serines and/or threonines are the phosphoprotein phosphatases (PPP) and Mg^{2+}-dependent protein phosphatases (PPM) (Moorhead, 2007). PPM is the largest family and contains protein phosphatases such as protein phosphatase 2A (PP2A), calcineurin (protein phosphatase 2B - PP2B) and protein phosphatase 1 (PP1).

The serine/threonine phosphatases PP2A and PP1 account for 80-90% of the total protein dephosphorylation activity in eukaryotic cells and are important regulators of the cell cycle, of development and differentiation of cells, and of other cellular activities (Janssens and Goris, 2001). PP2A is one of the most critical proteins involved in signaling pathways and comprises about 1% of the total cellular protein (Eichhorn et al.,

2009). PP2A is a multimeric protein requiring interactions between the A, B and C subunits to form a functional heterotrimer (Janssens and Goris, 2001). The A subunit primarily consists of 15 protein-binding domains termed HEAT repeats and functions as the scaffolding subunit that binds the B and C subunits. The B subunit is implicated in determining substrate specificity and localization of the PP2A holoenzyme. The C subunit is the site of catalytic activity and is a highly conserved protein in eukaryotes (Kerk et al., 2002). Study of mutants containing knockouts of A or C subunits in model organisms such as mice, yeast, and *Arabidopsis thaliana*, revealed that the complete absence of either type of PP2A subunit is lethal (Ronne et al., 1991; Gotz et al., 1998; Michniewicz et al., 2007).

Our lab studies Protein Phosphatase 2A in the popular model plant *Arabidopsis thaliana.* Arabidopsis is a small plant with a short life span that is easy to grow and transform. One important feature of Arabidopsis is that the genome has been sequenced (The Arabidopsis Genome Initiative, 2000). Over 25,000 genes have been identified and gene annotations and sequence data are available online. Other community resources include microarray expression data, extensive collections of mutants, cDNA clones, mutant seed stocks, and other useful tools, most of which are centralized at The Arabidopsis Information Resource (TAIR, http://www.arabidopsis.org/) and at the Arabidopsis Biological Resource Center (http://abrc.osu.edu/) for use by the Arabidopsis community.

A search of the Arabidopsis genome reveals that there are 3 genes encoding PP2A A subunits, 5 genes for C subunits and 17 B subunit genes (Table 1). The B and C subunits are further classified into subfamilies based on sequence similarities. If all

Table 1. Nomenclature and locus number of the Protein Phosphatase 2A subunits in *Arabidopsis thaliana.*

Subunit	Sub-family	Gene Symbol & Aliases	Arabidopsis Locus Number	NCBI Gene ID	Reference
A		RCN1, PP2A-A1, EER1, AtAα	At1g25490	839135	(Garbers et al., 1996; Thakore et al., 1999; Larsen and Cancel, 2003; Michniewicz et al., 2007)
		PP2AA2, AtAβ	At3g25800	822171	(Thakore et al., 1999; Zhou et al., 2004)
		PP2AA3, AtAγ	At1g13320	837892	(Thakore et al., 1999; Zhou et al., 2004)
C	I	PP2Ac-1, PP2A-1	At1g59830	842276	(Arino et al., 1993)
		PP2Ac-2, PP2A-2	At1g10430	837583	(Arino et al., 1993; Pernas et al., 2007)
		PP2Ac-5, PP2A-5	At1g69960	843333	
	II	PP2Ac-3, PP2A-3	At2g42500	818850	(Arino et al., 1993)
		PP2Ac-4, PP2A-4	At3g58500	825019	(Casamayor et al., 1994)
B	B	AtBα	At1g51690	841594	(Thakore et al., 1999)
		AtBβ	At1g17720	838348	(Thakore et al., 1999)
	B′	AtB′α	At5g03470	831828	(Latorre et al., 1997)
		AtB′β	At3g09880	820146	(Latorre et al., 1997)
		AtB′γ	At4g15415	827211	(Latorre et al., 1997)
		AtB′δ	At3g26030	822200	(Terol et al., 2002)
		AtB′ε	At3g54930	824658	(Terol et al., 2002)
		AtB′ζ	At3g21650	821719	(Terol et al., 2002)
		AtB′η	At3g26020	822199	(Terol et al., 2002)
		AtB′θ	At1g13460	837906	(Terol et al., 2002)
		AtB′ι	At5g25510	832626	(Terol et al., 2002)
	B′′	AtB′′α	At5g44090	834432	(Day et al., 2002; Reddy and Reddy, 2004)
		AtB′′β	At5g28900	833013	(Day et al., 2002; Reddy and Reddy, 2004)
		AtB′′γ	At1g54450	841887	(Day et al., 2002; Reddy and Reddy, 2004)
		AtB′′δ	At5g28850	833004	(Day et al., 2002; Reddy and Reddy, 2004)
		AtB′′ε	At1g03960	839361	(Day et al., 2002; Reddy and Reddy, 2004)
		FASS (FS), GORDO (GDO), TONNEAU 2 (TON2), AtB′′ζ	At5g18580	831976	(Torres-Ruiz and Jurgens, 1994; Fisher et al., 1996; Camilleri et al., 2002)

possible combinations of heterotrimers were able to form, there would be a total of 255 different combinations. Based on the numerous potential combinations of heterotrimers, there is opportunity for both specialization and redundancy. Conversely, a mutation in one A subunit could potentially affect the formation of 90 heterotrimers.

Pharmacological approaches have provided much information about the function of PP2A (Janssens and Goris, 2001). Okadaic acid (OA), a toxin extracted from marine invertebrates, is a non-competitive inhibitor of both PP1, PP2A, PP4, and PP5. PP4 (0.1 nM) is inhibited within the same range as PP2A (0.1-0.3 nM) and PP2A is sensitive to lower concentrations of OA than PP5 (3.5 nM) and PP1 (15-50 nM; Bialojan and Takai, 1988; Moorhead, 2007). A major drawback with using a pharmacological approach is the non-specific interactions off the inhibitor and effecting more than one phosphatase. Some of the potential functions of PP2A uncovered using OA include cell cycle control, arrangement of microtubules, and regulation of sucrose phosphate synthase, nitrate reductase, and K^+ channels (Li et al., 1994; Smith and Walker, 1996; Ayaydin et al., 2000; Polit and Kazmierczak, 2007).

A more nuanced understanding of the functions of PP2A has been revealed from analysis of plant mutants. In particular, analysis of the A1 subunit mutant *rcn1* has been very fruitful. The *rcn1* mutant exhibits a decrease in total cellular phosphatase activity indicating that the A1 subunit is likely a member of many critical holoenzymes and reinforcing the role of PP2A as a major phosphatase in plant cells (Deruere et al., 1999). Many of the phenotypes identified for *rcn1* mutants indicate involvement in hormone responses, especially auxin responses. For example, the *rcn1* mutant was originally identified in a screen for seedlings with an altered response to the auxin efflux inhibitor

N-1-naphthylphthalamic acid (NPA; Garbers et al., 1996). Subsequent studies monitoring the movement of radioactive auxin or visualizing the location of auxin with an auxin responsive promoter::reporter construct showed that *rcn1* mutants had increased basipetal auxin transport in roots (Rashotte et al., 2000). The functions of the other two A subunits, A2 and A3, are less well understood. There is no phenotype observed with single or double *a2* or *a3* mutants; however, double mutants between either *a2* or *a3* and *rcn1* had a severe phenotype (Zhou et al., 2004). Seven day old seedlings of *rcn* x *a2* or *rcn1* x *a3* double mutants grown in light exhibited an extreme decrease in root length and increased isotropic cell expansion compared to wild type. The *rcn* x *a2* and *rcn1* x *a3* mutants exhibited alterations in the number of cotyledons as well as their symmetry (Zhou et al., 2004). The cotyledon defects resembled defects observed in other mutants implicated in auxin efflux or regulation of auxin efflux.

Less is known about plants with mutations in the *C* and *B* subunit genes of PP2A. There are currently two reports on B or C subunit mutants in Arabidopsis. The PP2A C2 subunit was implicated as a negative regulator of abscisic acid responses (Pernas et al., 2007) while plants with mutations in a potential *B* subunit gene named *tonneau2* (*ton2*) have extreme developmental abnormalities including disorganization of the cortical cytoskeleton (Camilleri et al., 2002). Interestingly, none of the *A* subunit single or double mutant phenotypes were as extreme as the weakest *ton2* phenotype (Zhou et al., 2004). Needless to say, there is a need for additional PP2A mutant studies to further elucidate the function of PP2A in plants.

The Hrabak lab has been focusing on Protein Phosphatase 2A with the goal of understanding the function of the PP2A C subunits in Arabidopsis using a reverse

genetics approach. A previous graduate student, Enhua Wang, identified plants with T-DNA insertions in all five Protein Phosphatase 2A C subunit genes, for a total of 13 different alleles. T-DNA is a large (4-5 kb) fragment of DNA which can function as an insertional mutagen, disrupting genes into which it inserts (Alonso et al., 2003). DNA sequencing was used to determine the exact insertion site for the T-DNA in each allele. Homozygous lines were subjected to RT-PCR to determine if transcript was produced. At the time of this writing, three of the 13 homozygous C subunit mutant lines had been shown to have no detectable transcript and these three lines are considered to be null mutants (Table 2; M. Thompson, unpublished data).

These three null mutants looked very similar to wild type plants when grown under normal conditions (M. Thompson, personal observations; Wang, 2008). To detect potential phenotypes, the homozygous mutant plants were subjected to many of the screens described at the Arabidopsis Gantlet website (http://thale.biol.wwu.edu/). Some of the screens included growth at low temperature and growth in the presence of exogenous hormones or various salts. Of the 23 screens performed, a phenotype was observed for seedlings grown on vertically-oriented plates on medium supplemented with additional NaCl (Wang, 2008). In this screen, seedlings were germinated and grown for three days on vertically-oriented plates containing standard growth medium, then carefully transferred to new vertically-oriented plates containing additional NaCl and grown for seven days. Control seedlings were transferred to the same medium without supplemental NaCl. When grown on medium with no additional NaCl, roots of the wild type and *c4* mutant skewed slightly to the left (Figure 1). Skewing direction is based on viewing the seedlings from the back of the plate through the agar and a slight leftward

Table 2. C subunit knockout collection.

C Subunit	Allele Number	T DNA Identifier Number	Confirmed T-DNA Insertion Site
C1	*c1-1*	Salk-102599[1]	6th of 6 exons
C4	*c4-1*	Salk-035009[1]	9th of 11 exons
	c4-2	GABI-800G05[2]	1st of 10 introns

[1]Salk Institute (LaJolla, CA)
[2]German Plant Genomic Program (Potsdam, Germany).

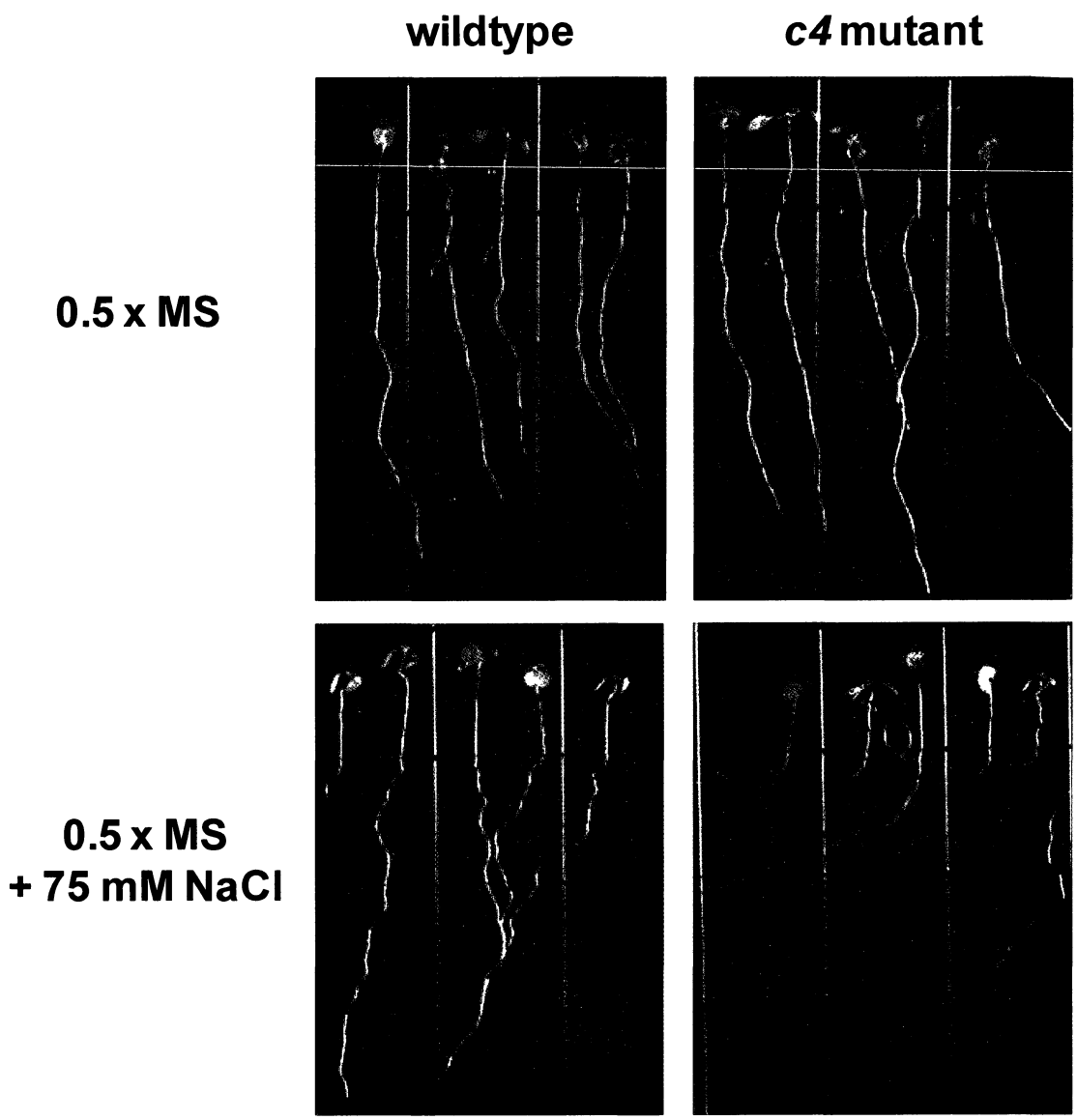

Figure 1. Growth of wildtype and PP2A *c4* mutant seedlings on standard medium or medium supplemented with NaCl.
Three day old seedlings grown on 0.5X MS were transferred to media containing either 0.5X MS or 0.5X MS + 75 mM NaCl and seedlings were transferred so their root tips were aligned. Seedlings were grown for another 7 days and photographed through the back of the plate.

angle is normal for *Arabidopsis thaliana* roots (Rutherford and Masson, 1996). In the presence of additional NaCl, the roots of *c4* mutant seedlings skewed strongly to the right while the wild type roots skewed slightly but the root angle was significantly different from the *c4* mutant roots (Figure 1; Wang, 2008). Supplementing the medium with other salts (LiCl, KCl or $CaCl_2$) did not cause root skewing nor did growth on medium containing mannitol at the same osmotic strength as the NaCl (data not shown), indicating that the phenotype is specific for sodium. The phenotype was complemented by transformation of the wildtype *C4* gene into the *c4-1* mutant plants, indicating that the skewing phenotype was due to a mutation in the *C4* gene (Wang, 2008). Although other root skewing mutants have been identified, to our knowledge, no other mutants have been identified which show root skewing only in the presence of Na^+.

The overall goal of this research is to generate a detailed cell expression profile of all of the *C* subunit genes to determine whether the expression patterns overlap and to correlate mutant phenotypes to the sites of gene expression. Online microarray data (assembled from www.genevestigator.com) cannot be used to answer this question because microarrays do not capture data at the cellular level. In addition, the Affymetrix Arabidopsis chip cannot differentiate between the *C3* and *C4* genes. The 557 bp probe (265857_S_AT) is located in the *C3* cDNA sequence, beginning 342 bp from the start codon, and is 91.7% identical to the corresponding *C4* cDNA region. Immunodetection would also not be a useful approach to distinguish the expression patterns of the *C4* and *C3* subunits because the two subunits are 98% identical at the protein level so that antibodies would not distinguish between the two subunits. I chose to study the expression pattern of the C subunits using a reporter gene approach. The reporter chosen

was the enzyme β-glucuronidase (GUS). The GUS histochemical assay can be used to determine global expression of a gene of interest, in this case the C subunit, at the level of single cells. Whenever the C subunit is normally expressed, the fused C subunit and GUS enzyme should be produced. When the tissue is incubated with the GUS substrate (X-Gluc), the GUS enzyme will cleave the substrate forming blue precipitate product that can accumulate over time. Therefore, by increasing the assay time, expression of genes with weak promoters can be detected. In addition, promoter strength can be determined by using a time course. Since the optimum pH for the plant's endogenous β-glucuronidase is pH 5 and there is little activity at neutral pH, these experiments were performed at pH 7 so that endogenous β-glucuronidase activity was not detected (Gallagher, 1992). The *E. coli* GUS or *uidA* gene was cloned downstream of the last codon of a large DNA fragment containing the genomic coding sequence and the C subunit promoter region. Following the production of multiple lines of transgenic plants, expression of each of the *C* subunit genes in Arabidopsis was determined.

The first goal of this research is to determine if the *C4* gene is expressed in roots during the developmental time period used for the NaCl root skewing assay (Figure 1). While the *C4* gene may be expressed in other places, I hypothesize that there will be expression in the roots because of the root-specific phenotype. The second goal is to determine where and when the *C4* gene is expressed throughout the Arabidopsis life cycle. My rationale for examining the global expression pattern is that, if a phenotype in another organ is discovered, it can be correlated with the established expression pattern. The third goal is to determine the expression pattern of the other four PP2A *C* subunit genes through the Arabidopsis life cycle and to investigate where the expression patterns

overlap and where they are distinct. The microarray data from *C1*, *C2*, and *C5* genes indicates similar organ- and tissue-specific expression; thus, I hypothesize that these genes will have overlapping expression patterns. It will be important to determine where the *C3* and *C4* genes are expressed because they cannot be distinguished on the microarray. The final goal is to examine the expression pattern of the *C4* gene and its close homologue *C3* in the presence of NaCl to determine if expression changes when seedlings are exposed to NaCl. This research will provide a detailed understanding of the expression pattern of the protein phosphatase 2A C subunits.

CHAPTER II

RESULTS

II.A. Generation of DNA constructs and transgenic plants

II.A.1. Plasmid construction

A translational fusion approach was used to document the expression pattern of the PP2A C subunit genes. In a translational fusion, the promoter and at least some the coding sequence of the gene-of-interest is cloned in-frame with a reporter gene. The amino-terminal sequence of a protein is one of the primary determinants of protein half-life (Varshavsky, 1997). Since the amino terminus of the fusion protein is identical to the native protein, the fusion construct is expected to have the same half-life as the native PP2A C subunit. This approach may yield more accurate results than using a transcriptional fusion approach in which only the promoter is fused to the reporter gene and no part of the native protein is expressed.

In the *C* subunit constructs used in this study, all of the introns and exons, except for the stop codon and 3' untranslated sequences downstream of the stop codon, were included. The reporter gene was inserted following the final codon of each C subunit gene (Figure 2-6). Splice variants have been documented from cDNA sequences for both the *C1* and *C3* transcripts (Figure 2 and 4). For the *C3* gene, the splice variation occurs after the first exon, thus both variants could be produced from the translational fusion construct. For *C1*, on the other hand, the splice variant occurs in the last exon, and the stop codon is affected. Only splice variant At1g59830.1 was fused to the reporter gene.

In the expression constructs, the last codon of each *C* subunit gene was cloned in

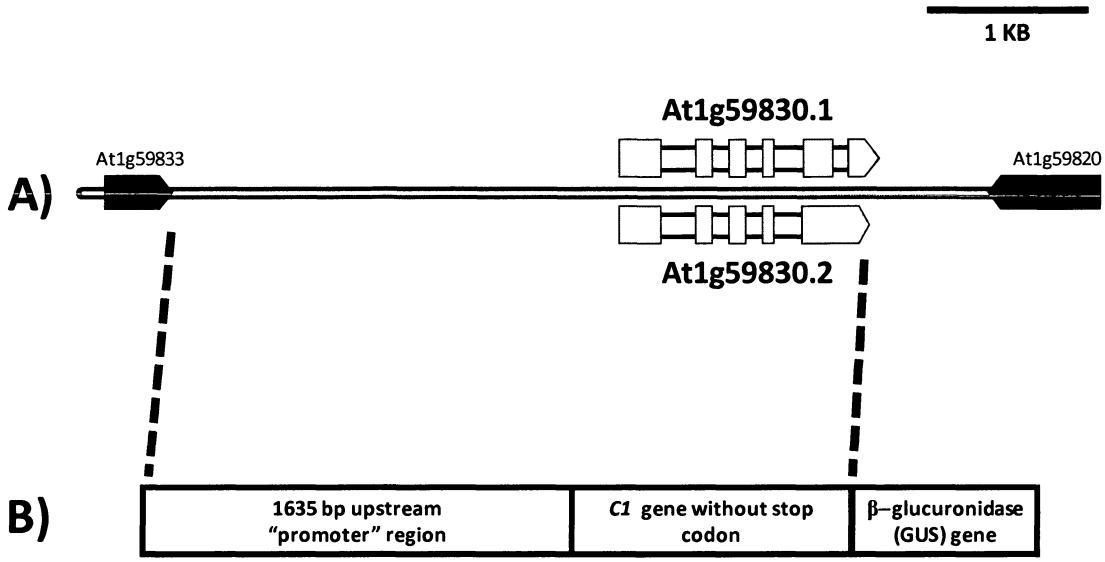

Figure 2. Schematic of the *C1* genomic region (At1g59830).
A) Genomic view of the chromosomal region encoding both splice variants for C1 subunit of Protein Phosphatase 2A (drawn to scale). Light grey boxes are exons and white boxes are introns. Black arrows indicate orientation of the upstream and downstream genes. **B)** Dashed lines delineate the approximate location of the genomic region amplified by PCR and fused *in vitro* to the GUS reporter gene in the C1 construct (not to scale).

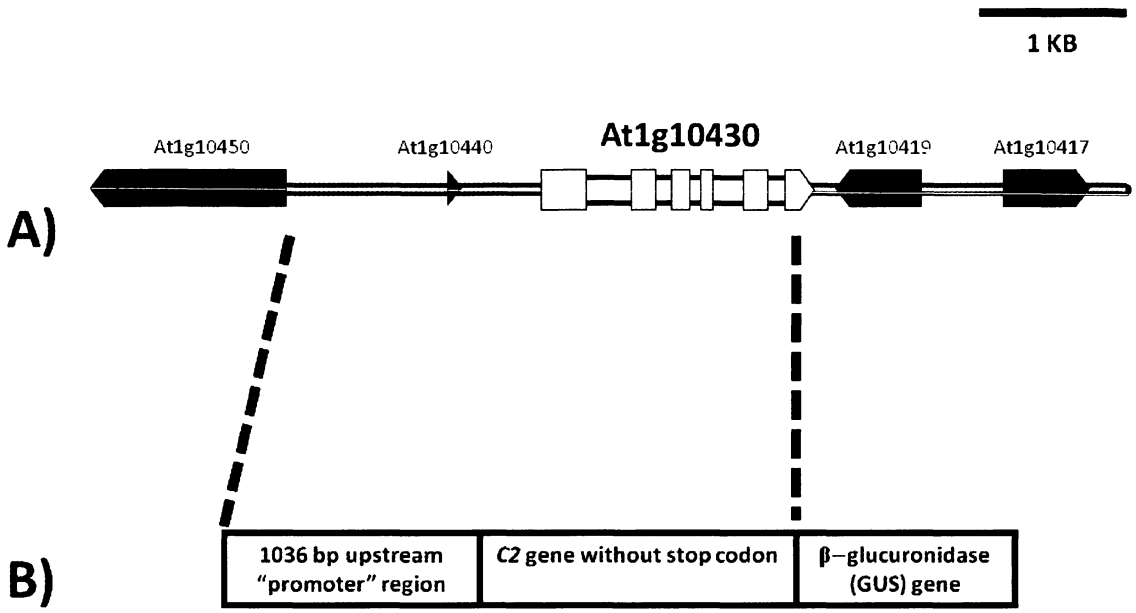

Figure 3. Schematic of the *C2* genomic region (At1g10430).
A) Genomic view of the chromosomal region encoding the C2 subunit of Protein Phosphatase 2A (drawn to scale). Light grey boxes are exons and white boxes are introns. Black arrows indicate orientation of the upstream and downstream genes. **B)** Dashed lines delineate the approximate location of the genomic region amplified by PCR and fused *in vitro* to the GUS reporter gene in the C2 construct (not to scale).

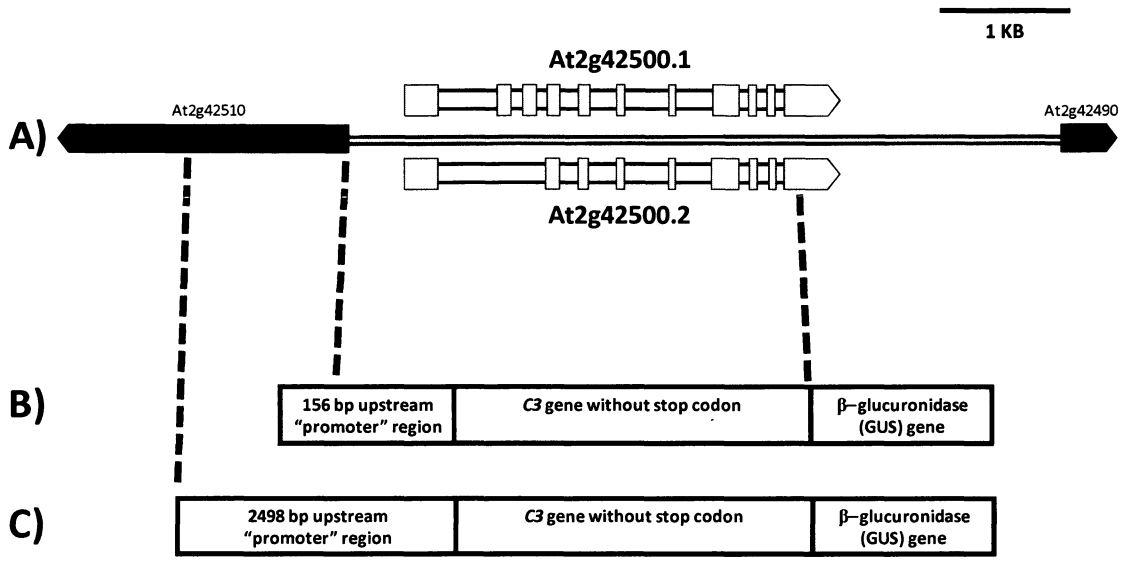

Figure 4. Schematic of the *C3* genomic region (At2g42500).
A) Genomic view of the chromosomal region encoding the C3 subunit of Protein Phosphatase 2A (drawn to scale). Light grey boxes are exons and white boxes are introns. Black arrows indicate orientation of the upstream and downstream genes. **B)** Dashed lines delineate the approximate location of the genomic region amplified by PCR and fused *in vitro* to the GUS reporter gene in the sC3 construct (not to scale). **C)** Dashed line delineate the genomic region amplified by PCR and fused *in vitro* to the GUS reporter gene in the LC3 construct (not to scale).

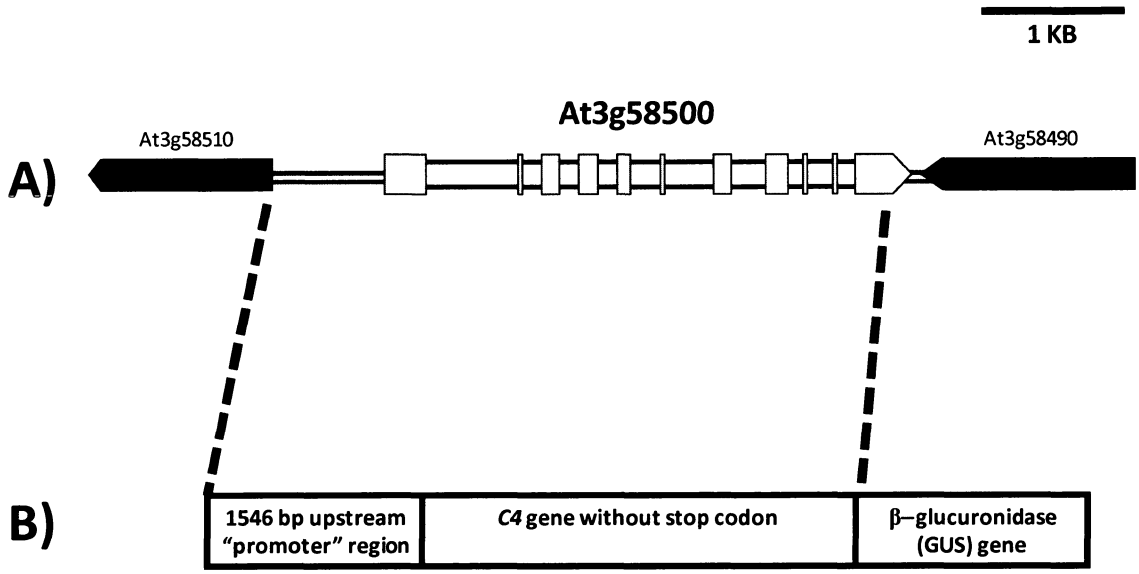

Figure 5. Schematic of the *C4* genomic region (At3g58500).
A) Genomic view of the chromosomal region encoding the C4 subunit of Protein Phosphatase 2A (drawn to scale). Light grey boxes are exons and white boxes are introns. Black arrows indicate orientation of the upstream and downstream genes. **B)** Dashed lines delineate the approximate location of the genomic region amplified by PCR and fused *in vitro* to the GUS reporter gene in the C4 construct (not to scale).

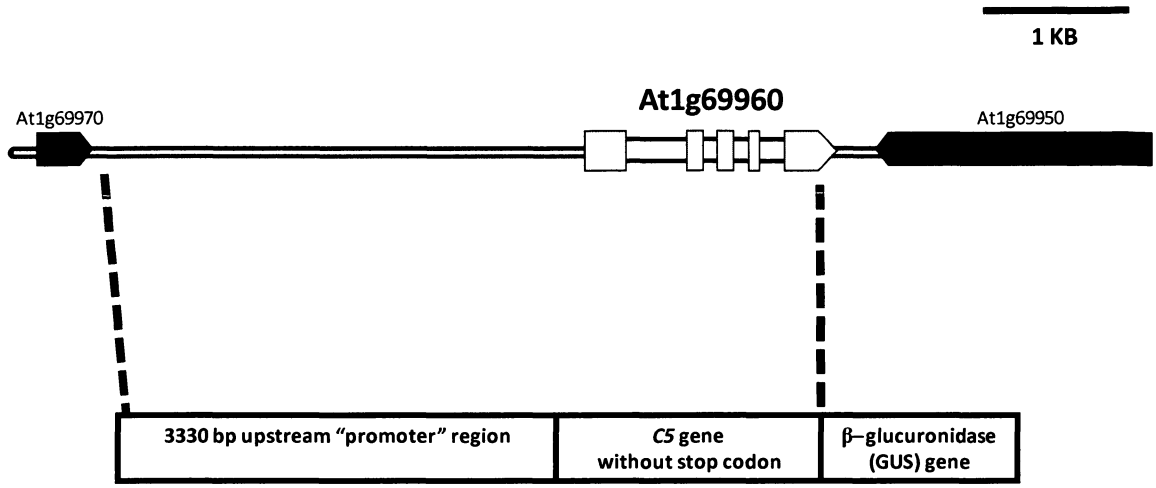

Figure 6. Schematic of the *C5* genomic region (At1g69960).
A) Genomic view of the chromosomal region encoding the C5 subunit of Protein Phosphatase 2A (drawn to scale). Light grey boxes are exons and white boxes are introns. Black arrows indicate orientation of the upstream and downstream genes. **B)** Dashed lines delineate the approximate location of the genomic region amplified by PCR and fused *in vitro* to the GUS reporter gene in the C5 construct (not to scale).

frame with the *uidA* reporter gene encoding β-glucuronidase (GUS). A short spacer region of 96 base pairs was introduced from the cloning vectors. When translated, the resulting fusion protein is predicted to consist of the full-length C subunit with its carboxy-terminus fused to a 32 amino acid spacer followed by the GUS reporter protein.

The expression of genes is controlled by their promoters. Promoters are essential for gene regulation but it is technically difficult to identify the exact location of all of the regulatory elements of a promoter from sequence data alone. Promoters include a core and an extended promoter region. The core promoter region (-1 to -70 bp) contains the basic regulatory sequences while the extended promoter (-70 to -500 or more bp) modifies expression. The extended promoter might contain binding sites for factors that regulate expression in response to light, stress, etc. (Riechmann, 2009). In Arabidopsis, the core promoter extends approximately 70 bp upstream of the transcription start site (Molina and Grotewold, 2005). Within this core region, the Y patch and TATA box are located at approximately -13 and -35 bp (Yamamoto et al., 2007). Within the extended promoter, most *cis* regulatory regions occur less than 1000 bp from the transcription start site (Yamamoto et al., 2007), although enhancers can be located much further away (Dean, 2006). In addition to the regulatory region upstream of transcription start, multiple studies indicate that cis-regulatory elements can be found in introns, untranslated regions (UTR), and downstream sequences (Larkin et al., 1993; Hong et al., 2003; Fiume et al., 2004). For this study, the 'promoter' region was defined as the intergenic region from the transcription start site of the *C* subunit gene to the transcribed sequence of the next upstream gene. Exceptions to this general approach were made for the *C2* and *C3* promoter regions as described below.

The Arabidopsis genome sequence was first released in 2000 and completely reannotated in 2003 (The Arabidopsis Genome Initiative, 2000; Wortman et al., 2003). The sequence in the 2007 Arabidopsis Information Resource genome release ((http://www.arabidopsis.org/; Swarbreck et al., 2008) was used for *in silico* construction of plasmids. Each of the five C subunit 'promoter' regions was determined from the annotated sequence available on the TAIR website (Figure 2-6). Promoter regions were defined as described previously except for the C2 and C3 constructs. For the *C2* gene construct, the upstream "promoter" region included a gene encoding a proline tRNA (At1g10440; Figure 3). For the *C3* gene constructs, the intergenic region containing the *C3* 'promoter' region was small (153 bp) and the adjacent gene (At2g42510) is likely a pseudogene because there are few expressed sequence tags (EST) for this gene and no reported full-length cDNA. Two constructs were made for the *C3* gene: one containing only the 153 bp intergenic region up to the next annotated gene (Figure 4B) and the other, termed the LC3 construct, extending 2313 bp upstream from the transcription start of the *C3* gene into the pseudogene (Figure 4C).

After the promoter region was defined, a two-step cloning process was used to create constructs which could be used to transform plants. Primers were designed to amplify the regions of interest by PCR from *Arabidopsis thaliana* Col-0 genomic template. An example of the PCR product is shown in Figure 7. To eliminate having to sequence the entire construct to check for PCR errors, three independent PCR products were amplified and cloned. The rationale was that, since each independent PCR product was from a separate reaction, if a PCR error which affected gene expression or introduced a stop codon or amino acid change in the open reading frame occurred in one

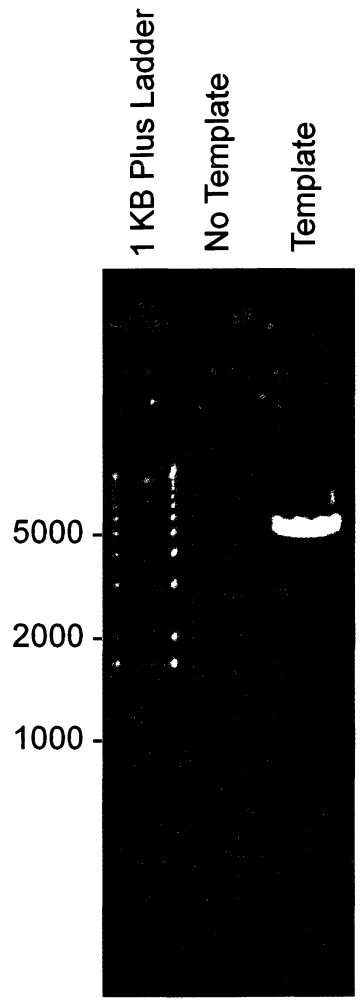

Figure 7. Amplification of *C4* genomic region from *Arabidopsis thaliana* Col-0 wild type genomic template.
The expected PCR product was 4974 bp. Ladder sizes are in base pairs.

reaction, it would not be present in a duplicate reaction. Thus, if the plants containing products from different PCRs had expression patterns that were indistinguishable, any PCR errors that might be present were inconsequential. After amplification, PCR products were inserted into the pCR8/GW/TOPO vector by TOPO cloning. pCR8/GW/TOPO is designed to clone PCR products with A-overhangs produced by *Taq* DNA polymerase. Some of the resulting clones were digested to determine insert orientation. An example of digestions to determine insert orientation is shown in Figure 8. pCR8/GW/TOPO is a Gateway entry vector and contains *attL1* and *attL2* sites. The correct orientation for all genes would have the *attL1* site adjacent to the C subunit promoter region. One clone with the insert in the desired orientation was selected and Gateway cloned into pMDC163, a plant binary vector containing the β-glucuronidase (GUS) reporter gene after the *attR2* site (Figure 9). After Gateway cloning, the PP2A *C* gene will be in-frame with the *GUS* gene. Several clones were restriction digested to identify those with the correct fragment patterns based on maps of the expected plasmid structures constructed *in silico* (Figures 10-15). An example of restriction digests of the PP2A *C4* subunit genomic region cloned into pMDC163 is shown in Figure 16. The fusion junction between the *C* subunit gene and the *GUS* gene was sequenced for all constructs to determine that the *C* subunit gene was in-frame with the *GUS* gene.

II.A.2. Generation of the negative control construct

A common control for experiments utilizing transgenic plants is to transform plants with an "empty" vector to ensure that the vector alone does not affect the plants. When the plasmid contains a reporter gene such as the *GUS* gene in pMDC163 (Figure

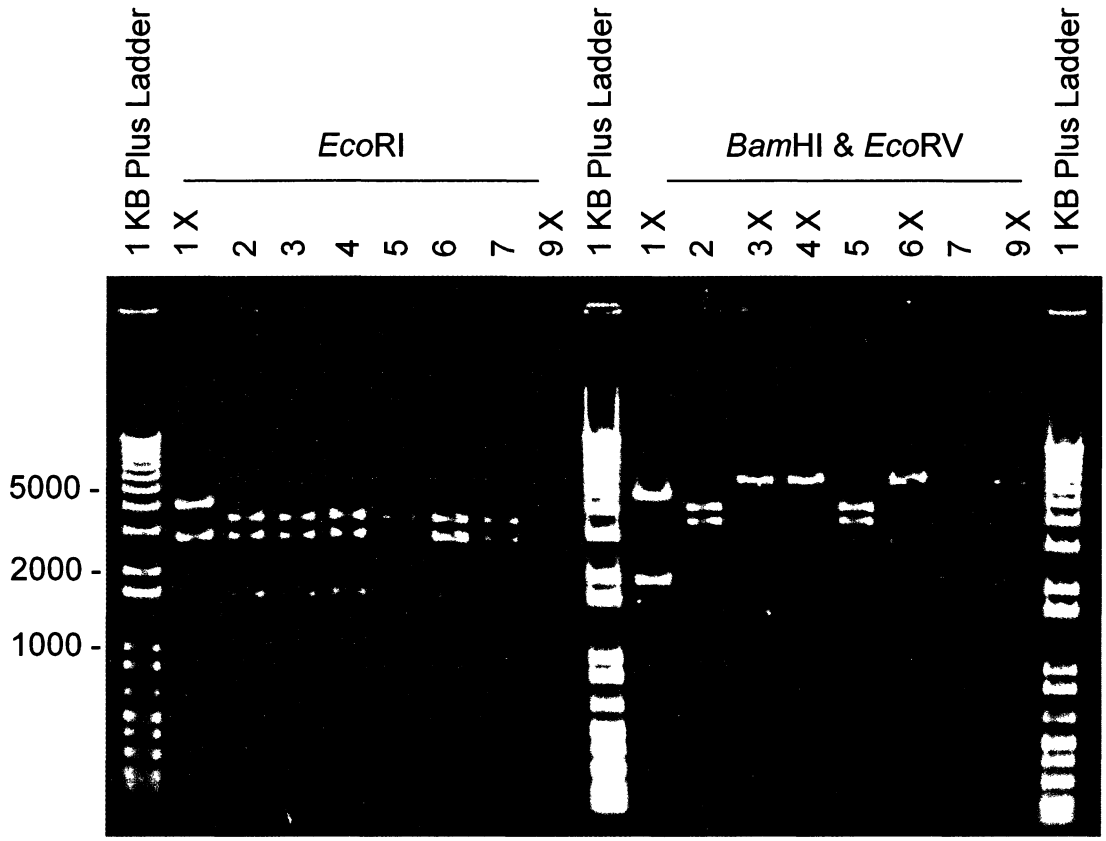

Figure 8. Restriction digests of plasmids putatively containing the *C4* genomic region cloned into pCR8/GW/TOPO.
Each clone was digested in two different reactions (*Eco*RI or *Bam*HI & *Eco*RV). *Eco*RI digests showed the insert released from the vector so all correct clones (#2-7) are expected to have the same digestion pattern. *Bam*HI and *Eco*RV digests were used to distinguish the orientation of the *C4* gene insert. In the desired clones (#2, 5 and 7), the inserts are oriented such that the *attL1* site of pCR8/GW/TOPO is adjacent to the gene's promoter region. Clones with undesirable digest patterns are marked with an X. Ladder sizes are in base pairs.

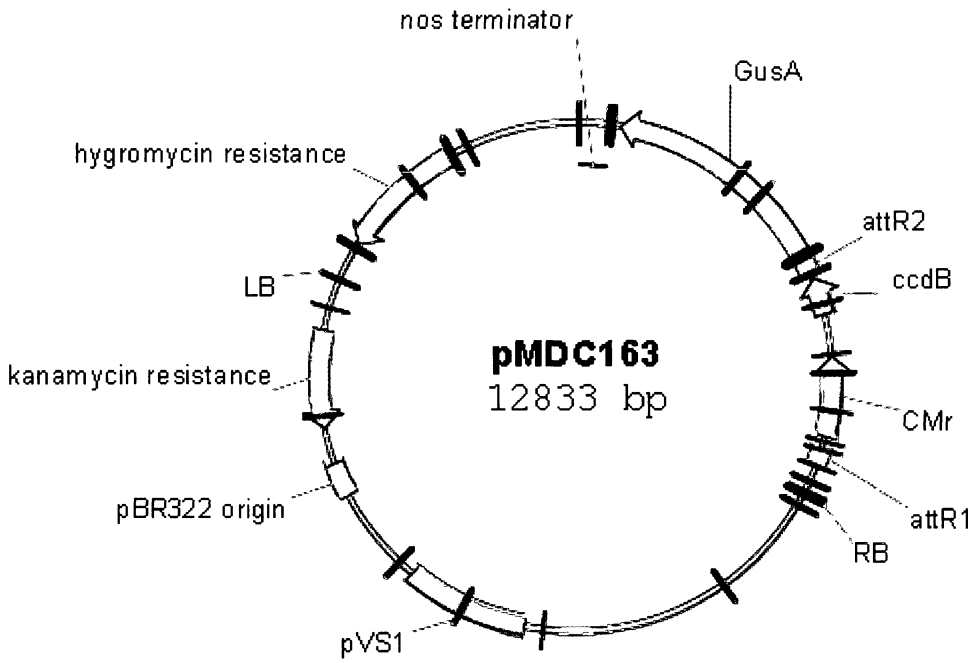

Figure 9. Plasmid map of pMDC163.
The *ccdB* gene, located between *attR1* and *attR2*, is exchanged with the DNA fragment-of-interest from the entry clone during Gateway cloning. Plasmid map from Curtis and Grossniklaus (2003).

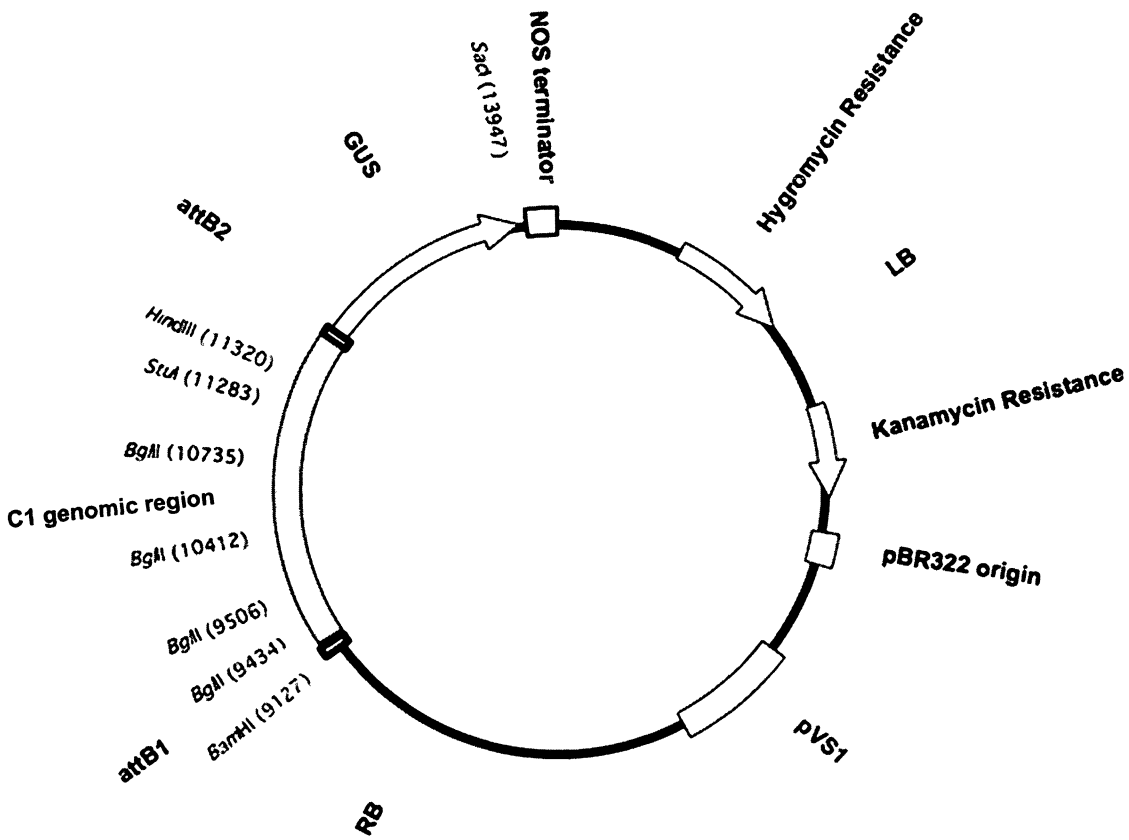

Figure 10. *C1* genomic region cloned into binary vector pMDC163.
C1 genomic region is diagrammed in Figure 2. Only the restriction enzymes used in digests are shown. Total plasmid size is 14.217 kb. Constructs from three independent PCRs are named pC1-4-2, pC1B-1-4, and pC1C-4-2.

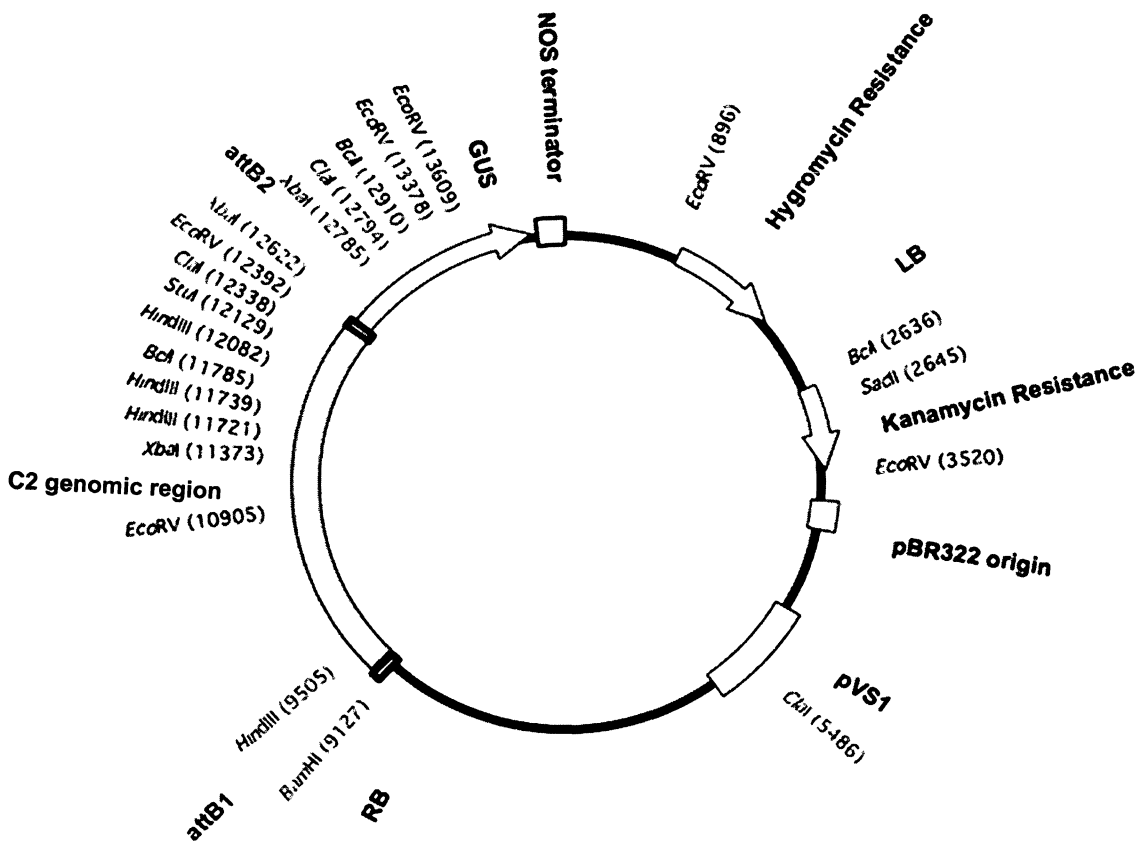

Figure 11. *C2* genomic region cloned into binary vector pMDC163.
C2 genomic region is diagrammed in Figure 3. Restriction enzymes shown were used in digests. Total plasmid size is 14.961 kb. Constructs from three independent PCRs are named pC2A-3-4, pC2E-1-4, and pC2D-4-1.

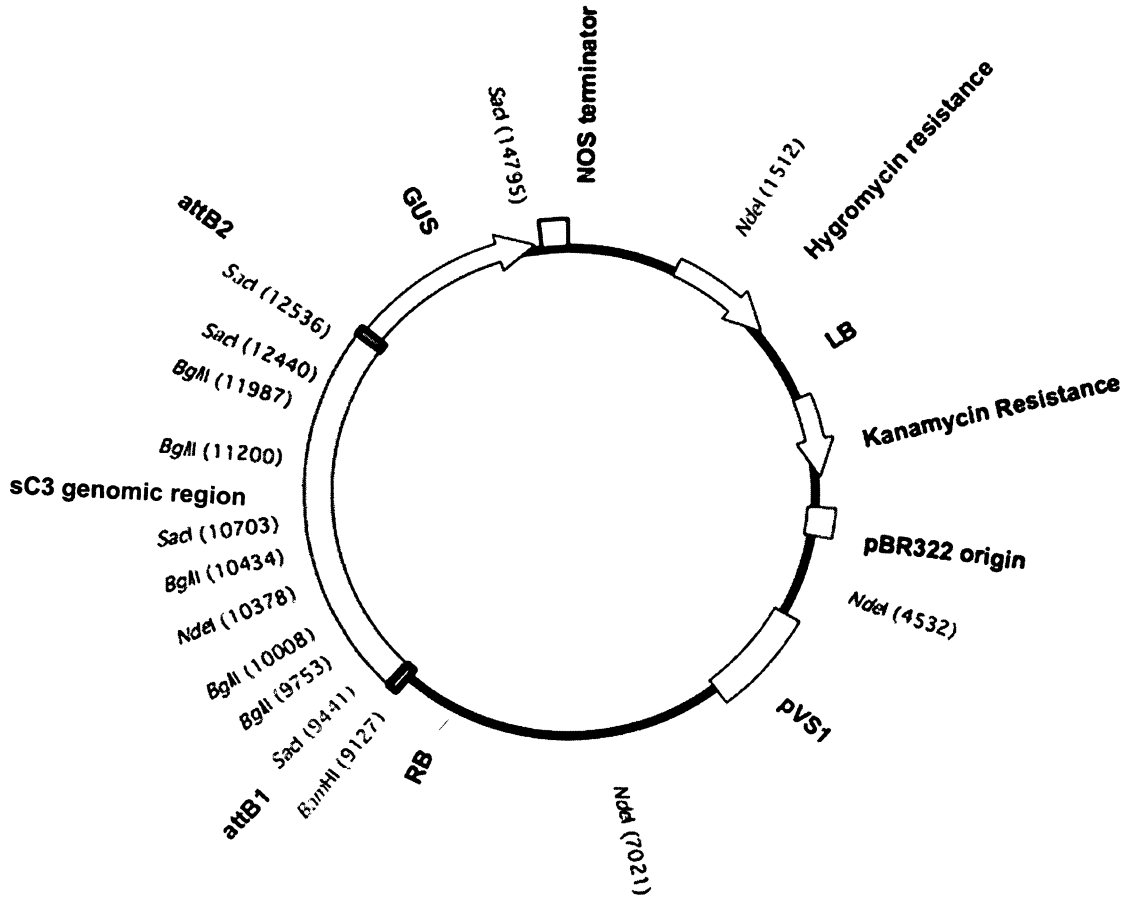

Figure 12. s*C3* genomic region cloned into binary vector pMDC163.
sC3 genomic region is diagrammed in Figure 4A and B. Restriction enzymes shown were used in digests. Total plasmid size is 15.065 kb. Constructs from three independent PCRs are named pC3-3-4, pC3B-9-5, and pC3C-5-3.

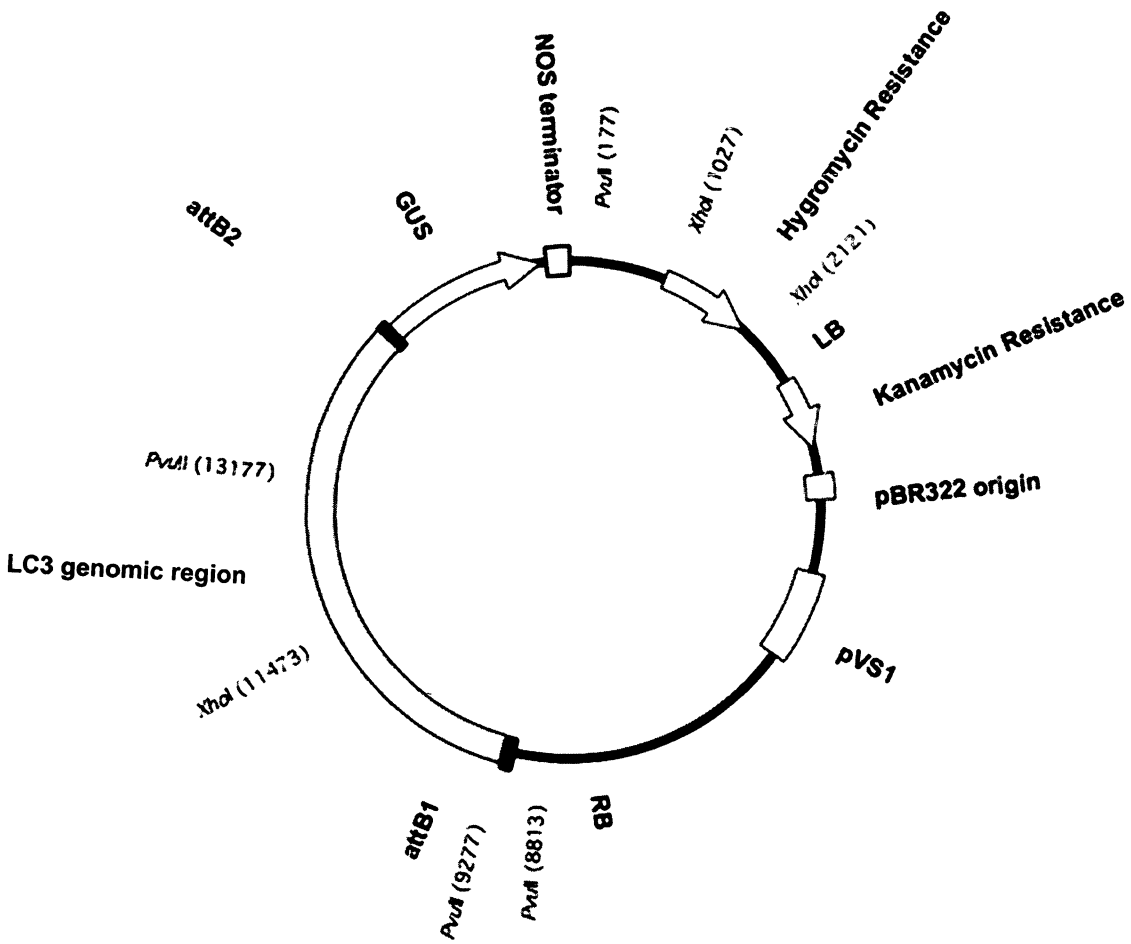

Figure 13. *LC3* genomic region cloned into binary vector pMDC163.
LC3 genomic region is diagrammed in Figure 4A and C. Restriction enzymes shown were used in digests. Total plasmid size is 17.219 kb. Constructs from three independent PCRs are named pLC3B-4-5, pLC3D-4-4, and pLC3E-4-5.

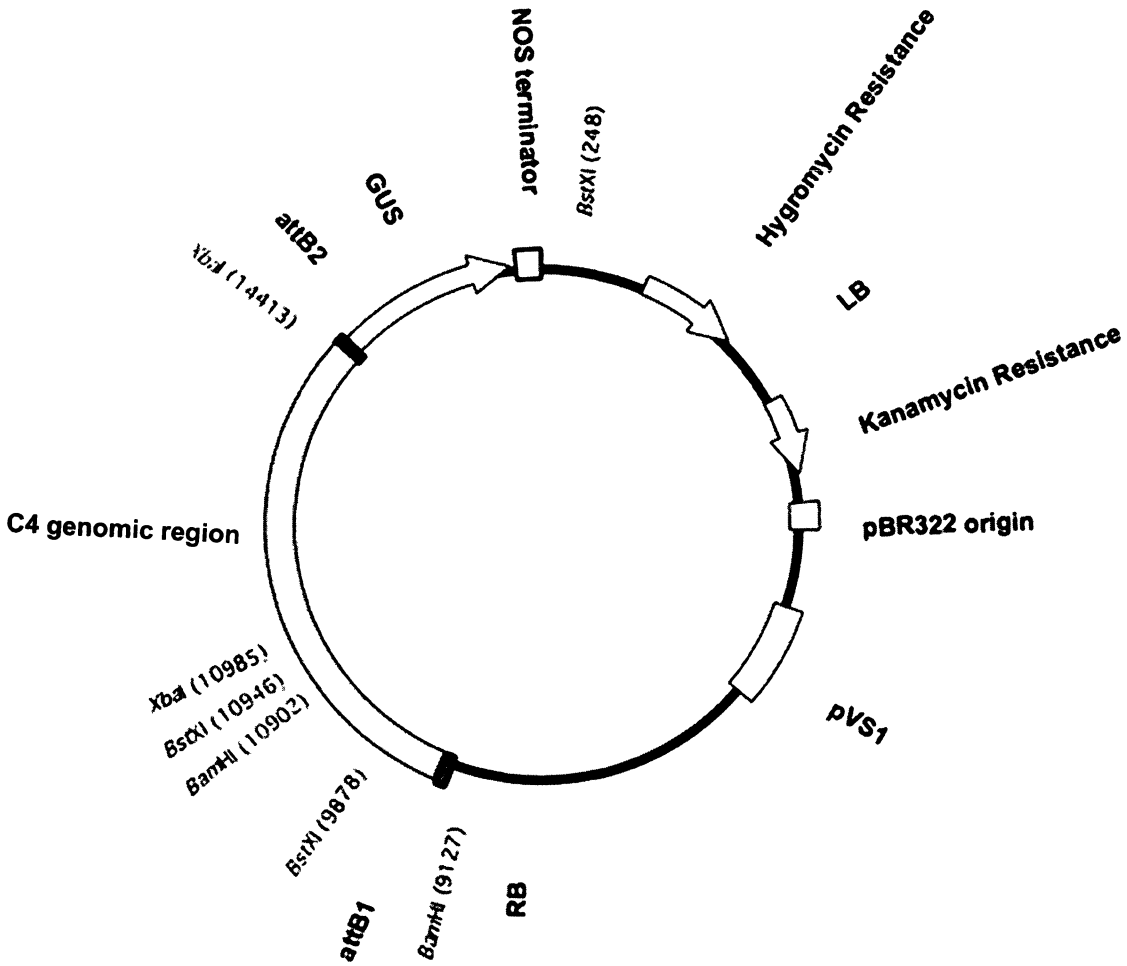

Figure 14. *C4* genomic region cloned into binary vector pMDC163.
C4 genomic region is diagrammed in Figure 5. Restriction enzymes shown were used in digests. Total plasmid size is 16.589 kb. Constructs from three independent PCRs are named pC4-5, pC4-7, and pC4B-4-2.

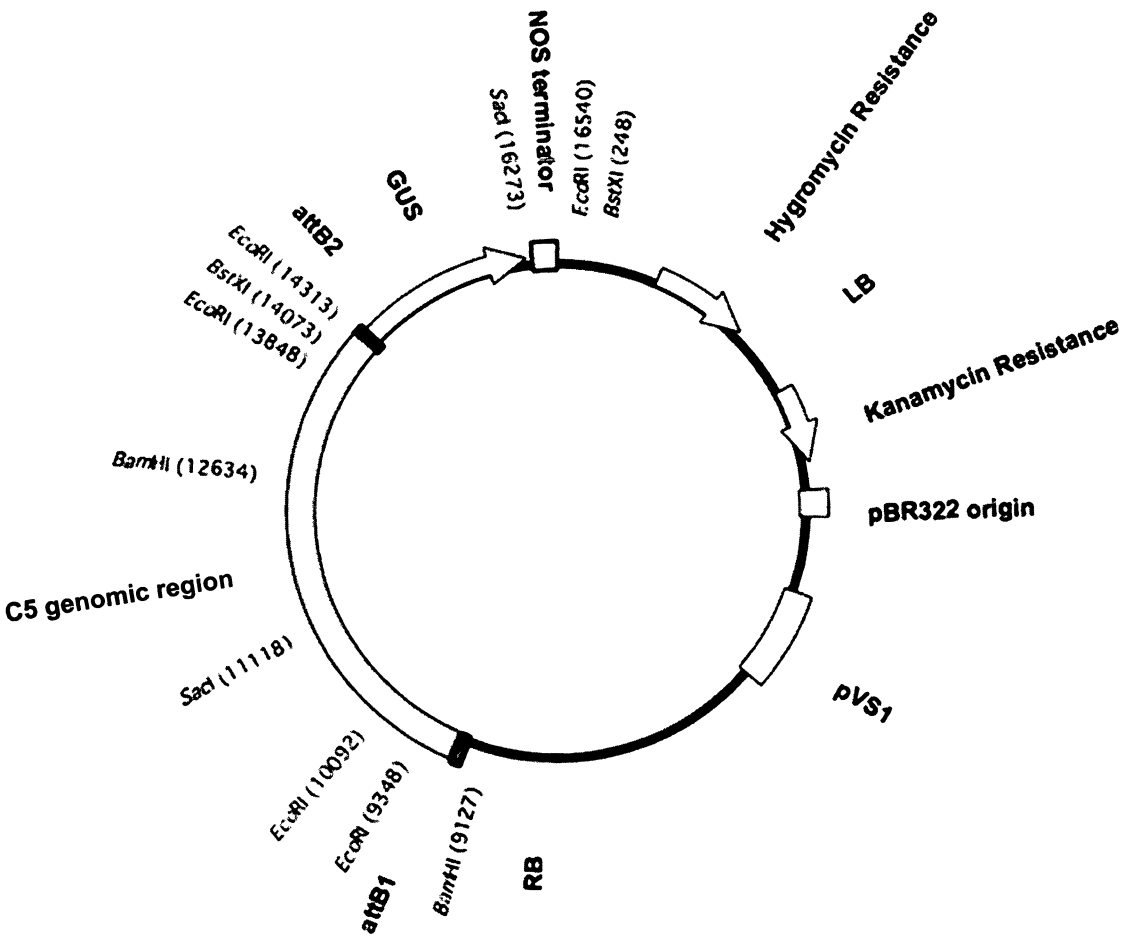

Figure 15. *C5* genomic region cloned into binary vector pMDC163.
C5 genomic region is diagrammed in Figure 6. Restriction enzymes shown were used in digests. Total plasmid size is 16.543 kb. Constructs from three independent PCRs are named pC5-7-12, pC5B-9-3,

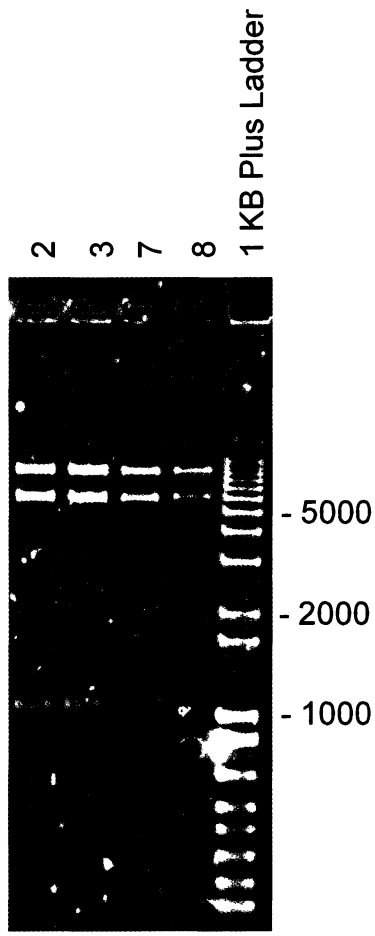

Figure 16. Digest of *C4* genomic region Gateway cloned into destination vector pMDC163.
Putative pC4-5 clones were digested with *Bst*XI and all clones showed the digest pattern expected from Figure 14.

9), a control construct would determine whether there are any *cis* regulatory sites upstream of the *attR1* site that could act as a promoter and induce expression of the *GUS* gene. pMDC163 contains the *ccdB* gene whose product was assumed to be lethal to *Agrobacterium* as it is to *E. coli*; thus a fragment of "neutral" DNA was Gateway cloned into pMDC163 to replace the *ccdB* gene. Ideally, a neutral DNA fragment would not contain any transcription factor binding sites and thus not be able to promote expression of the *GUS* gene, allowing evaluation of the region upstream of the *attR1* site. For this project, the *C4* cDNA open reading frame (ORF) was cloned into pMDC163 in reverse orientation so that the start codon was immediately upstream of the *attR2* site. The PLACE database of plant *cis* elements (http://www.dna.affrc.go.jp/PLACE/; Higo et al., 1999) was used to search for regulatory elements in the 939 bp *C4* ORF and the 356 bp region between the *RB* and the insert. The results from this search showed that many potential regulatory motifs were present in both regions (Figure 17-18). In eukaryotes, the typical length for transcription factor binding sites is 5-15 bp (Fickett and Hatzigeorgiou, 1997). Most of the regulatory regions found by PLACE were short sequences of about 5 bp and the odds that a particular 5 bp sequence will occur in a random sequence are 1 in 1024. Thus, it is almost impossible to identify a truly "neutral" DNA fragment for use in a control construct. Even though potential regulatory sequences are present, it is debatable whether any of these sequences would bind transcription factors and promote expression as the precise location, orientation and combination of *cis* regulatory sites is crucial for transcription factors to induce expression (Venter and Botha, 2004).

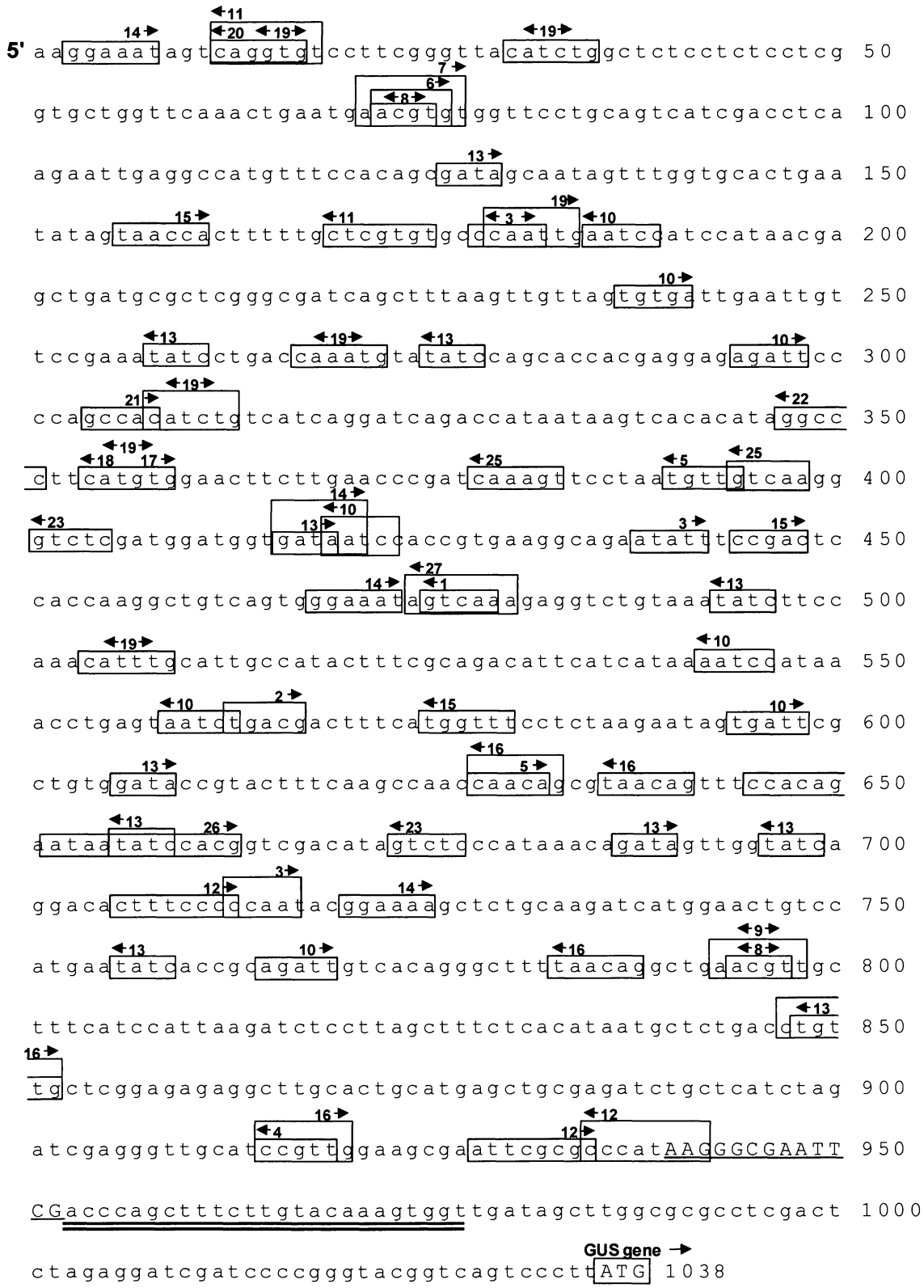

Figure 17. Location and orientation of transcription factor binding sites in the non-coding strand of the *C4* open reading frame cloned into pMDC163.

Nucleotides originating from pCR8/GW/TOPO are single underlined and double underlined nucleotides are the *att*B2 site. The *Arabidopsis thaliana cis*-regulatory sites are: 1) *TTGAC* - WBOXATNPR1 (Eulgem et al., 2000); 2) *TGACG* - ASF1MOTIFCAMV (Benfey and Chua, 1990; Klinedinst et al., 2000); 3) *CCAAT* - CCAATBOX1 - CAAT box (Haralampidis et al., 2002; Wenkel et al., 2006); 4) *AACGG* - MYBCOREATCYCB1 (Planchais et al., 2002; Abe et al., 2003) ; 5) *CAACA* - RAV1AAT (Kagaya et al., 1999); 6) *ACGTG* - ABRELATERD1 (Simpson et al., 2003; Nakashima et al., 2006) ; 7) *MACGYGB* - ABRERATCAL (Kaplan et al., 2006); 8) *ACGT* - ACGTATERD1 (Simpson et al., 2003); 9) *AACGTT* - ACGTTBOX (Foster et al., 1994); 10) *NGATT* - ARR1AT (Sakai et al., 2000); 11) *ACACNNG* - DPBFCOREDCDC3; 12) *WTTSSCSS* - E2FCONSENSUS (Vandepoele et al., 2005); 13) *GATA* - GATABOX (Benfey and Chua, 1990; Teakle et al., 2002); 14) *GRWAAW* - GT1CONSENSUS (Le Gourrierec et al., 1999); 15) *CCGAC* - LTRECOREATCOR15 (Busk and Pages, 1998); 16) *CNGTTR* - MYBCORE (Urao et al., 1993); 17) *CATGTG* - MYCATERD1 (Simpson et al., 2003); 18) *CACATG* - MYCATRD22 (Abe et al., 1997); 19) *CANNTG* - MYCCONSENSUSAT (Chinnusamy et al., 2003); 20) *CACCTG* - RAV1BAT (Kagaya et al., 1999); 21) *GCCAC* - SORLIP1AT (Hudson and Quail, 2003); 22) *GGGCC* - SORLIP2AT (Hudson and Quail, 2003); 23) *GAGAC* - SURECOREATSULTR11 (Maruyama-Nakashita et al., 2005); 24) *AACGTG* - T/GBOXATPIN2 (Boter et al., 2004); 25) *ACTTTG* - TBOXATGAPB (Chan et al., 2001); 26) *CCNNNNNNNNNNNCCACG* - UPRMOTIFIIAT (Martinez and Chrispeels, 2003); 27) *TTTGACY* - WBBOXPCWRKY1 (de Pater et al., 1996)

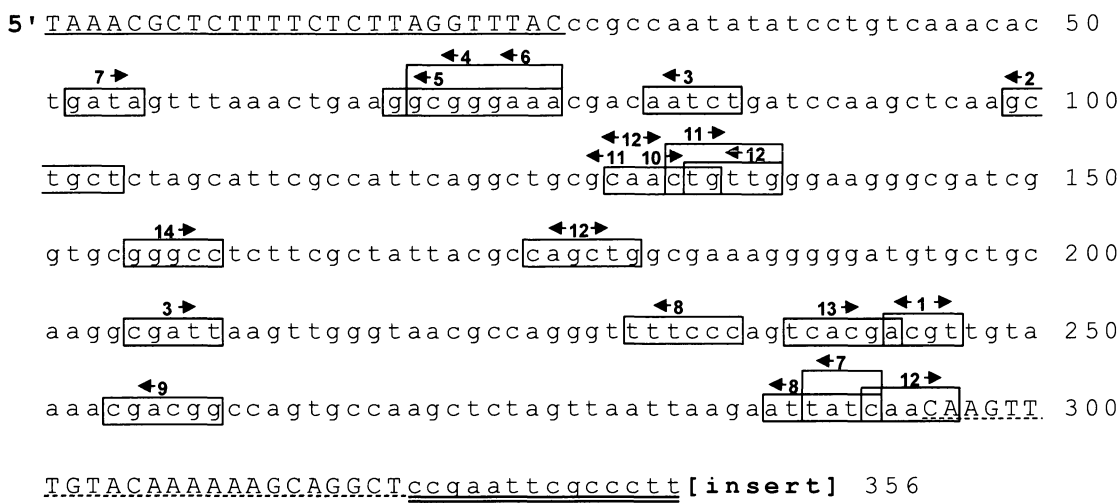

Figure 18. Location and orientation of transcription factor binding sites down stream of the RB site in pMDC163.

Single underlined nucleotides are the *RB* site, dashed underlined nucleotides are the *att*B1 site and nucleotides originating from pCR8/GW/TOPO are double underlined. The *Arabidopsis thaliana cis*-regulatory sites are: 1) *ACGT* - ACGTATERD1 (Simpson et al., 2003); 2) *AGCAGC* - ANAERO2CONSENSUS (Mohanty et al., 2005); 3) *NGATT* - ARR1AT (Sakai et al., 2000); 4) *TTTCCCGC* - E2FANTRNR (de Jager et al., 2001); 5) *TYTCCCGCC* - E2FAT (Ramirez-Parra et al., 2003); 6) *WTTSSCSS* - E2FCONSENSUS (Vandepoele et al., 2005); 7) *GATA* - GATABOX (Benfey and Chua, 1990; Teakle et al., 2002); 8) *GRWAAW* - GT1CONSENSUS (Le Gourrierec et al., 1999); 9) *CCGTCG* - HEXAMERATH4 (Chaubet et al., 1996); 10) *YAACKG* - MYB2CONSENSUSAT (Abe et al., 2003); 11) *CNGTTR* - MYBCORE (Urao et al., 1993); 12) *CAACA* - RAV1AAT (Kagaya et al., 1999); 13) *KCACGW* - RHERPATEXPA7 (Kim et al., 2006); 14) *GGGCC* - SORLIP2AT (Hudson and Quail, 2003).

II.A.3. Generation and genotyping of transgenic lines

All *C* gene constructs and the control construct were transformed into wildtype Col-0 plants by the floral dip method (Clough and Bent, 1998). T_1 seeds were selected on medium containing 65 mM hygromycin. From each independently-derived PCR construct, the goal was to select five independent T_1 lines. Nomenclatures for both plasmids and plants are in Table 3. For most of the T_1 lines, the presence of the T-DNA from the pMDC163-based constructs was detected by PCR with one primer in the *C* gene and the other primer in the *GUS* gene. An example of PCR genotyping is shown in Figure 19. For some T_1 lines, the presence of the T-DNA was confirmed by direct detection of the C subunit-GUS fusion protein in leaves using the GUS assay. T_1 plants confirmed to contain the T-DNA were allowed to self-pollinate and T_2 seeds were collected, representing segregating populations of hemizygous and homozygous plants. T_3 seeds from individual numbered T_2 plants were germinated on medium containing hygromycin to select for the T-DNA were genotyped by a progeny test to infer the genotype of the T_2 plant (Table 4). For the progeny test, T_3 progeny from individual T_2 plants were collected and expression of the *GUS* gene was assayed under non-selective conditions using at least 50 3-day-old T_3 seedlings from each T_2 plant. The pool of T_3 progeny were classified as: i) all showing GUS expression, ii) not all showing GUS expression or iii) other. If all of the T_3 progeny showed GUS expression, the genotype of the T_2 plant was inferred to be homozygous for the T-DNA and not undergoing silencing. If there were non-GUS-expressing T_3 progeny, then the T_2 plants in this class could be heterozygous for one or multiple T-DNAs or be homozygous undergoing silencing of the transgene. No inferences were made for the other category which might have displayed

Table 3. Nomenclature of constructs and plant lines.

DNA region	Name of clone in pCR8/GW/TOPO	Name of clone in pMDC163	Name of T_1 transgenic plant lines
C1	C1-4	C1-4-2	AC1::C1:GUS
	C1B-1	C1B-1-4	BC1::C1:GUS
	C1C-4	C1C-4-2	CC1::C1:GUS
C2	C2A-3	C2A-3-4	AC2::C2:GUS
	C2E-1	C2E-1-4	EC2::C2:GUS
	C2D-4	C2D-4-1	DC2::C2:GUS
sC3	C3-3	C3-3-4	AC3::C3:GUS
	C3B-9	C3B-9-5	BC3::C3:GUS
	C3C-5	C3C-5-3	CC3::C3:GUS
LC3	LC3B-4	LC3B-4-5	BLC3::C3:GUS
	LC3D-4	LC3D-4-4	DLC3::C3:GUS
	LC3E-4	LC3E-4-5	ELC3::C3:GUS
C4	C4-5	C4-5-2	AC4::C4:GUS
	C4-7	C4-7-2	CC4::C4:GUS
	C4B-4	C4B-4-2	BC4::C4:GUS
C5	C5-7	C5-7-12	AC5::C5:GUS
	C5B-9	C5B-9-3	BC5::C5:GUS
	C5C-3	C5C-3-3	CC5::C5:GUS
"Empty"	C4OOD-1	revC4::GUS	Rev

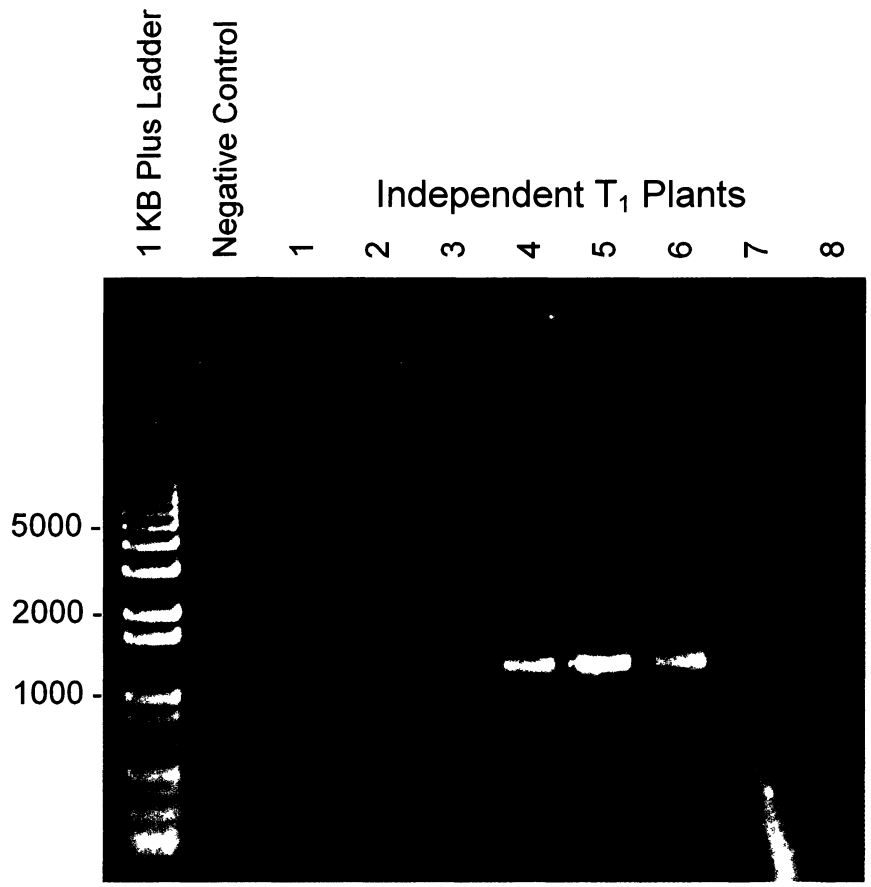

Figure 19. Genotyping of T_1 plants.
Detection of *CC4::C4:GUS* T-DNA in independent T_1 plants by PCR genotyping. Size markers are in base pairs. Expected size of PCR product is 1207 bp.

Table 4. Name and phenotype of transformed T_2 lines based of phenotype of T_3 progeny.

T_1 line	Phenotype of T_2 Line		
Line	All T_3 progeny GUS expressing	Not all progeny GUS expressing	Other†
AC1::C1:GUS -2	1 5 6 8 9	2 3 4 7	
AC1::C1:GUS -4	1 2 3 5 7 9	4 6 8 10 11 12	
BC1::C1:GUS -1	2 3 6 12	1 4 5 7 8 9 10 11	
BC1::C1:GUS -3	3 4	1 2 5 6 7	
BC1::C1:GUS -3.1		1 2 3	
BC1::C1:GUS -6		1 2 4	
BC1::C1:GUS -6.1	2 4	1 3 5 6 7 8 9	
AC2::C2:GUS -3	2 7 9 11	1 3 4 5 6 8 10	
AC2::C2:GUS -4	1	2	
AC2::C2:GUS -5	2 9 10	1 3 4 5 6 7 8 11	
AC2::C2:GUS -7		1 2 3 4 5 6 7 8 9 10 11 *	
AC2::C2:GUS -8	4 9	1 2 3 5 6 7 8 10	
AC2::C2:GUS -11	1 2	3 4 5 6 7	
DC2::C2:GUS -1	1 8	2 3 4 5 6 7 9 10	
EC2::C2:GUS -2	7	6 8 9 10 11	
EC2::C2:GUS -3	8	6 7 9 10 11 12 13	
EC2::C2:GUS -5	1 6 9 10	2 3 4 5 7 8	
EC2::C2:GUS -10	1 2 3 5 6 7	4 8 9 10 11	
AC3::C3:GUS -1	9 13	1 2 3 4 5 6 7 8 10 11 12 14	
AC3::C3:GUS -3	2 3 4 5 8 12	9 10 11	1 6 7
AC3::C3:GUS -5	1 2 3 4 5 6	7 8	
AC3::C3:GUS -6	3	1 5 9 11	2 4 6 7 8 10
BC3::C3:GUS -4	2 6 10 12	1 3 4 5 7 8 9 11	
BC3::C3:GUS -8		2 4 5 6 7 8	1 3
CC3::C3:GUS -1		1 2 3 4 5 6 7 8 9 10 11 12	
CC3::C3:GUS -8	8 10	1 2 3 4 5 6 7 9 11	
CC3::C3:GUS -9	1 3 4 5 6 7 8 9 11	2 10 12	
CC3::C3:GUS -11	4 6 11	1 2 3 5 7 8 9 10 12	
CC3::C3:GUS -12	6 7	1 2 3 4 5	
BLC3::C3:GUS -2	2 3 4 7	1 5 6	
BLC3::C3:GUS -3		1 2 3 4 5 6 7	
DLC3::C3:GUS -4	1 3 4 6 7 8 9 10 11 12	2 5	
DLC3::C3:GUS -6	2 5 8	1 3 4 6 7 9 10 11 12	
DLC3::C3:GUS -7	2 3 4 5 9	1 6 7 8 10	
DLC3::C3:GUS -11	3 7	1 2 4 5 6	

DLC3::C3:GUS -12	2 5 7 8	1 3 4 6	
AC4::C4:GUS -2		1 2 3 4 6 7 9	5 8 10
AC4::C4:GUS -3		3 5 7 10	1 2 4 6 8 9 11
AC4::C4:GUS -4		1 2 3 4 5 6 7 8 9	
AC4::C4:GUS -5		1 2 5 6 7 10 11	3 4 8 9
AC4::C4:GUS -6		1 4 6 7	2 3 5
AC4::C4:GUS -7		7 8 9 10	1 2 3 4 5 6
AC4::C4:GUS -8		1 2 3 4 5 6 7 8 9 10 11	
BC4::C4:GUS -3		1 2 3 4	
CC4::C4:GUS -1		1 2 3 4 5 6 7	
CC4::C4:GUS -2		1 2 3 4 5 6 7 9 10 11	8
CC4::C4:GUS -4	2	1 3 4 5 6 7 8 9 10 11 12	
CC4::C4:GUS -5		1 2 3 4 5 6 7 8 9	
CC4::C4:GUS -6	1	2 3 4 5 6 7 8	9 10
CC4::C4:GUS -9		1 2	3 4 5 6 8
AC5::C5:GUS -1	1 3 6 8 9	2 4 5	7 10
AC5::C5:GUS -6	2 3 4 5 6 7	1 8	9
AC5::C5:GUS -9			1 2 3 4 5 6 7 8 9 10 11 12
AC5::C5:GUS -10	5	3 4 6	1 2 7
BC5::C5:GUS -1	1 2 3 4 6 7 8 9	5 10	
BC5::C5:GUS -3	1 5 6 8	2 3 4 7	
BC5::C5:GUS -4	3 5 10	1 2 4 6 7 8 9 11 12	
BC5::C5:GUS -5	2 3 5 7 8 10 11	1 4 6 9	
BC5::C5:GUS -7	8 9 10	1 2 3 4 5 6 7 11 12	

* All lines have few individuals with no GUS expression.
† No or low seedling germination, severe contamination in assay well, no GUS expression

poor seedling germination, fungal contamination, or no GUS expression. When T_2 seeds were used for experiments, hygromycin-resistant (T-DNA-containing) plants were selected on agar plates. Homozygous T_3 lines were used in some experiments and those which were grown on plates were selected for hygromycin resistance while those which were grown on soil were not.

GUS construct-containing lines which were inferred to be homozygous and not silencing were isolated from most of the C subunits except for *C4* gene constructs. Of the 129 lines observed, only two *C4* gene constructs were homozygous for GUS expression. The exact reason for the limited number of plant lines observed to be homozygous for *C4* expression is unknown. One explanation could be that the position of the T-DNA in the genome inhibits the expression of the transgene gene. This is unlikely because each of the fourteen *C4* construct lines are likely in a different location in the genome and this effect is seen from all of the fourteen lines. Another explanation is that the lack of homozygous lines was due to the inability to produce plants homozygous for the T-DNA construct. This can occur because the insertion process of T-DNA into the genome can cause chromosomal translocations (Nacry et al., 1998). However, this also unlikely because T-DNA induced chromosomal arrangements do not occur every time the T-DNA is inserted. Also, from a hemizygous parent, 25% of the offspring would be expected to lack the transgene and thus be unable to generate GUS expression and this was observed for *C1*, *C2*, *sC3*, *LC3*, and *C5* construct lines. However, in the *C4* construct lines typically greater than 25% of the T_3 progeny lacked GUS expression. A third explanation is that the plant cannot tolerate extra copies of the *C4* subunit gene and will randomly silence (Schubert et al., 2004). Therefore, it is

possible that the *C4* lines are silencing.

II.B. Expression of Protein Phosphatse 2A *C4* subunit gene

The expression pattern of the PP2A *C4* subunit gene was determined from transgenic lines generated using constructs from three independent PCRs. First, the phenotype of T_1 plants and subsequent generations was examined. Ideally, the T_1 plants would: i) contain a single copy of the intact T-DNA inserted in an innocuous nuclear genomic region that does not disrupt a native gene; ii) appear phenotypically similar to wild type plants; and iii) have similar expression patterns to each other.

Different factors, including location of double stranded DNA breaks, affect where the T-DNA will insert (Windels et al., 2003). The ~130 Mb Arabidopsis genome contains 44.4% coding region (defined as the open reading frame) where 28.8% are coding sequences and 15.6% are introns (The Arabidopsis Genome Initiative, 2000). Ideally, my experimental plants should not contain a T-DNA insert within the coding sequence of any genes. Since the genome contains 44.4% coding sequence, there is a 55.6% chance that the T-DNA will insert in a non-coding region or promoter region; however the actual frequency of insertion into these regions has been found to be about 64.5% (Szabados et al., 2002; Kim et al., 2007) indicating that about 35% of the T-DNAs will insert into a gene. However, even if the T-DNA inserts into a gene, there may not be a detectable phenotype because Arabidopsis has many genes which appear to be functionally redundant (Briggs et al., 2006). Thus, I expect to find very few mutant plants with obvious phenotypes under normal growth conditions. In my experiments, the exact location and number of T-DNAs inserted were not determined. Instead, mutant

plant phenotypes were compared to wildtype plants. From the initial selection on hygromycin medium, up to 12 T_1 plants were saved. Only plants which were similar to wildtype under normal growth conditions were used for further experiments. T_1 plants which exhibited severe phenotypes (dwarfism, abnormal floral structure, etc.) were occasionally observed, and these lines were discarded from further analysis.

It is common to observe the same expression pattern but different expression levels from plants transformed with the same construct (Jones et al., 1985; Peach and Velten, 1991). Historically, such differences have been attributed to position effects, i.e., the location of the T-DNA in the genome affects its expression (Jaenisch et al., 1981). However, in studies using plants containing only single, intact, T-DNA inserts, similar expression of the reporter was usually found among the unique T-DNA insertion sites (Hobbs et al., 1990; Schubert et al., 2004; Nagaya et al., 2005). Thus differences in expression levels are better correlated with plant lines that contain multiple single copy insertions of the transgene or tandem copies of the transgene at a single insertion site (Hobbs et al., 1993; Schubert et al., 2004). After the visual screening and genotyping of the T_1 transgenic lines (Table 3), multiple T_2 and T_3 lines from the each independent PCR (Table 4) were generated and used in the GUS histochemical assay. Lines that were not consistent with the expression pattern observed in the majority of the population were discarded. Figure 20 shows an example of GUS assay results from different 4-week-old T_3 plant lines which arose from a single PCR (*AC4::C4:GUS*). These plants show very similar expression patterns as well as similar expression intensity in the leaves. In addition, these lines had very similar expression patterns in other developmental stages and tissues (data not shown). No expression or patchy expression seen in some of the

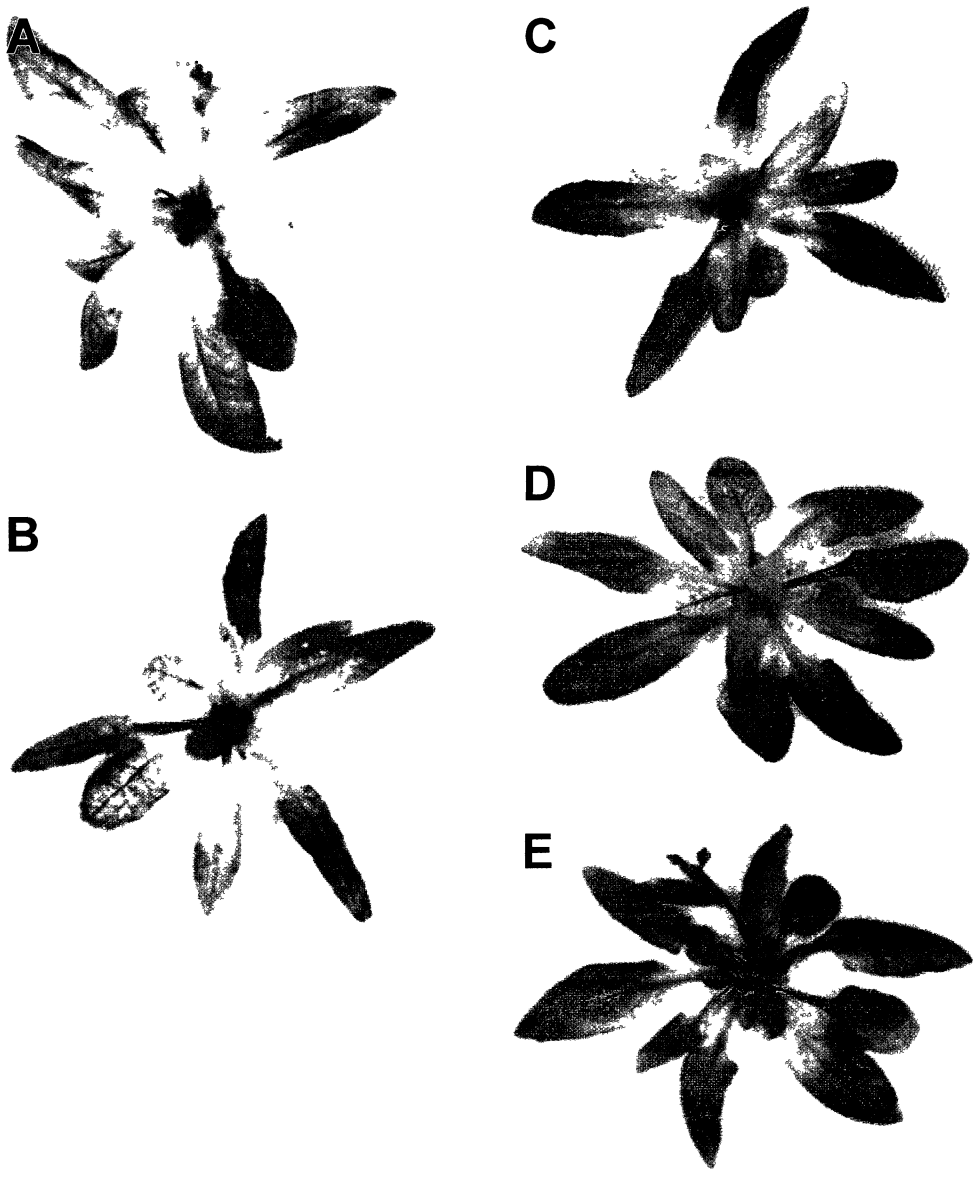

Figure 20. *C4* expression in 4-week-old plants from five independent lines.
All lines were incubated in the GUS substrate for 12 hours. The five independent lines are **A)** *AC4::C4:GUS-2*; **B)** *AC4.·C4:GUS-4*; **C)** *AC4::C4:GUS-5*; **D)** *AC4::C4:GUS-8*; **E)** *AC4::C4:GUS-7*.

leaves could be due to the GUS substrate ineffectively penetrating the leaves.

As described in section I.A, constructs were made from three independent PCRs for each C subunit. *Taq* DNA polymerase is known to randomly introduce errors during DNA synthesis. To determine if unknown errors might affect the expression pattern, for each of the C subunits, plants transformed with T-DNA from each of the three independent PCRs were compared at different developmental stages. Examples of the *C4* gene expression patterns from plants transformed with the products of two independent PCRs (*AC4::C4:GUS* and *CC4::C4:GUS*) are shown in Figure 21. The expression pattern of *BC4::C4:GUS* was also compared (data not shown). In all three constructs, the GUS expression pattern at different developmental stages was very similar. This result indicates that any DNA polymerase errors that occurred did not affect the expression pattern.

II.B.1. *C4* gene expression in organs, tissues and cell types throughout *Arabidopsis thaliana* development

To document the expression pattern of the *C4* gene throughout the Arabidopsis life cycle, GUS expression was observed at 1, 2, 3 or 4, 6 or 7, 10, and 14 days after germination and in 4- to 6-week-old plants. These time points were chosen because they represent major developmental transitions in Arabidopsis post-germination development (Boyes et al., 2001). *C4* gene expression was observed in various organs throughout the Arabidopsis life cycle (Figure 22). The details of *C4* gene expression will be described in following sections. A general trend was that the expression pattern in a particular organ remained constant even when the organ was compared over time. For example, expressio

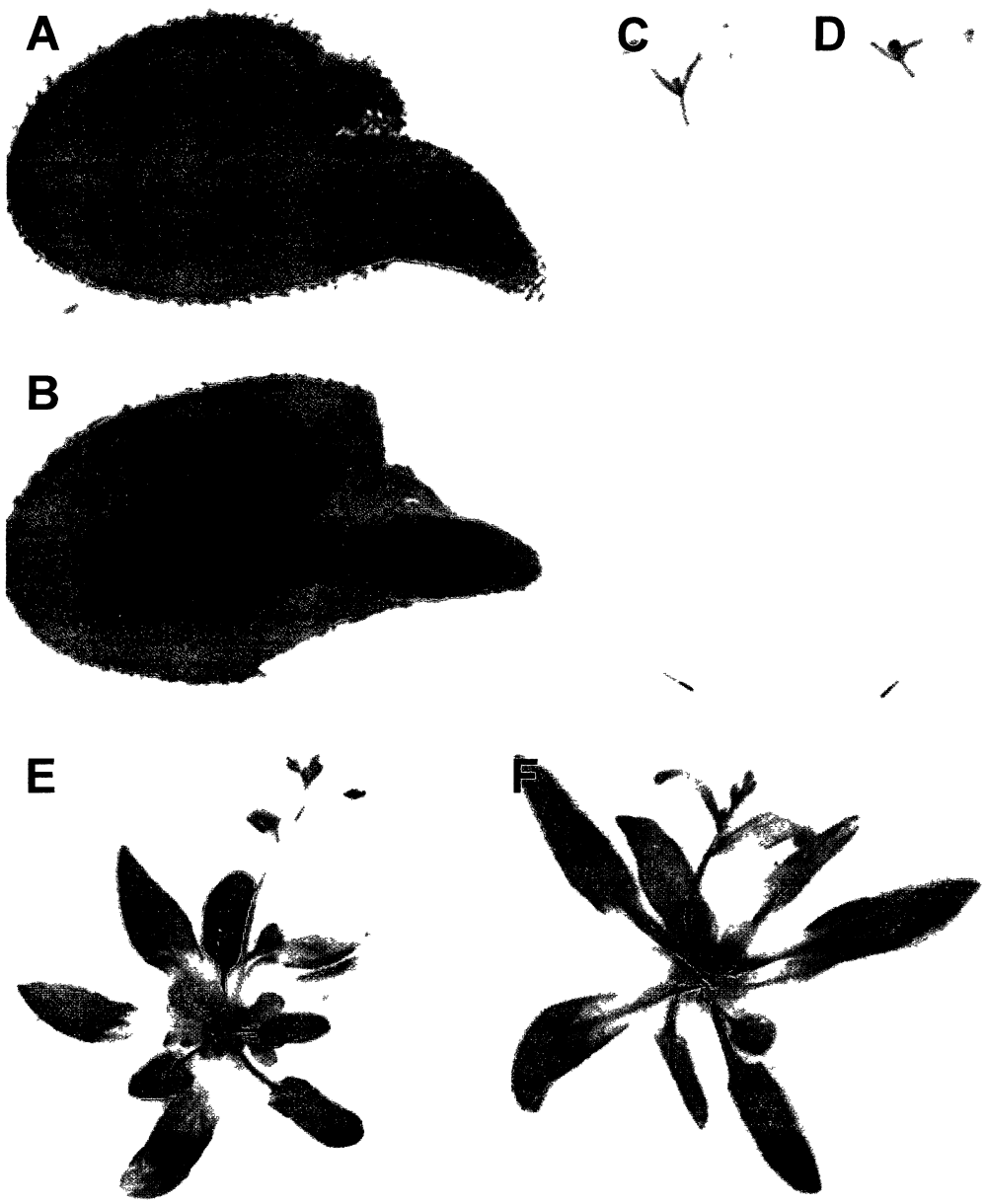

Figure 21. *C4* gene expression pattern of plants transformed with T-DNA from two independent PCRs.
1-day-old seedlings from **A**) *AC4::C4:GUS-2* and **B)** *CC4::C4:GUS-1* lines; 7-day-old seedlings from **C)** *AC4::C4:GUS-2* and **D)** *CC4::C4:GUS-1* lines; 4-week-old plants from **E)** *AC4::C4:GUS* and **F)** *CC4::C4:GUS* lines. Samples were incubated in the GUS substrate for **A)** 16 hours; **B)** 12 hours; **C-D)** 14 hours; **E-F)** 24 hours.

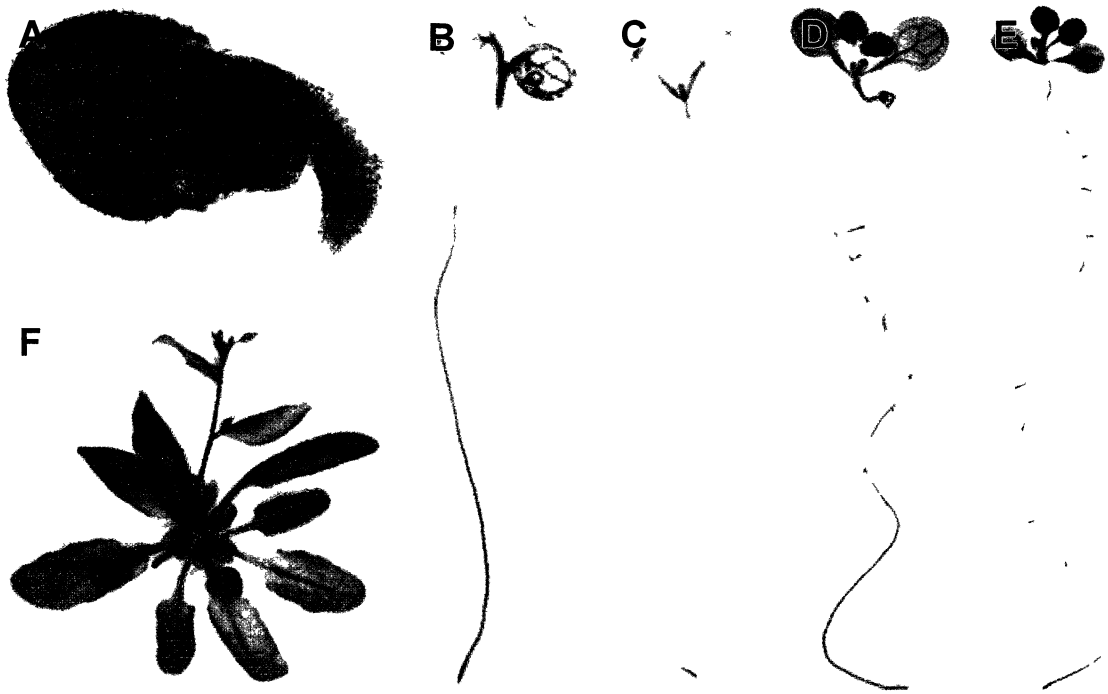

Figure 22. Expression pattern of the *C4* gene in Arabidopsis plants at different developmental stages.
A) 1-day-old *AC4::C4:GUS-2*; **B)** 4-day-old *AC4::C4:GUS-2* **C)** 7-day-old *AC4::C4:GUS-2*; **D)** 10-day-old; **E)** 14-day-old *AC4::C4:GUS-2*; **F)** 4-week-old *AC4::C4:GUS-7*. Lines used were **A-E)** *AC4::C4:GUS-2* and *AC4::C4:GUS-7* **F).** Samples were incubated in the GUS substrate for **A-B)** 24 hours; **C)** 14 hours; **D)** 12 hours; **E)** 18 hours; **F)** 24 hours.

expression in the root meristem was constantly strong no matter the age of the plant.

To determine the relative expression levels during development, the plants were assayed for different periods of time. The products of the GUS enzyme accumulate as insoluble diX-indigo and as a result, it is possible to determine the strength of the promoter by incubating the sample in the GUS substrate solution for various times. For 1-14 day-old plants, assay times of 1, 3, 12 and 24 hours were selected because, at each of these times, expression was detectable at additional sites that were not apparent at shorter assay times. For plants older than 14 days, the 1-hour assay time was not used because little product was detectable at that time. Twenty-four hours was chosen as the maximum assay time because preliminary experiments indicated that no additional information was gained from longer times (data not shown).

II.B.2. *C4* gene expression in roots

II.B.2.a. *C4* gene expression in primary roots

The root contains four zones: meristematic, elongation, differentiation, and mature (Dolan et al., 1993). Cells which are actively dividing are located in the meristematic zone and contain dense cytoplasm (Figure 23). The distal end of the meristematic region contains four mitotically inactive quiescent cells which maintain the identity of the surrounding stem cells and undergo cell division as needed to replenish the stem cells of the meristem (van den Berg et al., 1995; Kidner et al., 2000). Cell divisions establish columns or files of cells which extend along the length of the root. Cells in the elongation zone undergo anisotropic expansion and beginning to form large central vacuoles (Fluckiger et al., 2003). In the differentiation zone (not shown), cells begin to

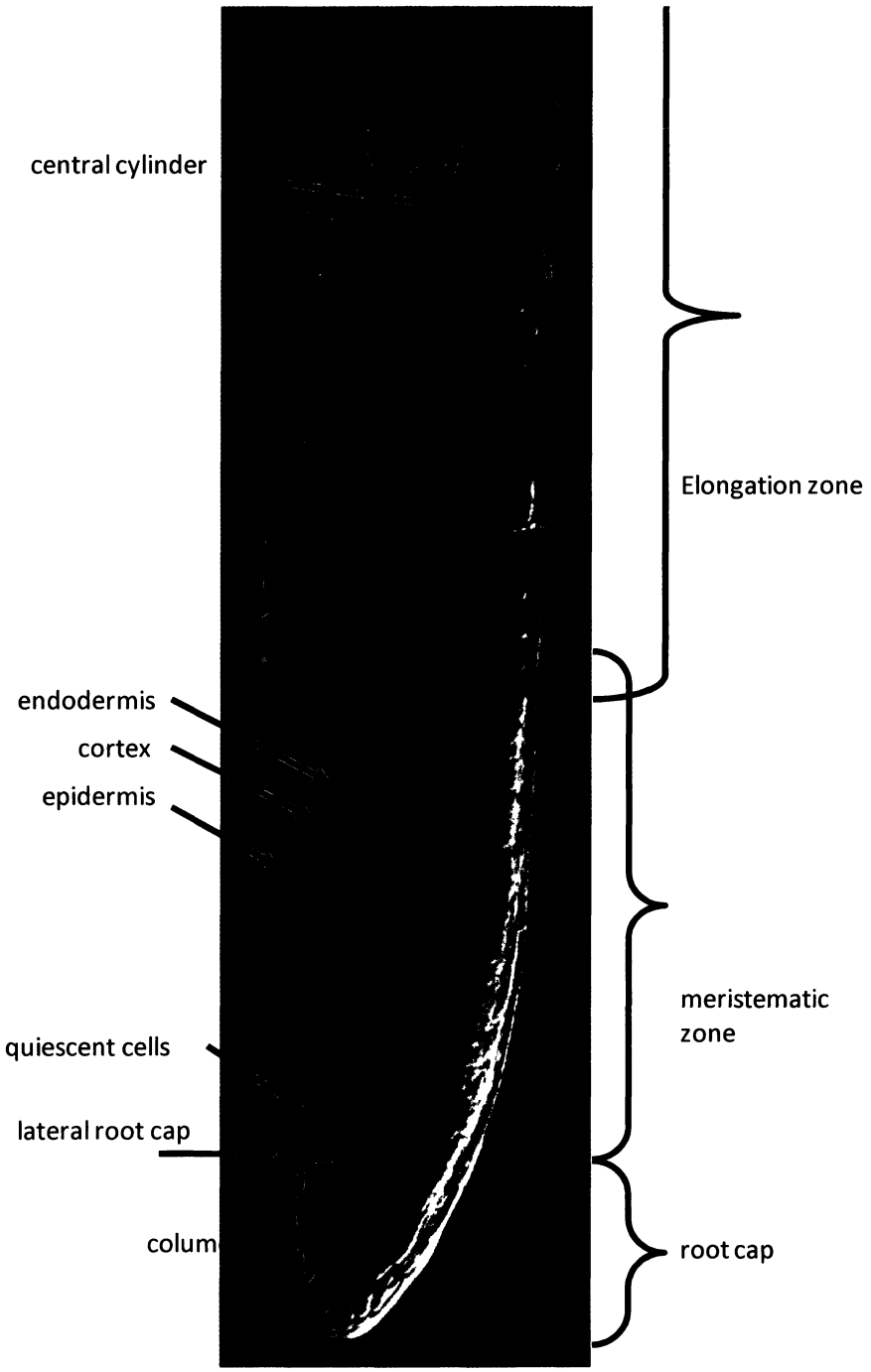

Figure 23. ***Arabidopsis thaliana*** **root anatomy.**
DIC image of 4-day-old *Arabidopsis thaliana* ecotype Columbia root tip. Photo courtesy of Whitney Hunter.

.

assume their final identity. A marker for the differentiation zone is the appearance of root hairs on trichoblast cells in the epidermal layer (Dolan et al., 1994). Root hairs are first detected on approximately three-day-old seedlings (Schiefelbein et al., 2009) indicating that it takes that long for cells to progress from the meristematic zone to the differentiation zone.

A cross section through a mature region of the root reveals that the root is made up of concentric layers of differentiated cells. The organization of these layers is established during embryogenesis (Scheres et al., 1994). The outermost layer of the root is the epidermis (containing trichoblasts and atrichoblasts), which overlays the ground tissue (one or more layers of cortical cells and one layer of endodermis) with the central cylinder in the middle. The central cylinder or stele is composed of the pericycle, xylem, and phloem. The root meristem is protected by the root cap made of columella cells that covers the most distal portion of the root and by lateral root cap cells that extend back towards the differentiation zone (Figure 23). Even in the mature embryo there are two layers of columella cells and one layer of lateral root cap cells. Additional columella layers are formed after germination.

C4::C4:GUS transgenic lines were examined for the expression of the *C4* gene in roots during the first two weeks of growth. These plants were grown in plates for ease of observation. Roots older than 14 days were not observed because those plants were grown in soil. An attempt to view older roots by growing plants in perlite was unsuccessful due to the inability to remove all of the perlite without severely damaging the delicate root system.

The first time when *C4* gene expression in roots was examined was during seed

germination. Cold stratification, imbibing dormant seeds in the dark at 4°C, was used to synchronize germination of the Columbia ecotype of *Arabidopsis thaliana* used in this study. Seedlings go through three stages of germination (Finch-Savage and Leubner-Metzger, 2006). In the first stage, the seed imbibes water which restarts metabolism in the dormant seed. The second stage involves further imbibition and it is at this stage that cold stratification can synchronize germination. These two stages occur during the cold stratification period. Once seeds are fully imbibed, they are removed from the cold and the third and final stage of germination occurs when the testa (seed coat) and endosperm rupture and the radicle emerges followed by the hypocotyl and cotyledons. Even with cold stratification, not all seeds germinate at the same rate and after 24 hours it is possible to observe seeds that are at different phases of emergence from the seed coat. Expression of the *C4* gene was observed in the radicle during the third stage of seed germination (Figure 24A-D). Soon after the seed coat ruptured, allowing for entry of GUS substrate), *C4* gene expression was detectable in the radicle (Figure 24A-B). The highest expression was always observed in the root meristematic zone. To determine if other regions of the radicle expressed the *C4* gene and to determine the relative levels of expression, samples were incubated in GUS substrate for 1, 3, 12 or 24 hours. At 1 and 3 hours, *C4* gene expression was not detected in the columella and lateral root cap cells (Figure 25A-B) but these cells did show expression after incubation with the GUS substrate for 12 and 24 hours (Figure 25C-D); thus there is weaker expression in the root columella and lateral root cap compared to the meristematic zone.

Once the radicle is fully emerged, it is referred to as the primary root. Primary root tips of plants from 2 to 14 days old were observed. At all ages, *C4* gene expression

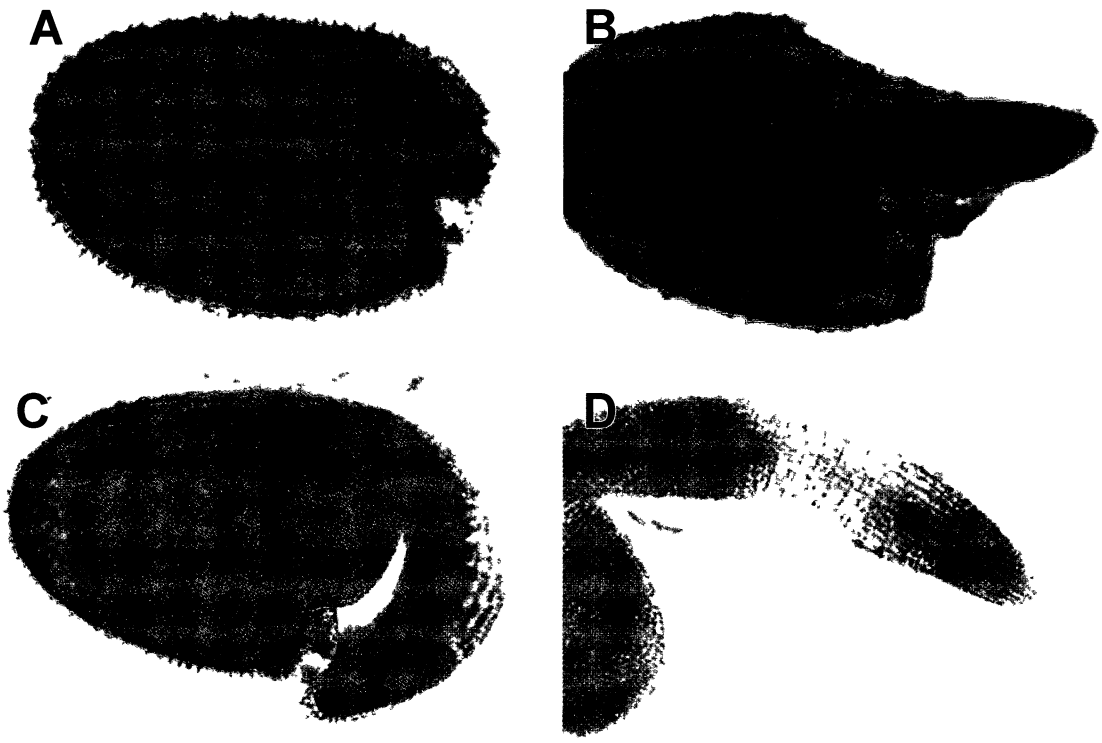

Figure 24. Expression pattern of *C4* gene during germination.
A) Seed coat ruptured; **B)** radicle emerged; **C)** partially emerged seedling; **D)** fully emerged seedling. **A)** and **C-D)** are *AC4::C4:GUS-2* and **B)** is *CC4::C4:GUS-1*. Samples were incubated in the GUS substrate for **A)** 3 hours; **B)** 24 hours; **C)** 12 hours; **D)** 24 hours.

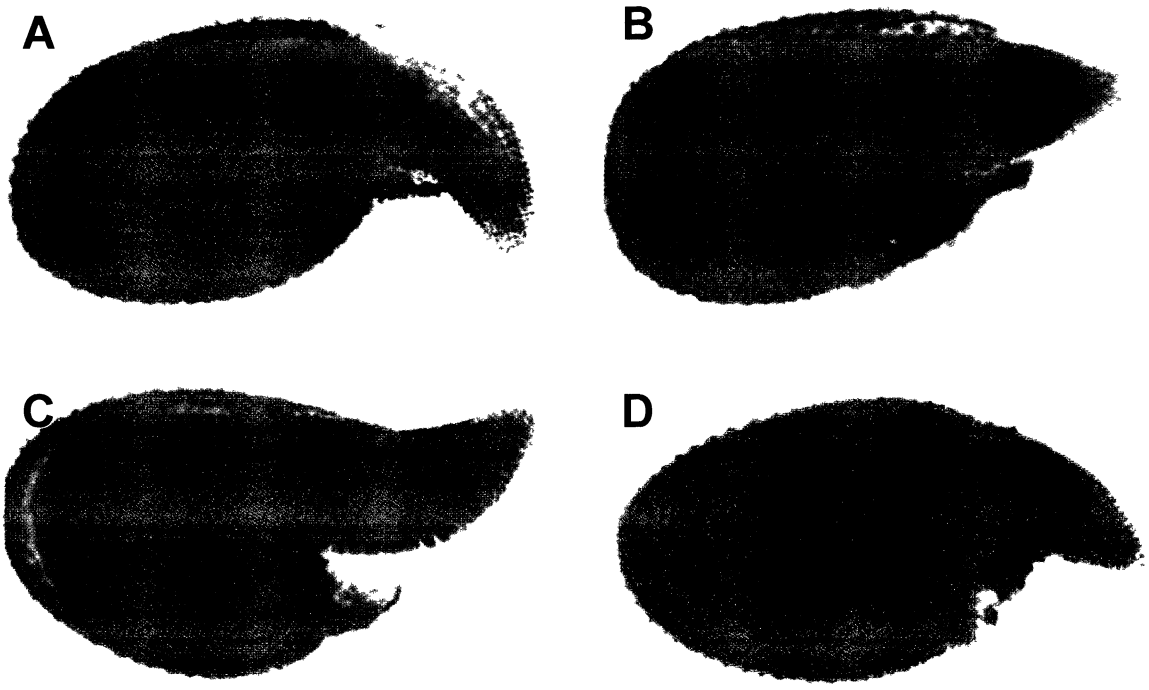

Figure 25. One-day-old seedlings assayed for different lengths of time.
All plants are *AC4::C4:GUS-2* and were assayed for **A)** 1 hour, **B)** 3 hours, **C)** 16 hours, or **D)** 24 hours.

was seen in the meristematic, elongation and differentiation zones. Representative 4 and 10 day old seedlings are shown in Figure 26. *C4* gene expression was observed in the cells in the meristematic zone and, to a lesser extent, in the cells of the elongation zone when the sample was incubated with GUS substrate for 1 hour; however expression was not seen in the root cap in this short assay time (Figure 26A-E). After 3 hours of incubation, faint accumulation of diX-indigo was seen in the root cap and, as expected, the meristematic and elongation zones showed more diX-indigo accumulation than was present at 1 hour (Figure 26B-F). Since the cells in the meristem are not highly vacuolated and have not yet begun to elongate, the apparent reduction in expression in cells in the elongation zone could be a result of increased cell volume rather than a true decrease in expression. Longer incubation periods of 12 and 24 hours showed high accumulation of diX-indigo throughout the root tip including the root cap (Figure 26C-D, G-H). This indicates that there is more *C4* gene expression in the root meristematic and elongation zones than in the columella cells and lateral root cap.

As described earlier, the differentiation zone is typically marked by the presence of root hairs. Figure 27 shows the meristematic, elongation and differentiation zones of a primary root incubated for 1 hour in the GUS substrate. Expression in the meristematic and elongation zones in this root is very similar to that shown in Figure 26. This image also shows the differentiation zone where expression was apparent in the developing root hairs. In the transition from elongation to differentiation zone, the cells of the central cylinder begin to assume their final cell identities as pericyle, xylem and phloem cells. The central cylinder region shows higher expression than the surrounding endodermal, cortical and epidermal cells although the precise identity of the cells which show *C4*

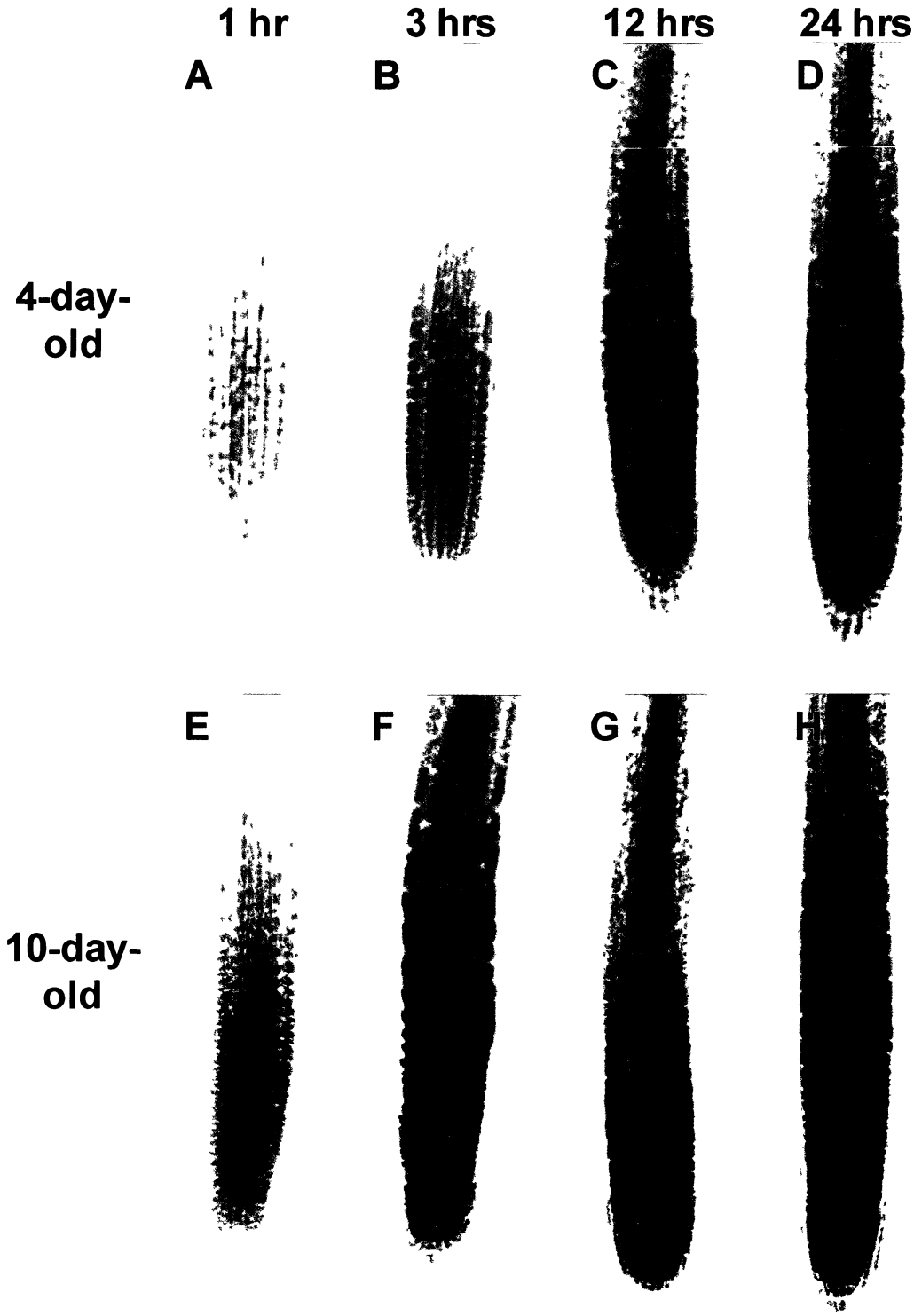

Figure 26. *C4* gene expression in primary root tip of 4- and 10-day-old *Arabidopsis thaliana* seedlings.
All 4-day-old plants were *AC4::C4:GUS-2* and 10-day-old plants were **E)** and **F)** *AC4::C4:GUS-5*, **G)** *BC4::C4:GUS-2*, and **H)** *AC4::C4:GUS-8*. Plants were incubated in the GUS substrate for times indicated.

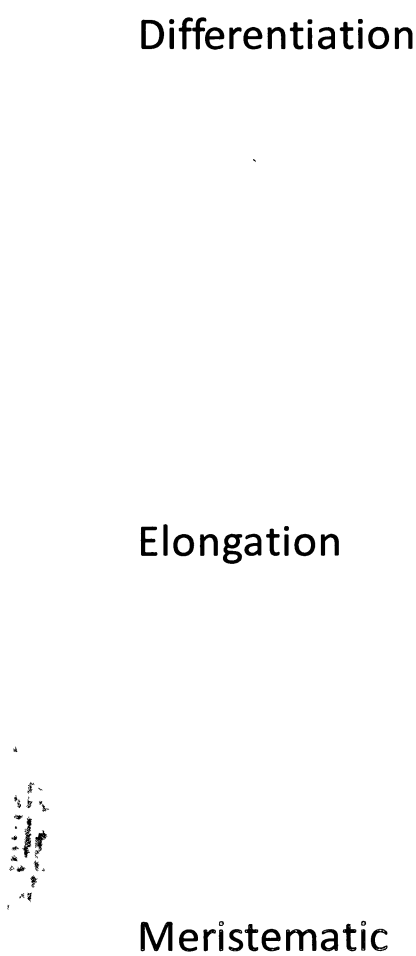

Figure 27. *C4* gene expression in primary root tips.
A 10-day-old *AC4::C4:GUS-2* root was assayed for 1 hour. The locations of the meristematic, elongation and differentiation root zones are indicated.

gene expression are unknown because root cross-sections were not done. The observed expression pattern is consistent with *C4* gene expression in multiple cell types of the central cylinder and is not consistent with expression in only one cell type which would result in a different pattern.

The mature zone of the primary root of 4-, 7-, 10-, and 14-day-old plants was examined next. Representative images from 4- and 14-day-old plants are shown in Figure 28. When roots were assayed for 1 hour, little expression was apparent in any of the cells in the mature zone. When assayed for 3 hours, the highest expression was associated with the central cylinder region, continuing the pattern observed in the differentiation zone. Expression in the central cylinder varied in intensity along the length of the root, decreasing with increasing distance from the root tip. In general, after 24 hours of incubation with the GUS substrate, all cells in the root appeared to express the *C4* gene with the greatest expression still in the central cylinder region. In summary, the levels of *C4* gene expression in the mature zone of the root were higher in the central cylinder and lower in the epidermis and cortex.

II.B.2.b. C4 gene expression in lateral roots

Arabidopsis has an indeterminate root structure in which the apical meristem remains active for the life of the plant. The primary root also develops new meristems to form lateral roots, also referred to as secondary roots; the secondary roots develop lateral roots called tertiary roots, and so on. Root branching increases the area of the root system resulting in a larger root surface available for uptake of nutrients and water. Because root growth and branching is an ongoing process, it is common to find lateral

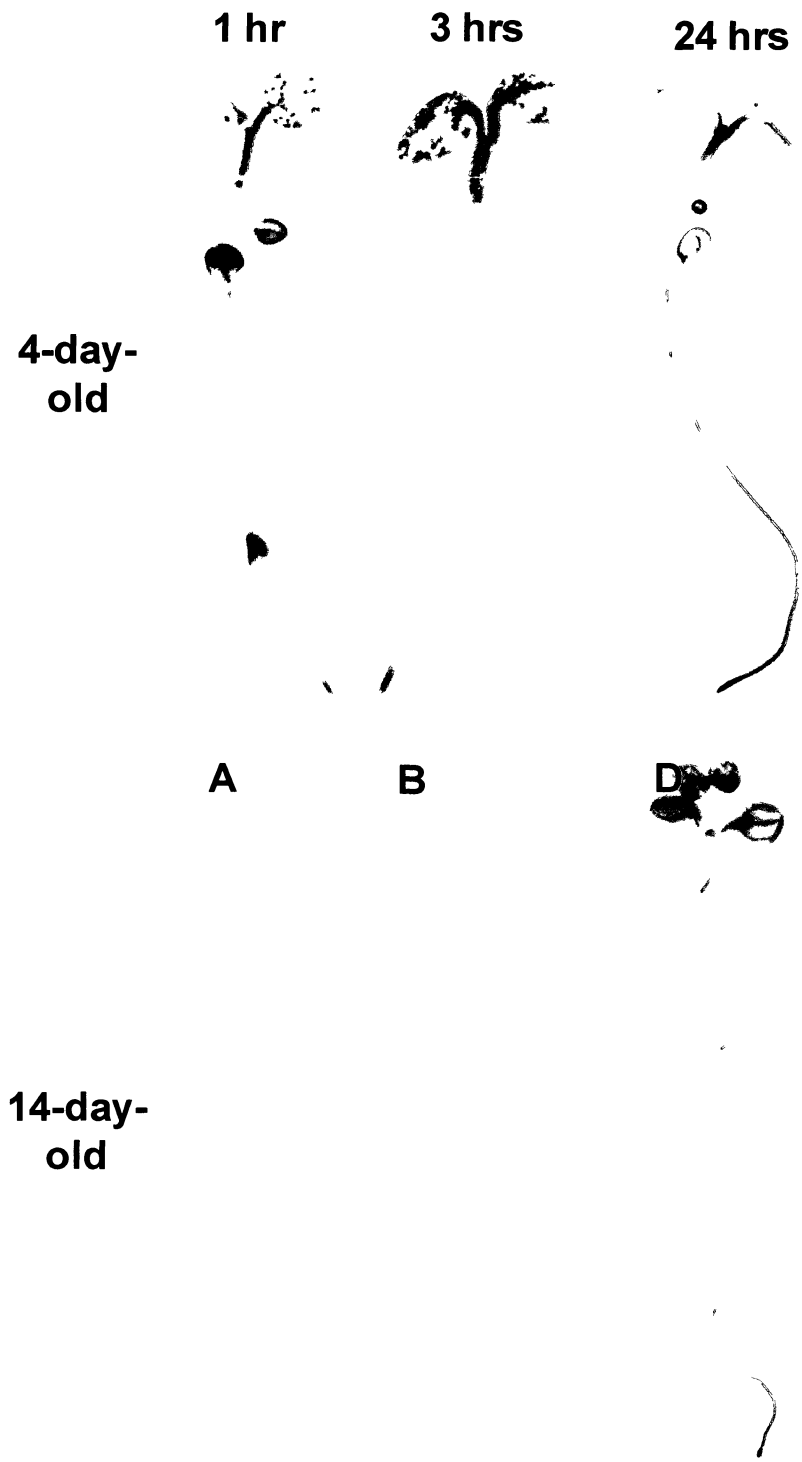

Figure 28. *C4* gene expression in 4- and 14-day-old seedlings.
All plant lines are from *AC4::C4:GUS-2*.

roots at different developmental stages on the same plant. From personal observations, the sites where the first lateral roots are initiating can be detected at about 4 days after germination using a compound microscope but these roots do not emerge from the primary root until about 7 days after germination. In dicots, lateral roots are formed from pericycle cells. Pericycle cells are suspended in different phases of the cell cycle; the cells nearest the phloem are suspended in G1 phase while those adjacent to the xylem are in G2 phase (Beeckman et al., 2001). Xylem-adjacent pericycle cells can re-enter the cell cycle to form lateral root primordia (Casimiro et al., 2003) in response to transient auxin maxima in the pericycle (Peret et al., 2009). Auxin maxima occur at ~15 hour intervals and as a result, lateral roots form at semi-regular intervals along the length of each root. Following an auxin maximum, Stage I of lateral root formation occurs when the two pericycle founder cells undergo anticlinal divisions to form a single layer of 8-10 small cells (Malamy and Benfey, 1997). Stage II is characterized by the formation of two layers, outer and inner, by periclinal divisions. Stage III involves periclinal division of the outer layer while the inner layer divides periclinally in Stage IV thus forming four layers. In Stages V and VI, cell divisions in the primordium continue that result in the formation of a dome of cells that extends into the cortical and epidermal layers of the root. In Stage VII, cell files similar to those in primary roots (described earlier) become apparent. By Stage VIII, the lateral root has fully emerged through the root epidermis. The emerged lateral root then forms meristematic, elongation, differentiation, and mature root zones, in a similar manner to primary roots as described earlier.

Lateral root primordia and emerged lateral roots were analyzed for *C4* gene expression at different developmental stages. Uniform expression was detected in all

cells of the lateral root primordium during Stages I-VIII after 1-3 hour incubation in the GUS substrate (Figure 29A-G and 30). After 12 and 24 hours of incubation, the lateral root primordia and central cylinder appear to have higher expression than the cells of epidermis, cortex, and endodermis (Figure 30). Although, the high expression observed in the rot primordia and central cylinder may be an artifact of the non-vacuolated nature of the primordium cells which is analogous to that described previously for the meristematic cells in the primary root. In addition, the knowledge that lateral roots initiate from the pericycle layer was used to determine that the expression of the *C4* gene in the central cylinder region included the pericycle layer and did not include the endodermis (Figure 29). After lateral root emergence, the expression pattern was similar to that in the primary root where the highest levels of *C4* gene expression were seen in the meristematic and elongation zones (Figure 29H-K). During the first 14 days when expression of the *C4* gene in roots was monitored, tertiary roots were sometimes observed forming on the secondary roots. Overall, the expression in the tertiary roots recapitulated that observed in the secondary roots (Figure 29L), indicating that expression of the *C4* gene likely occurred in a similar fashion in all lateral roots.

II.B.3. *C4* gene expression at the root-shoot junction

At the root-shoot junction, there are a few layers of root cells which formed in the embryo; this region is known as the collet (Compton, 1912; Scheres et al., 2009). In 1-day-old seedlings, *C4* gene expression was detected after three hours of incubation at the collet as a distinct line bisecting the root (Figure 31A-D). By 4 days of age, the line had disappeared (Figure 31E-H). Therefore, *C4* gene expression is detected in the collet in a

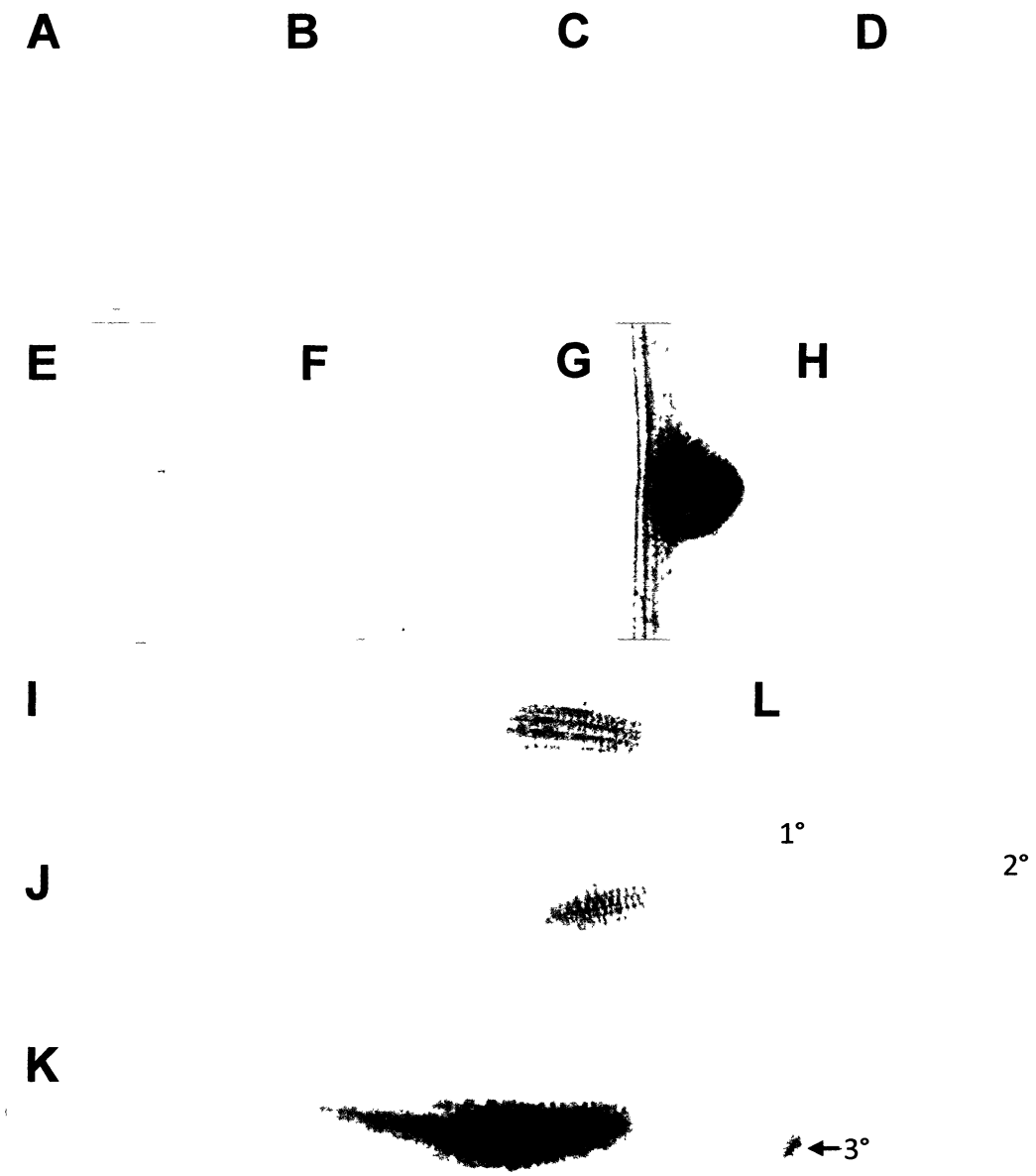

Figure 29. Expression pattern of *C4* gene during lateral root development.
Lateral root developmental stages are **A)** Stage-I primordia; **B)** Stage-II primordia; **C)** Stage-III primordia; **D)** Stage-IV primordia; **E)** Stage-V primordia; **F)** Stage-VI primordia; **G)** Stage-VIII primordia; **H)** emerged lateral root; **I)** lateral root; **J)** lateral root; **K)** lateral root tip; **L)** primary (1°), secondary (2°), and tertiary (3°) roots (*AC4::C4:GUS-2*; 14 days-old). **A), E), F), G), I), K),** and **L)** are *AC4::C4:GUS-2* plants. **B), C), D), H),** and **J)** are *BC4::C4:GUS-2* plants. All samples were incubated in the GUS substrate for 1 hour except for **G), K)** and **L)** which were incubated for 3 hours.

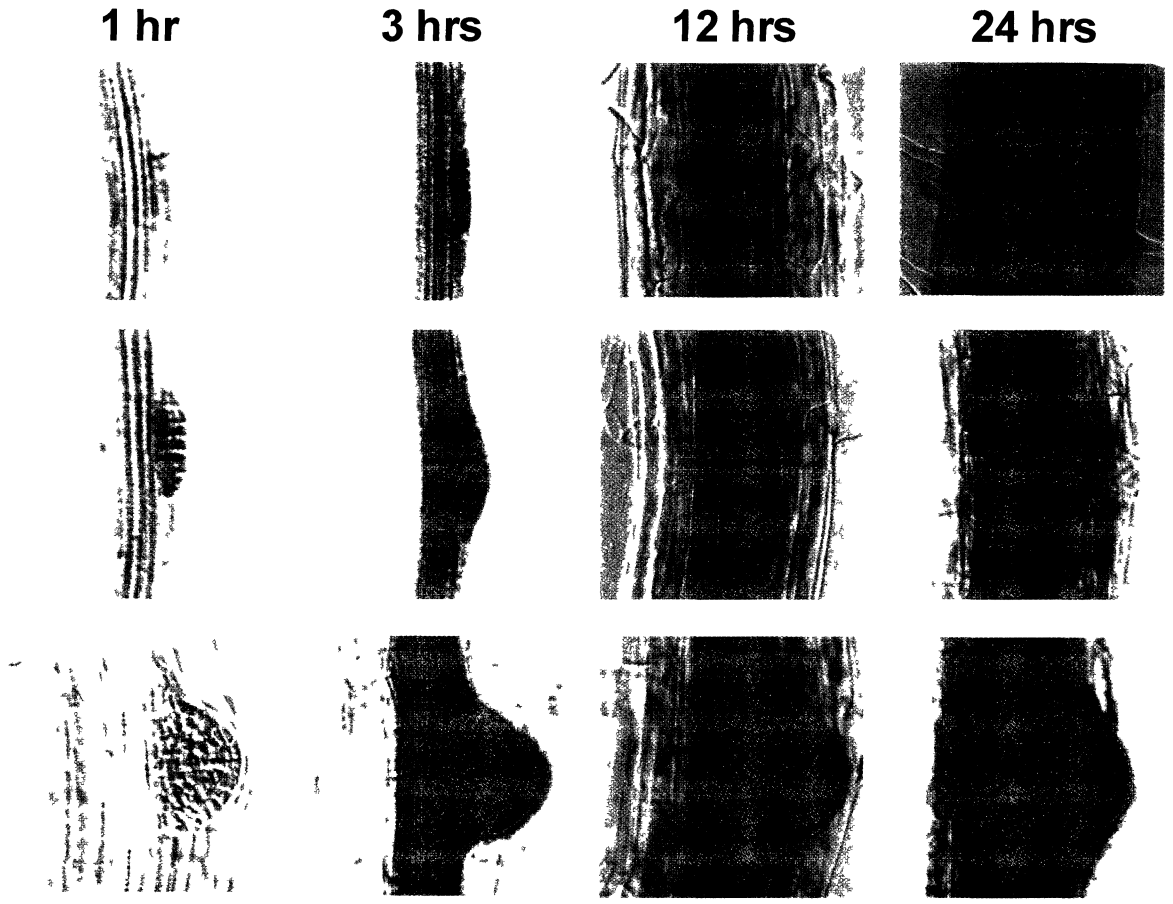

Figure 30. Stages of lateral root development assayed for *C4* gene expression at different periods of time.
The top row represents Stage-I primordia, middle row is Stage IV-V primordia, and bottom row is Stage-VIII primordia. Columns are labeled with incubation times in the GUS substrate. All roots assayed for 1, 3 and 12 hours were *AC4::C4:GUS-2* plants and all 24 hour assayed roots were *AC4::C4:GUS-8* plants.

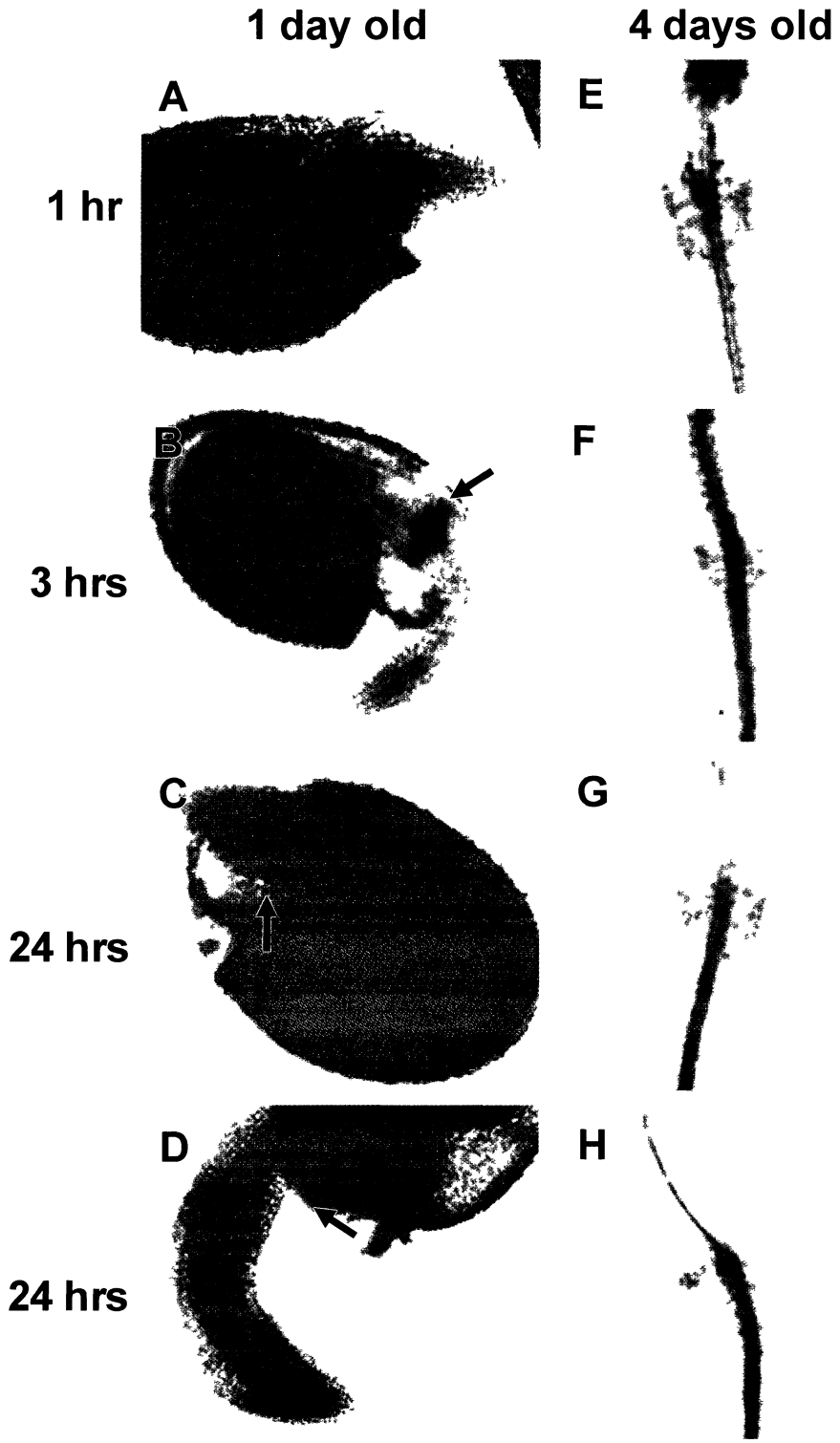

Figure 31. *C4* gene expression in the collet.
All plants are *AC4˙:C4:GUS-2* except for **B)** which is *BC4::C4:GUS-2* and assayed for times indicated.

limited time frame.

II.B.4. *C4* gene expression in stem

Simply put, most terrestrial vascular plants are composed of two parts: below-ground roots and above-ground shoots. In Arabidopsis, the shoot tissue between the root and the cotyledons is the hypocotyl. The cell number and tissue patterning of the hypocotyl is established in the embryo. After germination, the hypocotyl cells grow primarily by expansion and there are rarely any mitotic events (Gendreau et al., 1997). Cellular organization of the hypocotyl is similar to that of the root with a central cylinder, one layer of endodermis, two layers of cortex and one layer of epidermis.

In 1-day-old seedlings, the hypocotyl is often obscured by the seed coat, which may also prevent access of the GUS substrate to the tissues. Accurate observations of hypocotyl expression were thus restricted to those seedlings in which the seed coat had ruptured sufficiently. Little expression was seen in hypocotyls after 1 or 3 hours of incubation in the GUS substrate (Figure 32A and B). If expression was detected after 3 hours of incubation, it was confined to the central cylinder of the hypocotyl (Figure 32B). After 12 and 24 hours of incubation, there was expression throughout the hypocotyl with the highest expression in the central cylinder (Figure 32C and D).

Four day old seedlings exhibited no expression in the hypocotyl after 1 and 3 hours of incubation (Figure 33A and E). After 12 and 24 hours of incubation, *C4* gene expression was limited to the apex (near the cotyledon) of the hypocotyl and not detected in the base (near the crown; Figure 33I and M).

Likewise, at 7 days of age, no expression was observed after 1 and 3 hours of

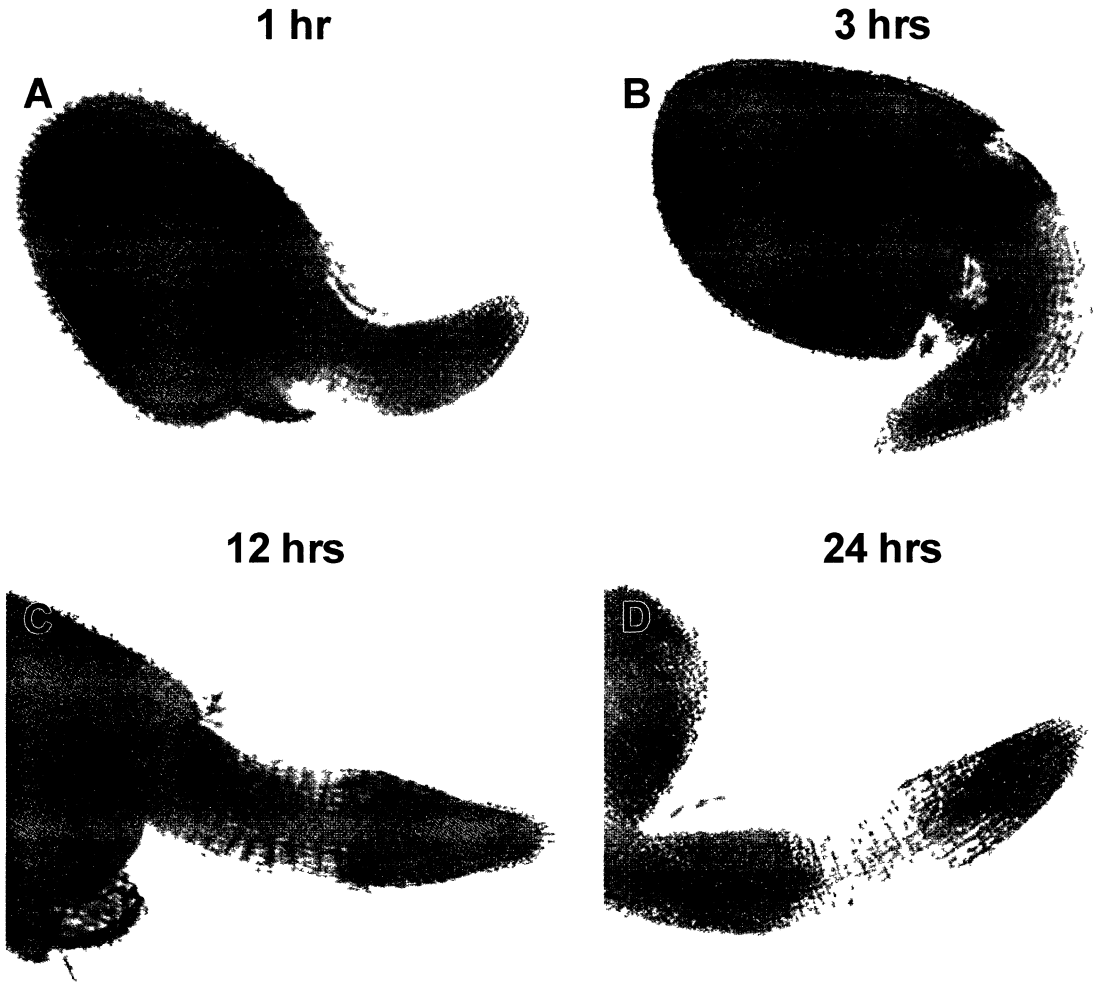

Figure 32. *C4* gene expression in the hypocotyl of 1-day-old seedlings.
A), **B)**, and **C)** *BC4::C4:GUS-2* and **D)** *AC4::C4:GUS-2*. Samples were incubated in the GUS substrate for the times indicated.

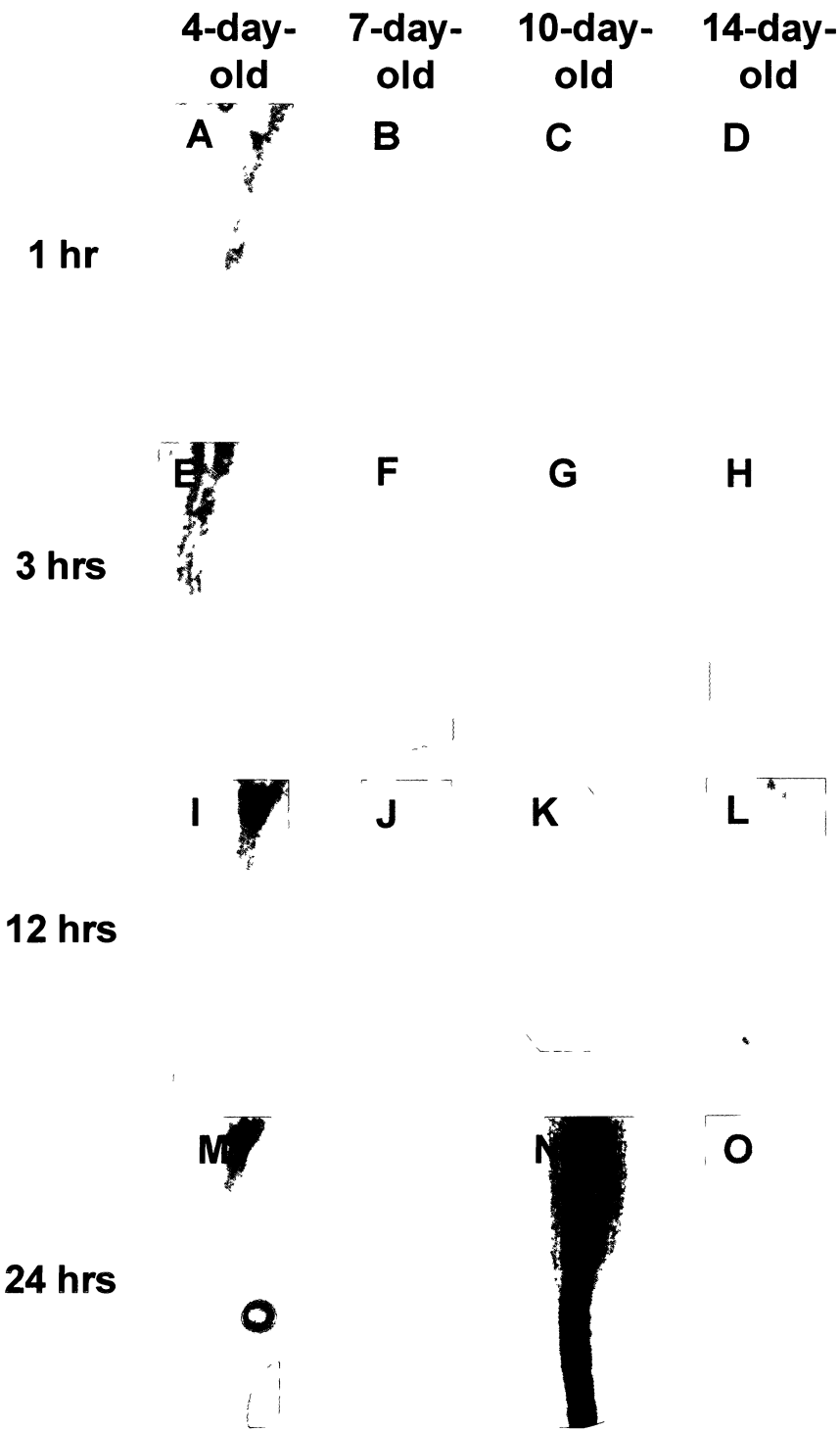

Figure 33. ***C4*** **gene expression in the hypocotyl of older seedlings.**
All samples are from the *AC4::C4:GUS-2* line with the exception of *AC4::C4:GUS-8* in **N)**. Samples were incubated in the GUS substrate for the times indicated.

incubation (Figure 33B and F). However after 12 hours, expression was detected in the upper part of the hypocotyl as well as throughout the vascular bundle (Figure 33J). Hypocotyls incubated for 24 hours were not photographed.

Ten-day-old seedlings, similar to 4- and 7-day-old plants, did not show expression after 1 and 3 hours of incubation (Figure 33C and G). After 12 hours, there was expression along the entire length of the hypocotyl vascular bundle but the level of expression varied, giving a blotchy appearance (Figure 33K). In addition, the regions of highest expression differed between plants and did not follow a consistent pattern. After 24 hours of incubation, the entire hypocotyl showed *C4* gene expression except for the hypocotyl base where less expression was observed in the outer layers of the hypocotyl (Figure 33N).

In 14-day-old plants, no expression was observed in the hypocotyl after 1 hour of incubation (Figure 33D), however weak expression was observed in the vascular bundle at the base of the hypocotyl after 3 hours of incubation (Figure 33H). After 12 hours of incubation, the expression was limited to the vascular bundle at the base of the hypocotyl (Figure 33L) and even at 24 hours only the vascular bundle and tissues surrounding the vascular bundle at the base were showing *C4* gene expression (Figure 33O). Therefore, the *C4* gene expression pattern in the hypocotyl changes depending upon the developmental stage. In the transition zone, located at the top of the hypocotyl near the cotyledons, the vascular patterning changes from one central vascular bundle to 5-8 vascular bundles separated by interfascicular fibers surrounding a pith (Zhong et al., 1999). Each of the vascular bundles are bilayered with the xylem located on the inside and the phloem on the outside. This vascular pattern continues throughout the highly

compact stem that bears the rosette leaves and into the inflorescence stem.

The inflorescence stems from flowering soil-grown plants (~6 weeks old) were analyzed for *C4* gene expression. Because of their length, stems were dissected into smaller sections prior to undergoing the GUS assay. No *C4* gene expression was detected in the stem after incubating the sample in the GUS substrate for 3 hours (Figure 34A and D). However, after 12 or 24 hours of incubation, *C4* gene expression was routinely seen at the cut end of the inflorescence stem or in parts of the stem that had been bent or damaged, especially in the vascular bundles (Figure 34B, C, E and F). These results indicate that either the *C4* gene is induced by wounding or that the GUS substrate was not able to easily penetrate the cuticular wax covering the stem tissue unless the stem was damaged in some way (Samuels et al., 2008). *C4* gene expression was also detected in the tissues surrounding the stem vascular bundles after 24 hours of incubation. Similar to the mature zone of roots, *C4* expression in inflorescence stems is highest in the vasculature.

II.B.5. *C4* gene expression in cotyledons and leaves

For most terrestrial vascular plants, leaves function as the major photosynthetic organ and transpiration site. Arabidopsis undergoes a well-defined progression of shoot developmental stages (Boyes et al., 2001). After the hypocotyl, the cotyledons are the second shoot structures to appear during germination. During embryogenesis, two cotyledons, also called seed leaves, are formed. After germination, the cotyledon's vascular system differentiates as the cotyledon expands in size due to increases in cell number and cell volume (Mansfield and Briarty, 1996). Mature cotyledons are petiolate,

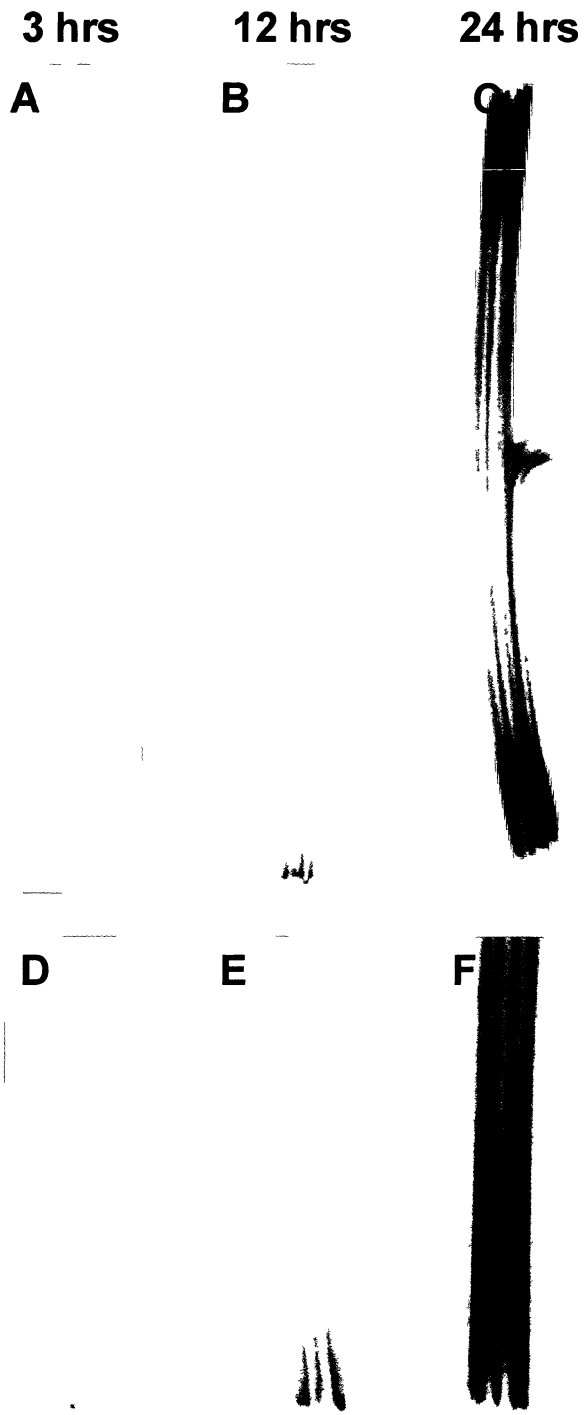

Figure 34. *C4* gene expression in the stem.
A portion of the stem including the cut site is shown in **A-C**). **D-F**) Higher magnification of cut ends of samples show *C4* gene expression in the vascular bundles. All sample are *CC4::C4:GUS-4* except **A)** *AC4::C4:GUS-4* and **C)** *CC4::C4:GUS-1*. Samples were incubated in the GUS substrate for the time indicated.

simple, entire and rounded.

In Arabidopsis, the dome-shaped shoot apical meristem is located between the cotyledons and differentiates to form leaves and eventually inflorescence structures during the course of plant development. Leaf morphogenesis stages are leaf primordia initiation, leaf adaxial and abaxial determination, tissue type differentiation, and leaf expansion (Cho et al., 2007). The basal leaves form a tight rosette due to the minimal spacing between the leaf internodes. In Arabidopsis ecotype Columbia, there are typically 10-15 rosette leaves formed when plants are grown under the long-day conditions used in these experiments (Boyes et al., 2001; Massonnet et al., 2010). Arabidopsis leaves undergo heteroblastic development in which subtle age-dependent changes in morphology are detectable between juvenile and adult leaves (Röbbelen, 1957; Medford et al., 1992). In general, rosette leaves are petiolate, simple, and entire (Al-Shehbaz and O'Kane, 2009) but the juvenile leaves have a smooth margin and are more round compared to the adult leaves which have partially serrulate to dentate margins and are more elliptic in shape (Medford et al., 1992). The transition from juvenile to adult leaves also includes changes in leaf phyllotaxy from opposite to spiral. Leaf hair or trichome distribution also changes in a heterochronic manner with juvenile leaves lacking trichomes on the abaxial side and adult leaves possessing trichomes on both the adaxial and abaxial sides (Telfer et al., 1997). After leaves are initiated from the shoot apical meristem, leaves expand from the tip to the base which results in a maturation gradient in expanding leaves with the most mature cells at the leaf apex (Donnelly et al., 1999).

Following the transition to flowering, cauline leaves subtend the lateral floral

buds on the inflorescence stem. Cauline leaves have a different morphology than the rosette leaves because they are apetiolate, more lanceolate to linear in shape, and rarely form dentate margins (Al-Shehbaz and O'Kane, 2009). In addition, cauline leaf morphology changes depending upon when in the plant's life cycle the cauline leaf was initiated (Meyerowitz and Somerville, 1994). The first cauline leaves are larger and broader than cauline leaves formed near the end of the plant's life cycle. Trichomes are present on both the abaxial and adaxial surfaces of cauline leaves, but trichome abundance on the adaxial surface decreases on cauline leaves formed further away from the rosette (Telfer et al., 1997).

Cross sections of cotyledonary and foliar tissues reveal various cell layers including the upper and lower epidermis, mesophyll (multi-layered spongy and single-layered palisade), and vascular bundles located within the spongy mesophyll (Pyke et al., 1991). The air space between the spongy mesophyll cells represents approximately 26% of the leaf volume. Each vascular bundle, with the xylem located on the adaxial side and the phloem on the abaxial side, is surrounded by a parenchyma layer called the bundle sheath (Kinsman and Pyke, 1998). Leaves and cotyledons have a reticulated vascular system that develops from the large primary vein or midvein. The cotyledon venation pattern consists of four areoles resulting from secondary veins splitting off the single primary vein (Sieburth, 1999). Leaves have a more complicated venation pattern in which the primary vein branches to form secondary branches, the secondary vein has tertiary branches, and tertiary veins branch to form quaternary veins (Hickey, 1973). Each successive branch is smaller in diameter than the previous branch.

II.B.5.a. *C4* gene expression in cotyledons

C4 gene expression in cotyledons was observed over a time course from 1 day to 4 weeks (Figure 35). In 1-day-old plants, vascular differentiation is underway and expression in the differentiating vascular cells could be observed when the seed coat was not present (Figure 35A). In general, expression in the 1-day-old cotyledon was in a diffuse pattern. In mature cotyledons, from 4-days to 4-weeks of age, expression was readily apparent in the vascular system and in the hydathode region (Figure 35B-F). Hydathodes, located at leaf margins, are modified pores which allow for release of excess water in a process called guttation (Evert and Esau, 2006). Low levels of expression were visible in other cell types like the mesophyll and epidermis upon longer incubation with the GUS substrate (Figure 35D and 36D and H). The petioles of cotyledons also exhibited expression in the vascular structures and to a lesser extent, in the mesophyll cells (Figure 37D). Similar to the stem and mature root, the highest levels of *C4* expression in the cotyledons were in the vascular system which was visible after 3 hours of incubation in the GUS substrate (Figure 36). In conclusion, *C4* gene expression was detected throughout the cotyledon with the strongest expression in the veins.

II.B.5.b. *C4* gene expression in rosette and cauline leaves

Compared to root tissues, relatively weaker *C4* gene expression was detected in leaves. *C4* gene expression in leaves at any developmental stage was not detectable or was extremely weak after 1 and 3 hours of incubation with the GUS substrate (Figure 38A-B; 39A and D). Only after 12 and 24 hours was expression easily observable in the leaves (Figure 38C and D; 39B-C, E-F), indicating that the *C4* gene is expressed at a

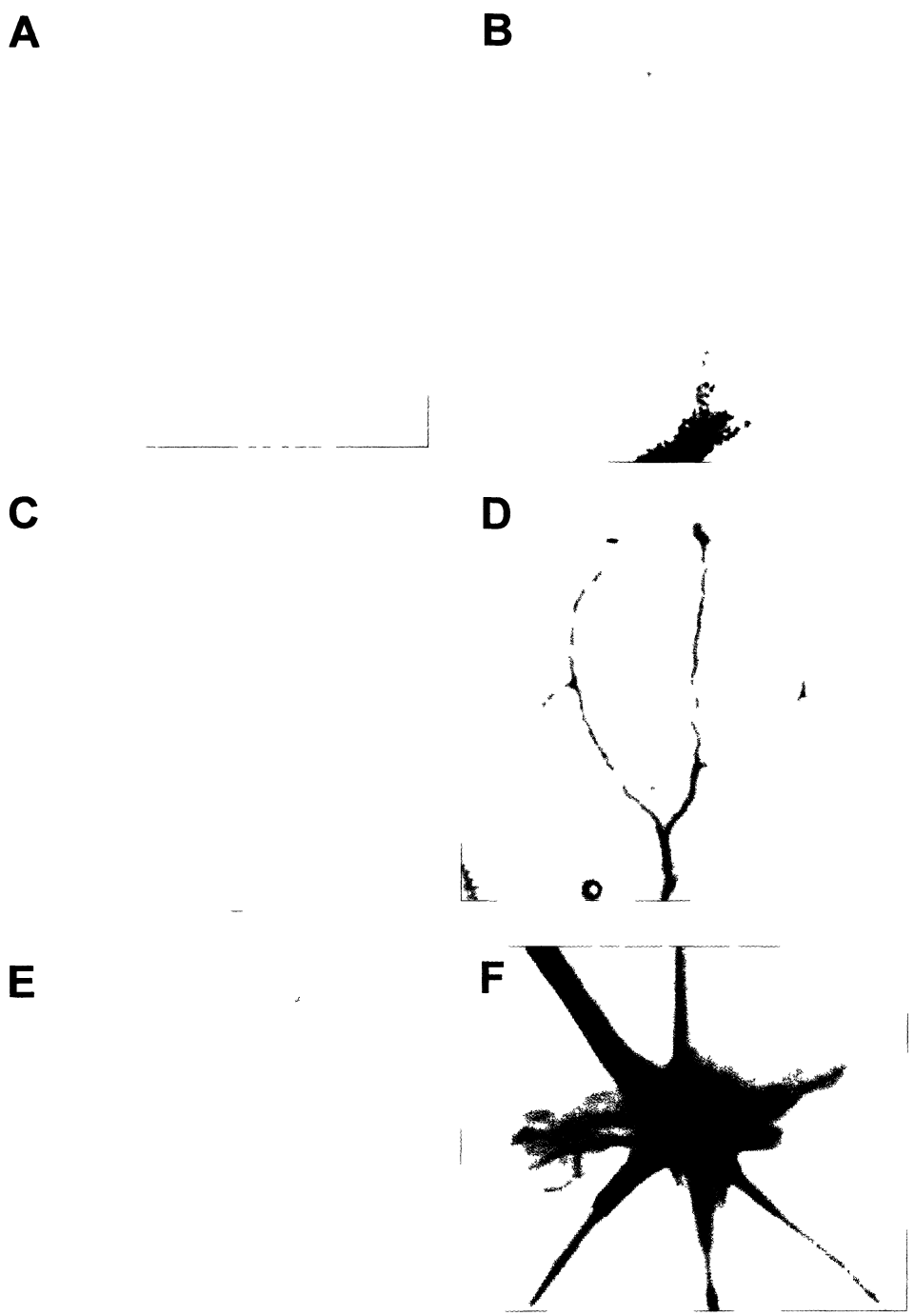

Figure 35. *C4* gene expression in cotyledons during development.
A) 1-day-old (*AC4::C4:GUS-2*); **B)** 4-day-old (*AC4::C4:GUS-2*); **C)** 7-day-old (*CC4::C4:GUS-1*); **D)** 10-day-old (*BC4::C4:GUS-2*); **E)**14-day-old (*CC4::C4:GUS-1*); **F)** 4-week-old (*AC4::C4:GUS-7*). Samples were incubated in the GUS substrate for **A)** 24 hours; **B)** 12 hours; **C)** 14 hours; **D)** 12 hours; **E)** 24 hours; **F)** 12 hours.

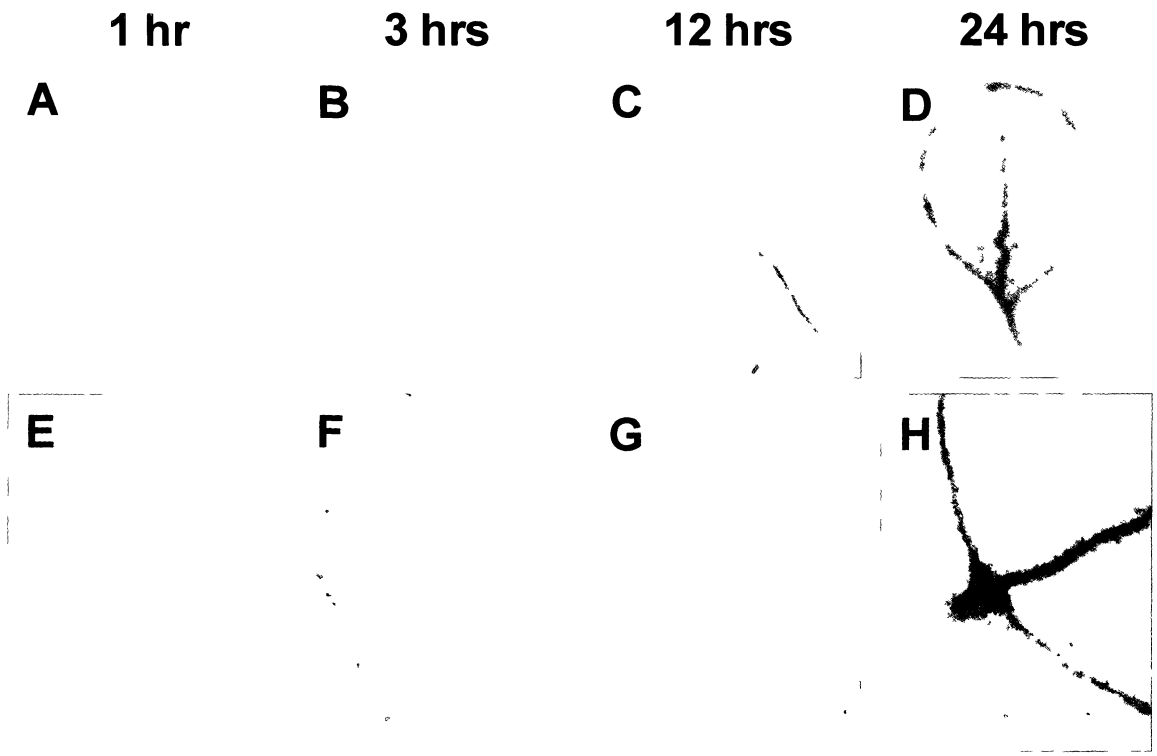

Figure 36. *C4* gene expression in cotyledons assayed for different periods of time. **A)** 14-day-old; **B)** 10-day-old; **C)** 10-day-old; **D)** 4-day-old; **E)** 10-day-old; **F)** 14-day-old; **G)** 14-day-old; **H)** 10-day-old. Samples were incubated in the GUS substrate as indicated above. All samples were from *AC4::C4:GUS-2* plants except **B)** *CC4::C4:GUS-2*.

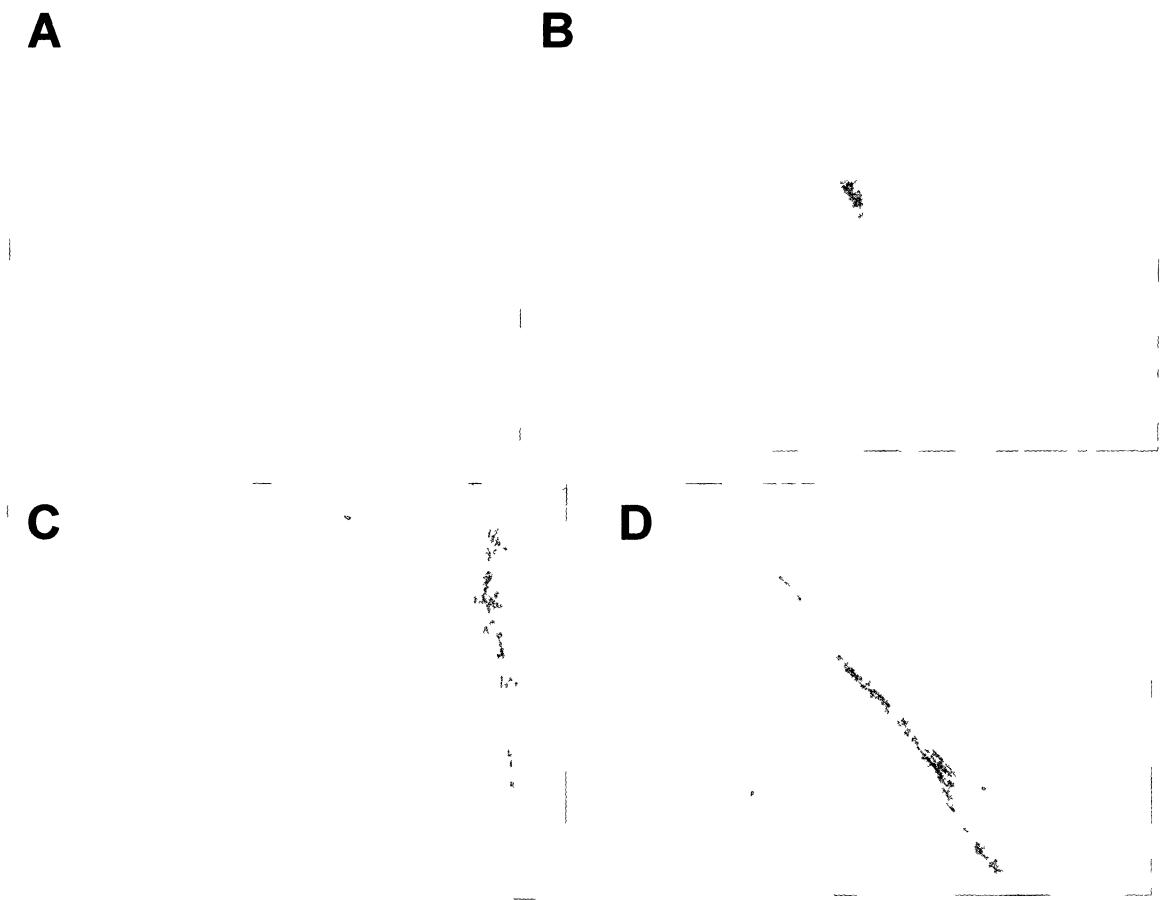

Figure 37. Expression pattern of *C4* gene in cotyledons.
A) entire cotyledon of *CC4::C4:GUS-1*, 7-day-old; **B)** apical terminus and hydathode of cotyledon of *BC4::C4:GUS-2,* 10-day-old; **C)** margin near the petiole of *AC4::C4:GUS-2*, 10-day-old; **D)** petiole of *BC4::C4:GUS-2*, 10-day-old. Samples were incubated in the GUS substrate for **A)** 14 hours; **B-D)** 12 hours.

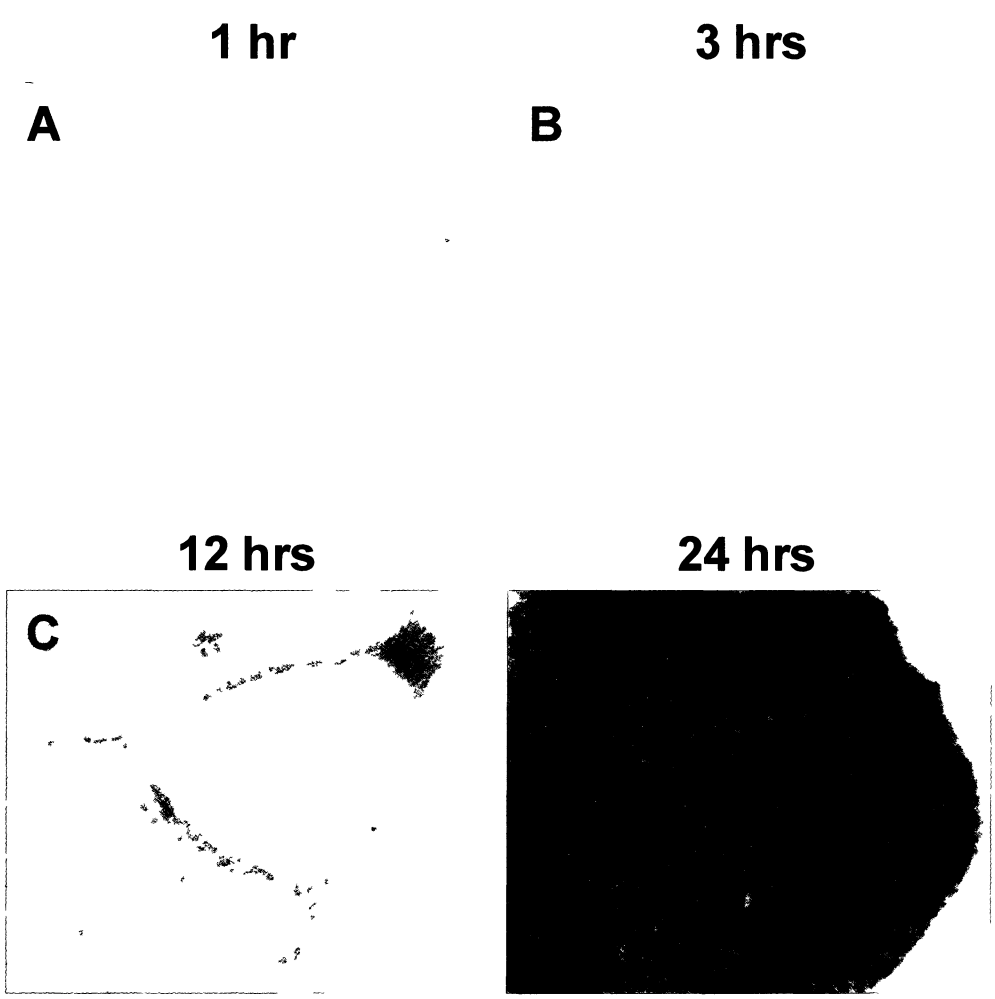

Figure 38. First true leaves assayed for different periods of time.
A) *BC4::C4:GUS-2*, 10-day-old; **B)** *CC4::C4:GUS-1*, 14-day-old; **C)** *BC4::C4:GUS-2*, 10-day-old; **D)** *AC4::C4::GUS-8*, 10-day-old. Samples were incubated in the GUS substrate for the times indicated.

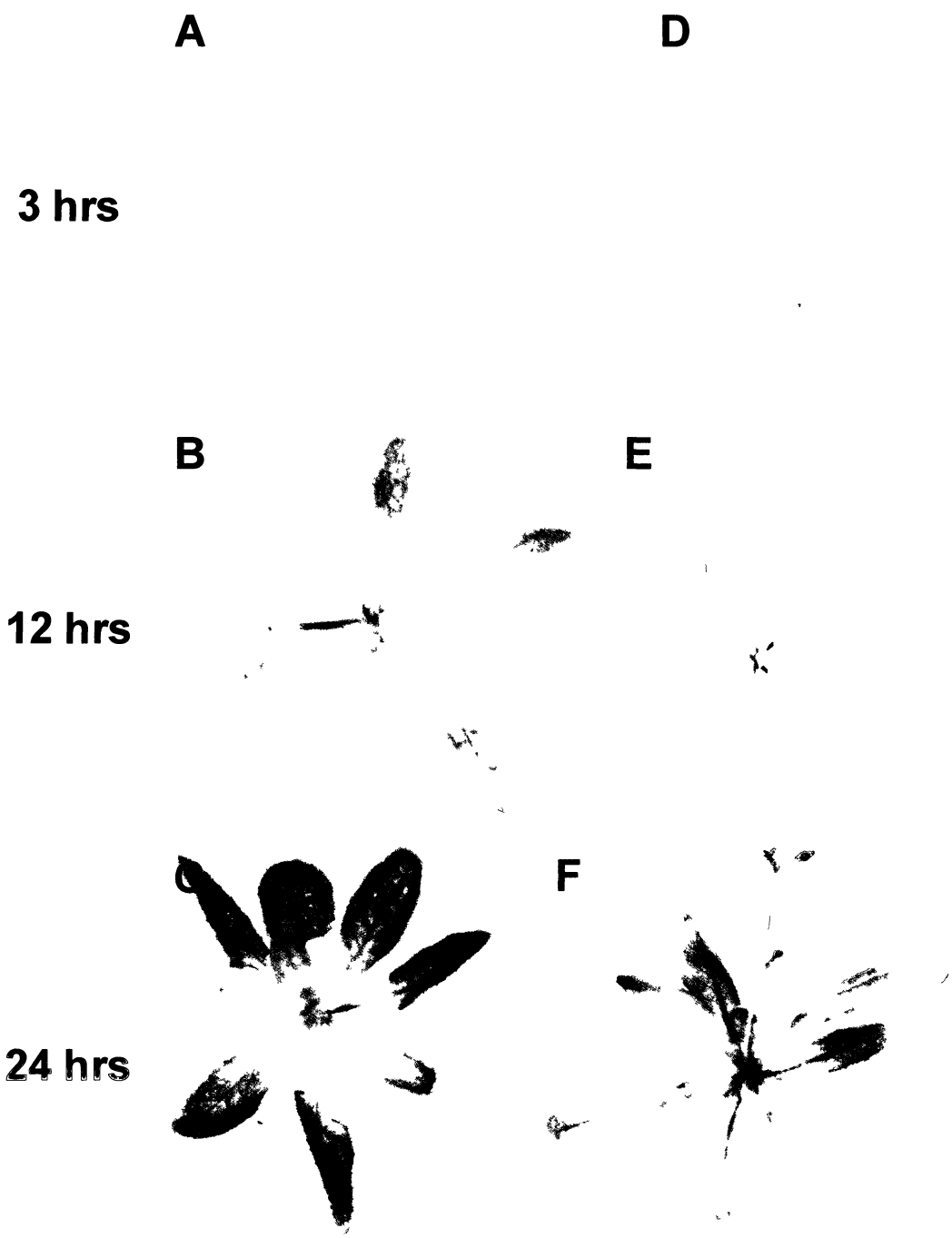

Figure 39. *C4* gene expression in leaves of 4-week-old plants.
A), **B)**, and **C)** are *AC4::C4:GUS-5*. **D)**, **E)**, and **F)** are *AC4::C4:GUS-7*. Samples were incubated in the GUS substrate for the times indicated.

lower level in leaves than roots.

C4 gene expression was detected in developing, differentiating, and mature leaves. An example of *C4* gene expression in a developmental series following the development of the first and second leaves is shown in Figure 40 A-D. The expression pattern observed in the first and second leaf can be extrapolated to other leaves because all rosette leaves develop similarly. Developing leaves, exemplified by leaf 1 and 2 of 4-day-old seedlings, showed constant expression throughout the leaf no matter the tissue type (Figure 40A). As the leaf develops, expression was seen throughout the differentiating and mature leaves with the highest expression seen in the veins and hydathode regions (Figure 40B-F). An overview of *C4* gene expression in rosette leaves can be seen in the 4-week-old plants which show most of the leaves that have already expanded or are almost expanded (Figure 40E-F). Some leaves assayed for 12 and 24 hours showed no expression which was likely due to incomplete infiltration of the GUS substrate into those tissues (Figure 39 and 40). Similar to the cotyledons, the *C4* gene expression pattern in leaves was most evident in the vascular bundle and hydathodes but still present at lower levels throughout the leaf.

Cauline leaves also showed expression in the reticulate vascular system and hydathode, and to a much lesser extent, in the interveinal regions (Figure 41). In general *C4* gene expression was less strong in the cauline leaves; expression was not detected at 3 hours of incubation with the GUS substrate and was weak after 12 hours but was easily detected after 24 hours (Figure 42). Therefore, the sites of expression in cotyledons and rosette and cauline leaves were alike.

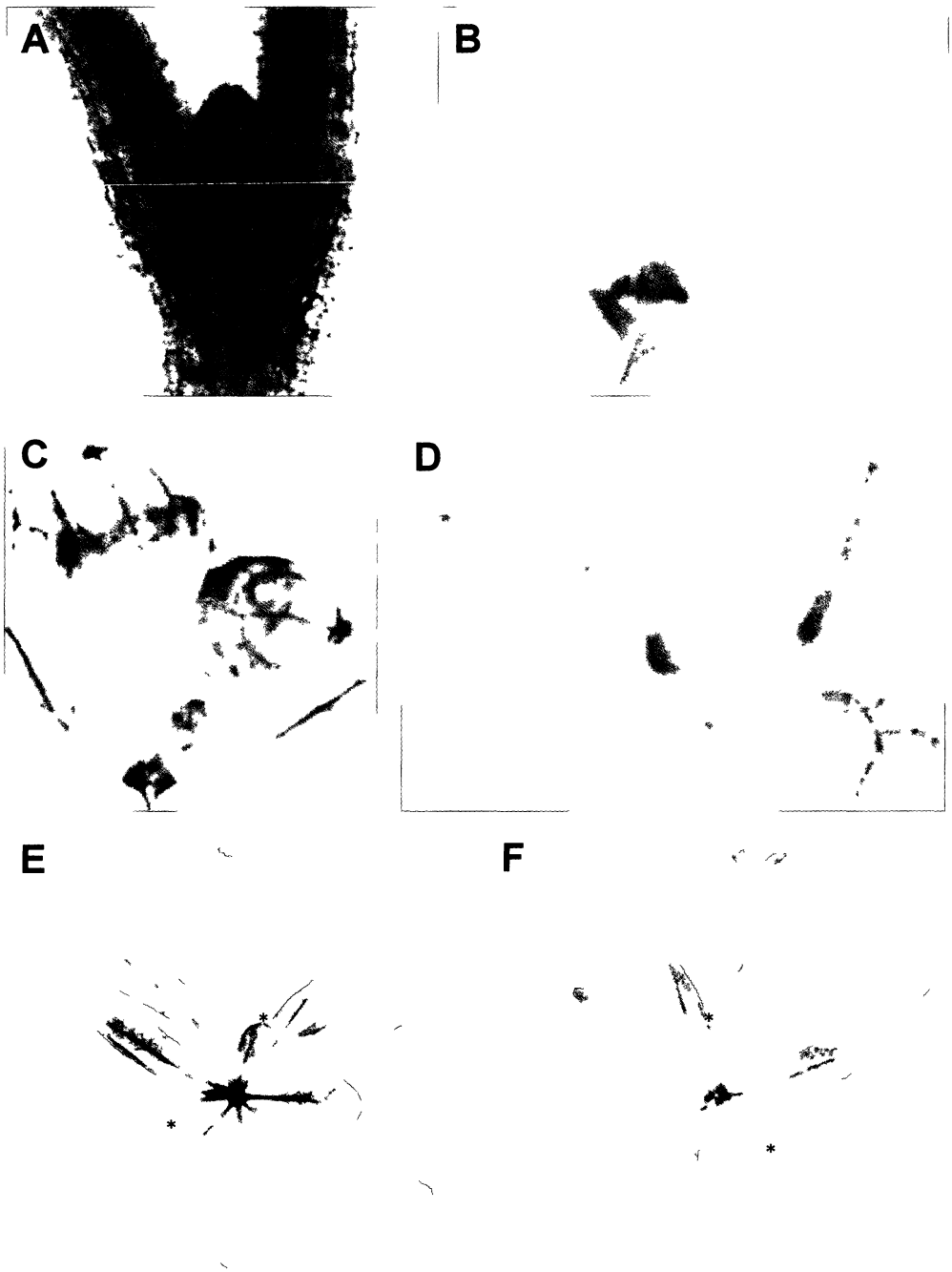

Figure 40. *C4* gene expression during leaf development.
A) Developing first and second leaf with developing trichome at leaf tip from 4-day-old plants. **B)** Primary vein and hydathode regions are detectable in 7-day-old plants. **C)** and **D)** Further development of the leaf and veins in 10- and 14-day-old plants. **E)** and **F)** top and bottom view of the same 4-week-old plant with partially and fully expanded leaves. Asterisk indicates first and second leaf of 4-week-old plants. **A)**, **B)**, **C)**, and **D)** are *AC4::C4:GUS-2*. **E)** and **F)** are *AC4::C4:GUS-7*. Samples were incubated in the GUS substrate for **A)** 12 hours; **B)** 14 hours; **C)** 12 hours; **D)** 24 hours; **E)** and **F)** 24 hours.

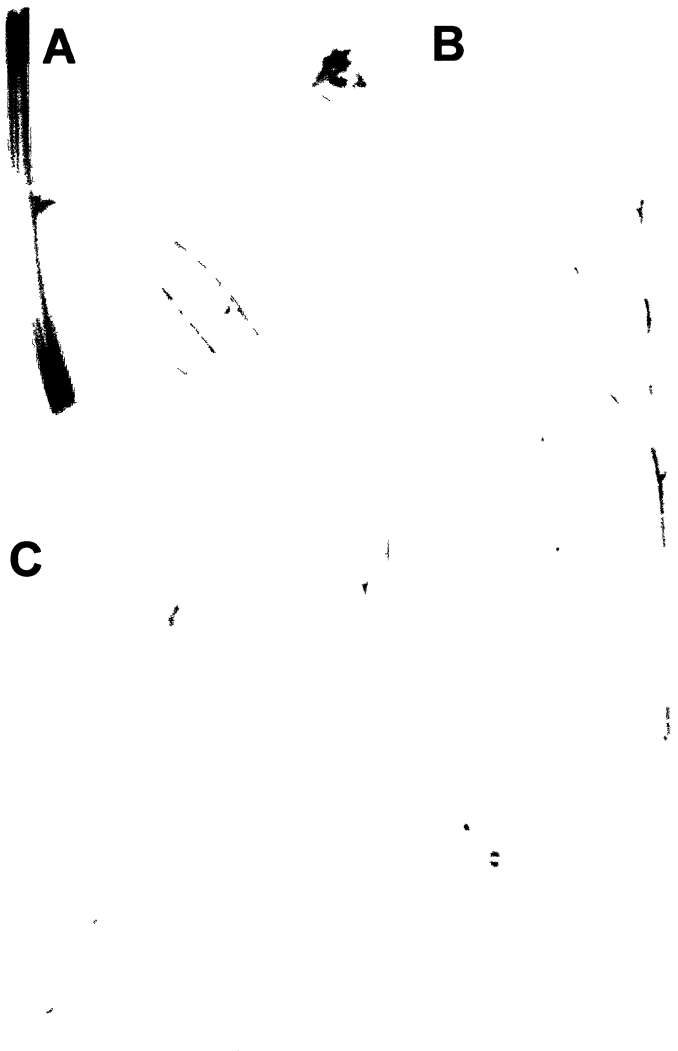

Figure 41. Expression pattern of the *C4* gene in cauline leaves.
A) Infloresence stem and entire cauline leaves including a secondary bolt (*CC4::C4:GUS-1*); **B)** entire cauline leaf (*AC4::C4:GUS-4*); **C)** leaf margin showing the veins, hydathode and trichomes (*CC4::C4:GUS-1*). All samples were incubated in the GUS substrate for 24 hours.

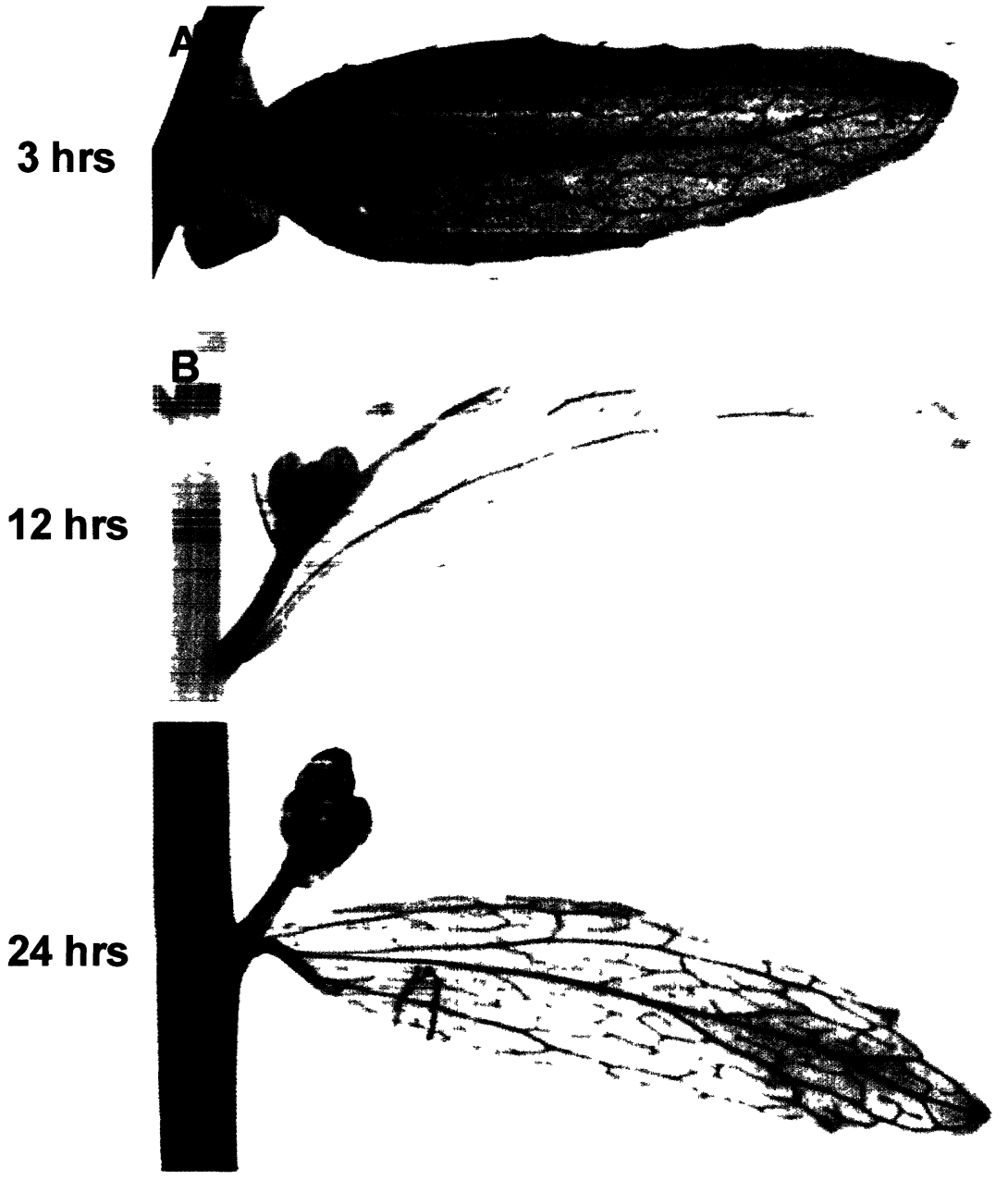

Figure 42. *C4* gene expression in cauline leaves.
A) *CC4::C4:GUS-5*; **B)** *AC4::C4:GUS-7*; **C)** *AC4::C4:GUS-8*. Samples were incubated in the GUS substrate for the times indicated.

II.B.5.c. *C4* gene expression in trichomes

Arabidopsis trichomes, or leaf hairs, are located on leaves (both rosette and cauline), inflorescence stems, and sepals (Bowman, 1994; Marks, 1997). Trichome morphology depends upon location; stems and sepals have predominantly unbranched trichomes while stellate trichomes are present on leaves. Trichomes are initiated from pluripotent epidermal cells (Morohashi and Grotewold, 2009) as a small outgrowth followed by further outward expansion (Marks, 1997). Stellate trichomes branch before reaching their final, fully expanded size. Once expanded, the cell walls thicken and form papillae on their surface. Mature trichomes are approximately 200-300 μm in length and have supporting epidermal cells surrounding the base of the trichome.

Developing leaf trichomes exhibited strong *C4* expression (Figure 43A-B), while fully-expanded trichomes had little expression (Figure 43C-D). Weak expression was also seen in mature inflorescence stem trichomes (Figure 43E). Sepal trichomes were not examined in this study. In conclusion, *C4* gene expression was seen in developing trichomes but not observed in fully expanded trichomes.

II.B.5.d. *C4* gene expression in guard cells

Gas exchange is a critical function of plants and is facilitated through pores in the epidermis called stomata (Nilson and Assmann, 2007). Stomata are found on all shoot epidermal surfaces except for petals and stamens (Geisler et al., 1998). The abundance of stomata varies between organs and even within an organ as there are typically more stomata on the abaxial than adaxial side of flat organs such as cotyledons, leaves and sepals. A stomate is opened and closed by two kidney bean-shaped guard cells. Guard

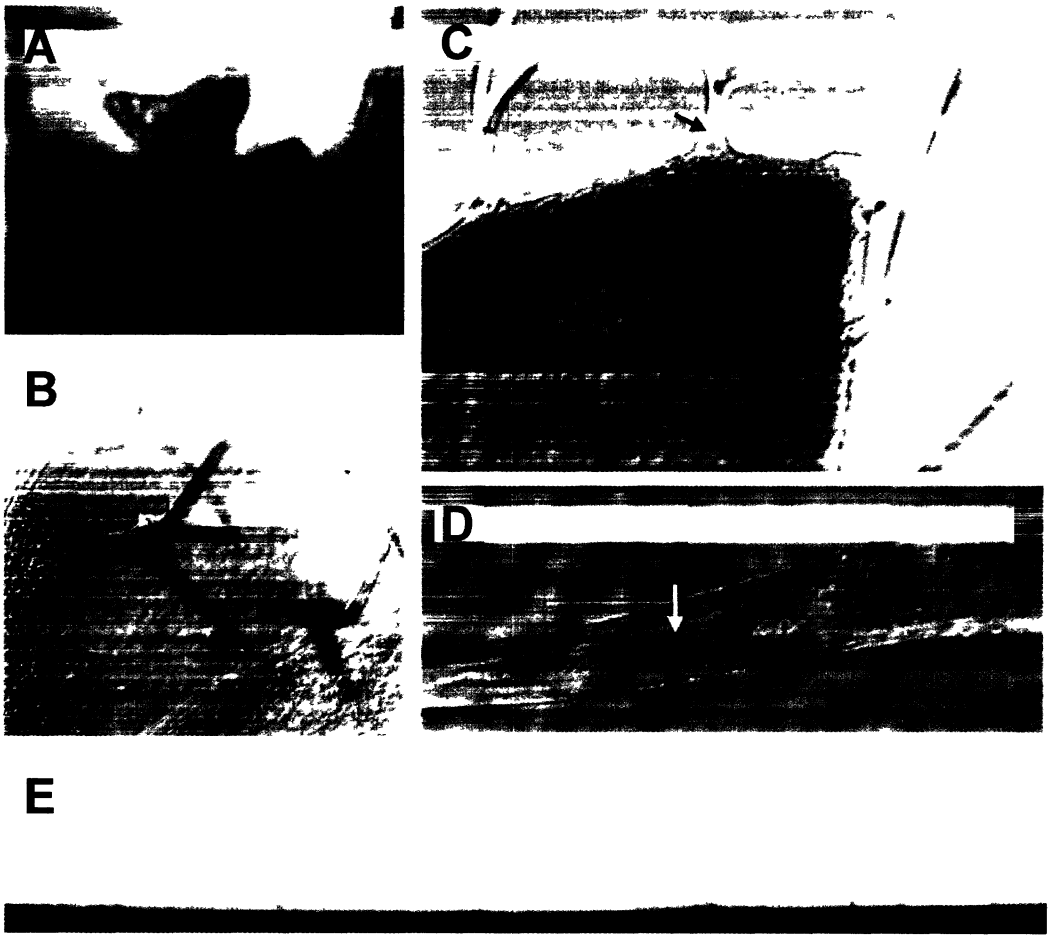

Figure 43. *C4* gene expression in trichomes.
A) and **B)** Developing leaf trichomes (*AC4::C4:GUS-2*); **C)** fully expanded leaf trichomes arrow indicates region of accumulating diX-indigo (*AC4::C4:GUS-2*); **D)** one branch of a trichome with accumulating diX-indigo indicated by the arrow; E) trichomes on inflorescence stem (*AC4::C4:GUS-4*). Samples were incubated in the GUS substrate for **A)** 24 hours; **B-D)** 12 hours; **E)** 24 hours.

cell development begins with an asymmetric division of a meristemoid mother cell to produce a triangular meristemoid as one of the daughter cells (Geisler et al., 1998; Nadeau and Sack, 2009). In the simplest scenario, the meristemoid cell can develop into an oval guard mother cell which divides symmetrically to form two immature guard cells. Another guard cell developmental pathway is when the meristemoid divides multiple times before differentiating into immature guard cells. Immature guard cells eventually differentiate into mature guard cells by thickening of their cell walls.

Leaf guard cells exhibited no detectable *C4* expression after 1 hour of incubation in X-gluc (Figure 44A), but by 3 hours weak accumulation of diX-indigo was detected (Figure 44B). By 12 and 24 hours, expression in guard cells was easily detected but was sometimes obscured by strong *C4* gene expression in the epidermis or the underlying mesophyll (Figure 44C-D). *C4* gene expression was frequently detected in the meristemoids, guard mother cells, and immature guard cells (Figure 45). Not all mature guard cells expressed the *C4* gene at the same level perhaps because different guard cells on the same leaf are at different developmental points. Similar to trichomes, *C4* gene expression was detected at higher levels during the development of guard cells from their precursor cells and appeared to be lower in mature guard cells on expanded leaves.

II.B.5.e. *C4* gene expression in stipules

Stipules are formed in the axil of true and cauline leaves but not in the axils of cotyledons (Chandler, 2008). *C4* gene expression was observed in stipules of rosette leaves of 7-, 10-, and 14-day-old plants (Figure 46A-C). In flowering plants, stipules at the base of cauline leaves also expressed the *C4* gene (Figure 46D). Therefore, the *C4*

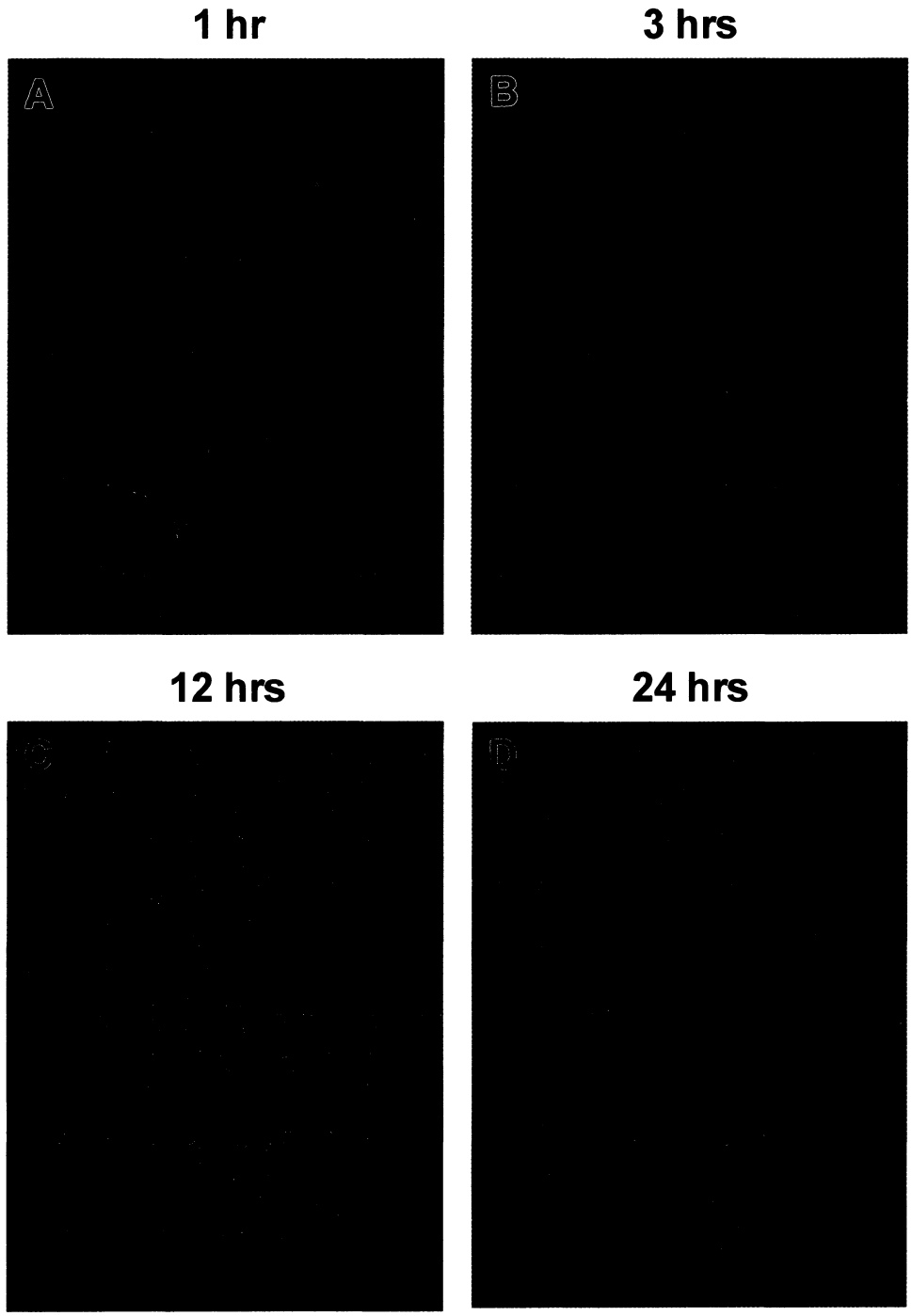

Figure 44. *C4* gene expression in guard cells.
A) *AC4::C4:GUS-2*, 10-day-old; **B)** *CC4::C4:GUS-2*, 14-day-old; **C)** *AC4::C4:GUS-2*, 10-day-old; **D)** *AC4::C4:GUS-8*, 10-day-old. Samples were incubated in the GUS substrate for times indicated.

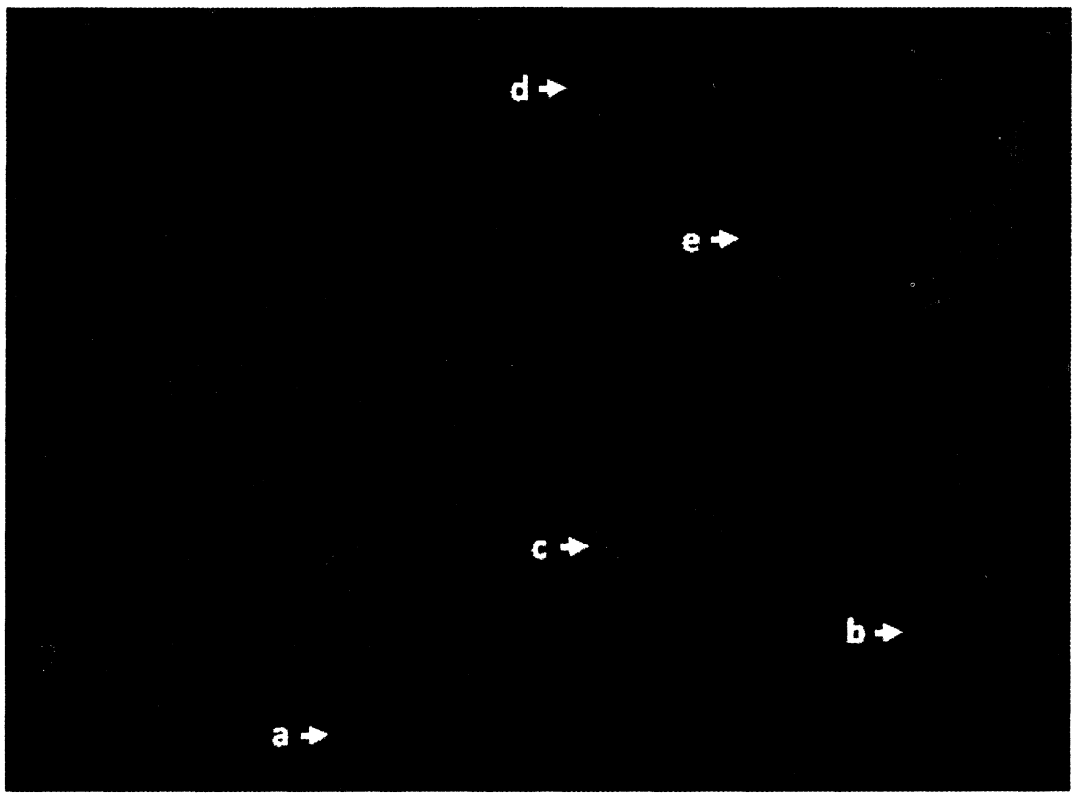

Figure 45. *C4* gene expression during guard cell development.
a) Meristemoids; **b)** guard mother cells; **c)** young immature guard cells; **d)** older immature guard cell; and **e)** mature guard cell. Sample was taken from a 10-day-old *AC4::C4:GUS-2* plant that was assayed for 12 hours.

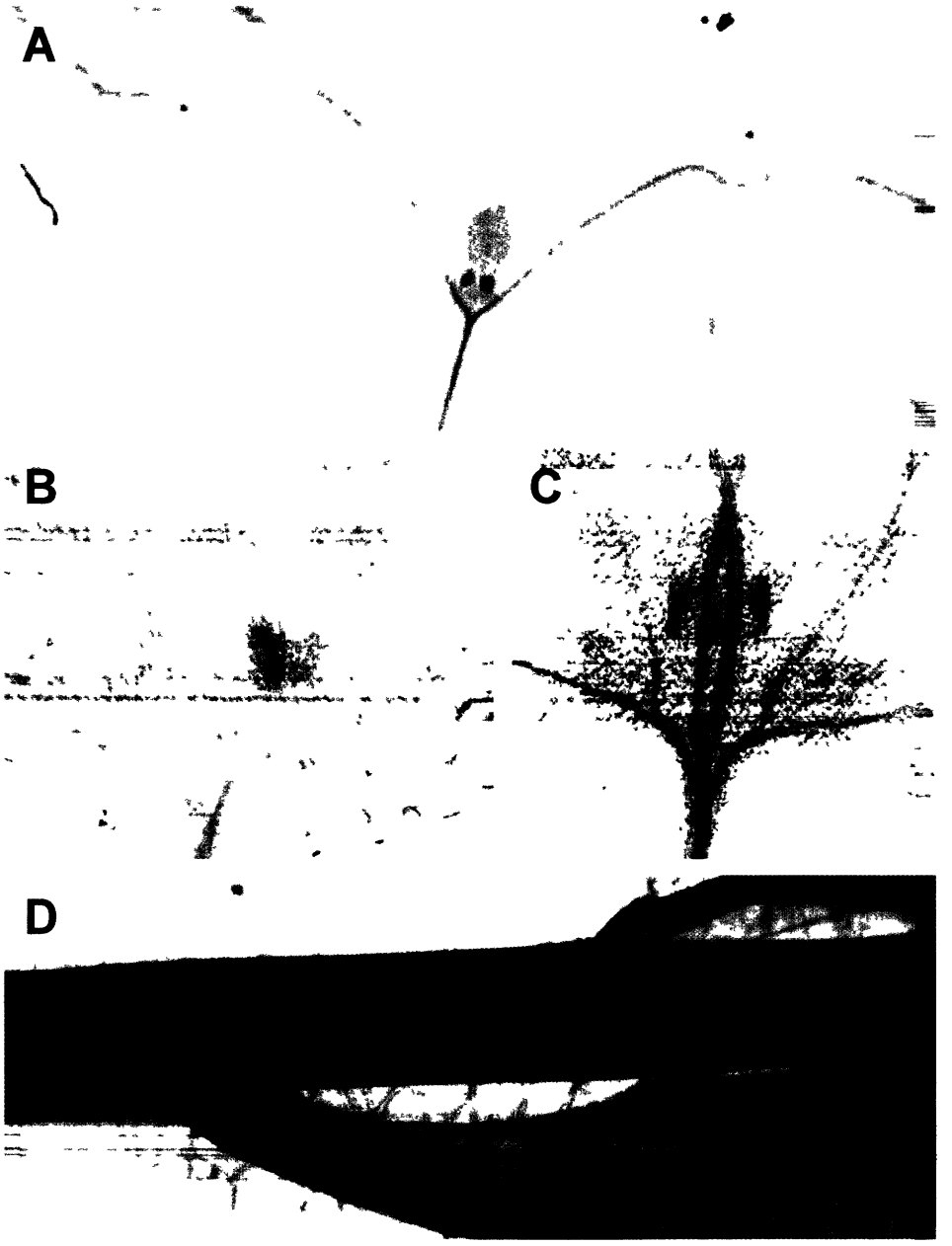

Figure 46. *C4* expression in stipules.
A) *CC4::C4:GUS-2*, 7-day-old; **B)** *AC4::C4:GUS-2*, 10-day-old; **C)** *AC4::C4:GUS-2*, 14-day-old; **D)** *CC4::C4:GUS-5*, flower stalk of mature plants. Samples were incubated in the GUS substrate for **A)** 3 hours; **B)** 12 hours; **C)** 3 hours; **D)** 24 hours.

gene was expressed in stipules no matter the developmental age of the plant or where the stipules were located.

II.B.6. *C4* gene expression in floral organs

After vegetative growth, the shoot apical meristem transitions into reproductive growth. The floral structure produced by Arabidopsis is a raceme that matures from the base to the apex; thus it is possible to observe flowers and siliques at different developmental stages on the same plant or even on the same inflorescence stem. The primary inflorescence stem usually branches to form secondary and tertiary offshoots. Arabidopsis, as is typical of most Brassicaceae, produces four-whorled flowers each supported on a separate pedicel. Flowers consist of a calyx made of four sepals, a corolla of four petals, six stamens which are tetradynamous (two short and four long), and a syncarpous gynoecium with two carpels. Each carpel consists of a central locule containing the ovules surrounded by an outer valve wall and separated from the other carpel by a septum. The septum spans the distance between the two replums located on opposite sides of the carpel (Al-Shehbaz and O'Kane, 2009; Roeder and Yanofsky, 2009). Both the valve and the replums contain vascular bundles. In sepals, the vascular system is different than the leaves because there is no midvein (Turner and Sieburth, 2009). Petals do have a midvein with secondary veins forming two areoles. The Arabidopsis fruit or silique can contain approximately 60-70 seeds depending upon the growth conditions of the plant (Meyerowitz and Somerville, 1994). Flower and silique stages were classified as stages 1-20 based on organ development (Table 5; Smyth et al., 1990; Roeder and Yanofsky, 2009).

Table 5. Floral and silique developmental stages.*

Stage	Description
1	Flower primordium (floral buttress) arises from flank of inflorescence meristem.
2	Flower primordium forms.
3	Sepal primordia arise and partially cover floral meristem.
4	Sepals overtie flower meristem. Flower meristem expands to form platform on which the gynoecium will develop.
5	Petal and stamen promordia arise.
6	Sepals enclose bud. Gynoecium begins to form.
7	Long stamen promordia stalked at base. Gynoecium forms a hollow tube.
8	Locules appear in long stamens.
9	Petal primordia stalked at base.
10	Petals level with four short stamens.
11	Stigmatic papillae appear.
12	Petals level with two long stamens. Gynoecium tissues become distinct.
13	Bud opens. Petals visible. Anthesis.
14	Long anthers extend above stigma. Fertilization occurs.
15	Stigma extends above long anthers.
16	Sepals, petals and stamens wither and fall.
17a	Fruit elongates in length and width until mature size.
17b	Fruit elongated completely.
18	Siliques turn yellow from apex to base.
19	Silique turns brown. Valves separate in dry siliques.
20	Seeds fall and leave dried replum and septum behind.

*modified from Smyth et al., 1990 and Roeder and Yanofsky 1996

All flowers, whether located on the primary inflorescence stem or on the offshoots, were found to have similar expression patterns when observed at the same developmental stage. Accurate identification of the different organs in flower bud stages earlier than stage 12 was not possible without dissection. The only structure that could be identified with confidence in these early flower buds was the carpel, which did show *C4* gene expression throughout (Figure 47A-C). The expression of *C4* gene in the carpel changed during development into a mature silique. In stage 12, expression was clearly seen in the entire carpel including the papillae. Stage 13 carpels exhibited expression near the apex and in the papillae while expression close to the pedicel was absent (Figure 47D). *C4* gene expression was only observed in the carpel region close to the pedicel but was absent or very weak in the papillae in stage 14 flowers (Figure 47C-D). In stage 15, *C4* gene expression was observed in both the apex and base of the carpel, but not in the papillae (Figure 48D). From stage 15 until full development of the silique (before stage 17b), expression was observed in the nectaries and surrounding tissue at the base of the carpel and the apex of the pedicel as well as the apical region of the silique (Figure 47A-C). Closer examination of siliques in stage 17a showed expression in the vascular system in the valve wall, the replum, and the funiculi which connect the ovule to the replum (Figure 48D-F). *C4* gene expression was also observed in structures which were either unfertilized ovules or embryos that arrested their development and viable embryos (Figure 48G).

C4 gene expression in the stamens changed during its development observed in stage 12 to 15. At stage 12, no expression was observed in the anther or filament of the stamen (Figure 47D). Filaments, but not anthers, of stage 13 stamens began to show

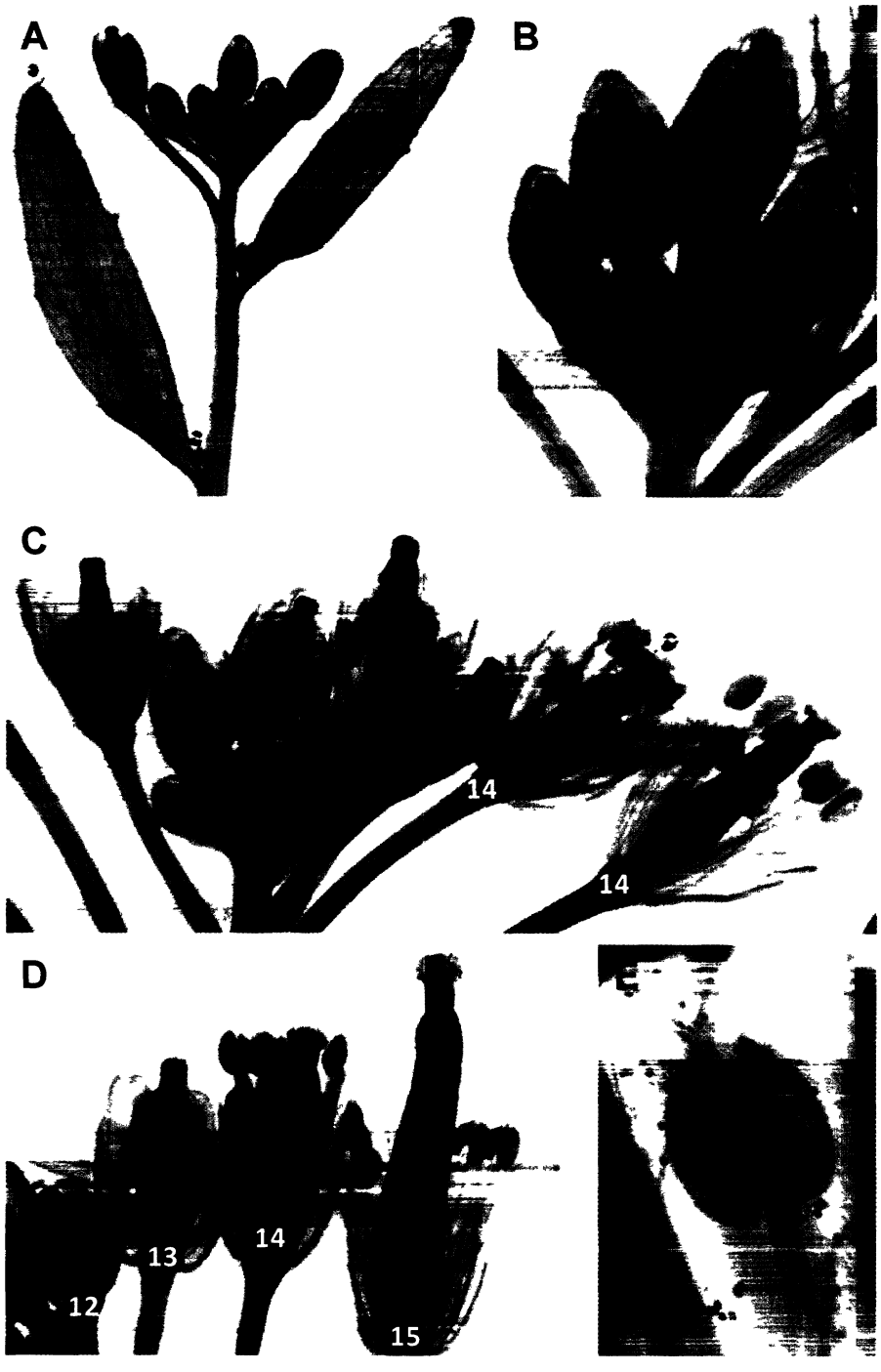

Figure 47. Expression pattern of the *C4* gene in flowers at different developmental stages.

A) Apical floral terminus of *CC4::C4:GUS-4*; **B)** floral apex of *CC4::C4:GUS-4*; **C)** *CC4::C4:GUS-4* and **D)** *AC4::C4:GUS-5*; **E)** dehiscent pollen of *AC4::C4:GUS-2*. All samples were incubated for 24 hours in the GUS substrate. Floral stages from Table 5 are indicated in **C)** and **D)**.

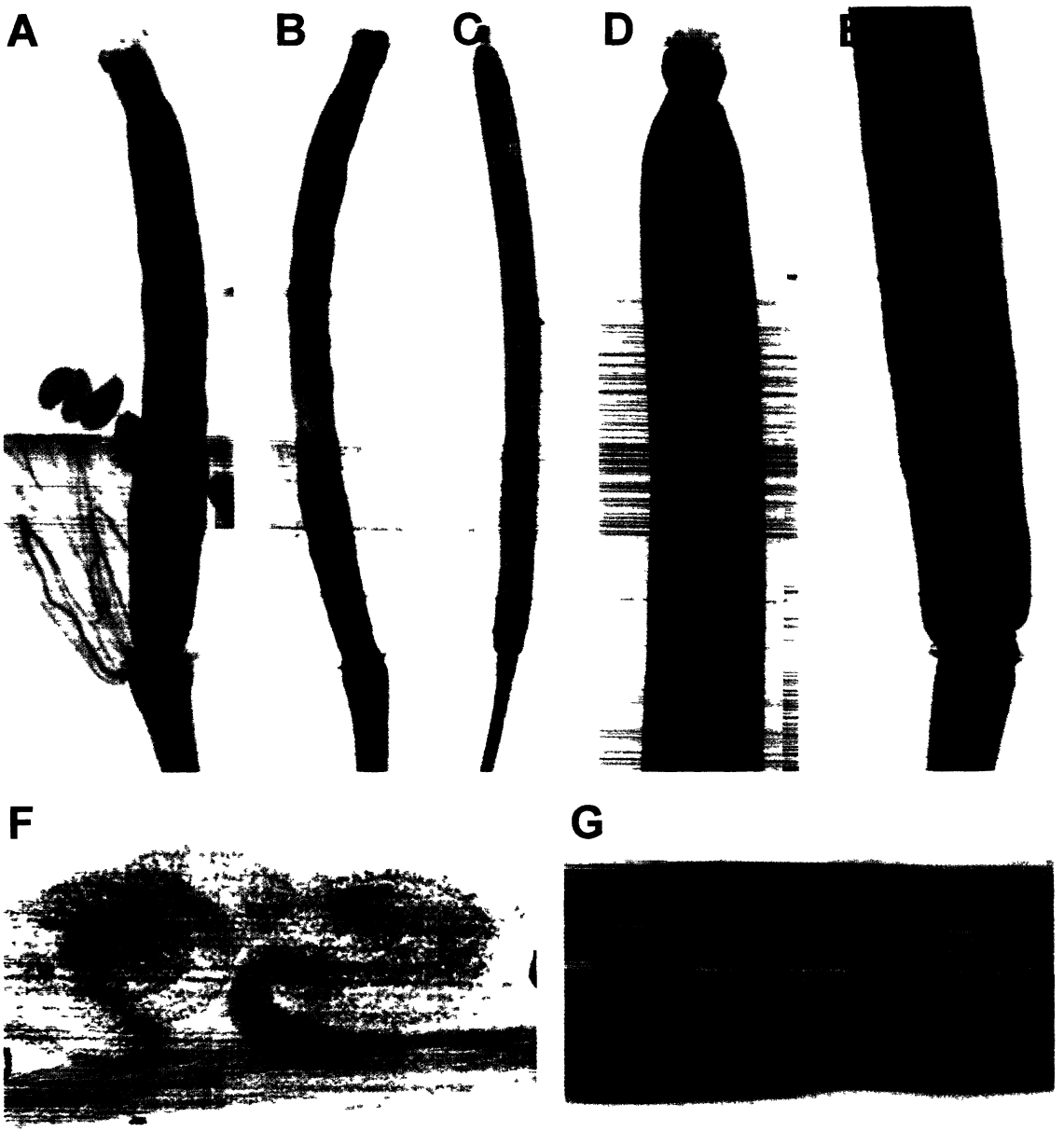

Figure 48. *C4* gene expression pattern in siliques at different developmental stages. **A)** Stage 16 silique (*AC4.:C4:GUS-5*); **B)** stage 17a silique (*CC4::C4:GUS-4*); **C)** stage 17b silique (*CC4.:C4:GUS-4*); **D)** apical region of stage 17b silique (*CC4::C4.GUS-1*); **E)** basal region of stage 17b silique (*CC4::C4:GUS-1*); **F)** dissected veins and funiculus of stage 17b silique (*AC4::C4:GUS-7*); **G)** close up of stage 17a (*CC4::C4:GUS-2*). All samples were incubated for 24 hours in the GUS substrate.

expression in the vascular and surrounding tissues (Figure 47D). Both vascular and nonvascular tissue of the filament and the pollen showed *C4* expression in stage 14 (Figure 47E). By stage 15, weak *C4* gene expression was observed in the filament and by stage 16, the stamens has withered and abscised. Petals did not show *C4* gene expression at any stage of floral development. Sepals of stage 12 through 14 flowers showed *C4* gene expression but only in the vascular system of the sepals. However, by stage 15 the expression level in the vascular tissue of the sepal had decreased (Figure 47D).

Flowers in Figure 47-48 were assayed for 24 hours. To determine which flower tissue had the highest expression, samples were incubated in the GUS substrate for 3, 12, or 24 hours. One hour was not included because expression was not typically detected in other shoot tissues after 1 or 3 hours of incubation. After three hours of incubation in the GUS substrate, weak expression was observed in the pollen and filaments in stage 14 flowers (Figure 49A). Faint expression was observed after 3 hour assay in the nectary region starting at stage 15 and through stage 17b (Figure 49A and 50A-E). Aftert 12 and 24 hours GUS assay, *C4* gene expression was observed in the carpel, stamen, and sepal, as described in the previous paragraph (Figure 49B-C; 50F-O). As expected, the expression patterns were much easier to detect after a 24 hour assay. In conclusion, the tissue with the highest level of expression in the flowers and siliques was the nectary region and stage 14 pollen and filaments. *C4* gene expression was also detected in various stages of flower and silique development, but no detectable C4 gene expression was ever observed in the petals.

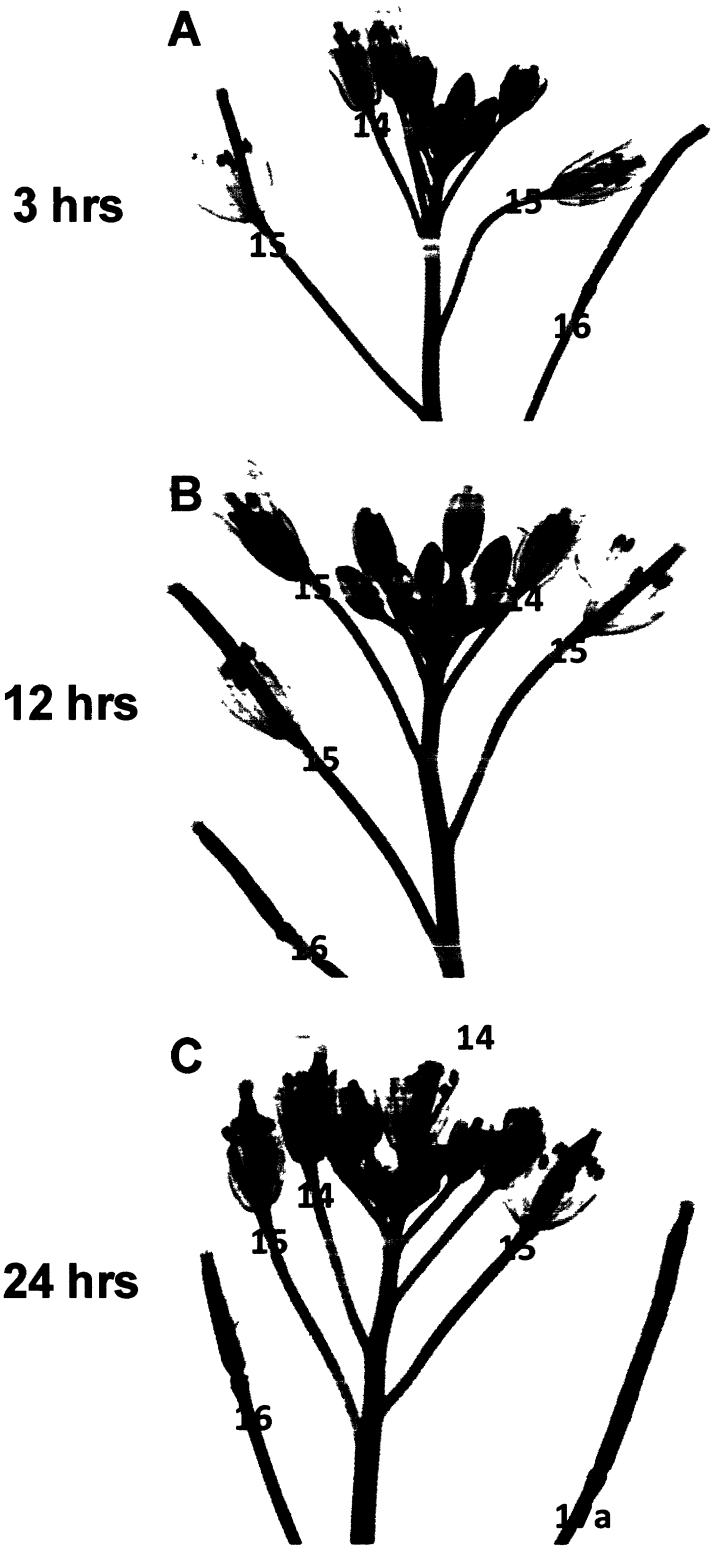

Figure 49. *C4* gene expression in floral apex assayed for different periods of time. **A)** *AC4::C4:GUS-2*; **B)** *AC4::C4:GUS-7*; **C)** *AC4::C4:GUS-4*. Samples were incubated in the GUS substrate for times indicated. Floral stages from Table 5 are indicated.

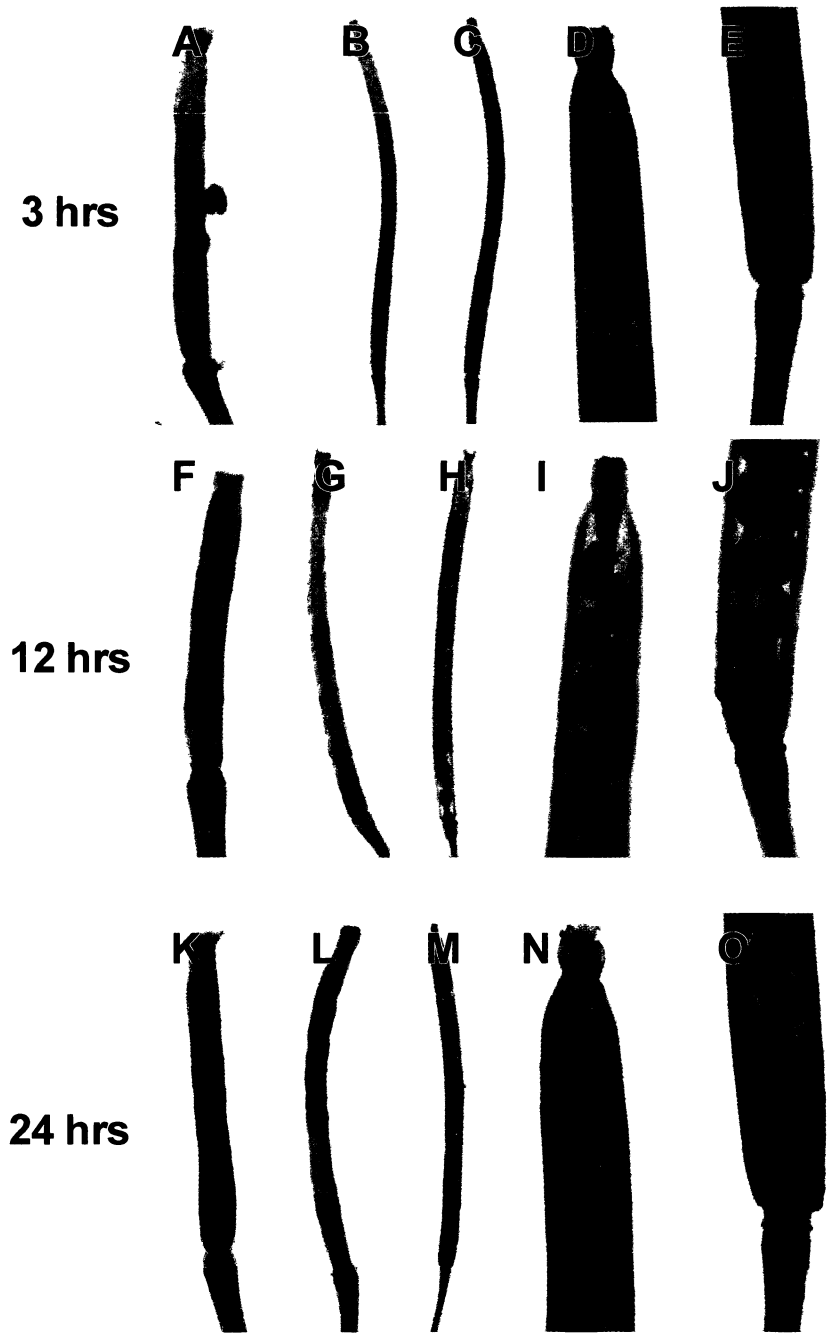

Figure 50. Siliques assayed for *C4* gene expression for different periods of time. Stage 16 siliques: **A)** *CC4::C4:GUS-4*; **F)** *AC4::C4:GUS-7*; **K)** *C4::C4:GUS-5*. Stage 17a siliques: **B)**, **G)**, and **H)** *CC4::C4:GUS-4*. Stage 17b siliques: **C)**, **H),** and **M)** *CC4::C4:GUS-4*. Apical region of silique: **D)** and **I)** CC4::C4:GUS-5; **I)** *CC4::C4:GUS-5*; **N)** *CC4::C4:GUS-1*. Basal region of silique: **E)** and **J)** *CC4::C4:GUS-5*; **O)** *CC4::C4:GUS-1*;. Samples were incubated in the GUS substrate for times indicated.

II.B.7. *C4* gene expression in the ovule and embryo

After the pollen has germinated, traveled down the transmitting tract of the carpel's septum and double fertilization has occurred, the zygote divides to form an apical and basal cell (Bowman, 1994). The apical cell will eventually form the embryo and the basal cell will form the hypophysis (suspensor) and the root. After multiple rounds of cell divisions, a single apical cell will become a 16-cell embryo or globular stage embryo (Capron et al., 2009). As the embryo develops, two lobes (the cotyledon primordia) form on the apical side of the embryo indicative of the heart stage. At the late heart stage, the root and shoot meristems are evident and the basic tissue patterning of Arabidopsis has been formed. The hypocotyl and the cotyledons expand, forming the torpedo stage and then, after further cell division, the embryo will bend into the walking stick (bent cotyledon) stage. After the final cell divisions, the mature embryo fills the developing seed coat.

An attempt was made to view embryos at different developmental stages. Due to the difficulties of working with microscopic embryos encased in a carpel, a limited number of embryos showing *C4* gene expression were observed. All embryos were assayed for GUS activity overnight. One-cell stage thru globular stage embryos were difficult to observe through the seed coat but expression was seen in the funiculus, chalazal endosperm, and outer and inner integument (Figure 51A and B). Because of the difficulty of observing the embryo through the developing seed coat, embryos from heart stage and older were excised from the seed and assayed directly in the GUS substrate overnight. *C4::C4:GUS* expression was observed throughout the embryo and the suspensor during heart stage (Figure 51C-H). In the older embryos, slightly higher *C4*

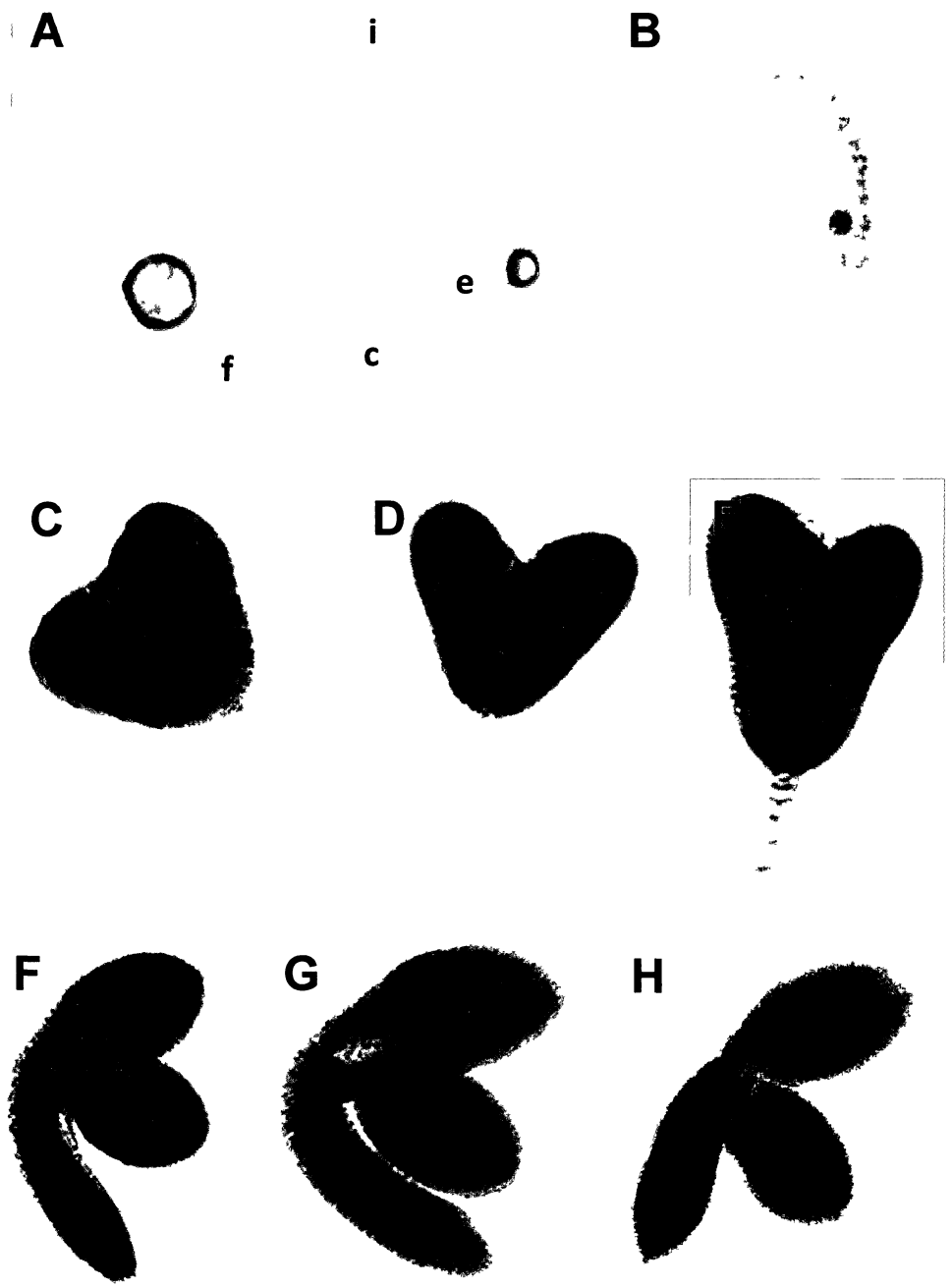

Figure 51. *C4* gene expression in embryos.
Developing embryos and endosperm in seed coat: **A)** *AC4::C4:GUS-7*, **B)** *CC4::C4:GUS-5*. Heart stage embryo with hypophysis: **C-E)** *CC4::C4:GUS-5*. Bent cotyledon stage: **F-G)** *AC4::C4:GUS-7*, **H)** *CC4::C4:GUS-5*. All samples were assayed overnight. Embryo structures indicated in Figure **A)** are funiculus (f), chalazal endosperm (c), embryo (e), and outer and inner integument (i).

gene expression was observed in the vascular system compared to the surrounding tissues (Figure 51H).

II.B.8. Sites of the greatest *C4* gene expression

One of the goals of this research was to determine which cells and tissues or organs had the most *C4* gene expression. Composite images of each of the four assay times (1, 3, 12, and 24 hours) was made to determine the site of highest expression. Following a 1 hour GUS assay, plants consistently showed expression only in the primary and secondary root meristems and elongation zones (Figure 52). A 3 hour GUS assay revealed only one additional site of expression: in the nectary region at the base of the silique (Figure 53). At 12 hours, all previously documented of the sites of *C4* gene expression in the roots and shoots are readily apparent (Figure 54); no floral expression was detectable after a 12 hour assay. A 24 hour GUS assay was required to detect expression in the floral structures. At 24 hours, regions of the plant that had expression at shorter assay times accumulated high amounts of diX-indigo. As expected, the highest expression was in the regions which showed expression after 1 hour (Figure 55). These composite images show that the highest *C4* gene expression is in the root meristem and elongation zone but that the *C4* gene is expressed throughout the plant at all developmental periods at differing levels.

II.C. Analysis of "empty" vector lines

Plants were transformed with the negative control construct, the anti-sense C4 coding region described in Section I.B. These plants were assayed for GUS enzyme

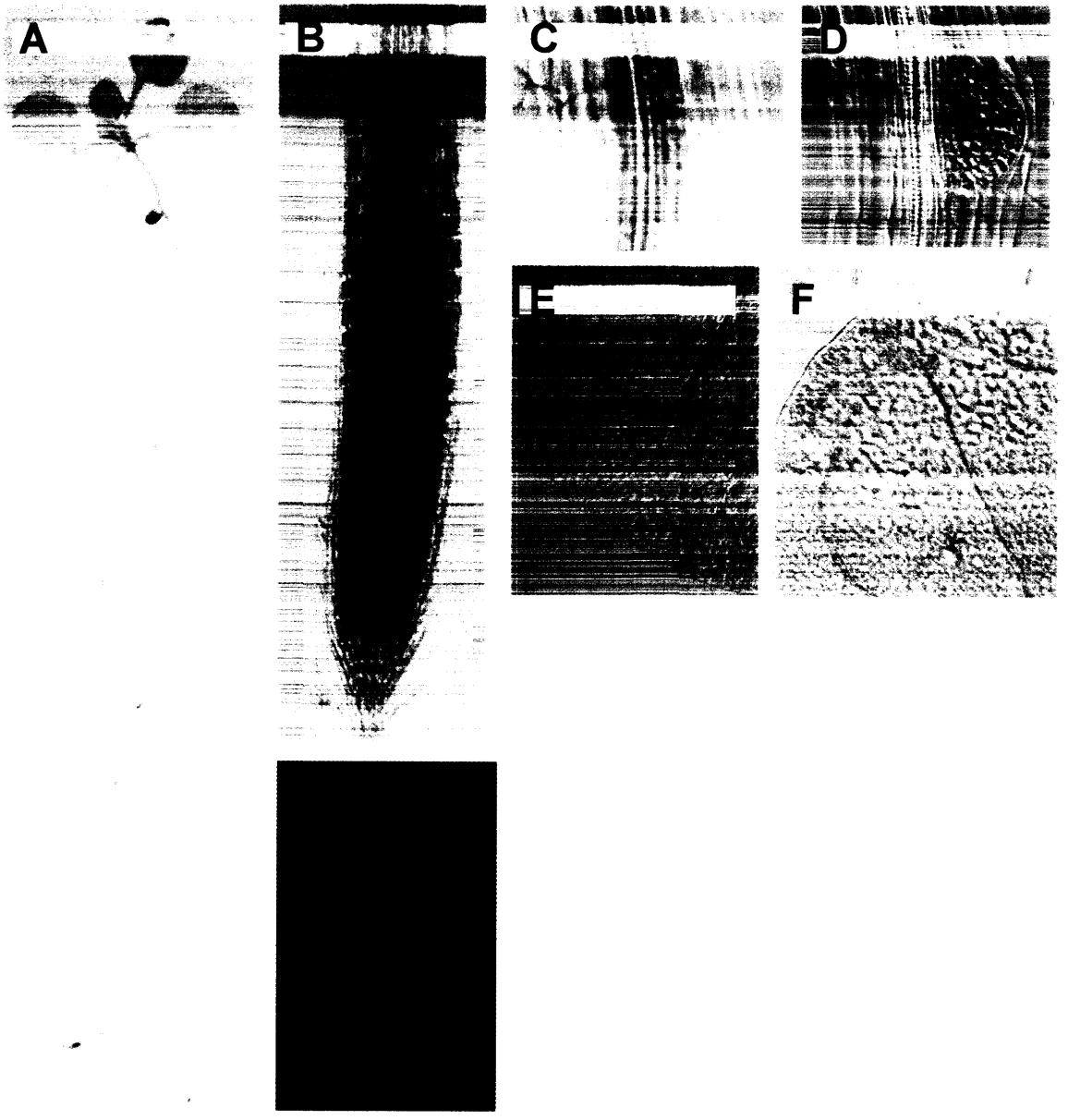

Figure 52. ***C4*** **gene expression in different Arabidopsis tissues after a 1 hour GUS assay.**
A) *AC4::C4:GUS-2*, 14-day-old; **B)** *AC4::C4:GUS-5*, 10-day-old; **C-G)** *AC4::C4:GUS-2*, 10-day-old.

Figure 53. ***C4*** **gene expression in different Arabidopsis tissues after a 3 hour GUS assay.**

A), C), and **D)** *AC4::C4:GUS-2*, 14-day-old; **B)** *AC4::C4:GUS-5*, 10-day-old; **E)** *AC4::C4:GUS-2*, 14-day-old; **F)** *AC4::C4:GUS-5*, 10-day-old; **G)** *AC4::C4:GUS-7*, 4-week-old; **H)** *CC4::C4:GUS-2*, 14-day-old; **I)** *AC4::C4:GUS-2*; **J)** *CC4::C4:GUS-4*; **K)** *CC4::C4:GUS-4*; **L)** *CC4::C4:GUS-5*.

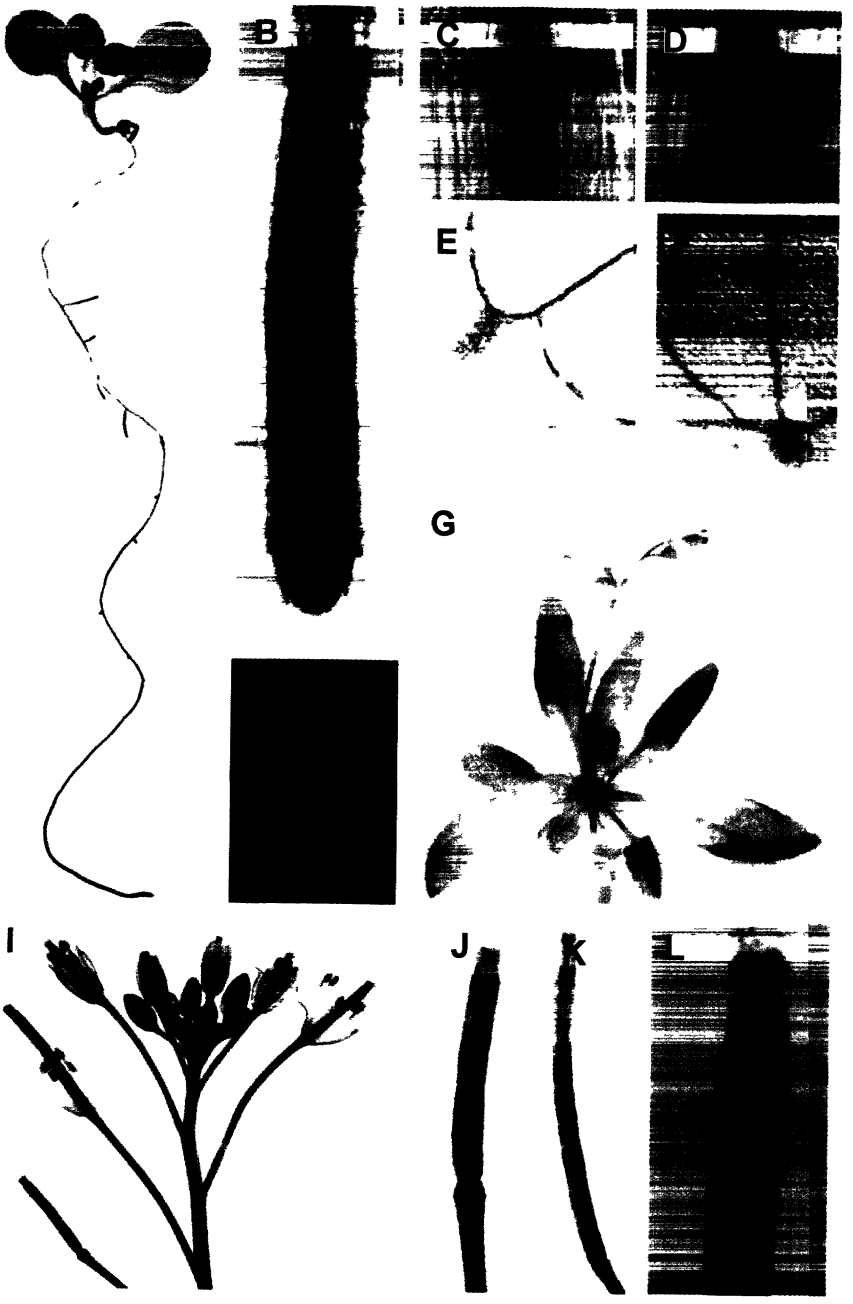

Figure 54. ***C4*** **gene expression in different Arabidopsis tissues after a 12 hour GUS assay.**

A) *AC4::C4:GUS-2*, 10-day-old; **B)** *BC4::C4:GUS-2*, 10-day-old; **C)** *AC4::C4:GUS-2*, 10-day-old; **D)** *AC4::C4:GUS-2*, 10-day-old; **E)** *AC4::C4:GUS-2*, 10-day-old; **F)** *AC4::C4:GUS-5*, 10-day-old; **G)** *AC4::C4:GUS-7*, 4-week-old; **H)** *AC4::C4:GUS-7*, 10-day-old; **I)** *AC4::C4:GUS-7*; **J)** *AC4::C4:GUS-7*; **K)** *CC4::C4:GUS-4*; **L)** *CC4::C4:GUS-5*.

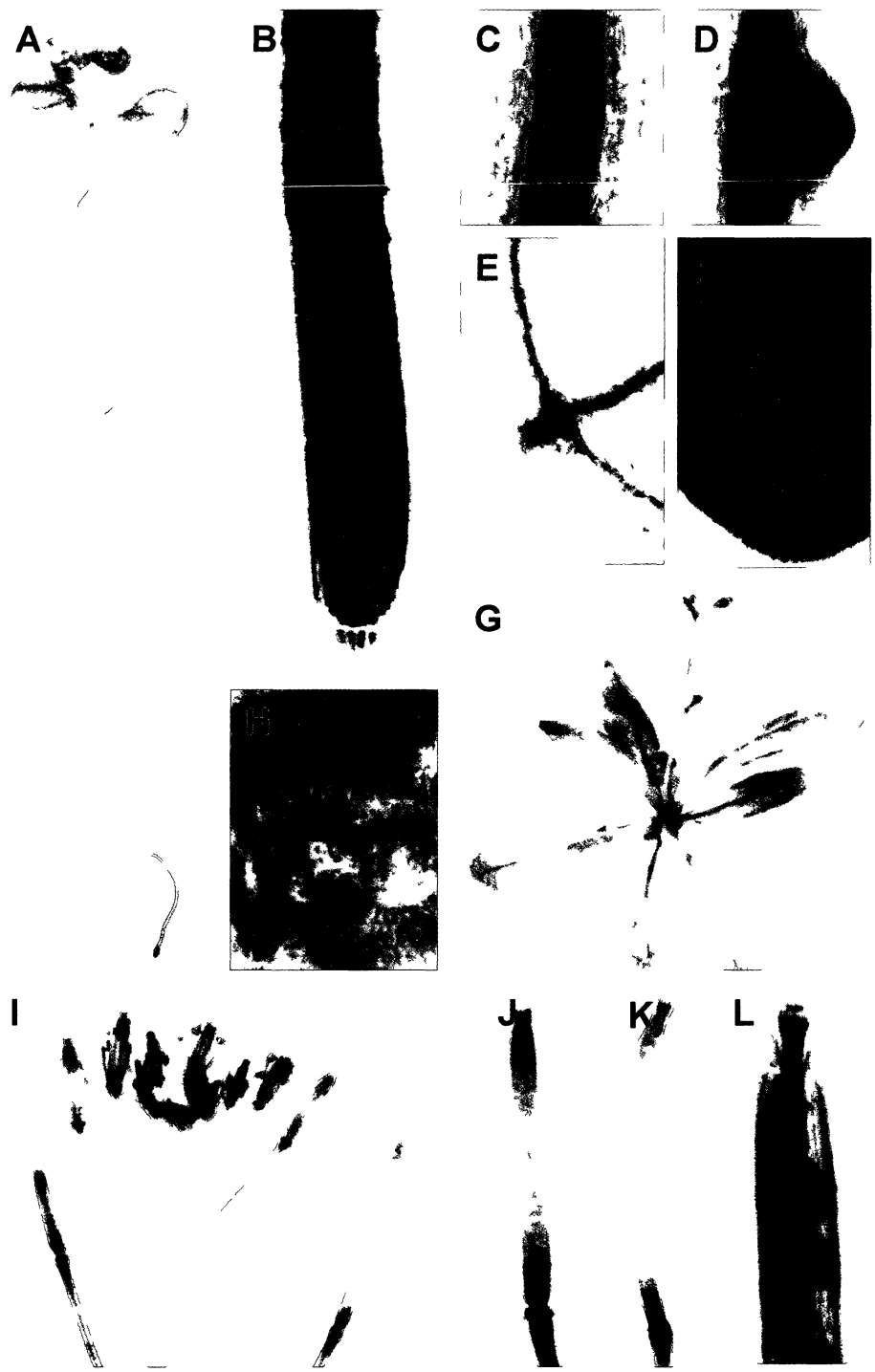

Figure 55. *C4* gene expression in different Arabidopsis tissues after a 24 hour GUS assay.

A) *AC4::C4:GUS-2*, 14-day-old; **B)** *AC4 :C4:GUS-5*, 10-day-old; **C)** *AC4::C4.GUS-8*, 10-day-old; **D)** *AC4: C4 GUS-8*, 10-day-old; **E)** *AC4::C4 GUS-2*, 10-day-old; **F)** *AC4::C4 GUS-8*, 10-day-old; **G)** *AC4.:C4:GUS-8*, 4-week-old; **H)** *AC4::C4.GUS-8*, 10-day-old; **I)** *AC4::C4:GUS-4*; **J)** *CC4::C4:GUS-5*; **K)** *CC4::C4:GUS-4*; **L)** *CC4::C4:GUS-1*.

activity after 1, 7, and 14 days and 4-6 weeks. At least 5 lines were examined at each time point. These lines were always incubated in the GUS substrate for the maximum assay time of 24 hours. A positive control line (*BC5::C5:GUS-5*) was also assayed at the same time to determine that the assay solution was made correctly.

Analysis of the plants after 24 hours of incubation time showed no detectable diX-indigo accumulation at any age (Figure 56). None of the lines observed contained any detectable diX-indigo accumulation in the root tissues. Some lines showed some very faint expression in the leaf petiole, vascular system and hydathode of the basal and cauline leaves. Even though some faint expression was observed in a few of the "empty" vector lines, the diX-indigo accumulation in the positive control line was much greater than that of the "empty" vector control.

II.D. Classification of *C1*, *C2*, *C3*, *C4* and *C5* subunit genes of protein phosphatase 2A

The Arabidopsis genome encodes five different PP2A C subunits; C1, C2, C3, C4 and C5. The subunits are divided into two classes based on similarities in amino acid sequence and genomic structure which indicates that C subunits likely had a common ancestor which eventually diverged into two classes (Blanc et al., 2000; Figures 57-60). The C1, C2 and C5 subunits belong to class I (Figure 58) while class II contains C3 and C4 subunits (Figure 59; DeLong, 2006). Genome-wide duplications have occurred in the Arabidopsis genome, therefore it is not uncommon to find gene families with multiple members (Bouche and Bouchez, 2001). As further support for the classification, I observed that genes in each class has similar coding sequence and intron- exon structure

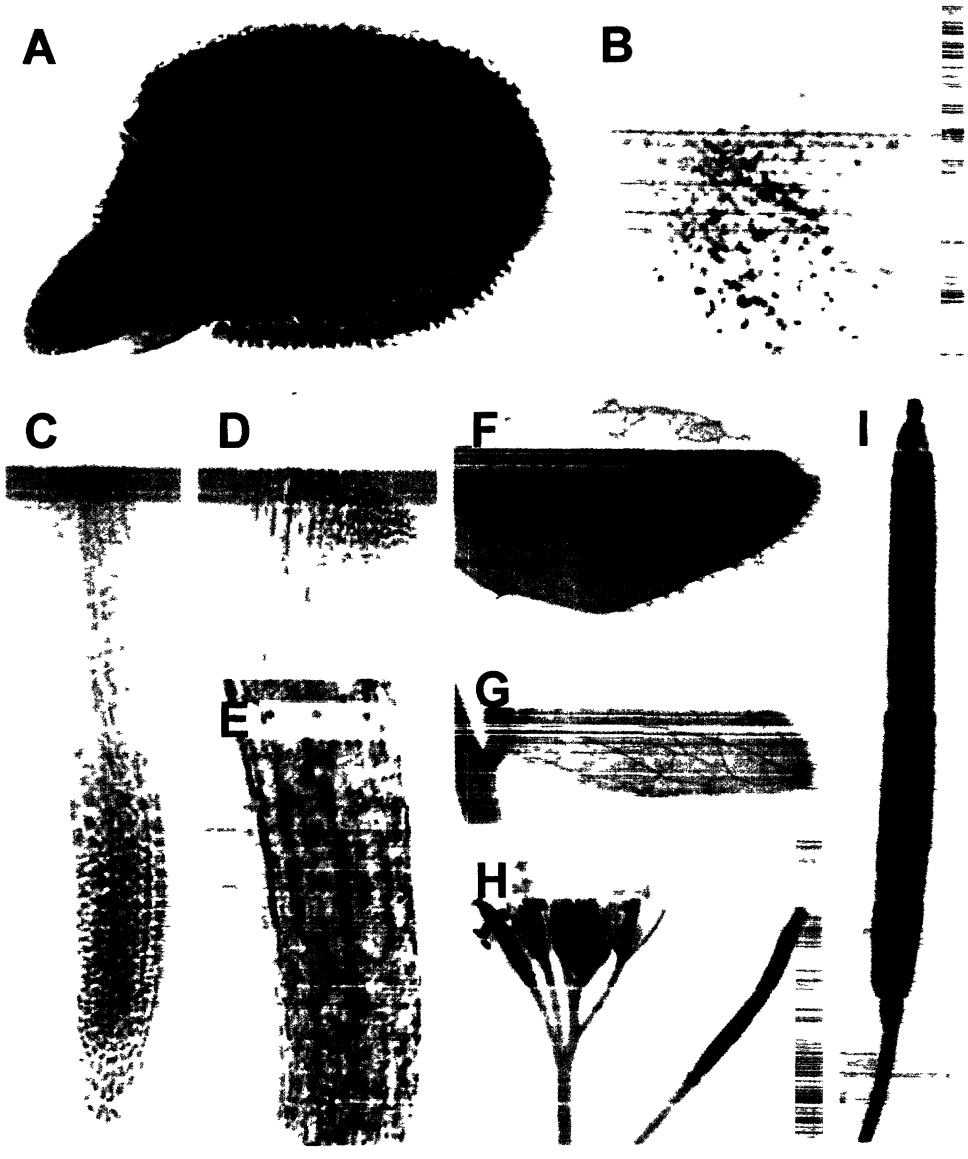

Figure 56. Expression of the negative control vector throughout Arabidopsis developmental.

A) 1-day-old (*Rev-2*); **B)** 7-day-old cotyledon (*Rev-3*); **C)** 7-day-old primary root tip (*Rev-1*); **D)** 7-day-old lateral root (*Rev-3*); **E)** 7-day-old hypocotyl (*Rev-5*); **F)** 4-week-old rosette leaf; **G)** cauline leaf (*Rev-5*); **H)** floral apex (*Rev-5*); **I)** silique (*Rev-1*). All samples were incubated for 24 hours in the GUS substrate.

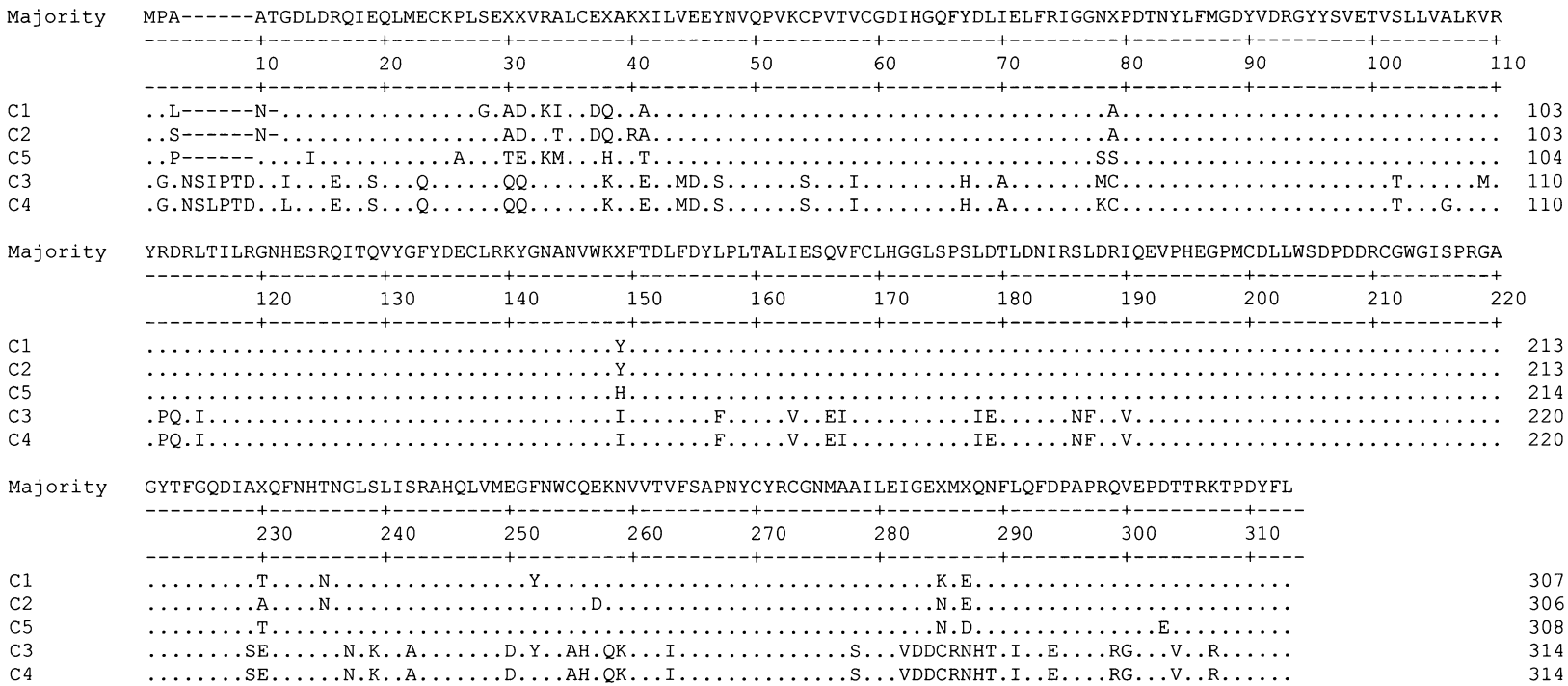

Figure 57. Alignment of *Arabidopsis thaliana* Protein Phosphatase 2A C subunit amino acid sequences.
Amino acid alignment was performed with DNASTAR MegAlign aligned using Clustal W.

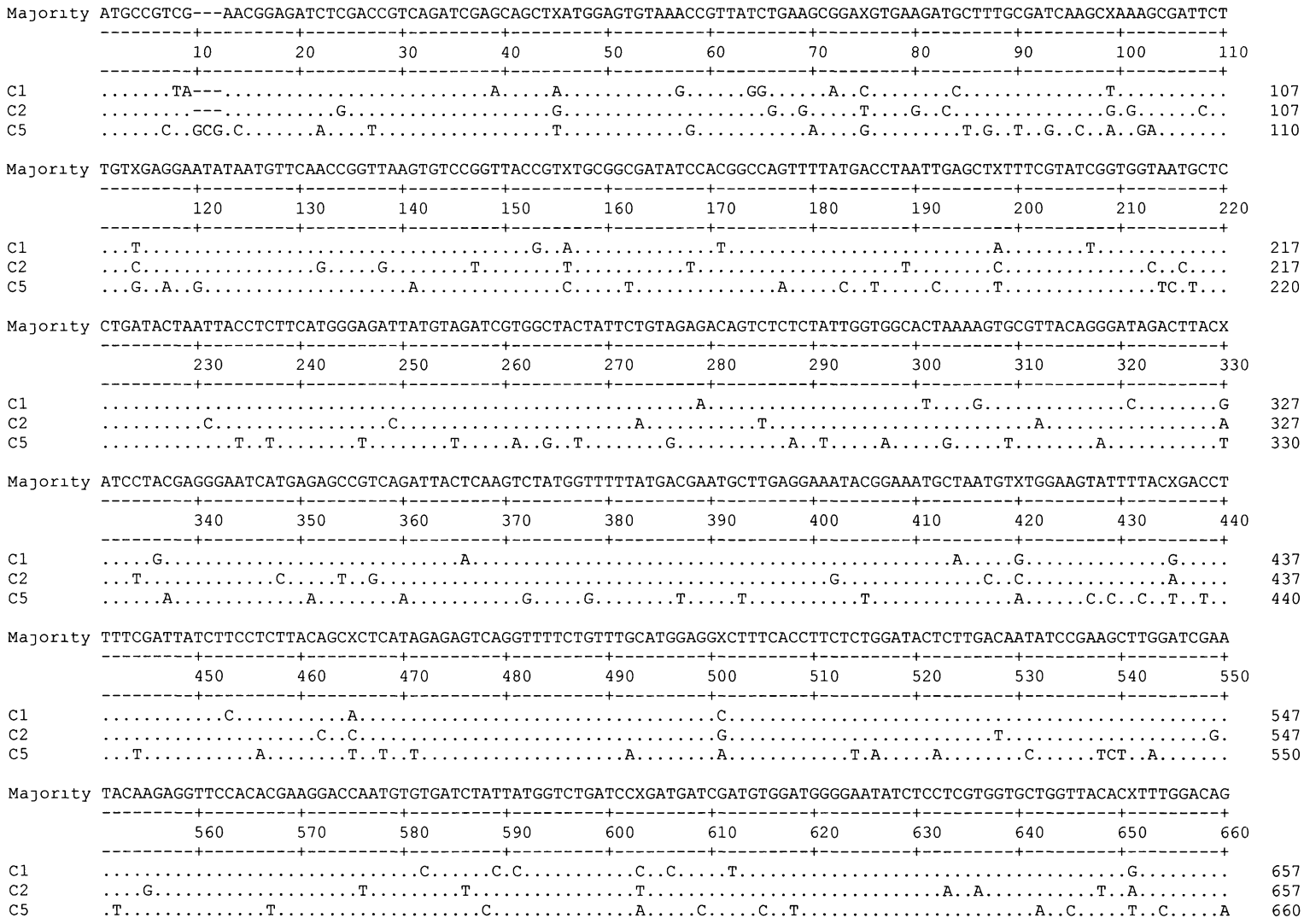

(continued on the next page)

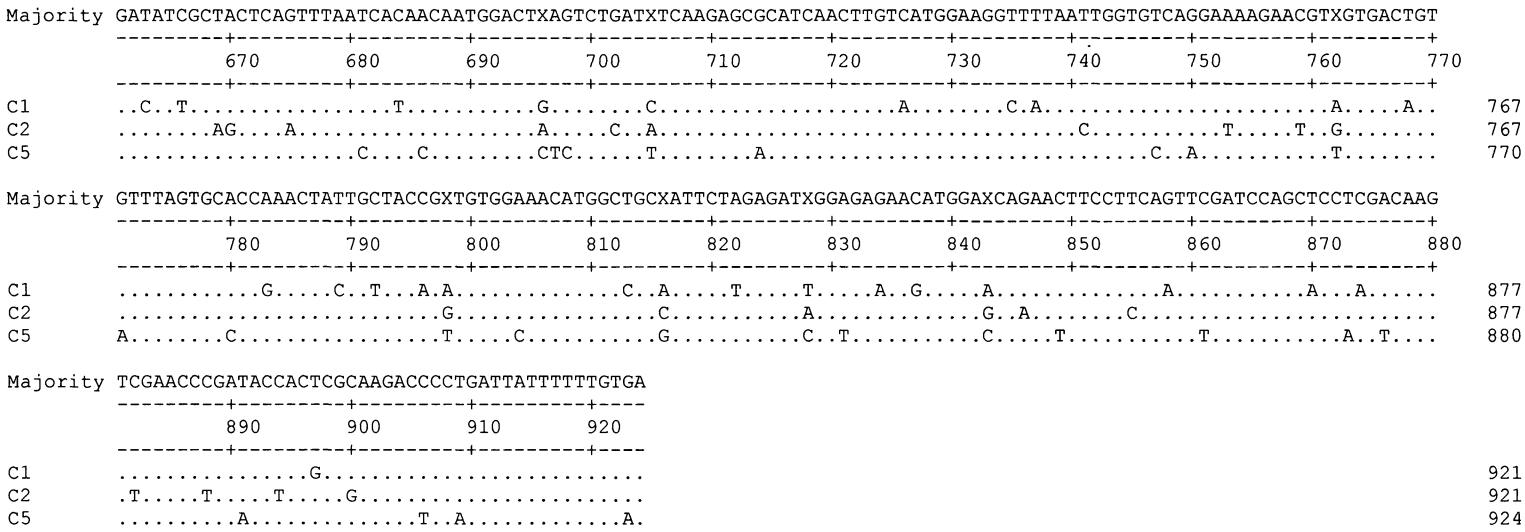

Figure 58. Alignment of *Arabidopsis thaliana* Class I PP2A coding sequences.
Nucleotide alignment was performed with DNASTAR MegAlign aligned using Clustal W.

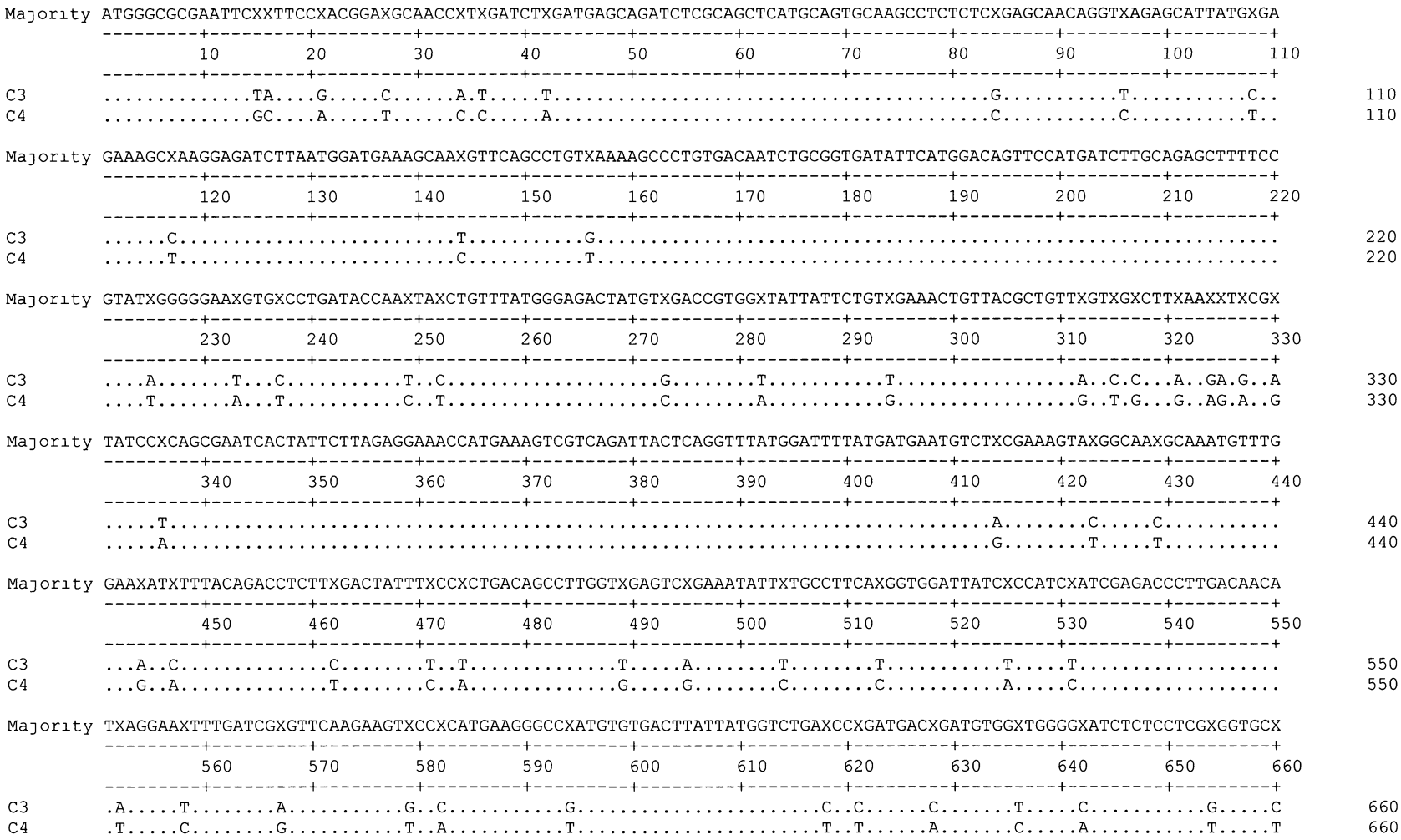

(continued on the next page)

Figure 59. Alignment of *Arabidopsis thaliana* Class II PP2A coding sequences.
Nucleotide alignment was performed with DNASTAR MegAlign aligned using Clustal W.

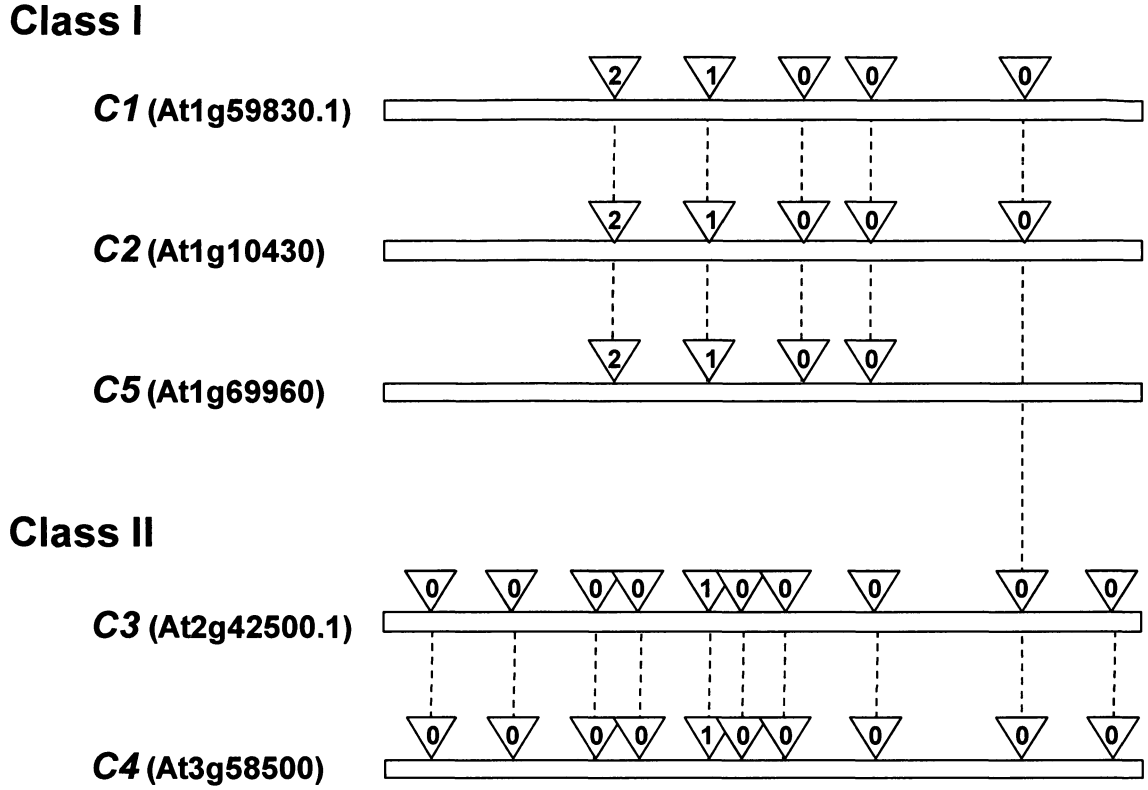

Figure 60. Intron and exon structure of PP2A C subunits
The C subunits amino acid sequences are diagramed as boxes. Introns are represented as triangles and the number indicates the phase of the intron: 0 = intron inserted between intact codons; 1 = intron inserted after first nucleotide of a codon; 2 = intron inserted after second nucleotide of a codon. Dotted lines connect introns at identical positions in the C subunits.

with additional evidence for intron gain or loss within each class (Figure 60). One goal of these experiments was to determine whether expression patterns of genes in each class are similar to each other or whether each *C* subunit gene has a unique expression pattern.

The upstream sequence was analyzed to determine if there were any *cis* regulatory elements in common between the C subunits which could potentially lead to similar expression patterns. Since the upstream boundary of each *C* subunit promoter region is not known, 2.1 kb upstream of the transcription start site of each gene was analyzed using the Athena website (http://www.bioinformatics2.wsu.edu/cgi-bin/Athena/cgi/home.pl; O'Connor et al., 2005). Little similarity was observed in the order or spacing of promoter elements (Figure 61); therefore, I expected that the expression patterns of the C1, C2, C3, C4, and C5 subunits may differ each other.

Various developmental stages and GUS assay times were used to analyze the expression of the *C1*, *C2*, *C3* and *C5* subunit genes. The developmental time points for observation were 1-, 2-, 3-4-, 6-7-, 10-, and 14-day-old, as well as 4-week-old. In addition to roots and shoots, parts of the flower stalk, including cauline leaves, buds, flowers and siliques, were examined. To determine relative promoter strength, tissues were incubated in the GUS substrate for 1, 3, 12 or 24 hours. For each C subunit, the complete expression pattern and the relative promoter strength were documented at each time point to allow for comparisons between the five *C* subunit genes during plant development.

II.D.1. Expression patterns of two different *C3* promoters

During preparation of the plant constructs for these studies, the *C3* gene was

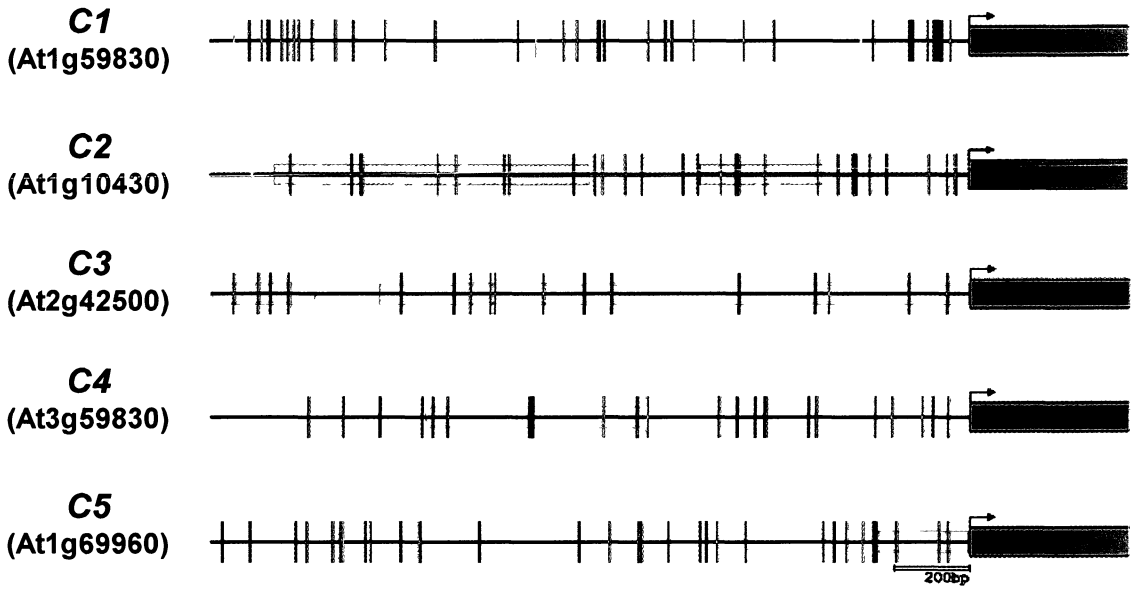

	P	N		P	N
ABFs binding site motif	1	1	ABRE binding site motif	1	1
ABRE-like binding site motif	2	3	ACGTABREMOTIFA2OSEM	1	2
ARF binding site motif	3	4	AtMYB2 BS in RD22	1	1
AtMYC2 BS in RD22	3	5	BoxII promoter motif	4	7
CACGTGMOTIF	2	4	CARGCW8GAT	4	30
CArG promoter motif	1	2	CCA1 binding site motif	1	1
DRE core motif	1	1	GADOWNAT	1	1
GAREAT	3	7	GBOXLERBCS	1	1
GCC-box promoter motif	2	2	Gap-box Motif	1	1
Ibox promoter motif	4	11	L1-box promoter motif	1	2
LEAFYATAG	1	2	MYB binding site promoter	2	2
MYB1 binding site motif	1	1	MYB1AT	5	18
MYB1LEPR	1	1	MYB2AT	3	4
MYB4 binding site motif	5	14	MYCATERD1	3	5
SV40 core promoter motif	2	3	T-box promoter motif	4	7
TATA-box Motif	4	21	TELO-box promoter motif	3	3
W-box promoter motif	5	15			

Figure 61. *Cis* regulatory motifs found 2100 bp upstream of transcription start of PP2A C subunit genes.

Regulatory motifs were found using the Athena website (O'Connor et al., 2005). Light blue boxes are CpG islands. Position of different motifs within the genomic region are marked with different colors. **P** corresponds to the number of promoters with this motif; **N** is the total number of times the motif is present in these five promoters.

found to be very close to a predicted upstream gene, At2g42510, which is located approximately 250 bp from the *C3* gene transcription start site. At2g42510 may be a pseudogene because no full length transcript has been reported. As 250 bp is quite short for a typical Arabidopsis promoter, two different GUS fusion constructs were made. The first construct, *sC3* (labeled *C3* or *C3::C3:GUS* on tubes and lab notebooks), contained 153 bp of the upstream region. The second construct, *LC3* (labeled *LC3* or *LC3::C3:GUS* on tubes and lab notebooks), included the 153 bp region as well as 2160 bp further upstream. Both constructs included the same *C3* genomic region, including the 5' UTR and unspliced coding region, fused in-frame to the GUS gene. The rationale for creating two constructs was to determine if the short upstream region produced the same expression pattern as the longer construct. If so, this could indicate that *C3* regulatory information was contained in the smaller upstream region. This approach represents a simple promoter deletion analysis, commonly used to compare expression from various sized promoter segments to determine location of *cis* regulatory elements (Donald and Cashmore, 1990).

To determine *C3* gene expression throughout the Arabidopsis life cycle, plants were assayed in the GUS substrate at major developmental points (1- , 2-, 3-4-, 6-7-, 10-, 14-day-old, and 4-week-old) and cauline leaves, buds, flowers and siliques were assayed from older plants. Relative expression levels were determined by incubating the plant sample in the GUS substrate for 1, 3, 12 or 24 hours. A total of 11 independent transformed lines from three independent PCRs were analyzed for *sC3* expression and seven independent transformed lines from two independent PCRs were analyzed for *LC3* expression (Table 4).

II.D.1.a. *sC3* and *LC3* expression pattern in roots

Arabidopsis root anatomy and development was described previously in Section II.A.1. In 1-day-old germinating seeds, the radicle, including the root cap, showed *sC3* expression as soon as it emerged from the seed coat (Figure 62A, C, E). The *LC3* expression pattern was indistinguishable from that of *sC3* (Figure 62B, D, F).

Additional root expression was analyzed from 2-14 days after germination. Representative examples of *sC3* and *LC3* expression in root tips are shown in Figure 63. After 1 hour of incubation with the GUS substrate, *C3* gene expression was readily detected in the meristematic, elongation, and differentiation zones. In the meristematic region, expression was detected in all cell types while in the elongation and differentiation zone, strongest expression was in the central cylinder. By 3 hours, expression was also detected in the root cap (both columella and lateral root cap) and in the epidermis and cortex of the elongation and differentiation zones. After 12 or 24 hours of incubation, the root tips perpetuated the expression pattern detected at 3 hours but, as expected, accumulated more diX-indigo. Expression was also seen throughout the tissues in the differentiated and mature roots (data not shown).

In developing lateral root meristems of either *sC3* or *LC3* seedlings, very weak expression was detected in stages I-VIII after 1 hour of incubation (Figure 64). Interestingly, expression in stage I or in stage IV-V meristems was more easily detected than in stage VIII, indicating a drop in expression at the later stages (Figure 64). With longer incubation times (3, 12 or 24 hours), strong *C3* gene expression was easily detected throughout the developing meristem in stages I-VIII. Once the lateral root had established meristematic and elongation zones, the expression of the *C3* gene during

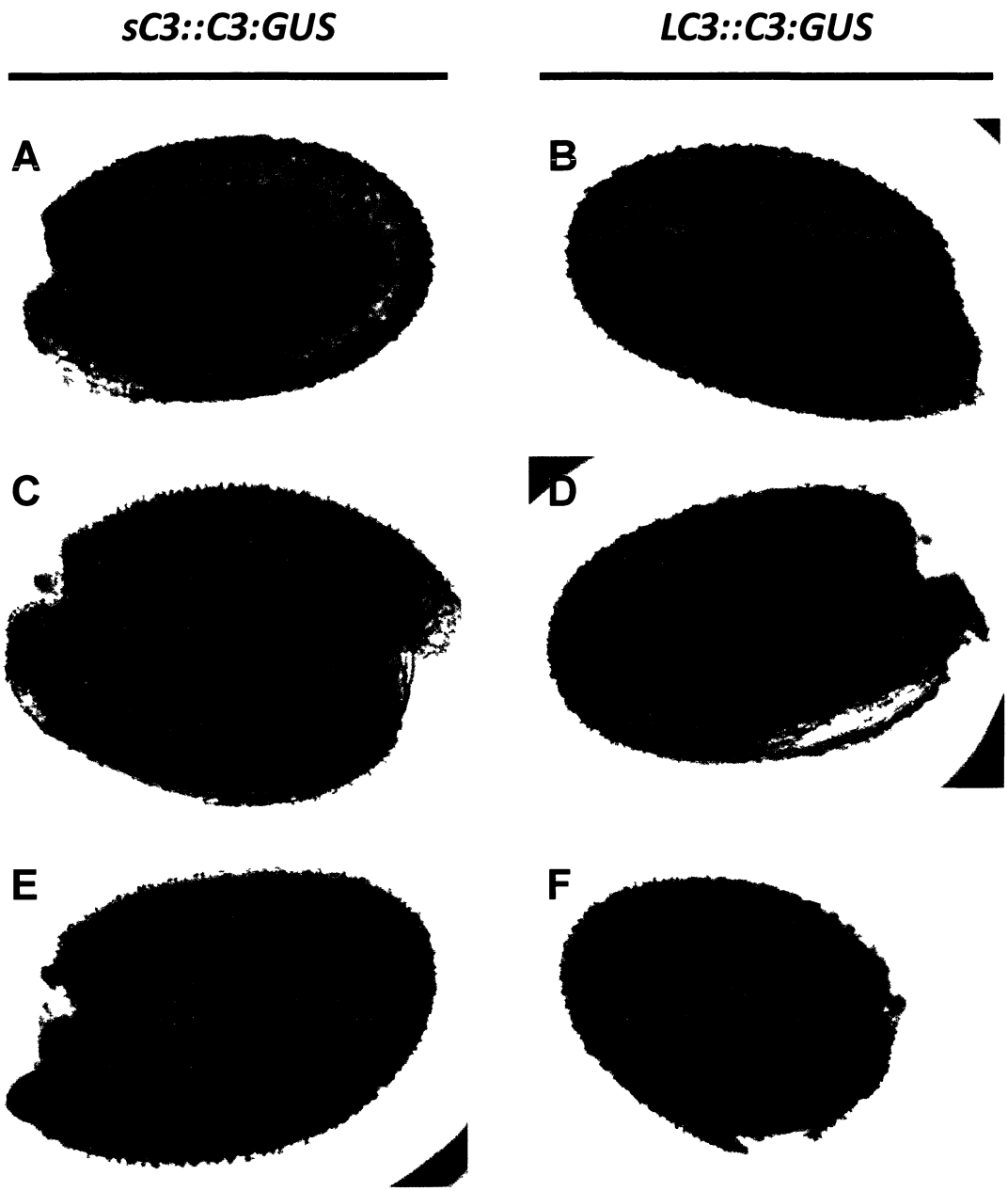

Figure 62. Expression of *sC3* and *LC3* in 1-day-old seedlings.
A) *AsC3::C3:GUS-1*; **B)** *DLC3::C3:GUS-11*; **C)** *AsC3::C3:GUS-1*; **D)** *DLC3::C3:GUS-11*; **E)** *CsC3::C3:GUS-9*; **F)** *DLC3::C3:GUS-11*. All samples were incubated for 24 hours in the GUS substrate.

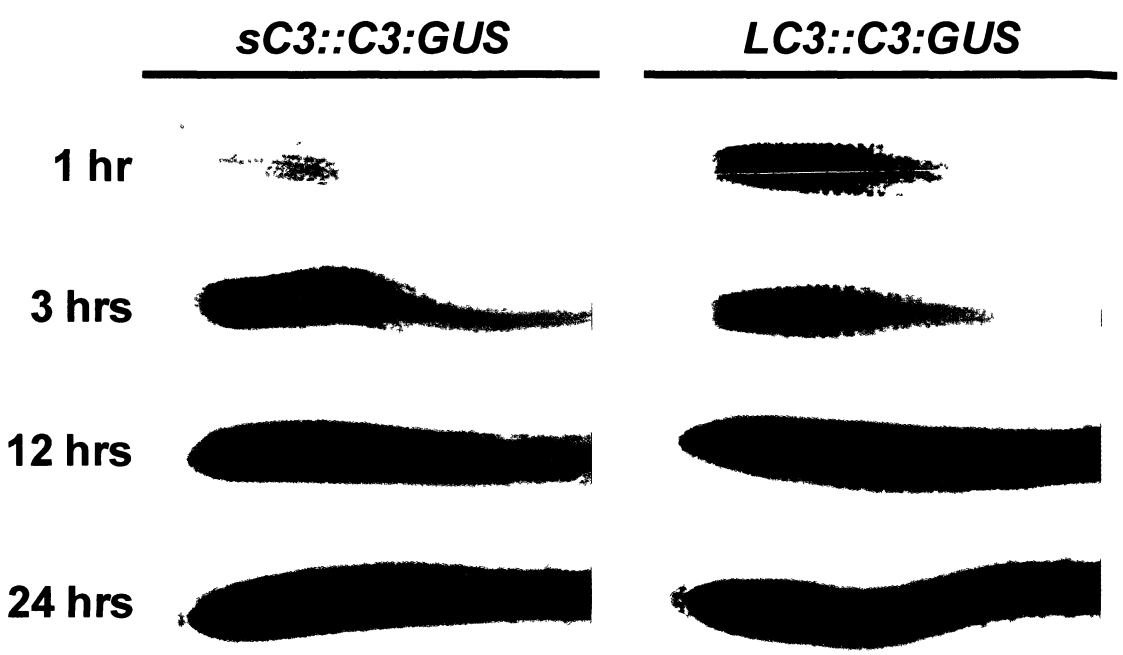

Figure 63. Expression of *sC3* and *LC3* in root tips.
sC3::C3:GUS lines were: *AsC3::C3:GUS-1* (1, 3, and 12 hours) and *AsC3::C3:GUS-6* (24 hours). *LC3::C3:GUS* lines were incubated for 1 hour (*DLC3::C3:GUS-11*); 3 hours (*DLC3::C3:GUS-4*); 12 hours (*DLC3::C3:GUS-3*); and 24 hours (*DLC3::C3:GUS-30*).

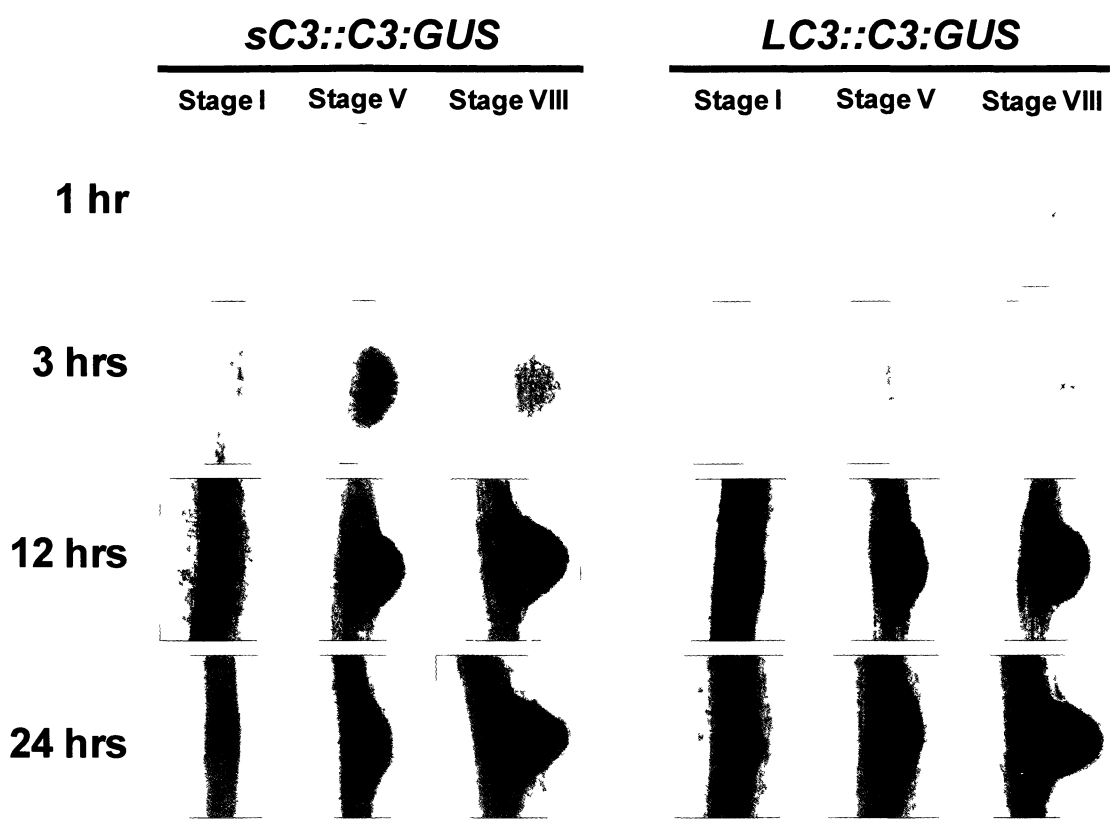

Figure 64. Expression of *sC3* and *LC3* in lateral root meristems.
sC3::C3:GUS stage I lines were: *CsC3::C3:GUS-9* (1 hour), *AsC3::C3:GUS-6* (3, 12, and 24 hours). *sC3::C3:GUS* stage V and VIII lines were all *AsC3::C3:GUS-6*. *LC3::C3:GUS* stage I lines were: *BLC3::C3:GUS-2* (1, 3, and 24 hours) *DLC3::C3:GUS-7* (12 hours). *LC3::C3:GUS* stage V lines were: *DLC3::C3:GUS-4* (1 hour), *BLC3::C3:GUS-2* (3 and 24 hours), *DLC3::C3:GUS-7* (12 hours). *LC3::C3:GUS* stage VIII lines were: *DLC3::C3:GUS-4* (1 hour), *BLC3::C3:GUS-2* (3 and 24 hours), and *DLC3::C3:GUS-7* (12 hours).

subsequent lateral root growth reiterated the overall expression pattern found in the primary root (data not shown).

In roots, the sites of *sC3* and *LC3* expression patterns were indistinguishable indicating that the *cis* regulatory elements could be contained in the short *sC3* promoter region. The *C3* gene was most highly expressed in actively dividing tissues such as primary and lateral root meristems although expression was also detected at lower levels throughout the differentiated root.

II.D.1.b. *sC3* and *LC3* expression pattern in shoots

II.D.1.b.i. *sC3* and *LC3* expression pattern in hypocotyl

A description of the anatomy and development of hypocotyls was provided in Section II.A.3. Observation of *C3* gene expression in hypocotyls included plants from 1- to 14-day-old. In all ages examined, the relative level and pattern of hypocotyl expression were equivalent for both *sC3* and *LC3* seedlings.

In 1-day-old germinating seeds, some samples showed very strong *C3* gene expression throughout the vascular system, cortex and epidermis while in other samples, expression was confined to the vascular system (Figure 62). The latter expression pattern correlated with seeds where the seed coat was barely ruptured by the emerging radicle while strong expression correlated with a more disrupted seed coat. Thus, the ability of the GUS substrate to access the tissues may contribute to the amount of expression observed.

In 7-day-old plants, little to no *C3* gene expression was detected in the hypocotyls after a 1 hour GUS assay (Figure 65). Weak *C3* gene expression was associated with the

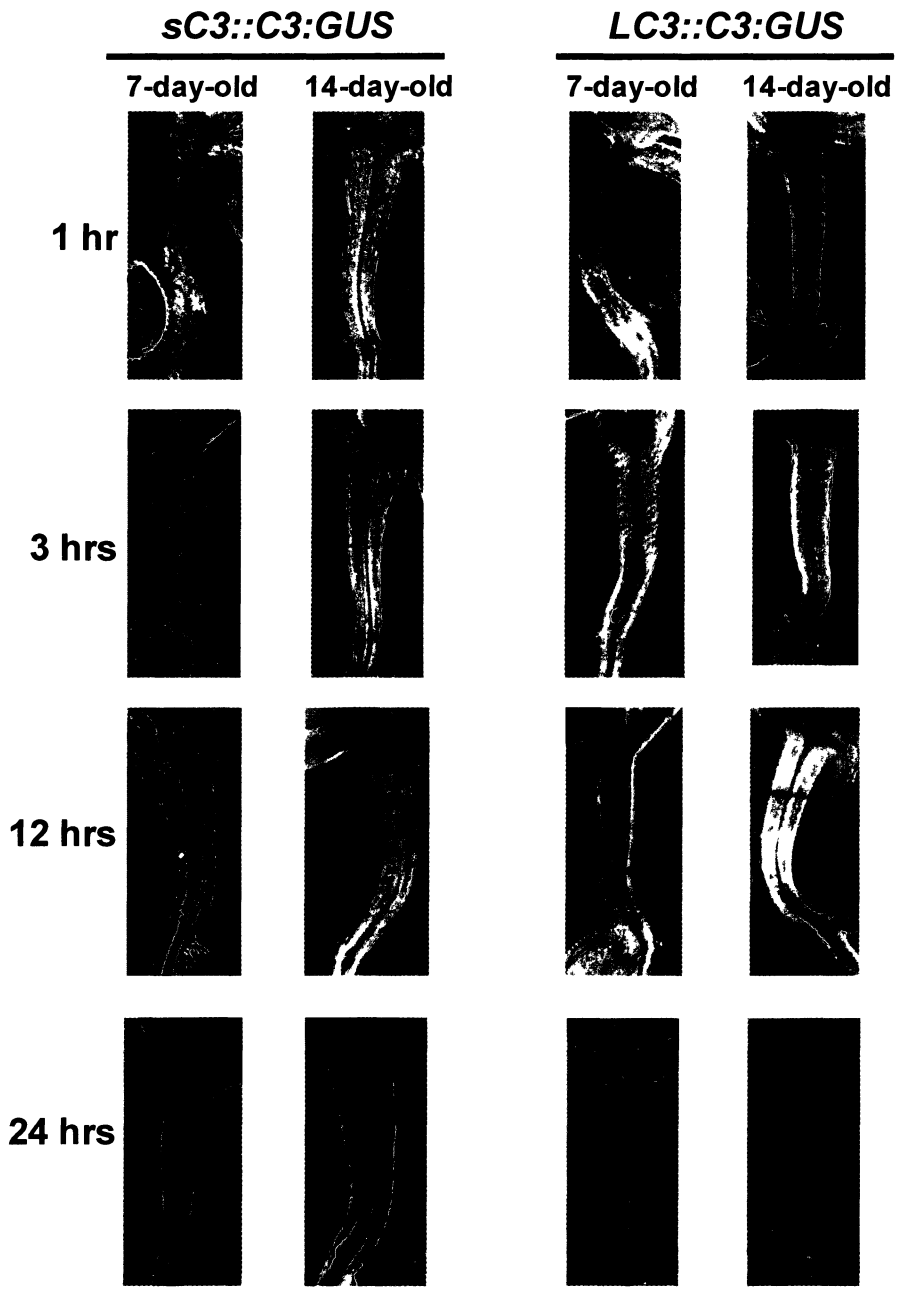

Figure 65. Expression of *sC3* and *LC3* in hypocotyls.
sC3::C3:GUS 7-day-old plants incubated for 1 hour (*CsC3::C3:GUS-9*), 3 hours (*CsC3::C3:GUS-9*), 12 hours (*AsC3::C3:GUS-6*), and 24 hours (*CsC3::C3:GUS-9*). *sC3::C3:GUS* 14-day-old plants incubated for 1 hour (*AsC3::C3:GUS-6*), 3 hours (*AsC3::C3:GUS-6*), 12 hours (*AsC3::C3:GUS-6*), and 24 hours (*AsC3::C3:GUS-1*). *LC3::C3:GUS* 7-day-old plants incubated for 1 hour (*DLC3::C3:GUS-4*), 3 hours (*BLC3::C3:GUS-2*), 12 hours (*DLC3::C3:GUS-6*), and 24 hours (*DLC3::C3:GUS-7*). *LC3::C3:GUS* 14-day-old plants incubated for 1 hour (*BLC3::C3:GUS-3*), 3 hours (*BLC3::C3:GUS-3*), 12 hours (*BLC3::C3:GUS-3*), and 24 hours (*DLC3::C3:GUS-11*).

longer incubation times (3, 12 or 24 hours), strong *C3* gene expression was easily detected throughout the developing meristem in stages I-VIII. Once the lateral root had established meristematic and elongation zones, the expression of the *C3* gene during vascular system near the base of the hypocotyl after 3 hours of incubation in both sC3 and LC3 seedlings. By 12 hours, conspicuous *C3* gene expression appeared throughout most of the hypocotyl but was reduced near the base of the hypocotyl in the epidermis, cortex and possibly the endodermis. After a 24-hour assay, *C3* gene expression was seen throughout the hypocotyl.

Expression of the *C3* gene was not detected in hypocotyls of 14-day-old plants after 1 or 3 hours of incubation. By 12 hours, limited *C3* gene expression occurred in the central cylinder near the base of the hypocotyl and occasionally near the apex of the hypocotyl. Expression was observed throughout the vascular system after 24 hours of incubation but not in the surrounding cortical or epidermal tissue.

Similar to the roots, expression of the *sC3* and *LC3* constructs in hypocotyls was indistinguishable, indicating that all of the regulatory regions need to drive expression in hypocotyls under normal growth conditions exists in the *sC3* construct. Additionally, analogous to the roots, the vascular system had stronger expression than the surrounding hypocotyl tissues. Relative *C3* gene expression strength decreased over time as exemplified by the reduced expression in hypocotyls of 14-day-old seedlings compared to 7-day-old seedlings.

II.D.1.b.ii. *sC3* and *LC3* expression pattern in cotyledonary and foliar organs

Arabidopsis anatomy and development of cotyledons and leaves were described

in Section II.A.4. Cotyledons and leaves were examined for *C3* gene expression throughout the development periods and assay times outlined in Section III.A. The *LC3* expression pattern was similar to *sC3* expression pattern in all developmental periods examined.

In 1-day-old germinating seeds, *C3* gene expression was observed in the cotyledons (Figure 62) in both *sC3* and *LC3* lines, but the exact pattern could not be elucidated due to obstruction by the seed coat. After germination, cotyledon expression was similar throughout the plant's life cycle. A representative example from 7-day-old cotyledons is shown in Figure 66. *C3* gene expression was not detectable after 1 hour of incubation in the GUS substrate; however, by 3 hours, extremely weak *C3* gene expression was occasionally seen in the vascular system. After 12 hours of incubation, distinct expression was seen throughout all cell types in the cotyledon with stronger expression in the vascular system and the hydathodal region. The same *C3* gene expression pattern, although stronger as expected, was observed after incubating for 24 hours.

C3 gene expression was observed in rosette leaves in both *sC3* and *LC3* lines. The first and second true leaves on 7-day-old seedlings, which were still expanding, were comparable to the fully-expanded counterparts on 14-day-old plants. *C3* gene expression was never detected after a 1 hour GUS assay (Figure 67) while weak expression in the veins was sometimes observed after 3 hours of incubation but in 14-day-old leaves only. After 12 or 24 hours of incubation, expression was observed throughout the leaf (Figure 67), although expression was usually higher in the distal versus the proximal region of the leaf at 7 days of age and was higher in proximal region on 14-day-old leaves. In

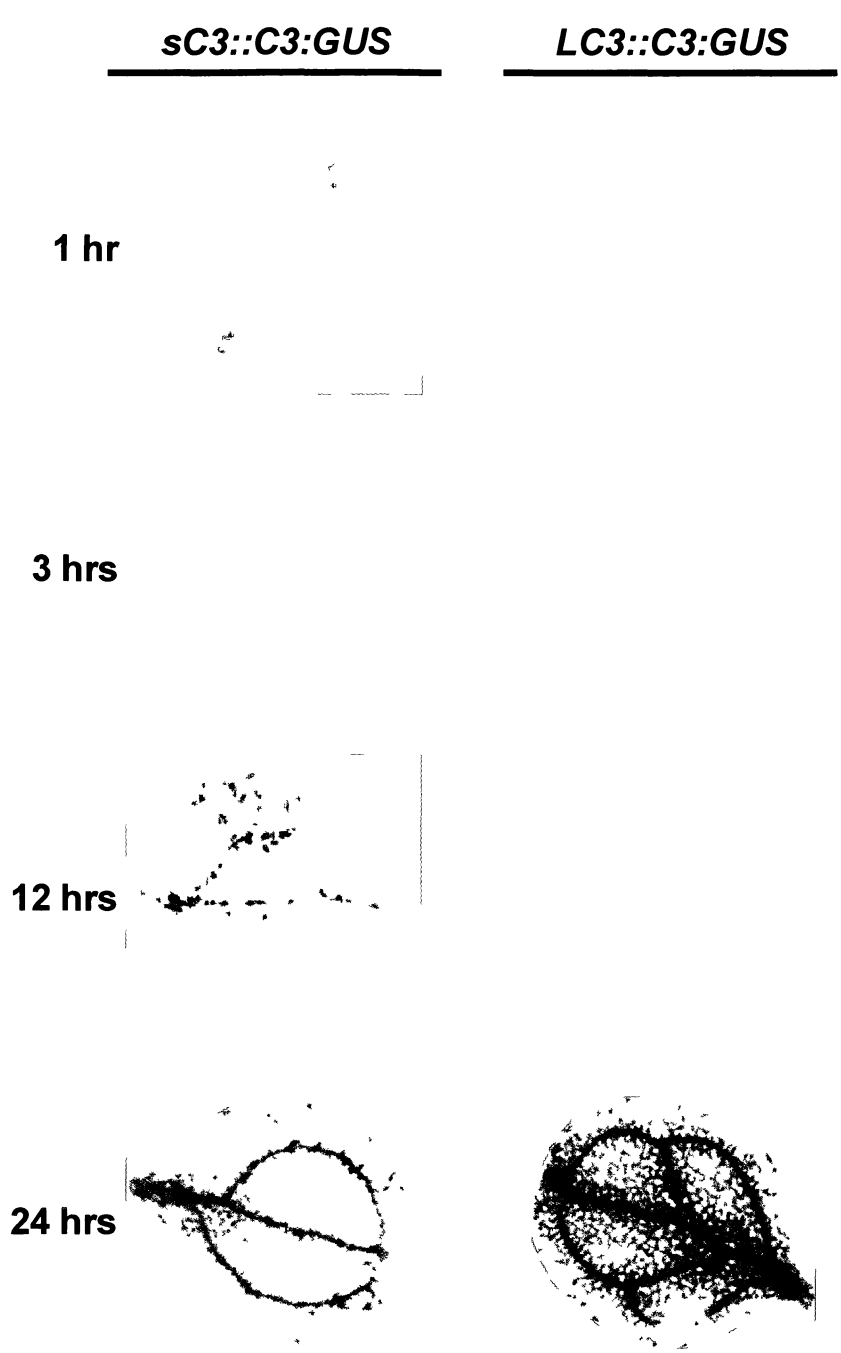

Figure 66. Expression of *sC3* and *LC3* in cotyledons.
sC3::C3:GUS 7-day-old plants incubated for 1 hour (*AsC3::C3:GUS-6*), 3 hours (*AsC3::C3:GUS-6*), 12 hours (*AsC3::C3:GUS-6*), and 24 hours (*AsC3::C3:GUS-6*). *LC3::C3:GUS* 7-day-old plants incubated for 1 hour (*DLC3::C3:GUS-6*), 3 hours (*DLC3::C3:GUS-6*), 12 hours (*DLC3::C3:GUS-3*), and 24 hours (*BLC3::C3:GUS-2*).

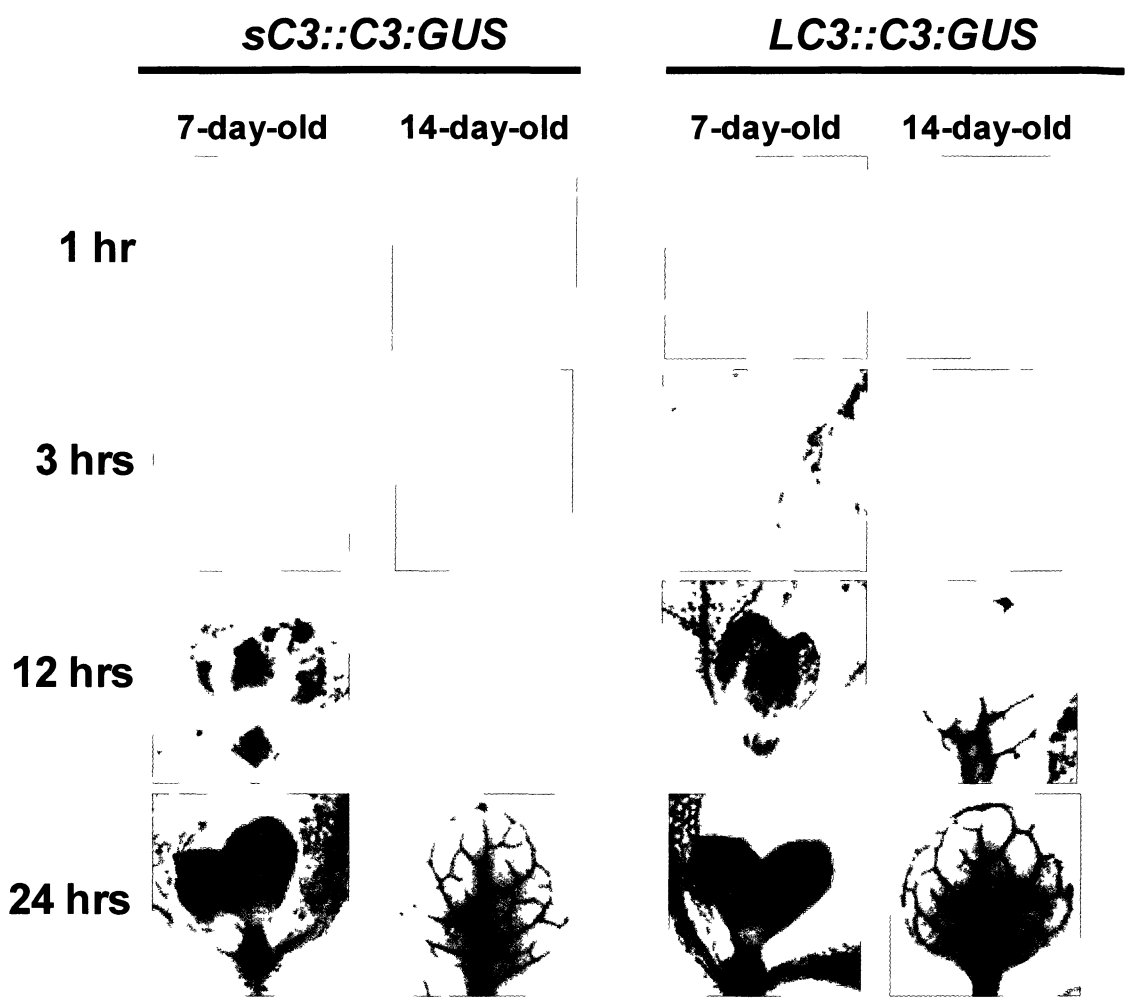

Figure 67. Expression of *sC3* and *LC3* in leaves.
sC3::C3:GUS 7-day-old plants GUS assayed for 1 hour (*CsC3::C3:GUS-11*), 3 hours (*AsC3::C3:GUS-1*), 12 hours (*CsC3::C3:GUS-9*), or 24 hours (*CsC3::C3:GUS-9*). *sC3::C3:GUS* 14-day-old plants GUS assayed for 1 hour (*AsC3::C3:GUS-6*), 3 hours (*AsC3::C3:GUS-1*), 12 hours (*AsC3::C3:GUS-6*), or 24 hours (*AsC3::C3:GUS-1*). *LC3::C3:GUS* 7-day-old plants GUS assayed for 1 hour (*DLC3::C3:GUS-6*), 3 hours (*BLC3::C3:GUS-3*), 12 hours (*BLC3::C3:GUS-3*), or 24 hours (*BLC3::C3:GUS-2*). *LC3::C3:GUS* 14-day-old plants GUS assayed for 1 hour (*BLC3::C3:GUS-3*), 3 hours (*BLC3::C3:GUS-3*), 12 hours (*BLC3::C3.GUS-3*), or 24 hours (*DLC3..C3.GUS-11*).

addition, leaf expression was strongest in the vascular system and the hydathode region at both 7 and 14 days. Four-week-old samples include all of the rosette leaves because these plants have transitioned to the reproductive stage. Most of the leaves are completely expanded and the newest leaves are completing expansion. Regardless of when the leaf developed, all leaves showed the same *C3* gene expression pattern and relative promoter strength as described above for 7- and 14-day-old seedlings (Figure 68). The "blotchy" expression observed in some of the tissues is likely due to difficulty infiltrating the GUS substrate into the sample. The exact reason for the lack of infiltration is not known but may be due to more waxy cuticle present on older plants, difficulty keeping large plant samples immersed in the substrate solution during vacuum infiltration or smaller air spaces available for substrate uptake in young leaves. Cauline leaves were also observed and detectable *C3* gene expression was limited to the leaf veins and hydathode regions after 24 hours of incubation with GUS substrate; there was little expression in epidermal or mesophyll cells (data not shown).

Expression in specialized leaf epidermal cells was also examined. Extremely weak expression in developing guard cells of 7-, 10-, and 14-day-old seedlings was first detected after 3 hours of incubation in the GUS substrate (data not shown). After 12 or 24 hours of incubation, expression was clearly seen in the meristemoids, guard mother cells, and immature guard cells (data not shown). Another specialized cell type is the trichome. Trichomes undergo massive cell expansion and branching to form prominent features of the leaf surface visible to the naked eye. *C3* expression was seen in expanding trichomes on all ages of leaves after 12 or 24 hours of incubation in the GUS substrate (Figure 69). No *C3* expression was observed in mature trichomes after

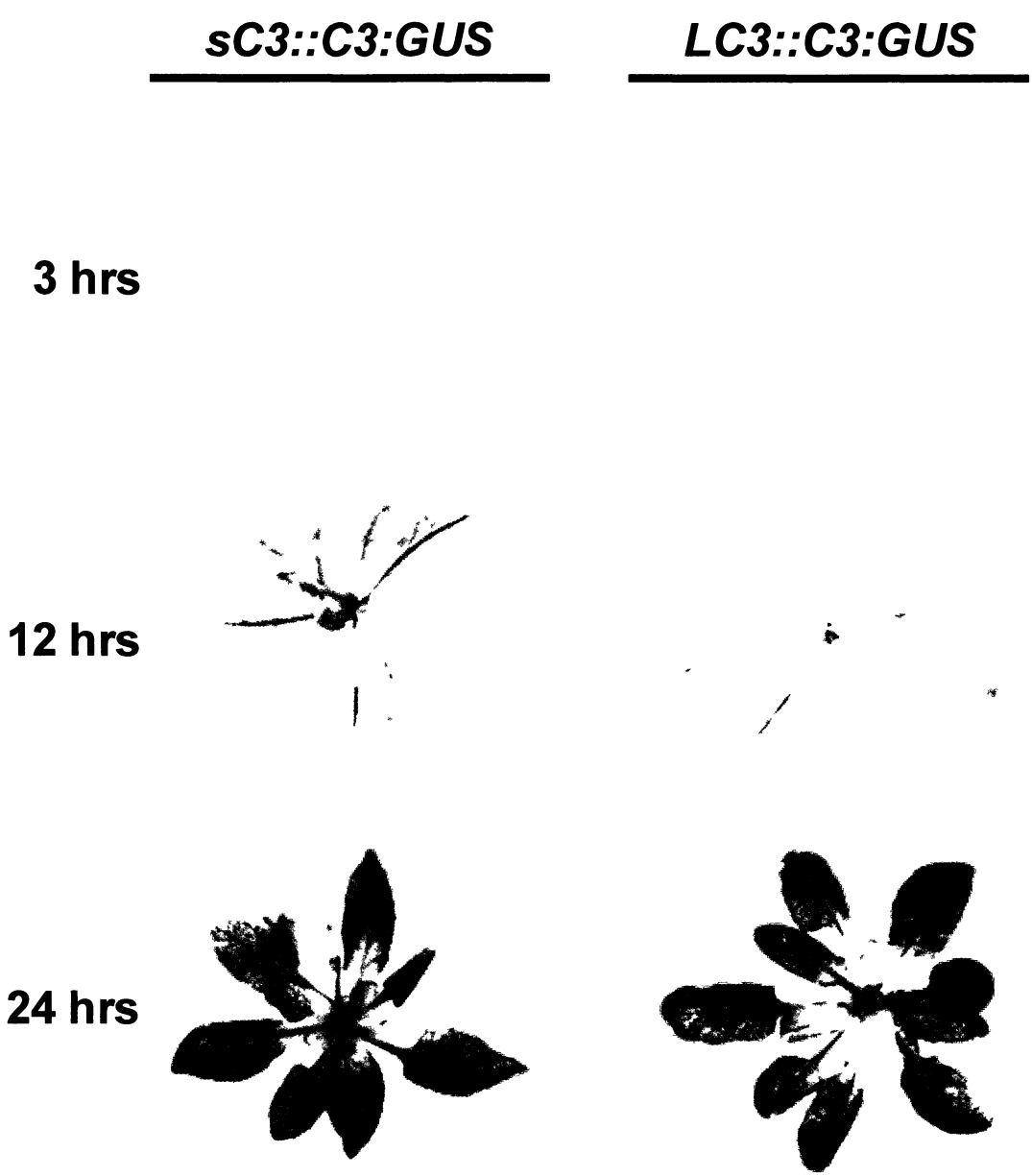

Figure 68. Expression of *sC3* and *LC3* in 4-week-old plants.
3 hour *sC3::C3:GUS* line was *AC3::C3:GUS-6* and *LC3::C3:GUS* line was *DLC3::C3:GUS-6*. 12 hour *sC3::C3.GUS* line was *CC3::C3:GUS-1* and *LC3::C3:GUS* line was *DLC3::C3:GUS-7*. 24 hour *sC3::C3:GUS* line was *AC3::C3:GUS-3* and *LC3::C3:GUS* line was *DLC3::C3:GUS-6.*

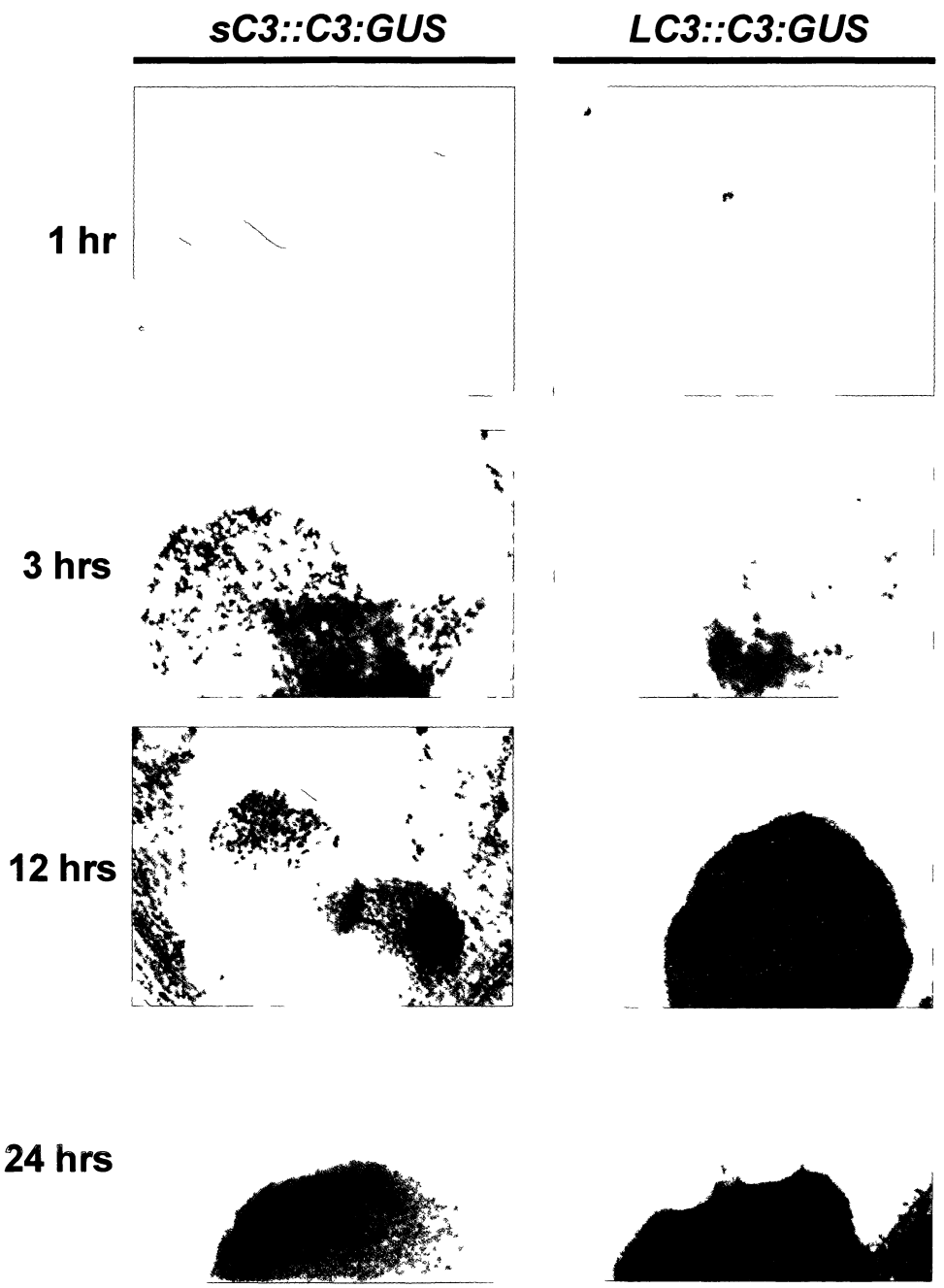

Figure 69. Expression of *sC3* and *LC3* in trichomes.
sC3::C3:GUS lines were all 7-days-old and incubated for 1 hour (*CsC3::C3:GUS-11*), 3 hours (*CsC3::C3:GUS-9*), 12 hours (*CsC3::C3:GUS-9*), and 24 hours (*CsC3::C3:GUS-9*). *LC3::C3:GUS* lines were 7-days-old and incubated for 1 hour (*BLC3::C3:GUS-2)*, 3 hours (*BLC3::C3:GUS-2)*, 12 hours (*BLC3::C3:GUS-3)*, and 24 hours (*BLC3::C3:GUS-2)*.

expansion was complete. In conclusion, both *sC3* and *LC3* constructs have the very similar expression patterns in cotyledons and leaves indicating that the regulatory elements required to drive expression in the cotyledons and leaves were located within the short *C3* promoter construct. The additional sequence in the longer construct did not provide any additional regulation of expression that could be detected with this method. *C3* gene expression in cotyledons, leaves, roots, and hypocotyls was typically higher in the vascular system than in the surrounding tissues. The highest *C3* expression in the vegetative parts of the plant occurred in the meristematic zone of roots, followed by vascular system of roots and shoots.

II.D.1.b.iii. *sC3* and *LC3* expression pattern in reproductive organs

Arabidopsis raceme anatomy and development were described in Section II.A.4. The inflorescence stems from 6-week-old plants were dissected and then assayed in the GUS substrate for *C3* gene expression. The results showed that, overall, there was fairly consistent expression between the *sC3* and *LC3* lines.

In all floral stages, expression was rarely observed in petals or sepals for either the *sC3* or *LC3* lines (Figure 70). When expression was observed, it occurred in the vascular tissues of these organs. The reason for this variability is not known but could be due to line-to-line variation caused by T-DNA position effects or to *C3* gene expression only occurring for a brief time during development which did not always coincide with the assay period. In contrast, the stamens revealed consistent expression in all lines assayed. The filament showed expression from stages 14 to 15, although filament expression in stage 15 was limited to the region nearest the anther (Figure 70).

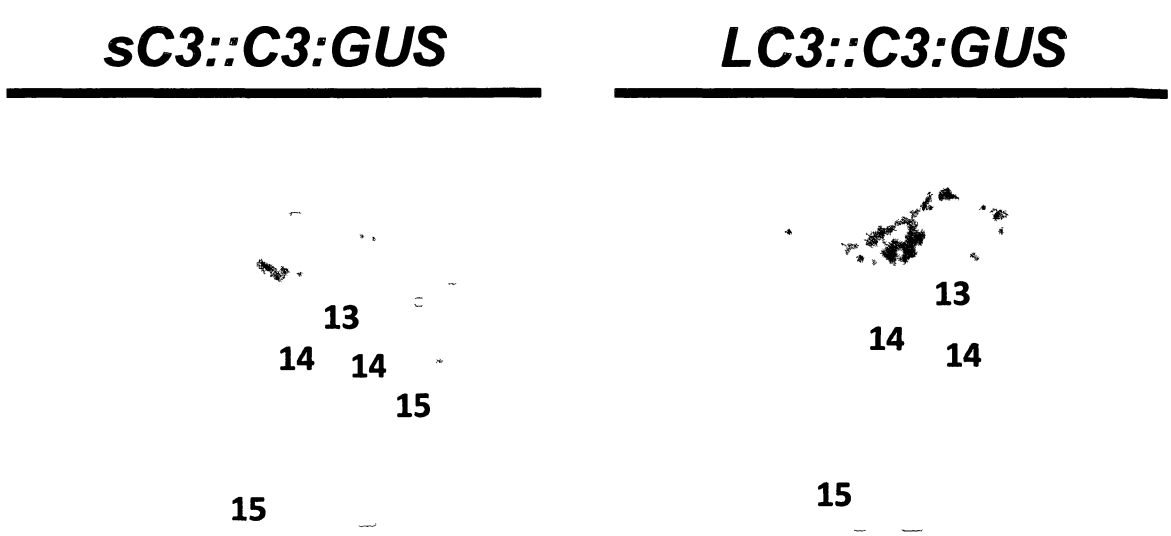

Figure 70. Expression of *sC3* and *LC3* in the floral apex.
Both *sC3* and *LC3* lines were incubated for 24 hours. The *sC3* line was *sC3::C3:GUS-6* and the *LC3* line was *LC3::C3:GUS-4*. Floral stages from Table 5 are indicated.

Expression was also seen in the dehisced pollen in stage 14 (not shown).

Expression was observed in the carpels from both *sC3* and *LC3* lines. Although the exact stage could not be determined without dissection, expression was seen throughout the carpels in buds of unknown easily floral stages (Figure 70). At stages 12-15, *sC3* and *LC3* expression in carpels was seen primarily at the apex, and included the stigma at stage 12 only. Also, at stage 15, strong expression was seen in the nectary.

In general, stage 16 siliques showed *C3* gene expression in the apex and base and there was less consistent expression in the vasculature (Figure 71). In stage 17a, siliques showed expression in most of the silique, which was easier to detect in *sC3* than *LC3* lines. Stage 17b *C3* expression was limited primarily to the basal region of the silique. Stage 18, 19 and 20 siliques had no detectable expression.

In conclusion, *C3* gene expression was observed in flowers, especially in carpels and stamens. Expression in both *sC3* and *LC3* lines were generally similar in all floral tissues. Therefore, similar to the vegetative tissue, the regulatory region needed to drive expression in floral structures was located within the *sC3* construct.

II.D.1.c. Summary of *C3* subunit gene expression pattern

Although images for all of the available transgenic lines were not included in this thesis, all of the *sC3* and *LC3* lines examined had similar expression patterns and similar relative expression levels all in vegetative tissues, indicating that the short promoter construct contained all of the necessary regulatory information. Both constructs included all of the introns and exons, and important regulatory information could be located in this region. Since multiple independent transgenic lines were examined for each construct,

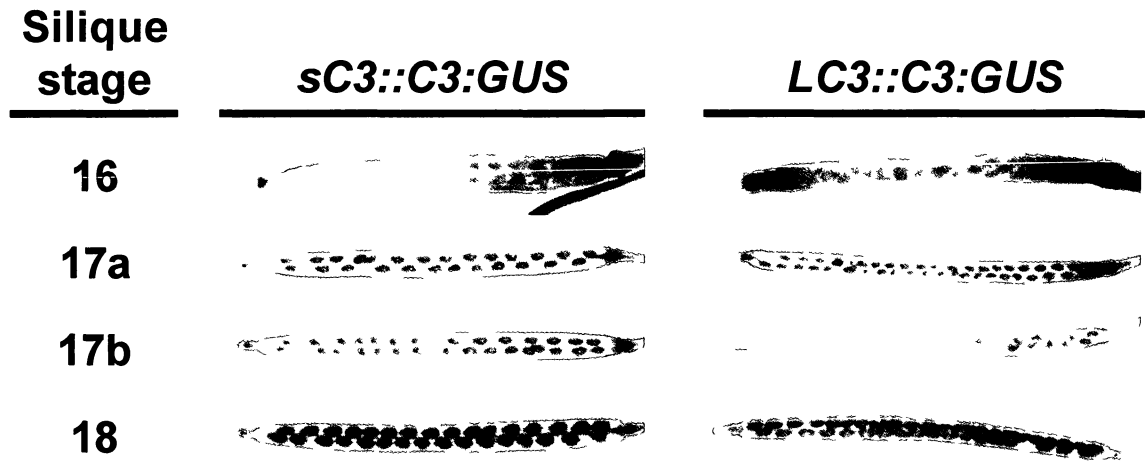

Figure 71. Expression of *sC3* and *LC3* in siliques.
sC3 lines were *AsC3 :C3.GUS-6* incubated for 24 hours. *LC3* lines were *DLC3:.C3: GUS-4* incubated for 24 hours.

these results also demonstrate that there was little or no effect from T-DNA insertion site and that any PCR errors that may have occurred in the constructs had no detectable effect on expression. A summary of the expression patterns of *sC3* and *LC3* is in Figure 72.

II.D.2. Class II C subunit (*C3* and *C4*) gene expression patterns

The Protein Phosphatase 2A class II subunits, C3 and C4, are 98% identical with only 6 amino acid differences out of 313 total amino acids (Figure 57). Even at the nucleotide sequence level, the coding sequences are 91.4% identical (Figure 59). From these observations, one might guess that these two subunits would be functionally redundant because of the high degree of similarity. However, despite being highly conserved in amino acid and nucleotide sequence, we discovered a sodium-induced root growth phenotype for the *c4* mutant plants. This led to the hypothesis that the *C3* gene may not be expressed in roots and therefore would be unable to compensate for the missing C4 subunit. The fact that the promoter sequences and regulatory elements of these two genes are very different (Figure 61) also led me to expect that the *C3* and *C4* genes might have different expression patterns but this is not what I found.

A detailed description of *C4* and *C3* gene expression is available in Sections II.B and II.D.1, respectively. A comparative overview of *C3* and *C4* gene expression patterns is shown in Figure 73 and key points will be summarized here. Root tip expression patterns of the *C3* and *C4* genes are extremely similar, especially in the elongation zone. The site of highest expression in both *C3* and *C4* lines is the roots, especially the primary root tip region and lateral root meristem (See Section II.B and III.D.1 for further details). All other shoot and reproductive tissues also revealed a high degree of similarity between

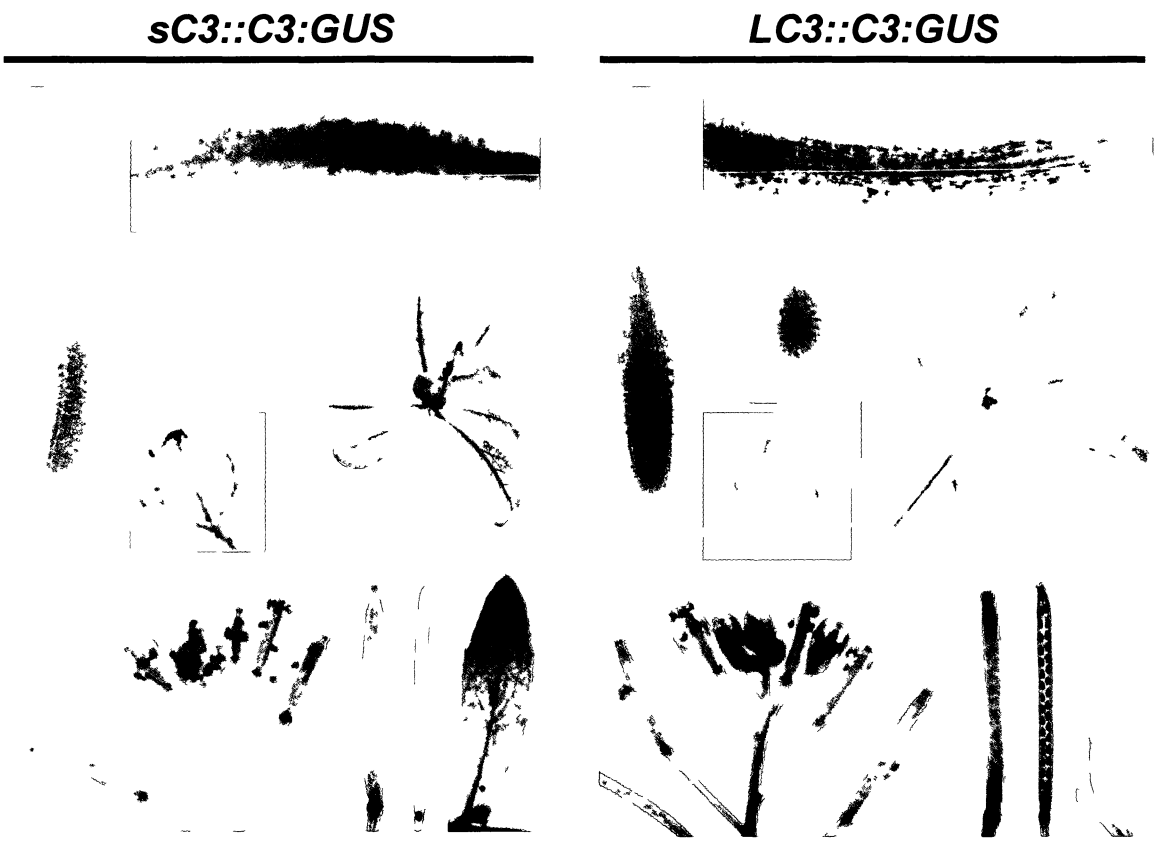

Figure 72. Comparison of the expression pattern of *sC3* and *LC3* promoter constructs in different tissues of *Arabidopsis thaliana*.

Organs shown for *sC3*, from top to bottom, were root tip (7-day-old, 1 hour assay), hypocotyl (7-day-old, 12 hour assay), lateral root (10-day-old, 3 hour assay), cotyledon (7-day-old, 12 hour assay), 4 week old plants (12 hour assay), floral apex (24 hour assay), siliques (24 hour assay) and cauline leaf (24 hour assay). Most samples were *AsC3::C3:GUS-6* except for the 4-week-old plant which was *CsC3::C3:GUS-1*.

Organs shown for *LC3*, from top to bottom, were root tip (*DLC3::C3:GUS-3*, 7-day-old, 1 hour assay), hypocotyl (*DLC3.::C3::GUS-7*, 7-day-old, 12 hour assay), lateral root (*DLC3::C3:GUS-11*, 10-day-old, 3 hour assay), cotyledon (*DLC3::C3:GUS-3*, 7-day-old, 12 hour assay), 4-week-old plant (*DLC3::C3:GUS-7*, 12 hour assay), floral apex (*DLC3::C3:GUS-4*, 24 hour assay), siliques (both *DLC3::C3:GUS-7*, 24 hour assay) and cauline leaf (*DLC3::C3:GUS-4*, 24 hour assay).

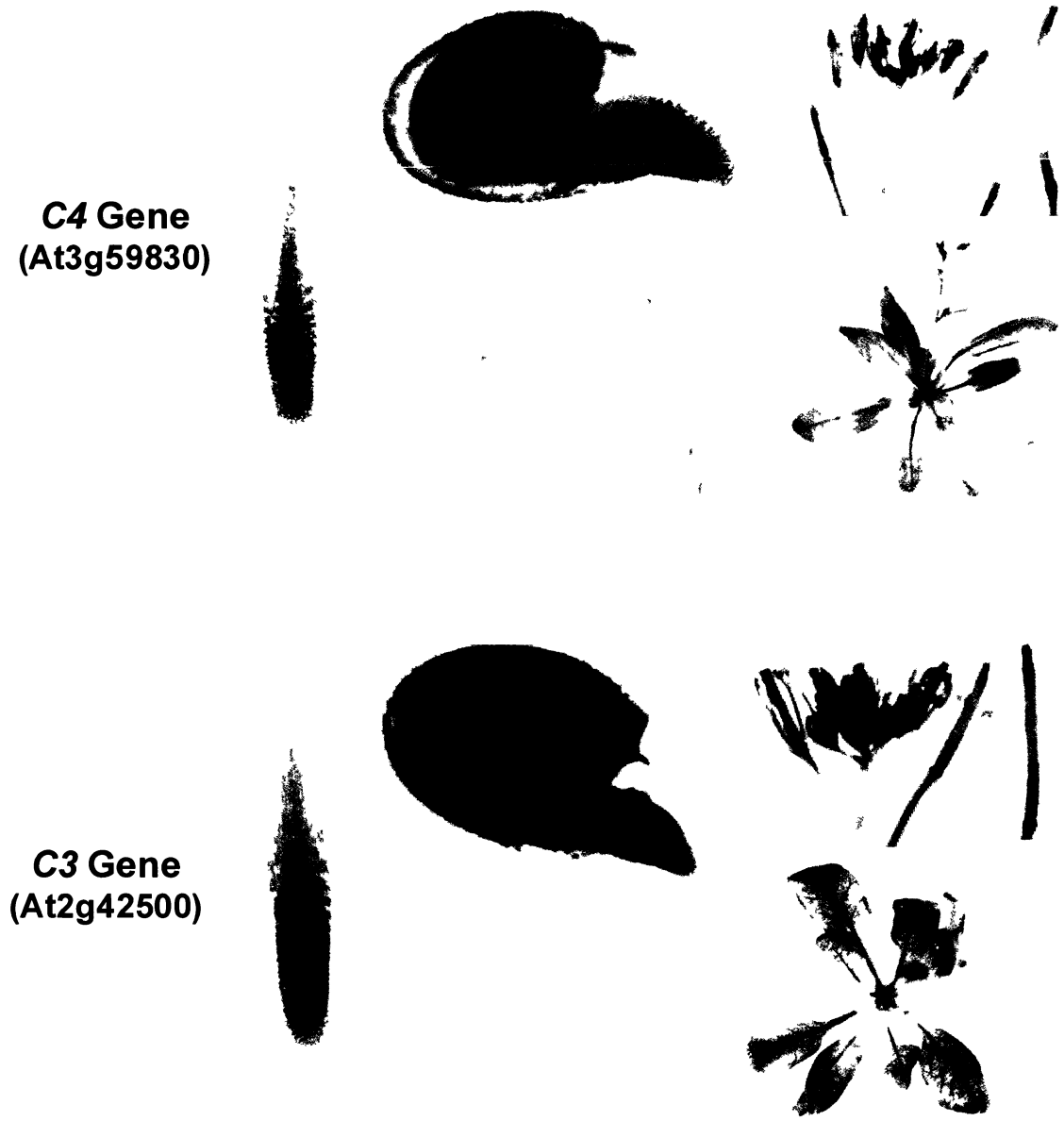

Figure 73. Comparison of Class II PP2A C subunit gene expression in Arabidopsis.
C4 gene: Representative examples of *C4* gene expression in the primary root tip (*AC4::C4:GUS-2* 7-day-old, 1 hour assay), 1-day-old seedling (*AC4::C4:GUS-2*, 16 hour assay), floral apex (*AC4::C4:GUS-4*, 24 hour assay), silique (*CC4::C4:GUS-4*, 24 hour assay), lateral root (*AC4::C4:GUS-2*, 10-day-old, 1 hour assay), cotyledon (*AC4::C4:GUS-2*, 10-day-old, 1 hour assay), and 4-week-old plant (*AC4::C4:GUS-7*, 24 hour assay).
C3 gene: Representative examples of *C3* gene expression in the primary root tip (*BLC3::C3:GUS-2*, 7-day-old, 1 hour assay), 1-day-old seedling (*AC3::C3:GUS-3*, 12 hour assay), floral apex (*DLC3::C3:GUS-7*, 24 hour assay), silique (*DLC3::C3:GUS-7*, 24 hour assay), lateral root (*AC3::C3:GUS-3*, 14-day-old, 1 hour assay), cotyledon (*AC3::C3:GUS-3*, 8-day-old, 12 hour assay), and 4-week-old plant (*CC4::C4:GUS-8*, 24 hour assay).

the *C3* and *C4* gene expression patterns. Relative expression strength in the cells of each organ was also similar. Therefore, I conclude that the *C3* and *C4* gene expression patterns and relative expression levels are almost identical. As a result, the initial hypothesis that the *C3* and *C4* genes would have disparate expression patterns was not supported.

II.D.3. Class I C subunit (*C1*, *C2*, and *C5*) genes expression patterns

Class I of the Arabidopsis PP2A C subunits has three members: C1, C2, and C5. C5 is 93.2% identical to both the C1 and C2 subunits at the amino acid level (Figure 57) while C1 and C2 are 97.1% similar to each other, meaning that C5 is the most divergent Class II subunit. *C1*, *C2*, and *C5* gene expression was determined during multiple developmental timepoints and for several incubation times in the GUS substrate as described previously in Section II.B. When equivalent developmental times and incubation times were compared, I observed similar expression patterns and expression intensities between all of the Class I C subunits.

Expression was detected throughout the roots, with the highest gene expression in the primary root tips and the lateral root meristems (Figure 74). Expression was also observed throughout the cotyledons and rosette leaves with the highest expression in the vascular system. Cauline leaf expression was restricted primarily to the veins. Floral expression was universally observed in the filaments, dehisced pollen, carpels, and siliques while expression in the petal veins was only detected in the *C2* lines. In conclusion, the *C1*, *C2*, and *C5* subunit genes have highly overlapping expression patterns and similar relative expression levels.

II.D.4. Highly overlapping and similar protein phosphatase 2A C subunit gene expression patterns

C1, *C2*, *C3*, *C4* and *C5* gene expression was compared at all developmental stages previously defined (Section II.B). The root expression pattern for all five subunits was very similar (Figure 75 and data not shown). All subunits are expressed throughout the root and the root tips are the site of the highest relative gene expression for all subunits.

In general, the cotyledon, rosette leaf and cauline leaf expression was similar for all five subunits with the highest relative expression in the vascular tissue compared to the other leaf tissues (Figure 75). Additionally, gene expression of each C subunit was observed in expanding trichomes and developing guard cells (not shown). Despite these similar expression patterns in the vegetative tissues, there was some difference in the expression pattern in the reproductive structures particularly in the sepals and petals. Stamen, carpel and silique expression was similar for all subunits but expression in the petal veins was often visible in the *C2* lines, occasionally observed in *C3* lines, and not seen for the other C subunits. Sepal expression in the veins was sometimes observed for *C1*, *C2*, and *C4* but was inconsistently observed for the *C3* lines. *C5* gene expression was not observed in either petals or sepals.

These results indicate that the highly homologous C subunits have very similar expression patterns. Intriguingly, similar expression was observed from constructs containing the sequence upstream and gene sequence from the different C subunits indicating that the elements that are present are able to drive similar expression of all the C subunits.

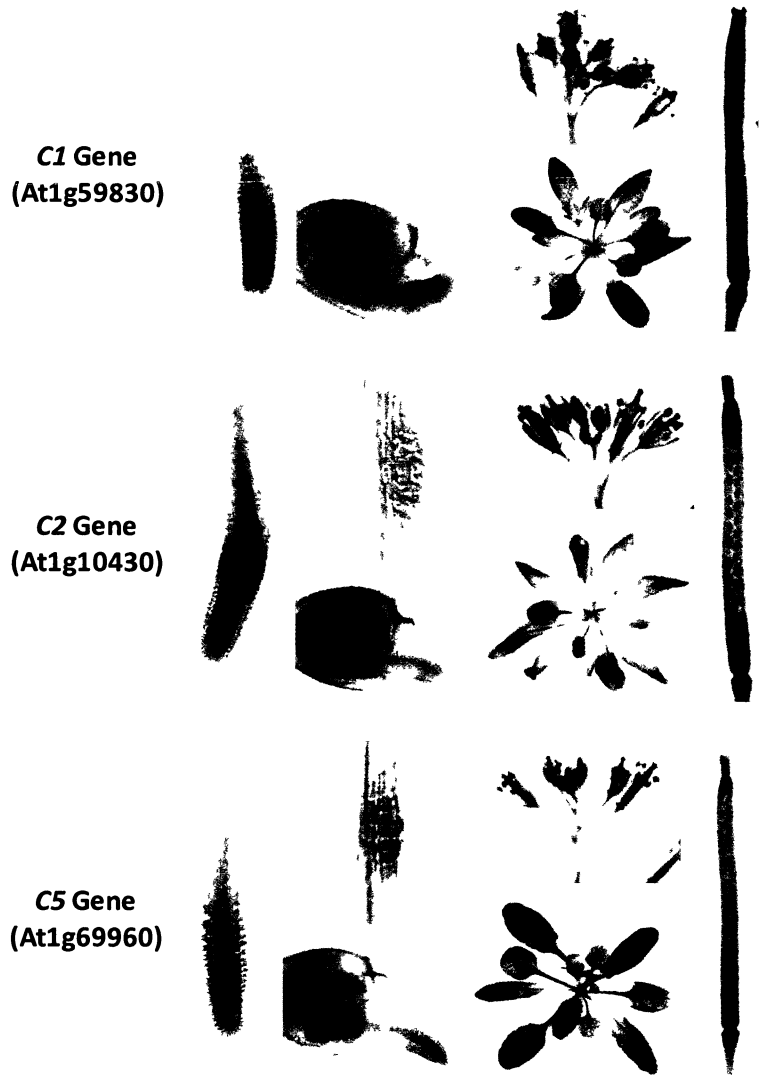

Figure 74. Class I PP2A C subunit gene expression in *Arabidopsis thaliana.*
Representative examples of *C1* gene expression in the primary root tip (*AC1::C1:GUS-2* 10-day-old, 1 hour assay), lateral root (*AC1::C1:GUS-2* 10-day-old, 1 hour assay), floral apex (*BC1::C1:GUS-1*, 24 hour assay), silique (*AC1::C1:GUS-4*, 24 hour assay), 1-day-old seedling (*BC1::C1:GUS-6*, 16 hour assay), and 4-week-old plant (*AC1::C1:GUS-2*, 24 hour assay).
Representative examples of *C2* gene expression in the primary root tip (*AC2::C2:GUS-8*, 14-day-old, 3 hours assay), lateral root (*AC2::C2:GUS-8*, 14-day-old, 1 hour assay), floral apex (*AC2::C2:GUS-8*, 24 hour assay), silique (*AC4::C4:GUS-8*, 24 hour assay), 1-day-old seedling (*AC2::C2:GUS-5*, 16 hour assay), and 4-week-old plant (*EC2::C2:GUS-3*, 24 hour assay).
Representative examples of *C5* gene expression in the primary root tip (*BC5::C5:GUS-4* 4-day-old, 1 hour assay), lateral root (*BC5::C5:GUS-4* 4-day-old, 1 hour assay), floral apex (*BC5::C5:GUS-11*, 24 hour assay), silique (*BC5::C5:GUS-11*, 24 hour assay), 1-day-old seedling (*BC5::C5:GUS-1*, 24 hour assay), and 4-week-old plant (*AC5::C5:GUS-2*, 24 hour assay).

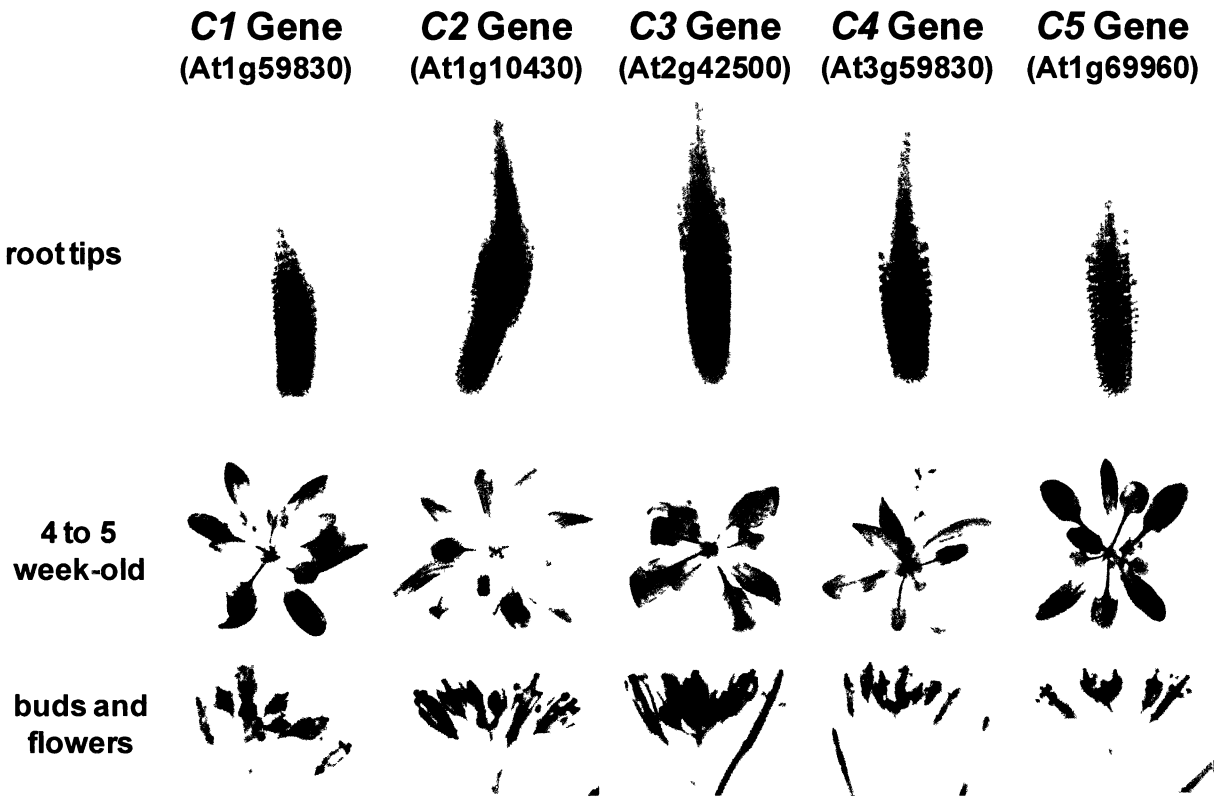

Figure 75. Gene expression of all five Protein Phosphatase 2A C subunit genes in *Arabidopsis thaliana*.
Root tip expression pattern from *C1* (*AC1::C1:GUS-2*, 10-day-old, 1 hour assay), *C2* (*AC2::C2:GUS-8*, 14-day-old, 3 hour assay), *C3* (*BLC3::C3:GUS-2*, 7-day-old, 1 hour assay), *C4* (*AC4::C4:GUS-2*, 7-day-old, 1 hour assay), and *C5* (*BC5::C5:GUS-4*, 4-day-old, 1 hour assay).
Expression pattern at 4-5-weeks from *C1* assayed for 24 hours (*AC1::C1:GUS-2*), *C2* (*EC2::C2:GUS-3*), *C3* (*CC4::C4:GUS-8*), *C4* (*AC4::C4:GUS-7*), and *C5* (*AC5::C5:GUS-2*).
Flower apex expression pattern from *C1* assayed for 24 hours (*BC1::C1:GUS-1*), *C2* (*AC2::C2:GUS-8*), *C3* (*DLC3::C3:GUS-7*), *C4* (*AC4::C4:GUS-4*), and *C5* (*BC5::C5:GUS-11*).

II.E. *C3* and *C4* gene expression pattern under different growth conditions

Plants with mutated C*4* gene have an altered root growth response to Na^+ (Wang, 2008). The expression pattern of the *C4* gene was examined on medium supplemented with NaCl to determine if a change in expression could be associated with the root skewing phenotype. To determine when to observe *C4* gene expression, the angle of root skewing was measured daily to establish when the most skewing occurred during the seven days post-transfer to NaCl supplemented medium. *C3* gene expression was also observed to see if there was a change in expression of this highly homologous C subunit.

II.E.1. Daily measurement of NaCl-induced root skewing

As described previously, *c4* mutant plants display a NaCl-induced root skewing phenotype. This phenotype is observed as an alteration in root growth direction. After transfer to medium containing additional NaCl, *c4* mutant plants undergo a permanent change in root growth direction and do not align to the gravity vector. To determine the time course of root skewing, wildtype and *c4-2* seedlings (Table 2) were grown for three days on vertically-oriented 0.5X MS plates, then transferred to fresh plates. The time of transfer is considered time 0 (Figure 81A). Plates were oriented vertically in a growth room. The experiment consisted of 10 plates of basal media and 10 plates with additional NaCl; each plate received 5 wildtype seedlings and 5 *c4-2* mutant seedlings. The experimental design was a 2X2 ANOVA and significance was determined by Tukey's test. Wildtype and *c4-2* seedlings grown on 0.5X MS medium exhibited slight positive (rightward) skew and were statistically indistinguishable at all time points (Figure 76A). Slight rightward root skewing of wildtype seedling roots is normal and has been reported

previously (Rutherford and Masson, 1996; Oliva and Dunand, 2007). Wildtype seedlings grown on 0.5X MS+75 mM NaCl had a slight leftward skew which was significantly different from wildtype seedlings grown on 0.5X MS at days 1 through 7. An effect of NaCl on the direction of root growth of wildtype seedlings has also been described previously (Sun et al., 2008; Wang, 2008). Roots of *c4-2* seedlings grown on 0.5X MS+75 mM NaCl displayed a pronounced negative (leftward) skewing that was significantly different from wildtype seedlings grown on the same medium. Wildtype and *c4-2* root angles were significantly different from day 1 through day 7. These results indicate that there are significant differences in the angle of root skewing for the *c4-2* mutant grown on 0.5X MS+75 mM NaCl compared to the other condition and genotype and that this effect is apparent within 24 hours after transfer of seedlings to the NaCl-supplemented medium. The greatest changes in direction of root growth seemed to occur soon after transfer to NaCl-supplemented medium. To determine when the greatest amount of change in growth direction occurred, the absolute day-to-day change in the skewing angle was calculated (Figure 76B). The most dramatic change in skewing angle occurred on the first and second days after *c4-2* seedlings were transferred to 0.5X MS+75 mM NaCl medium. After the first two days, little daily change in the angle of root growth was observed.

II.E.2. *C4* and *C3* gene expression pattern when exposed to NaCl

A dramatic change in the angle of root growth occurred for *c4* mutant roots, but not wildtype roots, when exposed to increased concentrations of NaCl (Figure 76). One

A)

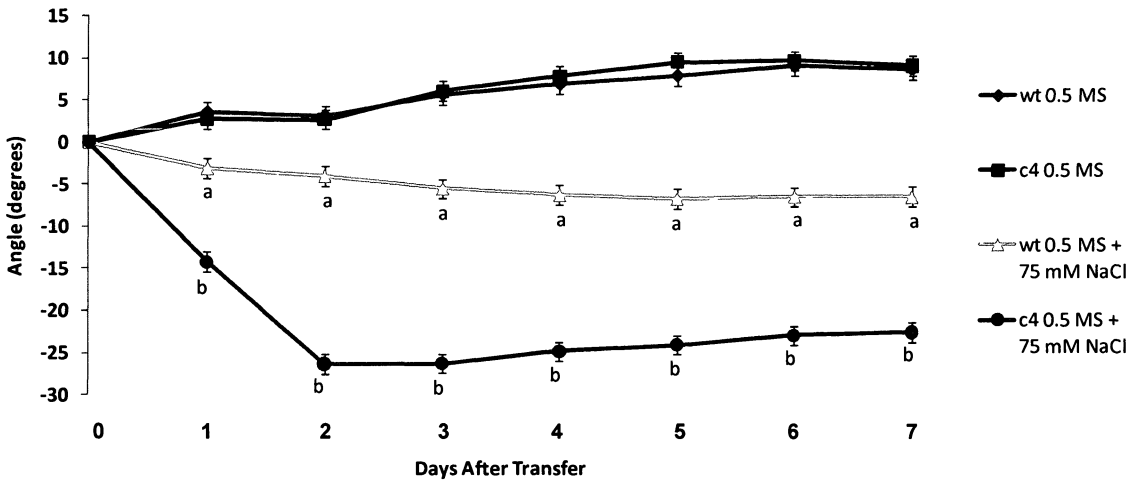

B)

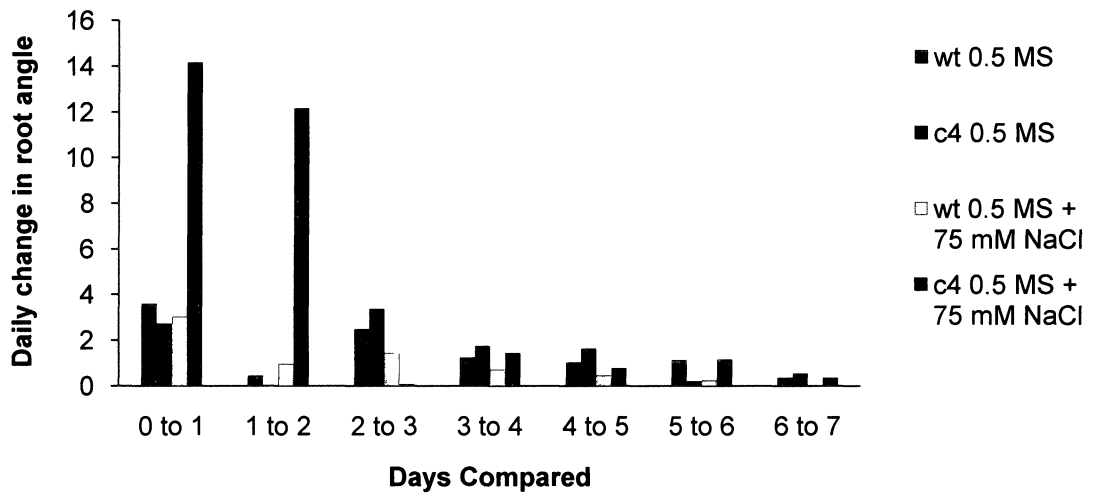

Figure 76. Angle of root growth of wild type (wt) and *c4-2* mutant on 0.5X MS or 0.5X MS+75 mM NaCl.

A) Average root angle measurements of wild type and *c4-2* on different media over seven days of growth. Approximately ten plates per experimental condition (~10 0.5X MS and ~10 0.5X MS + 75 mM NaCl) were measured, The experiment was repeated once. Error bars represent standard deviation of the population of the entire experiment. The p value resulting from an ANOVA was 0.000 and significance between the genotypes and media per day was determined by a Tukey's test. For each day, values differing significantly from each other are represented by no letter, a or b. **B)** Change in root growth angle from day to day.

hypothesis to explain this phenotype is that changes in *C4* gene expression are needed to help roots adapt to high levels of NaCl. Changes in *C4* gene expression might indicate a role for the C4 subunit in response to NaCl stress. To determine if there was a change in *C4* gene expression after transfer of seedlings to medium containing elevated NaCl concentrations, *C4* gene expression in roots was examined using a wildtype plant line containing the *AC4::C4:GUS-2* reporter construct at 1, 2 and 7 days after transfer to 0.5X MS+NaCl. One representative line was used for all experiments. Seedlings were incubated with the GUS substrate for 1 hour or 3 hours. Based on the promoter strength determined in section II.B, these assay times would easily show expression on basal media. There was no observable difference in expression between seedlings grown on the two media or assayed for 1 or 3 hours (Figure 77). However, the data does not rule out the possibility that changes in NaCl concentration may have other effects on the C4 subunit of PP2A, such as altering subcellular localization or affecting protein-protein interactions.

Expression patterns of the *C3* and *C4* subunit genes in plants undergoing NaCl stress were compared because these two subunits are highly homologous. The C3 and C4 proteins are 98% identical, differing in only 6 of 313 amino acids, although the motifs in the *C3* and *C4* subunit gene promoter regions are dissimilar (Figure 61 and data not shown). From analysis of the *c4* mutant, we have detected a NaCl-induced root skewing phenotype indicating that either the C4 protein has a unique function or that a correct C subunit dosage is needed. As described previously, the expression patterns of the *C4* and*C3* genes on basal medium (0.5X MS) are very similar. Therefore representative *C3* (A*C3::C3:GUS-3*) and *C4* (A*C4::C4:GUS-2*) lines were chosen and compared at 1 and

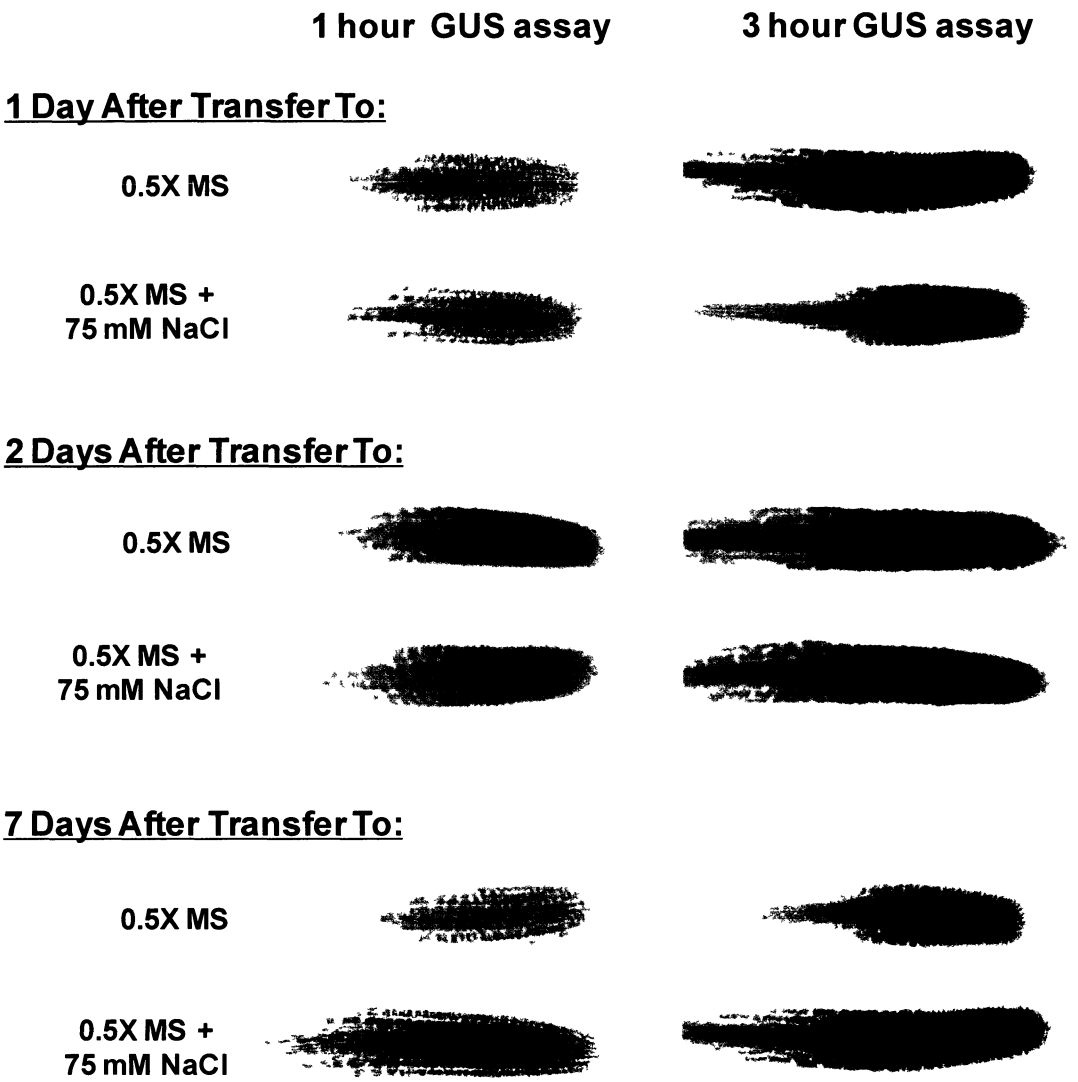

Figure 77. ***C4::C4:GUS-2*** **expression in root tips of transgenic seedlings transferred to 0.5X MS or 0.5X MS+75 mM NaCl.**
3 day-old seedlings were transferred from 0.5 X MS plates to either 0.5X MS or 0.5X MS+75 mM NaCl media and assayed 1, 2, or 7 days later.

7 days after transfer to medium supplemented with NaCl. The expression patterns of *C3::C3:GUS* in seedling root tips at 1 and 7 days post-transfer were similar (Figure 78). In addition, no obvious differences in *C3* gene expression were apparent whether seedlings were transferred to unsupplemented or NaCl-supplemented medium. A comparison of the expression pattern of *C4::C4:GUS* and *C3::C3:GUS* roots grown on the two media showed strong similarity between the two C subunits (Figure 79). From this result, it does not appear that the *C3* and *C4* genes are regulated by the presence of NaCl.

II.E.3. *C4* gene expression on NaCl or equivalent osmoticum

Real-time PCR was used as a more sensitive method than using qualitiative GUS assay experiments to determine if *C4* gene expression in roots changed after transfer to medium supplemented with NaCl. In addition, medium supplemented with mannitol at an equivalent osmolarity was used. Mannitol, a non-metabolizable sugar alcohol, was chosen to mimic the increase in osmotic strength caused by the addition of NaCl. When compared to the leftward skewing induced by NaCl, the addition of mannitol to the media causes a slight leftward root skewing (data not shown). Experimental design was the same as described in Section II.E.2 except that: 1) only wildtype was used, 2) 25°C and a photoperiod of 12 hours were used for the growth room conditions, 3) the seeds were sown in rows with almost no space between the seeds so plants would grow together in small clumps to enable faster transfer to the experimental media, and 4) three rows of seedlings were placed on the plates with experimental media. The roots were harvested 24 hours post-transfer to the experimental media. The three experimental media were

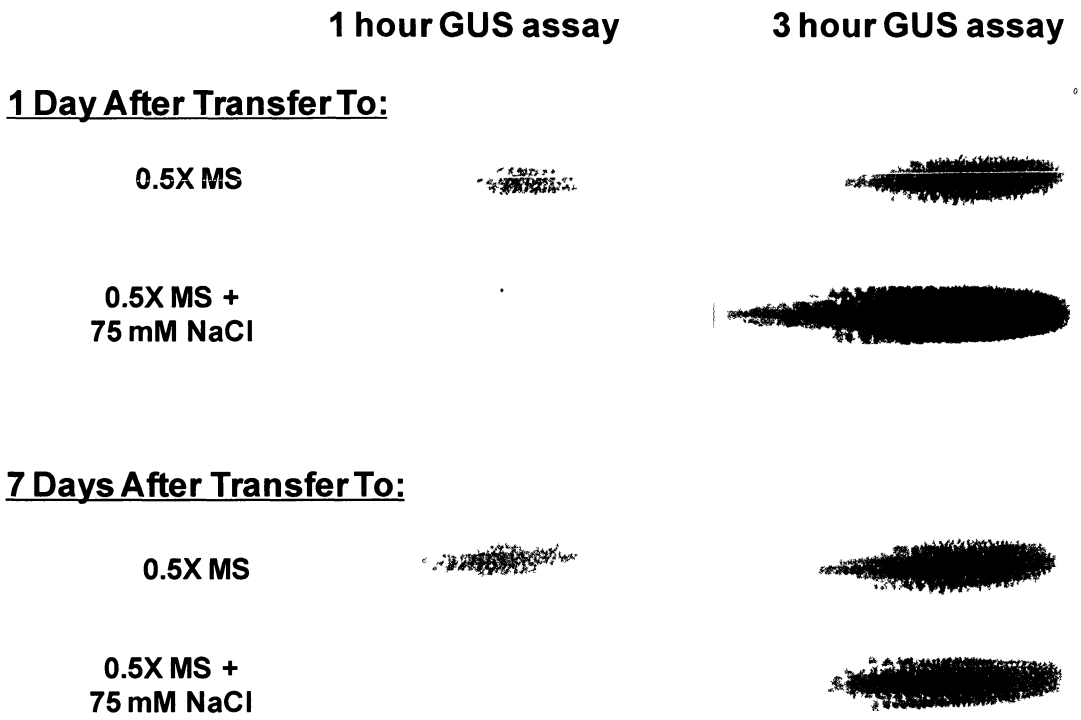

Figure 78. ***C3::C3:GUS-3*** **expression in root tips of transgenic seedlings transferred to 0.5X MS or 0.5X MS+75 mM NaCl.**
Three-day-old seedlings were transferred from 0.5 X MS plates to either 0.5X MS or 0.5X MS+75 mM NaCl media and assayed for GUS activity 1 or 7 days later. Two different GUS assay times were used.

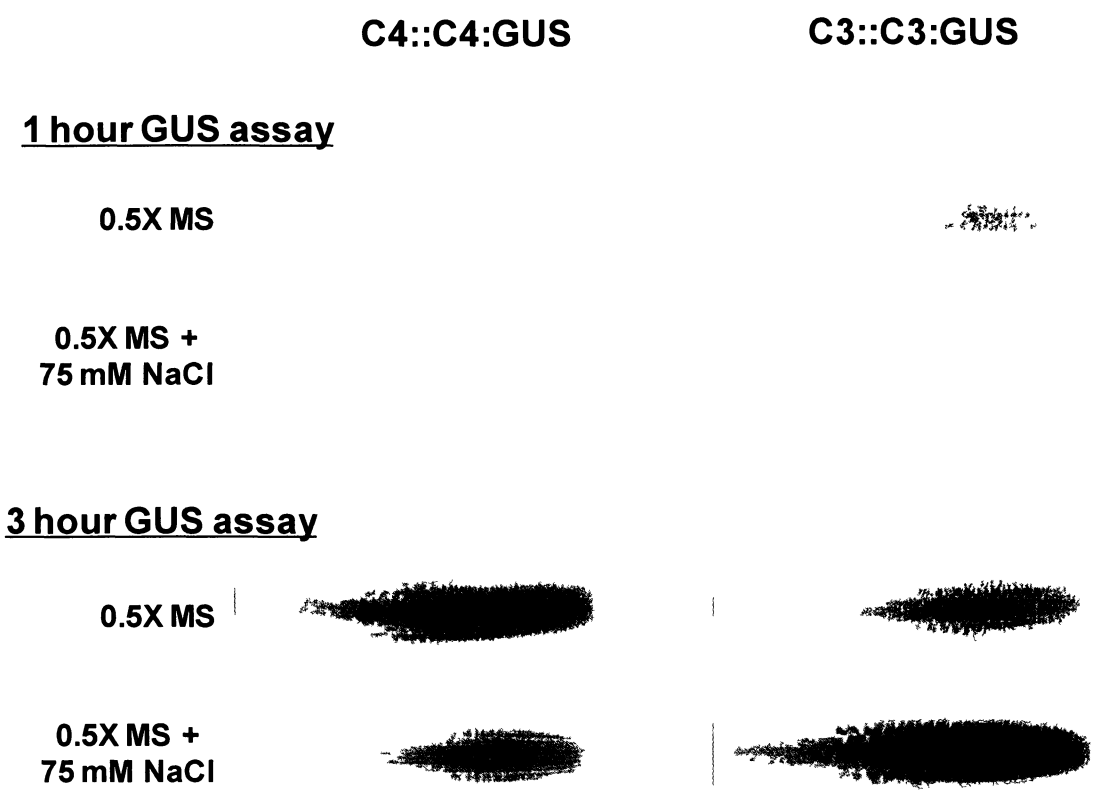

Figure 79. Comparison of *C4::C4:GUS* and *C3::C3:GUS* expression in root tips. Seedlings were transferred from 0.5 X MS plates to either 0.5X MS or 0.5X MS+75 mM NaCl media and assayed 1 day later. Two different GUS assay times were used.

basal medium (0.5X MS), basal medium supplemented with 75 mM NaCl, and basal medium supplemented with 150 mM mannitol. Two biological replicates were prepared for the basal and NaCl medium and only one replicate for mannitol. RNA was extracted, reverse transcribed into cDNA, and expression was determined using relative quantitative real-time PCR (Figure 80). Results indicated that neither NaCl nor mannitol caused a significant change in the level of *C4* gene expression.

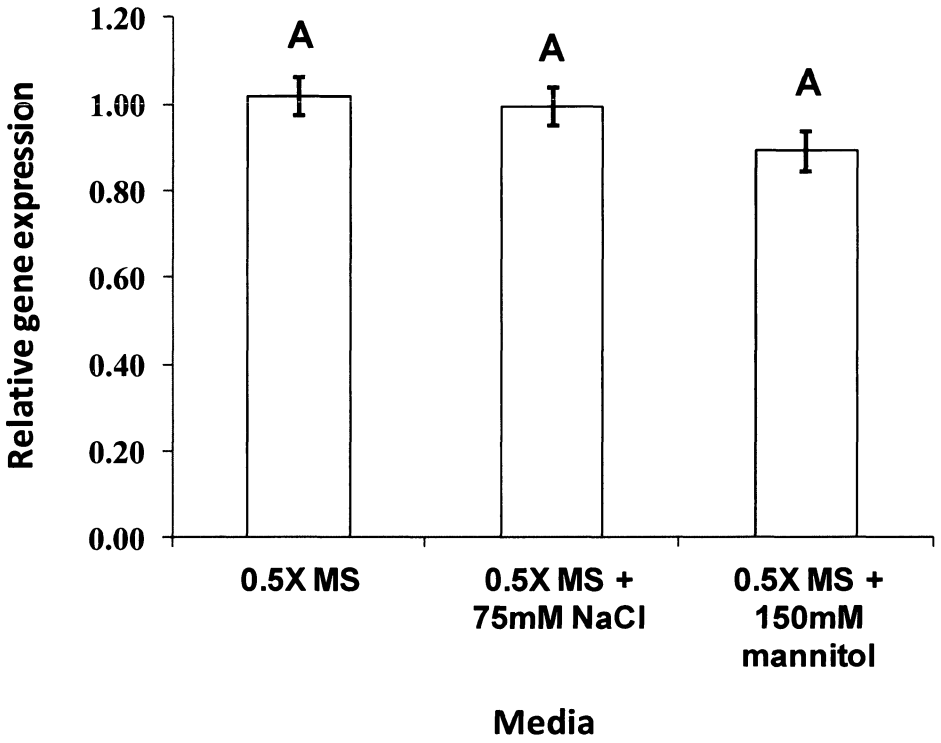

Figure 80. *C4* gene expression in roots measured by Real-Time PCR.
Data are represented as the ratio between the normalized critical thresholds (C_t) of the control condition versus the experimental condition and significance was determined by a Tukey's test. A indicates no significance.

CHAPTER III

DISCUSSION

The heterotrimeric protein phosphatase 2A is a biologically important enzyme that regulates many signaling pathways (Janssens and Goris, 2001). Previous work in the Hrabak lab demonstrated a Na^+-induced root skewing phenotype for the fourth isoform of the PP2A catalytic subunit in *Arabidopsis thaliana* (Wang, 2008). The first goal of this thesis was to document the expression of the *C4* gene during the life cycle of Arabidopsis and correlate the observed expression with the root skewing phenotype. The second goal was to document the expression patterns of the four other *C* subunit genes (*C1*, *C2*, *C3*, and *C5*) and compare the expression patterns of all five *C* subunit genes.

To elucidate the expression of the *C* subunits, constructs were made containing an upstream genomic region defined as the 'promoter' and the unspliced coding region upstream of the stop codon fused to the reporter *uidA* gene. The resulting protein would encode the entire C subunit with β-glucuronidase (GUS) fused to the C terminus. Similar constructs were made for each of the five C subunit genes and transformed into plants. Transgenic plants were selected using the antibiotic hygromycin and resistant plants were propagated. Plants were routinely assayed for β-glucuronidase for 1, 3, 12, and 24 hours. Assays were performed on plants that were 1, 2, 3-4, 6-7, 10, and 14 days-old, as well as on 4-week-old plants and on reproductive structures (buds, flowers and siliques) of mature plants. After clearing the chlorophyll with ethanol, the samples were photographed.

The results from this research showed that the *C4* gene was expressed in most cell

types throughout the plant at all stages of development. The highest expression was in the root tips and lateral root meristems which correlates with the expected location of the cells that would differentially elongate during Na^+-induced root skewing. The *C1*, *C2*, *C3*, and *C5* genes had very similar and overlapping expression patterns to the *C4* gene. Therefore, all PP2A C subunits are expressed throughout Arabidopsis development.

III.A. Rationale for constructs

A common molecular biology technique to determine expression of a gene-of-interest at the cellular level is to use a reporter gene. There are many reporter genes available and each has advantages and disadvantages and is dependent on the application. The reporter gene used for this study was β-glucuronidase (GUS), which is often utilized in plant molecular biology. The main advantage of GUS as a reporter is that low levels of expression in a single cell can be detected. The *uidA* gene encodes the very stable GUS enzyme which can be used to generate either quantitative or qualitative data. Qualitative data uses the colorless X-Gluc substrate which is cleaved by GUS resulting in an easily detectable blue diX-indigo precipitate. The product from this reaction accumulates over time as long as the substrate and enzyme are available. Therefore, weak expression can be detected by increasing the assay time. By using various assay times, it is possible to determine relative expression levels in different cells within a sample. Another advantage is that, for this application, the GUS assay is easier to use than other reporters such as green fluorescent protein (GFP). GFP is excited by a specific wavelength of light and the emission of the fluorophore is detected by fluorescence microscopy. A limitation of GFP is detecting weak expression if not enough GFP molecules have accumulated and

the amount of fluorescence is below the detection limit (Mantis and Tague, 2000). Also, GFP can undergo photobleaching upon prolonged exposure to the excitation wavelength, thus further reducing the GFP signal. Unlike GFP which requires a microscope capable of exciting the fluorophore, viewing and documenting the GUS assay samples does not require a special light source nor do the samples undergo bleaching. Therefore, there are many benefits to using the GUS reporter to determine *C* subunit gene expression.

Even though GUS is commonly used as a reporter gene in plant molecular biology, there are some drawbacks to this technique. One disadvantage is that endogenous GUS exists in plants and is active in acidic conditions and inactive at neutral to slightly alkaline pH (Martin et al., 1992). Neutral pH was used in all experiments to ensure that the observed diX-indigo precipitate occurred because of the GUS expressed from the transgene and not the endogenous GUS. Accumulation of diX-indigo in the reproductive tissue has been reported to occur in non-transformed plants at neutral pH (Martin et al., 1992); however, blue percipitate in reproductive tissues was not observed under the assay conditions used for this study (Figure 56). A second disadvantage is that detection of GUS is a destructive assay. If an entire plant is assayed, then clearly it is not possible to obtain progeny from this individual. A third disadvantage is that, to perform the assay, the sample must be immersed in the GUS substrate, vacuum infiltrated to remove as much air in the tissue as possible, and incubated for the desired assay period. These manipulations could alter the expression pattern if the promoter is induced by anoxic stress. Another issue observed in my study was that no expression was seen in parts of the leaf while other leaves at the same developmental level showed expression patterns in these areas. This non-reproducible pattern of expression was probably due to

the substrate did not fully penetrate the tissue (Guivarc'h et al., 1996). This problem was overcome by either viewing multiple samples to generate a clear picture of the expression patterns or by analyzing regions where the GUS substrate could easily penetrate the tissue. A fourth potential drawback is the stability of the GUS enzyme. In protoplasts, the intact GUS enzyme is estimated to be stable for approximately 50 hours (Jefferson et al., 1987). Because of the stability of the GUS enzyme, it can be difficult to determine when promoter function ceases. My constructs were made to fuse the protein of interest (C subunit) to the N-terminus of the GUS enzyme. Since protein half-life is typically controlled by the N-terminal amino acid (Varshavsky, 1997), the half-life of the fusion protein should be the same as the native protein. Another drawback is the cost of the GUS substrate, which may be cost prohibitive for some researchers. Despite these limitations, GUS was chosen because its many advantages.

A qualitative approach was used in this study to determine the cell specificity and the relative strength of PP2A C subunit gene expression. A region that should contain the entire promoter as well as the entire coding sequence (introns and exons) was fused upstream of and in-frame with the *uidA* gene. In plants transformed with such a construct, when the *C* subunit promoter region is activated, the protein product will be the C subunit with the GUS enzyme fused to its carboxy terminus. Due to technical limitations, potential regulatory information in the native 3' UTR and terminator were not included in this study although it is known that, in some genes, these downstream sequences may affect the level of expression (Larkin et al., 1993; Wickens et al., 2002; He and Hannon, 2004). In addition, mRNA half-life may be regulated by the 3' UTR. However, many reporter gene studies where the constructs did not include the native 3'

UTR or terminator have generated results consistent with microarray expression data or with in situ hybridization expression data (Becnel et al., 2006), indicating that these domains are not essential in many cases. The vector in this study, pMDC163, used the *NOS* terminator from the *Agrobacterium tumefaciens* nopaline synthase gene downstream of the *uidA* gene.

A plasmid control was constructed to determine if the flanking sequences in the T-DNA were able to induce expression of the *uidA* gene. No accumulation of the GUS product was observed in multiple control sample lines. This control also indicates that there was no endogenous GUS activity detected in the assay conditions used.

III.B. Comparison of results to previously-published C subunit expression patterns

Microarray data available online at the Genevestigator website (www.genevestigator.com) was examined to determine the native transcript expression of PP2A C subunit genes in whole tissues. Unfortunately, the *C3* and *C4* transcripts cannot be distinguished because of the probe used on the chip but expression data for the other C subunits was analyzed. In agreement with the results presented here, the microarray data shows that the *C1*, *C2*, and *C5* subunit genes are expressed at high levels throughout the plant and throughout Arabidopsis development. In contrast to the GUS expression data presented in this thesis, the microarray database does not reveal cell-specific expression and does not distinguish between the *C3* and *C4* subunits.

Like microarrays, northern blots have been use to detect the expression of C subunits in whole tissues. Expression data from various reports indicates that the *C1*, *C2*, *C3* and *C4* genes are expressed at different strengths throughout the plant (Arino et al.,

1993; Perez-Callejon et al., 1993; Casamayor et al., 1994). No northern blot data has been reported for the *C5* gene. These reports indicated that the highest expression for the C subunits was consistently in flowers and roots while the weakest expression was in the leaves of adult plants (Perez-Callejon et al., 1993; Casamayor et al., 1994). The high expression in flowers observed for the four C subunits is not consistent with the data presented in this thesis where flower expression was much weaker than the expression in other tissues. Both the expression data presented in this thesis and microarray data indicate that there is *C3* or *C4* expression in the leaves while Perez-Callejon et al. (1993) report no *C3* subunit expression in leaves using a northern technique. These blots were probed with 25S cytoplasmic ribosomal RNA to determine if the same amount of RNA was loaded in each lane, but this loading control was not published. Therefore, a potential reason for this discrepancy is that the transcript level was too low for detection using the northern technique. In all three studies, the strength of expression of the C1, C2, C3 and C4 subunits was not similar which is different from the relatively consistent levels of expression reported here. Similar to the microarray, northern analysis does not reveal expression patterns at the level of single cells. It is also unclear from the work of Perez-Callejon et al. (1993) and Casamayor et al. (1994) whether the probes used for northern analysis were specific to each C subunit. In summary, differences between the data presented here and previously published data are most likely due to the technical limitations of the different approaches used to determine C subunit expression.

Immunodetection of individual C subunits is complicated by their extremely high degree of amino acid conservation. Therefore, information generated by western blotting can only determine the presence of one or more C subunits in a tissue but cannot

differentiate between individual C subunits. C subunit(s) were detected in the root, hypocotyl, cotyledons and leaves of dark and light grown plants using monoclonial antibodies raised against the conserved amino acids near the carboxyl terminus of the human PP2A C subunits (Zhou et al., 2004). In mature plants, C subunit(s) protein was reported in roots, flowers, stem and whole rosettes of both Columbia and Wassilewskija plants and these data are congruent with the GUS expression data presented in this thesis. Zhou et al. (2004) also showed little to no C subunit expression in siliques of either ecotype using immunoblotting while in young siliques all three A subunits were detected. The GUS expression data presented in this thesis showed that all C subunits were expressed in siliques, albeit at a low level. The descrepancy may be explained if the expression of the C subunits in siliques is too low to detect with antibodies but can be detected with the GUS enzymatic assay.

The novel data presented in this thesis is the first documentation of the *C1*, *C3*, *C4* and *C5* subunit expression patterns determined by GUS. There are two previous reports documenting *C2* gene expression. In one study, nucleotides -561 to +23, counting from the transcription start site of the *C2* gene, were fused to the *GUS* reporter gene and the resulting expression pattern at various stages of development was documented (Thakore et al., 1999). The promoter region used by Thakore et al. (1999) included the region up to the preceeding gene encoding tRNA-proline. In my study the tRNA-proline gene and the sequence upstream to the next protein encoding gene was included as the *C2* "promoter" region. Their GUS assay procedure also included an initial fixation step of 20 minutes in cold 90% acetone before vacuum infiltration and incubation in the GUS substrate overnight. However, acetone fixation can reduce the

amount of diX-indigo accumulation (personal observations). Thakore et al. (1999) observed *C2* gene expression in the shoots, crown and root tip of 3- and 8-day-old seedlings. The vascular system of the leaves of older plants showed *C2* gene expression, while only a few lines showed expression in the root vascular system. In mature plants, expression was detected in leaves, stem, anthers, pollen, and some carpels. The expression profile described above is similar to the one presented in this thesis. One difference is that every line observed had expression throughout the root including, but not limited to, the root tip. This difference could be explained by the longer time of my assays.

The second report on *C2* expression used a promoter trap method (Pernas et al., 2007). After screening through a random population of T-DNA insert lines, a line was found which had *GUS* inserted in frame with the *C2* coding sequence. Therefore, this line should contain all of the upstream regulatory information, but any potential 3' UTR regulatory information would be likely be non-functional due to the NOS terminator at the end of the GUS gene. After 6 hours of incubation with the GUS substrate, Pernas et al. (2007) reported *C2* gene expression in and near the root tips, lateral root meristems, vascular tissues and guard cells in leaves, as well as in anthers. The data I collected are consistent with their results. However, unlike my data, they did not detect expression in the siliques, in petals or any other flower part, or in trichomes. In my assay conditions, detectable *C2* gene expression in the siliques, flower organs, and trichomes only occurred after 12 or 24 hours of incubation, therefore their allotted 6 hour assay period may not have been long enough to observe expression.

The histochemical GUS assay used in this thesis provides a detailed description of

C subunit expression at the cellular level throughout Arabidopsis development. The GUS data provides a cellular analysis of gene expression for each of the PP2A C subunit genes, unlike microarrays and northerns which provide expression data at the tissue and organ level only. In comparison to immunodetection, which cannot distinguish the different C subunits, the PP2A-GUS fusion constructs detected with the GUS assay can analyze each C subunit independently. By varying the assay length, it is possible to determine which tissues had the highest and lowest levels of expression. At the longest assay time, weak expression was observed in floral organs which had not been previously reported. Therefore, this approach in general correlates well with published data and provides even more detailed information about *C* subunit gene expression.

III.C. Root expression of the *C4* subunit gene

Mutants in the Protein Phosphatase 2A *C4* subunit have a root skewing phenotype which is induced in the presence of elevated levels of Na^+ (Wang, 2008). The data presented in this thesis showed that the skewing response occurs within the first two days after transfer to medium supplemented with Na^+. The new growth direction is then maintained for the remainder of the assay. Changes in *C4* gene expression were assayed in roots to determine if there was a correlation between *C4* expression and the Na^+-specific root phenotype. Two approaches, *in situ* GUS assays of plant reporter lines and real-time PCR, were used to determine if *C4* expression changed in the first two days after transfer to medium with elevated NaCl. The GUS assays showed no observable change in expression pattern either 1 or 2 days post-transfer to NaCl-supplemented medium. GUS expression was also observed for plant lines containing the *C3* subunit

reporter gene fusion and no expression differences were observed between basal and NaCl-supplemented media. Data from real-time PCR also showed that there was no change in expression 1 day post-transfer to medium supplementated with NaCl or with the osmotic equivalent concentration of mannitol. Together, these data indicated that *C4* gene expression was not changed by NaCl or osmotic stress. Thus the role of the C4 subunit is maintaining normal root growth under high Na^+ conditions is not regulated at the level of transcription.

A common genetic approach to understand which genes are involved with various pathways is to determine whether gene expression changes under a particular stress. Based on microarray data, *C1*, *C2*, *C3/C4*, and *C5* subunits show little to no change in expression upon exposure to various stresses. The stress-induced expression data presented in this thesis also is consistent with the microarray data (Czechowski et al., 2005). Arabidopsis *C2* gene expression has been reported to be induced upon treatment with abscisic acid (Pernas et al., 2007). Thus, even though PP2A has been implicated in many cellular pathways, regulation of the C subunit does not occur at the level of transcription.

Microarray data indicate that the A subunit shows only very slight changes in expression when exposed to various stresses. The A subunits are also expressed ubiquitously throughout Arabidopsis during all stages of development (Zhou et al., 2004). It is likely that all of the A and C subunits are expressed in most cells regardless of plant age or growth conditions; expression of many B subunits is altered when exposed to various stresses. Therefore, regulation of the PP2A holoenzyme is probably dependent upon various B subunits that are induced by different stresses.

III.D Partial dissection of the *C3* promoter

Promoter deletions are a common approach to study promoter structure. Successively shorter promoters are analyzed to determine the location of promoter elements by detecting an effect on gene expression. A modified promoter deletion approach was used to determine the location of the promoter of the *C3* gene. One construct, *sC3*, contained 153 bp upstream of the transcription start site while *LC3* included 2313 bp upstream. Both constructs included the 5' UTR, introns, and exons of the *C3* gene. The *sC3* construct ended near the transcription start site of the adjacent predicted gene At2g42510 (Figure 4), but since the function of At2g42510 is unknown and it could be a pseudogene, a second construct was made which included 2160 bp of additional upstream sequence. Comparison of the expression pattern and relative promoter strength of transgenic plants carrying either *sC3* or *LC3* demonstrated that both "promoter" regions produced similar expression patterns at all developmental stages and in all tissues. This result indicates that the regulatory information needed to drive *C3* gene expression is encompassed in the *sC3* construct containing 153 bp upstream of the transcription start site and the exons and introns of the gene itself.

The promoter regions of the *C3* subunit gene were mapped previously using a promoter deletion approach (Perez-Callejon et al., 1998). The *C3* subunit constructs included 89, 212, 322, 569, or 914 bp upstream of the transcription start site fused to the entire 5' UTR and first four codons. The *C3* gene fragments were then fused to GUS, transformed into protoplasts, and assayed to determine promoter strength. For the C3 subunit, GUS activity from the 914 and 569 bp promoter regions was similar. GUS activity from the 322 and 212 bp constructs decreased approximately 80% when

compared to the two longer constructs, while approximately 10% activity was observed from the 89 bp promoter. These results indicate that at least one major positive transcription factor binding site occurs between -569 and -322 bp of the *C3* promoter. While the data presented in this thesis indicated no difference between expression of a 153 and 2313 bp *C3* promoter, the promoter deletion study showed a dramatic decrease in expression in promoter regions shorter than 322 bp. However, my experiment differs from that of Perez-Callejon et al. (1998) in several ways. First, my constructs contain all of the introns and the coding regions of the *C3* gene, while Perez-Callejon et al. (1998) used only 158 bp of the first exon. Important regulatory information key to driving the *C3* expression may be present in the introns and this information is lacking in the Perez-Callejon et al. (1998) constructs. Second, the *C3* promoter may drive expression differently in intact plants than in protoplasts.

Interestingly, the 5' UTR of the *C3* gene contains a simple sequence repeat (SSR) of the dinucleotide GA repeated 22 times. The exact regulatory nature of the GA SSR is unknown, but this type of SSR is enriched in the 5' UTRs of both Arabidopsis and Brassica genomes and has been hypothesized to be involved in gene regulation (Zhang et al., 2006).

III.E. Comparison of C subunit expression patterns

Similar to other gene families with multiple members, the nucleotide sequences of the promoters of the five *C* subunit are highly variable (unpublished observation; Thakore et al., 1999). Variability in promoter sequence is reflected in the different predicted arrangements of transcription factor binding sites which could lead to differential

regulation (Figure 61). Despite the different upstream regions, expression patterns of the five C subunit genes were almost indistinguishable. The upstream regions of the A subunits are also highly variable and also display very similar expression patterns (Zhou et al., 2004). It is difficult, if not impossible, to predict the expression patterns from sequences gazing and there are certainly cases where expression patterns from members of a gene family are very different. For example, 1-aminocyclopropane-1-carboxylate synthase (ACS) gene family members have overlapping but unique expression patterns (Tsuchisaka and Theologis, 2004). The same is true for the xyloglucan endotransglucosylases/hydrolase (XTHs) family whose 33 members have unique but overlapping expression patterns (Becnel et al., 2006).

The almost identical expression patterns of the five PP2A C subunit genes indicate that all five C subunits are probably available in most cells for formation of holoenzymes. As a result, it is unlikely that the C subunits are the limiting subunit for heterotrimer formation. In fact, in *Saccharomyces cervisiae*, there are three C subunits for every A subunit and eight B subunits (Gentry and Hallberg, 2002), indicating that the A subunit is limiting in that organism.

Despite highly similar amino acid sequences between the C3 and C4 subunit, a sodium-induced root skewing phenotype was found in *c4* mutant plants. There are a number of alternative explanations that might explain how two genes with very similar expression patterns and sequences might not be functionally redundant. First, a knockout of *any C* subunit gene might produce a root phenotype if it is the levels of total C protein that are important rather than which specific subunits are present. Second, the 6 amino acids that differ between the C3 and C4 proteins may alter the catalytic site of the enzyme

and result in different substrate specificities for C3- versus C4-containing heterotrimers. Third, the amino acid differences might affect the stability of the heterotrimers or subunit binding affinity resulting in holoenzymes with different half-lives. Further experiments are required to elucidate the specific roles of these two subunits in Arabidopsis.

III.F. Expression patterns of PP2A gene family members in other organisms

To date, all sequenced eukaryote genomes encode A, B, and C subunits of PP2A (Kerk et al., 2002; Janssens et al., 2008; Moorhead et al., 2009). All known C subunits contain the same six amino acids (TPDYFL) at their carboxy terminus, an internal phosphoesterase signature motif (DXH-(-25)-GDXXD-(-25)-GNH), and an okadaic acid binding sequence (YRCG) (Mayer-Jaekel and Hemmings, 1994; Zhuo et al., 1994; Janssens et al., 2008). The most amino acid divergence occurs near the amino terminus of the C subunit.

Many plants contain multiple copies of the C subunit genes which are classified into two subfamilies - class I and II. In Arabidopsis, the C1, C2 and C5 subunits are grouped into Class I while C3 and C4 belong to Class II. A new C subunit nomenclature, using an abbreviated form of the organism's scientific name followed by the subunit name and number, will be used from this point on to distinguish between the C subunits of different species.

III.F.1. PP2A in *Oryza sativa*

In the monocot *Oryza sativa* (Asian Rice), there are five C subunit isoforms. Class I contains OsPP2AC1 and OsPP2AC3, while Class II contains OsPP2AC2,

OsPP2AC4, and OsPP2AC5 (Yu et al., 2005; Yang et al., 2010). Microarray analysis indicates that all C subunits are ubiquitously and highly expressed at different stages of rice development (Yang et al., 2010). A more nuanced picture of C subunit expression was obtained from notherns.

OsPP2AC1 and *OsPP2AC3* are expressed in the leaf, stem and root of rice from 2-14 weeks of age and in all stages of panicle (flower) development (Yu et al., 2003). *OsPP2AC1* is highly expressed in the stems, roots and flowers, but weakly expressed in the leaves. *OsPP2AC3* is expressed similarly, except there is also weak expression in the roots. No changes in expression for *OsPP2AC1* or *OsPP2AC3* are observed in the stem when exposed to stresses such as drought, heat shock, or salinity, but both *OsPP2AC1* and *OsPP2AC3* are up-regulated in the leaves when exposed to drought or high salinity. *OsPP2AC3* expression in roots is down-regulated when exposed to drought. *In situ* hybridization shows highly similar expression patterns for both *OsPP2AC1* and *OsPP2AC3* in the root apex and elongation zone, stem, and inner and outer flower sheath. *OsPP2AC1* and *OsPP2AC3* are expressed in the meristematic and elongation zones of the root. The only difference is observed in the leaf where *OsPP2AC3*, but not *OsPP2AC1*, expression is detected in the leaf epidermis.

By northerns, *OsPP2AC2*, *OsPP2AC4*, and *OsPP2AC5* vary in expression levels throughout development (Yu et al., 2005). In the leaf, *OsPP2AC2* and *OsPP2AC4* are weakly expressed while *OsPP2AC5* expression is much stronger. All three are expressed strongly in the stem but levels decrease with plant age. In the root, consistent expression is observed from *OsPP2AC2* and *OsPP2AC4* at different ages of the plant, while *OsPP2AC5* expression decreases with age. Addition of 300 mM NaCl causes no

expression change of *OsPP2AC2* in the leaf, stem or root. Expressions of both *OsPP2AC4* and *OsPP2AC5* is induced by 300 mM NaCl in the leaf, but expression was not altered in the stem or root. The application of heat and drought stress cause down-regulation of *OsPP2AC2*, *OsPP2AC4* and *OsPP2AC5* subunit genes in the leaf and stem, but no change in the root.

III.F.2. PP2A in *Medicago sativa*

There are three known C subuntis in *Medicago sativa* (alfalfa): MsPP2A Cα/pp2aMs, MsPP2A Cβ, and MsPP2A Cγ (Pirck et al., 1993; Toth et al., 2000). *MsPP2A Cα/pp2aMs* expression, determined by northern analysis, is detected in somatic embryos, roots, stems, nodes, young and old leaves, flower buds and mature flowers (Pirck et al., 1993). The highest expression is found in stems while the weakest expression is found in mature flowers. The expression of the two other C subunits is currently unknown.

III.F.3. PP2A in *Nicotiana tabacum*

There have been two reports on PP2A C subunits in *Nicotiana tabacum* (cultivated tobacco). Two C subunit genes, *NPP4* and *NPP5*, were isolated from a cDNA library made from floral bud mRNA (NPP1, NPP2, and NPP3 encode PP1 catalytic subunits. Suh et al., 1998). Northern blots indicate that *NPP4* is expressed in roots, stems, leaves and flowers, while *NPP5* is predominatly expressed in leaves and all stages of flower development. *NPP4* is grouped in Class I and *NPP5* is in Class II (Yu et al., 2005).

III.F.4. PP2A in *Solanum tuberosum*

The *Solanum tuberosum* (potato) genome encodes six C subunit isoforms. The three C subunits in Class I are StPP2AC1, StPP2AC2a and StPP2AC2b whereas StPP2AC3, StPP2AC4, and StPP2AC5 are in Class II (Pais et al., 2009a). Western blots using an antibody that recognizes all C subunits reveal that PP2A C subunit(s) are present in all potato tissues, but the lowest amount is present in the flower bud and root compared to the open flower, shoot apex, leaf and stem (Pais et al., 2010). RT-PCR product was not generated in the roots for *StPP2AC1* and *StPP2AC2b* indicating that these two subunits are not expressed in roots, while the other four C subunits are expressed at various levels in the root. In developing potato tubers the expression of PP2A C subunit genes varies depending on the subunit. *StPP2AC3* and *StPP2AC4* expression is observed throughout tuber development, while *StPP2AC1*, *StPP2AC2a*, *StPP2AC2b*, and *StPP2AC5* expression is primarily limited to the developmentally older tuber stages. An increase in overall C subunit expression in older tubers was also observed as higher accumulation of C subunit protein (Pais et al., 2010).

Isoform-specific northern probes were used on detached leaflets to determine the expression of the six C subunits and westerns were used to determine the total C subunit protein accumulation when exposed to various stresses (Pais et al., 2009a). When the plant was exposed to cold, no change in expression or protein levels was observed for any of the isoforms. Salt exposure induced expression in all C subunits and increased C subunit protein accumulation. Mechanical wounding caused an isoform specific induction only in *StPP2AC2b* which also resulted in an increase in total C subunit protein. Chitosan and PGA (polygalacturonic acid) caused *StPP2AC1*, *StPP2AC2a* and

StPP2AC2b gene expression to be upregulated which also resulted in an increase in total C subunit protein.

III.F.5. PP2A in *Solanum lycopersicum*

Solanum lycopersicum (garden tomato) has five C subunit isoforms, the same as Arabidopsis. Isoforms LePP2AC1 and LePP2AC2 belong to subfamily class I and class II contains LePP2AC3, LePP2AC4, and LePP2AC5 (Pais et al., 2009a). Only a partial transcript for *LePP2AC5* has been found and expression has not been observed by northern blot in any of the tissues or stress conditions. The same stress experiments performed on *Solanum tuberosum* and described above were used on detached leaflets of *Solanum lycopersicum.* Cold stress down-regulated *LePP2AC1*, *LePP2AC2* and *LePP2AC3* expression while no change in *LePP2AC4* gene expression was observed. The decrease in expression correlated with the decrease in C subunit protein. Salt stress caused no change in expression or protein accumulation in any C subunit genes. *LePP2AC1* and *LePP2AC2* and the total PP2A protein level was up-regulated in response to mechanical wounding while the rest of the C subunits expression was not changed. PGA and chitosan stress response was similar to what was observed for mechanical wounding.

III.F.6. PP2A in humans

In human, the C subunits are not divided into subfamilies because there are only two subunits - Cα and Cβ. The C subunits are expressed ubiquitously, albeit Cα is

typically more abundant than Cβ (Khew-Goodall and Hemmings, 1988; Zhou et al., 2003).

III.F.7. Comparison of C subunit expression in different organisms to Arabidopsis

A common pattern observed for many organisms where C subunit expression has been investigated is that C subunits are expressed ubiquitously. This is consistent with the notion that PP2A is a essential enzyme (Michniewicz et al., 2007; Janssens et al., 2008). Interestingly, in some organisms, C subunits have undergone specialization and are expressed at different levels either under basal conditions or when exposed to stress. Potentially, these C subunits may regulate pathways involved with a particular stress. According to the Arabidopsis microarray data and the data presented in this thesis, Arabidopsis PP2A C3 and C4 subunit expression is not significantly altered by NaCl or other stresses (Czechowski et al., 2005). This is different from many other plant species and indicates either that Arabidopsis PP2A C subunits have diverged recently and specialization has not yet occurred or that all five C subunits have unique functions that are required in each cell.

In the monocot *Oryza sativa*, *OsPP2AC1* and *OsPP2AC3* are both expressed in the root meristematic and elongation zone. This expression pattern is similar to the dicot Arabidopsis C subunit expression pattern. It would be interesting to determine if C subunits are commonly expressed in these root regions in other monocots or dicots. If so, this could indicate that PP2A is required for root organization and development in all vascular plants (Michniewicz et al., 2007; Blakeslee et al., 2008).

III.G. Conclusions

The data presented in this thesis provide a detailed analysis of the expression patterns of Protein Phosphatase 2A C subunit gene expression throughout Arabidopsis development. Gene expression from all C subunit genes were very similar and were observed throughout most organs during the life cycle of the plant. The primary and secondary root tips were the regions of the plant with the highest gene expression for all C subunits. Consistent with the sodium-induced root skewing phenotype of the *c4* mutants, the *C4* gene was highly expressed in both the root tips and the root elongation zone. *C4* gene expression was not altered by the addition of NaCl to the medium. These data are useful because the expression patterns can be correlated with any new C subunit phenotypes and can be used to develop questions regarding PP2A holoenzyme regulation in Arabidopsis.

CHAPTER IV

METHODS

IV.A. Primer design, PCR amplification, and TOPO cloning

Primers (Table 6) were designed by using Oligo Primer Analysis Software (Molecular Biology Insights, Inc. Cascade, CO) and synthesized by Integrated DNA Technologies (Coralville, IA).

PCR was performed using either a PTC-100 or PTC-200 thermal cycler (MJResearch, Watertown, MA). Large genomic fragments were amplified using *ExTaq* DNA polymerase (Takara, Moutain View, CA). A 50 µl reaction contained 1.25 units DNA polymerase, 200 µM dNTP mix (Takara), 1x buffer (Takara), 0.2 µM of each primer, and 100 ng *Arabidopsis thaliana* ecotype Columbia genomic DNA. The PCR temperature profile was 94°C for 1 minute, followed by 30 cycles of 94°C for 30 seconds, the primer specific annealing temperature for 1 minute, and 72°C for 45 sec/Kb, and ending with 2 minutes at 72°C. All products were visualized by electrophoresis through a 1% GenePure LE agarose gel (BioExpress, Kaysville, UT) in 1X TAE (40 mM Tris-acetate (pH 8.0), 1 mM EDTA). Gels were stained with ethidium bromide and visualized under 312 nm UV light with a transilluminator (Fotodyne, Inc., Hartland, WI).

PCR products were separated by using 1% SeaPlaque agarose (Lonza Rockland, Inc., Rockland, ME) and DNA fragments were purified from agarose slices using a Wizard PCR Prep DNA Purification System following manufacturer's instructions (Promega Corp., Madison, WI). To generate the 3′ adenine overhang needed for TOPO cloning, the PCR product was incubated with 0.7-1 unit of *Taq* DNA polymerase, 0.16

Table 6. Primers used in this study.

Gene Amplified	Primer Name	Primer Sequence (5′-3′)	Purpose of Primer
C1 (At1g59830)	C1 GWC 5′	ATT TTC ACT ATG AAC TCT ATT GAG	Paired with C1/C2 GWC 3′ to amplify genomic region; product size 2621 bp
	C1/C2 GWC 3′	CAA AAA ATA ATC AGG GGT	See C1 GWC 5′
	C1 5′	TCA ACT TGT AAT GGA AAG	Sequencing gene/GUS junction
C2 (At1g10430)	C2 GWC 5′	TAC TCA AAC GGT GAA GAG AGC	Paired with C1/C2 GWC 3′ to amplify genomic region; product size 3365 bp
	C2 5′	ACA ACA ATG GAC TAA GTC	Sequencing gene/GUS junction
C3 (At2g42500)	C3 GWC 5′A	GTA GAA GTT AGT ATT AAA CCG	Paired with C3 GWC 3′ to amplify genomic region; product size 3469 bp
	C3 GWC 5′B	TCA AGT AGT TAA GTC ATC	Paired with C3 GWC 3′ to amplify genomic region; product size 5623 bp
	C3 GWC 3′	CAG GAA ATA GTC TGG AGT	See C3 GWC 5′A and C3 GWC 5′B
	C3 5′	ACT ATT GTT ACC GTT GTG	Sequencing gene/GUS junction
C4 (At3g58500)	C4 GWC 5′A	GCA AAT ACC AAA TAG GTC	Paired with C4 GWC 3′A to amplify genomic region; product size 4974 bp
	C4 GWC 3′A	AAG GAA ATA GTC AGG TGT	See C4 GWC 5′A
	C4 5′	CCA AAC TAT TGC TAT CG	Sequencing gene/GUS junction
	AtPP2AC4F2	TTG TGT TCC AGG TTG CTT CTC TT	Amplifying 3′ UTR for Real-time PCR.
	AtPP2AC4R2	TTC ATG AGA GGT TTT AAA GTT CAT TGA C	Amplifying 3′ UTR for Real-time PCR.
C5 (At1g69960)	C5 GWC 5′	TTA GTT AGG TCT AAG TTC AAG	Paired with C5 GWC 3′ to amplify genomic region; product size 4930 bp
	C5 GWC 3′	CAA AAA ATA ATC TGG AGT	See C5 GWC 5′
	C5 5′	GTG CCA AGA AAA GAA C	Sequencing gene/GUS junction
Other	AtTIP41exF	CGA GGT TTA CGC ATC CAT GA	Amplifying housekeeping gene for real-time PCR
	AtTIP41exR	TCG ACA GCG AGA GAA GTG AGA A	Amplifying housekeeping gene for real-time PCR
	GUS Rev	CGA CCA AAG CCA GTA AAG	Amplification of junction between C and GUS gene

mM dATP, and 1x Promega PCR buffer (50 mM KCl, 10 mM Tris/HCl (pH 9.0), 1.5 mM $MgCl_2$, 0.1% Triton X) for 10-15 minutes at 72°C.

One µl of fresh PCR product was added to 1 µl dilute salt solution (1:4), 3.5 µl deionized, autoclaved water, and 0.5 µl pCR®8/GW/TOPO® (Invitrogen, Cat. No. K250020SC). The reaction was mixed by gentle flicking, centrifuged briefly, and incubated at room temperature for a minimum of 15 minutes.

IV.B. Gateway cloning and DNA sequencing

TE (10 mM Tris-Cl, 1 mM EDTA, pH 8.0) was added to 50-150 ng of Gateway entry clone (PCR product cloned into pCR®8/GW/TOPO® vector) and 150 ng destination vector (pMDC163) to a final volume of 8 µl. One µl of thawed and briefly vortexed LR Clonase (Invitrogen, Cat. No. 11791-020) was added, mixed gently and incubated for 1 hour at room temperature. Two µl of Proteinase K was added, mixed, and incubated for 30 minutes at 37°C.

The *attB2* junction region from Gateway expression plasmids was sequenced using BigDye Terminator c3.1 cycle sequencing reagents (Applied Biosystems, Foster City, CA) per manufacturer's instructions. Sequencing reactions contained 1 µl sequencing mix, 3 µl sequencing buffer, 150 ng plasmid and 5 pmol primer in a 10 µl reaction. The cycling profile was 95°C for 1 minute, followed by 25 cycles of 95°C for 10 seconds, 50°C for 5 seconds, 60°C for 4 minutes. After sequencing, the DNA was mixed with 1 µl 125 mM EDTA (pH 8), 1 µl 3 M sodium acetate (pH 5.2) and 25 µl 100% ethanol. The samples were vortexed and centrifuged for 30 minutes at 3,000 x g. The pellet was washed with 70% ethanol and centrifuged for 15 minutes at 1,700 x g.

The 70% ethanol wash was repeated and the pellet was completely dried and resuspended in 10 µl deionized formamide. Samples were analyzed at the University of New Hampshire Hubbard Center for Genome Studies.

IV.C. Preparation of electrocompetent *Escherichia coli* and *Agrobacterium tumefaciens*

A starter culture was used to inoculate 400 ml of LB medium to an OD_{600} of less than 0.05. Cultures were grown at the appropriate temperature with vigorous agitation. Once the OD of the culture reached 0.550, the culture was cooled on ice and kept cold throughout the rest of the procedure. The OD was checked again to confirm that it was below 0.700. The culture was pelleted at 4,000 x g at 4°C for 10 minutes in sterile centrifuge bottles. The pellet was resuspended in sterile, ice-cold, deionized water and pelleted again. This step was repeated with another deionized water wash and finally with 10 ml of 10% glycerol. The pellet was resuspended in 2 ml of 10% glycerol, aliquoted in 40 µl volumes and stored at -80°C.

IV.D. Bacterial transformation

An aliquot of a cloning reaction or purified plasmid was added directly to electrocompetent cells on ice. The bacteria-DNA mixture was immediately transferred into a 1-mm gap electroporation cuvette (Bio-Rad) and cells were transformed by electroporation. Following a 1-hour incubation in SOC (0.5% yeast extract, 2% tryptone, 10 mM NaCl, 2.5 mM KCl, 10 mM $MgCl_2$, 10 mM $MgSO_4$, 20 mM glucose), cells were plated on LB plates (1% tryptone, 0.5% yeast extract, 1% NaCl, 1.3% bacto-agar)

containing the appropriate antibiotic and grown at the appropriate temperature until colonies were visible.

IV.E. Plasmid isolation by alkaline lysis

An overnight bacterial culture grown in LB containing appropriate antibiotic was pelleted by centrifugation at 10,000 x g. The pellet was resuspended by vortexing in 100 µl GET buffer (50 mM glucose, 25 mM Tris-HCl, pH 8.0, 10 mM EDTA). A 200 µl aliquot of freshly prepared 0.2N NaOH and 1% SDS was added and mixed by inverting followed by the addition of 150 µl of potassium acetate (pH 5.2) and mixing by inversion. Samples were centrifuged at 10,000 x g and the supernatant was extracted with an equal volume of phenol:chloroform (25:24). After centrifugation, the aqueous phase was mixed with two volumes of 100% ethanol and centrifuged for a minimum of 10 minutes. The pellet was washed with 600 µl and centrifuged for 2 minutes. The pellet was completely dried and resuspended in 20 µg/ml DNase-free RNase A.

IV.F. DNA quantitation and restriction digestion

DNA was quantitated with a DyNA Quant 200 fluorometer (Hoefer Inc., Holliston, MA) and digested with restriction enzymes per manufacturer's instructions.

IV.G. Plant materials and growth conditions

Arabidopsis thaliana ecotype Columbia (Col-0) was used for most experiments. Most plants were grown at 21°C with an 18-hour photoperiod of 100 µmol m-2 s-1 fluorescent light. For real-time PCR, plants were grown at 25°C with a 12-hour

photoperiod at 100 μmol m-2 s-1 fluorescent light. The defined medium for plant growth was 0.5X MS (0.22% [w/v]) Murashige and Skoog w/ Gamborg's vitamins (Caisson Laboratories, North Logan, UT, Cat No. MSP0506) and 0.8% Phytoblend (Caisson Laboratories, Cat No. PTC001). Seeds on plates were stratified at 4°C for 3 days. Seeds were germinated in liquid medium (0.5-X MS containing 1% sucrose) to generate tissue for genomic DNA extraction. Soilless plant medium was a 1:1 ratio of perlite (Whittemore Company, Inc, Lawrence, MA) and Metromix 360 (SUN GRO Horticulture, Bellevue, WA).

IV.H. Seed sterilization

One drop of 10% Triton X-100 (~15 μl) and 1.5 ml 70% ethanol was added to approximately 50 seeds in a 1.5 mL tube. The tubes were agitated at least once per minute for five minutes and the ethanol was decanted. Next, 1.5 ml of 100% ethanol and one drop of 10% Triton X-100 was added and the tube was agitated for 5 minutes. Finally 100% ethanol was used for the final 5-minute sterilization step. Seeds were completely dried in a laminar flow hood before use. The seed sterilization procedure was proportionately scaled to accommodate the larger number of seeds in 15 ml polystyrene Falcon tubes.

IV.I. Root skewing assay

Sterilized seeds were plated on starter 0.5X MS medium plates and stratified as described previously. Seeds were germinated at 21°C with a 18-hour photoperiod on vertically-oriented plates. Three-day-old plants were transferred to either 0.5X MS or

0.5X MS supplemented with 75mM NaCl and grown for an additional 7 days on vertical plates. For time course experiments, plates were photographed daily after transfer. Root skewing angles were calculated using ImageJ (Abramoff et al., 2004) and significance determined by a Tukey's test. Root skewing angle was defined by three points: the actual position of the root tip at time of measurement, the location of the root tip at Time 0, and the theoretical position of the root tip if root growth had proceeded parallel to the gravity vector (Figure 81B). Angles were defined as positive if the root skewed to the right of vertical and negative if skewing was to the left of vertical when seedlings were viewed from the back of the plate.

IV.J. Plant transformation and selection of transformants

Arabidopsis transformation was performed by the floral dip method (Clough and Bent, 1998). A stationary-phase liquid culture of *Agrobacterium tumefaciens* strain GV3101 in LB was used to inoculate 200 ml of LB. After overnight incubation, the culture was pelleted at 5,000 x g for 10 minutes. The pellet was resuspended in 5% non-molecular grade sucrose containing 0.05% Vac-In-Stuff (Silwet L-77, Lehle Seeds, Round Rock, TX, Cat. No. VIS-02) to an OD_{600} of 0.800±0.200 as determined with a GENESYS 20 spectrophotometer (Thermo Fisher Scientific Inc., Waltham, MA). Flowering T_0 Arabidopsis plants (10 per pot) were inverted in the *Agrobacterium* suspension for 10 seconds. The pots containing the inoculated plants were placed on their sides in a flat and covered with plastic wrap or a clear plastic dome. The next day, the plants were gently washed with cool tap water and the pots were placed upright in the growth chamber. In some cases, the plants were re-transformed with *Agrobacterium* 1

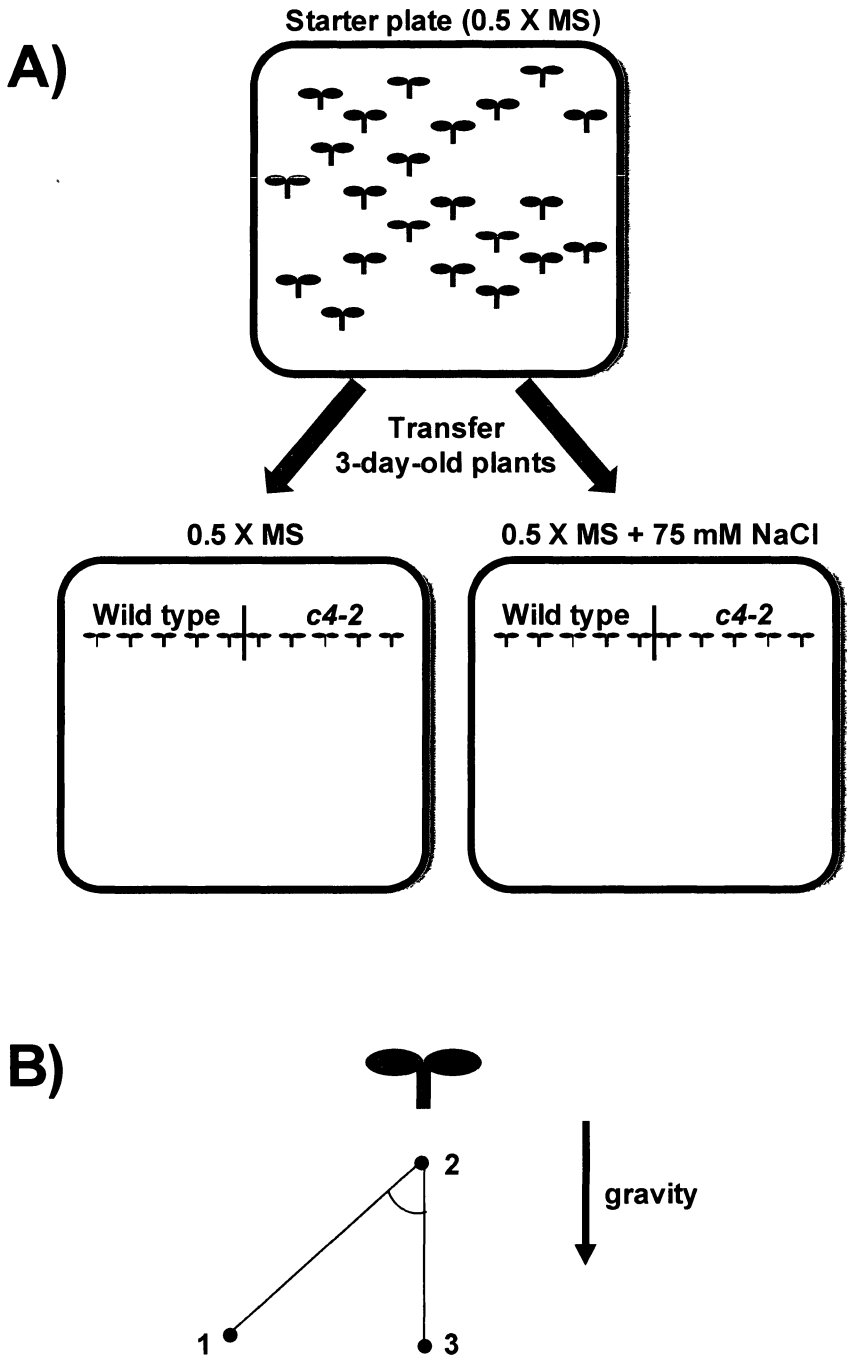

Figure 81. Experimental design and measurement of NaCl-induced root skewing phenotype.

A) Starter plates of 0.5 X MS were sprinkled with seeds, stratified for 3 days and the plants were grown for three days. Seedlings of desired genotype were transferred to plates containing 0.5 X MS or 0.5 X MS+75 mM NaCl. **B)** Root angles were measured from the tip (1) to the origional root tip position at Time 0 (2) to the vertical gravity vector (3).

week later.

T_1 seeds were harvested and dried for at least one week before use. Seeds (40 mg) were surface-sterilized and scattered evenly on 0.5X MS plates containing the appropriate antibiotic. For hygromycin selection, the appropriate amount of hygromycin (Roche Molecular Biochemicals, Indianapolis, IN, Cat No. 14937400) was determined experimentally by plating hygromycin resistant and sensitive seeds on MS medium containing various concentrations of hygromycin. For the lot of hygromycin used for these experiments, a final concentration of 65 μg/ml was used for selection. After no more then 14 days of growth on plates, plants were transplanted to soil. Once transferred to soil, flats were covered and kept under low light conditions at room temperature overnight. The cover was kept on the flats for 2 days after returning to the growth room.

Rosette or cauline leaves from hygromycin-resistant T_1 plants were removed for a GUS assay to detect the presence of the GUS enzyme expressed from the T-DNA. Plants which tested positive for expression of GUS were grown to maturity and T_2 seeds were collected. To quickly identify homozygous lines, 25-100 non-sterilized seeds from individual T_3 lines were plated on sterile water agar (tap water and 0.8% Phytoblend) in sterile 24-well plates. At 4-days-post-germination, ~500 μl of GUS assay solution (100 mM sodium phosphate buffer, pH 7.0, 1 mM potassium ferrocyanide, 1 mM potassium ferricyanide, 5 mM EDTA, 0.1% Triton X-100, and 1 mM X-GLUC [5-bromo-4-chloro-3indolyl-β-D-glucuronide; Rose Scientific] dissolved in dimethylformamide) was added to each well. The plates were incubated overnight at 37°C. The seedlings were observed directly with a dissecting microscope and the ratio of seedlings containing the blue product of the GUS enzyme reaction was used to determine whether the seed stock was

homozygous for the transgene.

IV.K. *Arabidopsis thaliana* genomic DNA isolation

Genomic DNA isolation was performed using the CTAB method. Tissue from plants grown in liquid culture for less than 2 weeks was blotted dry, separated into 100 mg samples and frozen at -80°C. For DNA isolation, 100 mg of tissue frozen with liquid nitrogen was ground into a fine powder with a cold mortar and pestle. Following addition of 1 ml of grinding buffer (100 mM Tris-HCl, pH 8.0, 1.4 M NaCl, 20 mM EDTA, 2% CTAB, 0.004% β-mercaptoethanol), the mixture was ground until a slurry formed. The slurry was transferred to a microfuge tube and incubated at 60°C for 30 minutes. Samples were cooled to room temperature. To each sample, 650 µl of chloroform:octanol (24:1) was added, followed by vortexing for 10 seconds. The debris was pelleted by centrifugation for 5 min at 14,000 x g. The aqueous layer was transferred to a clean tube, slowly overlaid with ice cold 100% ethanol, and incubated at -20°C for 1 hour. After 1 hour, white precipitate had usually formed at the phase interface. The tube was inverted 5 times and incubated overnight at -20°C. DNA was pelleted at 14,000 x g for 5 minutes, then 1 ml 70% ethanol was added and the sample was incubated at -20°C overnight. Ethanol was decanted and the pellet was dried completely. The pellet was incubated at 4°C in 50 µl of TE overnight. After incubation, 50 µl of 10 ug/ml RNase was added and the sample was incubated for 37°C for 1 hour. Long term storage of genomic DNA was at -20°C.

IV.L. Isolation of *Arabidopsis thaliana* cDNA

Arabidopsis tissue was collected and stored at -80°C until RNA isolation. RNA was isolated from 50-100 mg of tissue using the RNeasy Plant Mini Kit (Qiagen, Valencia, CA) with the following modifications to the manufacturer's instructions: the second RPE wash was not done, the optional spin step to dry the membrane was included, and the RNA was eluted with 40 µl RNase free water. Total RNA was quantitated with a spectrophotometer (NanoDrop ND-1000; Thermo Fisher Scientific Inc., Wilmington, DE). DNA was removed from the RNA by using the routine DNase treatment procedure in the TURBO DNA-free kit (Applied Biosystems/Ambion, Austin, TX). PCR was performed to confirm that all of the DNA was degraded. SuperScript III reverse transcriptase (Invitrogen, Carlsbad, CA) was used per manufacturer's directions to produce cDNA and modified by doubling the volume of all of the reagents to a 40 µl reaction.

IV.M. Real-time PCR

Each 10 µl reaction contained 0.15 µM of each primer, 1x ABI Power SYBR Green Master Mix (Applied Biosystems, Carlsbad, CA; PN: 4367659), and 2 µl of cDNA template. Reactions were placed in a MicroAmp™ Fast Optical 96-Well Reaction Plate (Applied Biosystems, Carlsbad, CA; PN: 4346907). Real-time PCR was performed using a 7500 Fast Real-Time PCR System using the Standard Curve (Absolute Quantitation) assay and Standard 7500 run mode. The thermal profile was 50°C for 2 minutes, 95°C for 10 minutes for *Taq* activation, followed by 40 cycles of 95°C for 15 sec and 60°C for 1 minute for amplification.

Critical threshold (C_t) values were calculated by the SDS software component of the 7500 Fast Real-Time PCR System. The percent efficiency was calculated for all primers using $E = 10^{(-1/slope)}$. The Pfaffl method (Pfaffl, 2001) was used to calculate the fold-change in expression of a gene under control and experimental conditions. Statistical significance was determined using a Tukey's test.

IV.N. GUS assay and documentation of expression pattern

To determine the expression pattern, plants were chosen at major developmental stages or specific tissues such as flowers, siliques and cauline leaves were collected. Plants were submerged in GUS assay solution and vacuum infiltrated. The time of vacuum infiltration was dependent upon the age of the sample; seedlings 7-day-old or younger were infiltrated for 5 minutes, 10-day-old plants for 10 minutes, and 14-day-old plants and dissected inflorescences for 15 minutes. Four-week-old plants were infiltrated for 15 minutes, the vacuum was released and samples were re-infiltrated for an additional 5 minutes. Samples were incubated in GUS assay solution for 1, 3, 12-18 or 24 hours and the assay was stopped by removing the assay solution and adding 70% ethanol. The 70% ethanol was changed daily until the plants were completely decolorized. For plants between 1-14 days old that were to be mounted on microscope slides, the 70% ethanol was replaced with deionized water for a minimum of 1 hour, then samples were transferred to 50% glycerol for a minimum of 1 hour, and finally to 100% glycerol before mounting on microscope slides. Flowers, siliques and cauline leaves were processed similarly but mounted in 50% glycerol.

Images of intact young seedlings and high magnification images for all sample

types were collected with an Axioplan 2 Imager compound microscope (Carl Zeiss, Jena, Germany) using either 10X, 20X or 40X objectives and differential interference contrast (DIC) optics. Compound microscope digital images were captured with an AxioCam MRC camera (Zeiss). Young intact plants and dissected older tissues were photographed with a SZX9 dissecting microscope (Olympus) equipped with a Q-color 3 digital camera (Olympus). Intact older plants and flowering plants were arranged on a waterproof white surface and photographed with a Pentax K100 digital camera using manual settings (aperture 8.0 and F stop 20-60).

REFERENCES

Abe H, Urao T, Ito T, Seki M, Shinozaki K, Yamaguchi-Shinozaki K (2003) Arabidopsis AtMYC2 (bHLH) and AtMYB2 (MYB) function as transcriptional activators in abscisic acid signaling. Plant Cell **15:** 63-78

Abe H, Yamaguchi-Shinozaki K, Urao T, Iwasaki T, Hosokawa D, Shinozaki K (1997) Role of arabidopsis MYC and MYB homologs in drought- and abscisic acid-regulated gene expression. Plant Cell **9:** 1859-1868

Abramoff M, Magelhaes P, Ram S (2004) Image processing with ImageJ. Biopho Int **11:** 36-42

Al-Shehbaz IA, O'Kane SL (2009) Taxonomy and phylogeny of Arabidopsis (Brassicaceae). *In* The Arabidopsis Book. The American Society of Plant Biologists

Alonso JM, Stepanova AN, Leisse TJ, Kim CJ, Chen H, Shinn P, Stevenson DK, Zimmerman J, Barajas P, Cheuk R, Gadrinab C, Heller C, Jeske A, Koesema E, Meyers CC, Parker H, Prednis L, Ansari Y, Choy N, Deen H, Geralt M, Hazari N, Hom E, Karnes M, Mulholland C, Ndubaku R, Schmidt I, Guzman P, Aguilar-Henonin L, Schmid M, Weigel D, Carter DE, Marchand T, Risseeuw E, Brogden D, Zeko A, Crosby WL, Berry CC, Ecker JR (2003) Genome-wide insertional mutagenesis of Arabidopsis thaliana. Science **301:** 653-657

Arino J, Perez-Callejon E, Cunillera N, Camps M, Posas F, Ferrer A (1993) Protein phosphatases in higher plants: multiplicity of type 2A phosphatases in Arabidopsis thaliana. Plant Mol Biol **21:** 475-485

Ayaydin F, Vissi E, Meszaros T, Miskolczi P, Kovacs I, Feher A, Dombradi V, Erdodi F, Gergely P, Dudits D (2000) Inhibition of serine/threonine-specific protein phosphatases causes premature activation of cdc2MsF kinase at G2/M transition and early mitotic microtubule organisation in alfalfa. Plant J **23:** 85-96

Becnel J, Natarajan M, Kipp A, Braam J (2006) Developmental expression patterns of Arabidopsis XTH genes reported by transgenes and Genevestigator. Plant Mol Biol **61:** 451-467

Beeckman T, Burssens S, Inze D (2001) The peri-cell-cycle in Arabidopsis. J Exp Bot **52:** 403-411

Benfey PN, Chua NH (1990) The cauliflower mosaic virus 35S promoter: combinatorial regulation of transcription in plants. Science **250:** 959-966

Bernards R (2005) A functional approach to questions about life, death, and phosphorylation. Cancer Cell **7:** 503-504

Bialojan C, Takai A (1988) Inhibitory effect of a marine-sponge toxin, okadaic acid, on protein phosphatases. Specificity and kinetics. Biochem J **256:** 283-290

Blakeslee JJ, Zhou H-W, Heath JT, Skottke KR, Barrios JAR, Liu S-Y, DeLong A (2008) Specificity of RCN1-mediated protein phosphatase 2A regulation in meristem organization and stress response in roots. Plant Physiol. **146:** 539-553

Blanc G, Barakat A, Guyot R, Cooke R, Delseny M (2000) Extensive duplication and reshuffling in the Arabidopsis genome. Plant Cell **12:** 1093-1101

Boter M, Ruiz-Rivero O, Abdeen A, Prat S (2004) Conserved MYC transcription factors play a key role in jasmonate signaling both in tomato and Arabidopsis. Genes Dev **18:** 1577-1591

Bouche N, Bouchez D (2001) Arabidopsis gene knockout: phenotypes wanted. Curr Opin Plant Biol **4:** 111-117

Bowman JL (1994) Arabidopsis : an atlas of morphology and development. Springer-Verlag, New York

Boyes DC, Zayed AM, Ascenzi R, McCaskill AJ, Hoffman NE, Davis KR, Gorlach J (2001) Growth stage-based phenotypic analysis of Arabidopsis: a model for high throughput functional genomics in plants. Plant Cell **13:** 1499-1510

Briggs GC, Osmont KS, Shindo C, Sibout R, Hardtke CS (2006) Unequal genetic redundancies in Arabidopsis--a neglected phenomenon? Trends Plant Sci **11:** 492-498

Busk PK, Pages M (1998) Regulation of abscisic acid-induced transcription. Plant Mol Biol **37:** 425-435

Camilleri C, Azimzadeh J, Pastuglia M, Bellini C, Grandjean O, Bouchez D (2002) The Arabidopsis TONNEAU2 gene encodes a putative novel protein phosphatase 2A regulatory subunit essential for the control of the cortical cytoskeleton. Plant Cell **14:** 833-845

Capron A, Chatfield S, Provart N, Berleth T (2009) Embryogenesis: Pattern Formation from a Single Cell. *In* The Arabidopsis Book. The American Society of Plant Biologists

Casamayor A, Perez-Callejon E, Pujol G, Arino J, Ferrer A (1994) Molecular characterization of a fourth isoform of the catalytic subunit of protein phosphatase 2A from Arabidopsis thaliana. Plant Mol Biol **26:** 523-528

Casimiro I, Beeckman T, Graham N, Bhalerao R, Zhang H, Casero P, Sandberg G, Bennett MJ (2003) Dissecting Arabidopsis lateral root development. Trends Plant Sci **8:** 165-171

Chan CS, Guo L, Shih MC (2001) Promoter analysis of the nuclear gene encoding the chloroplast glyceraldehyde-3-phosphate dehydrogenase B subunit of Arabidopsis thaliana. Plant Mol Biol **46:** 131-141

Chandler JW (2008) Cotyledon organogenesis. J Exp Bot **59:** 2917-2931

Chaubet N, Flenet M, Clement B, Brignon P, Gigot C (1996) Identification of cis-elements regulating the expression of an Arabidopsis histone H4 gene. Plant J **10:** 425-435

Chinnusamy V, Ohta M, Kanrar S, Lee BH, Hong X, Agarwal M, Zhu JK (2003) ICE1: a regulator of cold-induced transcriptome and freezing tolerance in Arabidopsis. Genes Dev **17:** 1043-1054

Cho K, Jun S, Jeong S, Lee Y, Kim G (2007) Developmental processes of leaf morphogenesis in *Arabidopsis*. J Plant Biol **50:** 282-290

Clough SJ, Bent AF (1998) Floral dip: a simplified method for Agrobacterium-mediated transformation of Arabidopsis thaliana. Plant J **16:** 735-743

Cohen P (2000) The regulation of protein function by multisite phosphorylation--a 25 year update. Trends Biochem Sci **25:** 596-601

Cohen P (2002) The origins of protein phosphorylation. Nat Cell Biol **4:** E127-130

Compton RH (1912) Theories of the anatomical transition from root to stem. New Phytologist **11:** 13-25

Cozzone AJ (1997) Diversity and specificity of protein-phosphorylating systems in bacteria. Folia Microbiol (Praha) **42:** 165-170

Curtis MD, Grossniklaus U (2003) A gateway cloning vector set for high-throughput functional analysis of genes in planta. Plant Physiol **133:** 462-469

Czechowski T, Stitt M, Altmann T, Udvardi MK, Scheible WR (2005) Genome-wide identification and testing of superior reference genes for transcript normalization in Arabidopsis. Plant Physiol **139:** 5-17

Day IS, Reddy VS, Shad Ali G, Reddy AS (2002) Analysis of EF-hand-containing proteins in Arabidopsis. Genome Biol **3:** RESEARCH0056

de Jager SM, Menges M, Bauer UM, Murra JA (2001) Arabidopsis E2F1 binds a sequence present in the promoter of S-phase-regulated gene AtCDC6 and is a member of a multigene family with differential activities. Plant Mol Biol **47:** 555-568

de Pater S, Greco V, Pham K, Memelink J, Kijne J (1996) Characterization of a zinc-dependent transcriptional activator from Arabidopsis. Nucleic Acids Res **24:** 4624-4631

Dean A (2006) On a chromosome far, far away: LCRs and gene expression. Trends Genet **22:** 38-45

DeLong A (2006) Switching the flip: protein phosphatase roles in signaling pathways. Curr Opin Plant Biol **9:** 470-477

Deruere J, Jackson K, Garbers C, Soll D, Delong A (1999) The RCN1-encoded A subunit of protein phosphatase 2A increases phosphatase activity in vivo. Plant J **20:** 389-399

Dolan L, Duckett CM, Grierson C, Linstead P, Schneider K, Lawson E, Dean C, Poethig S, Roberts K (1994) Clonal relationships and cell patterning in the root epidermis of Arabidopsis. Development **120:** 2465-2474

Dolan L, Janmaat K, Willemsen V, Linstead P, Poethig S, Roberts K, Scheres B (1993) Cellular organisation of the Arabidopsis thaliana root. Development **119:** 71-84

Dombradi V, Krieglstein J, Klumpp S (2002) Regulating the regulators. Conference on protein phosphorylation and protein phosphatases. EMBO Rep **3:** 120-124

Donald RG, Cashmore AR (1990) Mutation of either G box or I box sequences profoundly affects expression from the Arabidopsis rbcS-1A promoter. EMBO J **9:** 1717-1726

Donnelly PM, Bonetta D, Tsukaya H, Dengler RE, Dengler NG (1999) Cell cycling and cell enlargement in developing leaves of Arabidopsis. Dev Biol **215:** 407-419

Eichhorn PJ, Creyghton MP, Bernards R (2009) Protein phosphatase 2A regulatory subunits and cancer. Biochim Biophys Acta **1795:** 1-15

Eulgem T, Rushton PJ, Robatzek S, Somssich IE (2000) The WRKY superfamily of plant transcription factors. Trends Plant Sci **5:** 199-206

Evert RF, Esau K (2006) Esau's plant anatomy: meristems, cells, and tissues of the plant body: their structure, function, and development, Ed 3. John Wiley & Sons, Hoboken, NJ

Fickett JW, Hatzigeorgiou AG (1997) Eukaryotic promoter recognition. Genome Res **7:** 861-878

Finch-Savage WE, Leubner-Metzger G (2006) Seed dormancy and the control of germination. New Phytol **171:** 501-523

Fisher RH, Barton MK, Cohen JD, Cooke TJ (1996) Hormonal studies of *fass*, an Arabidopsis mutant that is altered in organ elongation. Plant Physiol **110:** 1109-1121

Fiume E, Christou P, Giani S, Breviario D (2004) Introns are key regulatory elements of rice tubulin expression. Planta **218:** 693-703

Fluckiger R, De Caroli M, Piro G, Dalessandro G, Neuhaus J-M, Di Sansebastiano G-P (2003) Vacuolar system distribution in Arabidopsis tissues, visualized using GFP fusion proteins. J Exp Bot **54:** 1577-1584

Foster R, Izawa T, Chua NH (1994) Plant bZIP proteins gather at ACGT elements. FASEB J **8:** 192-200

Gallagher SR (1992) GUS protocols : using the GUS gene as a reporter of gene expression. Academic Press, San Diego

Garbers C, DeLong A, Deruere J, Bernasconi P, Soll D (1996) A mutation in protein phosphatase 2A regulatory subunit A affects auxin transport in Arabidopsis. EMBO J **15:** 2115-2124

Geisler M, Yang M, Sack FD (1998) Divergent regulation of stomatal initiation and patterning in organ and suborgan regions of the Arabidopsis mutants too many mouths and four lips. Planta **205:** 522-530

Gendreau E, Traas J, Desnos T, Grandjean O, Caboche M, Hofte H (1997) Cellular basis of hypocotyl growth in Arabidopsis thaliana. Plant Physiol **114:** 295-305

Gentry MS, Hallberg RL (2002) Localization of Saccharomyces cerevisiae protein phosphatase 2A subunits throughout mitotic cell cycle. Mol Biol Cell **13:** 3477-3492

Gotz J, Probst A, Ehler E, Hemmings B, Kues W (1998) Delayed embryonic lethality in mice lacking protein phosphatase 2A catalytic subunit Calpha. Proc Natl Acad Sci U S A **95:** 12370-12375

Guivarc'h A, Caissard JC, Azmi A, Elmayan T, Chriqui D, Tepfer M (1996) *In situ* detection of expression of the *gus* reporter gene in transgenic plants: ten years of blue genes. Transgenic Res **5:** 281-288

Haralampidis K, Milioni D, Rigas S, Hatzopoulos P (2002) Combinatorial interaction of cis elements specifies the expression of the Arabidopsis AtHsp90-1 gene. Plant Physiol **129:** 1138-1149

He L, Hannon GJ (2004) MicroRNAs: small RNAs with a big role in gene regulation. Nat Rev Genet **5:** 522-531

Hickey LJ (1973) Classification of the architecture of dicotyledonous leaves. Am J Bot **60:** 17-33

Higo K, Ugawa Y, Iwamoto M, Korenaga T (1999) Plant cis-acting regulatory DNA elements (PLACE) database. Nucleic Acids Res **27:** 297-300

Hobbs SL, Kpodar P, DeLong CM (1990) The effect of T-DNA copy number, position and methylation on reporter gene expression in tobacco transformants. Plant Mol Biol **15:** 851-864

Hobbs SL, Warkentin TD, DeLong CM (1993) Transgene copy number can be positively or negatively associated with transgene expression. Plant Mol Biol **21:** 17-26

Hong RL, Hamaguchi L, Busch MA, Weigel D (2003) Regulatory elements of the floral homeotic gene AGAMOUS identified by phylogenetic footprinting and shadowing. Plant Cell **15:** 1296-1309

Hudson ME, Quail PH (2003) Identification of promoter motifs involved in the network of phytochrome A-regulated gene expression by combined analysis of genomic sequence and microarray data. Plant Physiol **133:** 1605-1616

Hunter T (1995) Protein kinases and phosphatases: the yin and yang of protein phosphorylation and signaling. Cell **80:** 225-236

Jaenisch R, Jahner D, Nobis P, Simon I, Lohler J, Harbers K, Grotkopp D (1981) Chromosomal position and activation of retroviral genomes inserted into the germ line of mice. Cell **24:** 519-529

Janssens V, Goris J (2001) Protein phosphatase 2A: a highly regulated family of serine/threonine phosphatases implicated in cell growth and signalling. Biochem J **353:** 417-439

Janssens V, Longin S, Goris J (2008) PP2A holoenzyme assembly: in cauda venenum (the sting is in the tail). Trends Biochem Sci **33:** 113-121

Jefferson RA, Kavanagh TA, Bevan MW (1987) GUS fusions: β-glucuronidase as a sensitive and versatile gene fusion marker in higher plants. EMBO J **6:** 3901-3907

Jones JD, Dunsmuir P, Bedbrook J (1985) High level expression of introduced chimaeric genes in regenerated transformed plants. EMBO J **4:** 2411-2418

Kagaya Y, Ohmiya K, Hattori T (1999) RAV1, a novel DNA-binding protein, binds to bipartite recognition sequence through two distinct DNA-binding domains uniquely found in higher plants. Nucleic Acids Res **27:** 470-478

Kaplan B, Davydov O, Knight H, Galon Y, Knight MR, Fluhr R, Fromm H (2006) Rapid transcriptome changes induced by cytosolic Ca2+ transients reveal ABRE-related sequences as Ca2+-responsive cis elements in Arabidopsis. Plant Cell **18:** 2733-2748

Kerk D, Bulgrien J, Smith DW, Barsam B, Veretnik S, Gribskov M (2002) The complement of protein phosphatase catalytic subunits encoded in the genome of Arabidopsis. Plant Physiol **129:** 908-925

Khew-Goodall Y, Hemmings BA (1988) Tissue-specific expression of mRNAs encoding alpha- and beta-catalytic subunits of protein phosphatase 2A. FEBS Lett **238:** 265-268

Kidner C, Sundaresan V, Roberts K, Dolan L (2000) Clonal analysis of the Arabidopsis root confirms that position, not lineage, determines cell fate. Planta **211:** 191-199

Kim DW, Lee SH, Choi SB, Won SK, Heo YK, Cho M, Park YI, Cho HT (2006) Functional conservation of a root hair cell-specific cis-element in angiosperms with different root hair distribution patterns. Plant Cell **18:** 2958-2970

Kim SI, Veena, Gelvin SB (2007) Genome-wide analysis of Agrobacterium T-DNA integration sites in the Arabidopsis genome generated under non-selective conditions. Plant J **51:** 779-791

Kinsman EA, Pyke KA (1998) Bundle sheath cells and cell-specific plastid development in Arabidopsis leaves. Development **125:** 1815-1822

Klinedinst S, Pascuzzi P, Redman J, Desai M, Arias J (2000) A xenobiotic-stress-activated transcription factor and its cognate target genes are preferentially expressed in root tip meristems. Plant Mol Biol **42:** 679-688

Larkin JC, Oppenheimer DG, Pollock S, Marks MD (1993) Arabidopsis GLABROUS1 gene requires downstream sequences for function. Plant Cell **5:** 1739-1748

Larsen PB, Cancel JD (2003) Enhanced ethylene responsiveness in the Arabidopsis eer1 mutant results from a loss-of-function mutation in the protein phosphatase 2A A regulatory subunit, RCN1. The Plant Journal **34:** 709-718

Latorre KA, Harris DM, Rundle SJ (1997) Differential expression of three Arabidopsis genes encoding the B' regulatory subunit of protein phosphatase 2A. Eur J Biochem **245:** 156-163

Le Gourrierec J, Li YF, Zhou DX (1999) Transcriptional activation by Arabidopsis GT-1 may be through interaction with TFIIA-TBP-TATA complex. Plant J **18:** 663-668

Lemeer S, Heck AJ (2009) The phosphoproteomics data explosion. Curr Opin Chem Biol **13:** 414-420

Li W, Luan S, Schreiber SL, Assmann SM (1994) Evidence for protein phosphatase 1 and 2A regulation of K+ channels in two types of leaf cells. Plant Physiol. **106:** 963-970

Luan S (2003) Protein phosphatases in plants. Annu Rev Plant Biol **54:** 63-92

MacKeigan JP, Murphy LO, Blenis J (2005) Sensitized RNAi screen of human kinases and phosphatases identifies new regulators of apoptosis and chemoresistance. Nat Cell Biol **7:** 591-600

Malamy JE, Benfey PN (1997) Organization and cell differentiation in lateral roots of Arabidopsis thaliana. Development **124:** 33-44

Mansfield SG, Briarty LG (1996) The dynamics of seedling and cotyledon cell development in *Arabidopsis thaliana* during reserve mobilization. Int J Plant Sci **157:** 280-295

Mantis J, Tague BW (2000) Comparing the utility of β-glucuronidase and green fluorescent protein for detection of weak promoter activity in *Arabidopsis thaliana*. Plant Mol Biol Rep **18:** 319-330

Marks MD (1997) Molecular genetic analysis of trichome development in Arabidopsis. Annu Rev Plant Physiol Plant Mol Biol **48:** 137-163

Martin T, Wohner R-V, Hummel S, Willmitzer L, Frommer W (1992) The GUS reporter system as a tool for the study of plant gene expression. *In* SR Gallagher, ed, Gus Protocols: Using the GUS Gene as a Reporter of Gene Expression. Academic Press, San Diego, CA, pp 23-43

Martinez IM, Chrispeels MJ (2003) Genomic analysis of the unfolded protein response in Arabidopsis shows its connection to important cellular processes. Plant Cell **15:** 561-576

Maruyama-Nakashita A, Nakamura Y, Watanabe-Takahashi A, Inoue E, Yamaya T, Takahashi H (2005) Identification of a novel cis-acting element conferring sulfur deficiency response in Arabidopsis roots. Plant J **42:** 305-314

Massonnet C, Vile D, Fabre J, Hannah MA, Caldana C, Lisec J, Beemster GT, Meyer RC, Messerli G, Gronlund JT, Perkovic J, Wigmore E, May S, Bevan MW, Meyer C, Rubio-Diaz S, Weigel D, Micol JL, Buchanan-Wollaston V, Fiorani F, Walsh S, Rinn B, Gruissem W, Hilson P, Hennig L, Willmitzer L, Granier C (2010) Probing the reproducibility of leaf growth and molecular phenotypes: a comparison of three Arabidopsis accessions cultivated in ten laboratories. Plant Physiol **152:** 2142-2157

Mayer-Jaekel RE, Hemmings BA (1994) Protein phosphatase 2A--a 'menage a trois'. Trends Cell Biol **4:** 287-291

Medford JI, Behringer FJ, Callos JD, Feldmann KA (1992) Normal and abnormal development in the Arabidopsis vegetative shoot apex. Plant Cell **4:** 631-643

Meyerowitz EM, Somerville CR (1994) Arabidopsis. Cold Spring Harbor Laboratory Press, Plainview , N.Y.

Michniewicz M, Zago MK, Abas L, Weijers D, Schweighofer A, Meskiene I, Heisler MG, Ohno C, Zhang J, Huang F, Schwab R, Weigel D, Meyerowitz EM, Luschnig C, Offringa R, Friml J (2007) Antagonistic regulation of PIN phosphorylation by PP2A and PINOID directs auxin flux. Cell **130:** 1044-1056

Mohanty B, Krishnan SP, Swarup S, Bajic VB (2005) Detection and preliminary analysis of motifs in promoters of anaerobically induced genes of different plant species. Ann Bot **96:** 669-681

Molina C, Grotewold E (2005) Genome wide analysis of Arabidopsis core promoters. BMC Genomics **6:** 25

Moorhead G (2007) Protein phosphatase protocols. Humana Press, Totowa, N.J.

Moorhead GB, De Wever V, Templeton G, Kerk D (2009) Evolution of protein phosphatases in plants and animals. Biochem J **417:** 401-409

Morohashi K, Grotewold E (2009) A systems approach reveals regulatory circuitry for Arabidopsis trichome initiation by the GL3 and GL1 selectors. PLoS Genet **5:** e1000396

Nacry P, Camilleri C, Courtial B, Caboche M, Bouchez D (1998) Major chromosomal rearrangements induced by T-DNA transformation in Arabidopsis. Genetics **149:** 641-650

Nadeau JA, Sack FD (2009) Stomatal development in Arabidopsis. *In* The Arabidopsis Book. The American Society of Plant Biologists

Nagaya S, Kato K, Ninomiya Y, Horie R, Sekine M, Yoshida K, Shinmyo A (2005) Expression of randomly integrated single complete copy transgenes does not vary in Arabidopsis thaliana. Plant Cell Physiol **46:** 438-444

Nakashima K, Fujita Y, Katsura K, Maruyama K, Narusaka Y, Seki M, Shinozaki K, Yamaguchi-Shinozaki K (2006) Transcriptional regulation of ABI3- and ABA-responsive genes including RD29B and RD29A in seeds, germinating embryos, and seedlings of Arabidopsis. Plant Mol Biol **60:** 51-68

Nilson SE, Assmann SM (2007) The control of transpiration. Insights from Arabidopsis. Plant Physiol **143:** 19-27

O'Connor TR, Dyreson C, Wyrick JJ (2005) Athena: a resource for rapid visualization and systematic analysis of Arabidopsis promoter sequences. Bioinformatics **21:** 4411-4413

Oliva M, Dunand C (2007) Waving and skewing: how gravity and the surface of growth media affect root development in Arabidopsis. New Phytol **176:** 37-43

Olsen JV, Blagoev B, Gnad F, Macek B, Kumar C, Mortensen P, Mann M (2006) Global, *in vivo*, and site-specific phosphorylation dynamics in signaling networks. Cell **127:** 635-648

Pais SM, Garcia MN, Tellez-Inon MT, Capiati DA (2010) Protein phosphatases type 2A mediate tuberization signaling in Solanum tuberosum L. leaves. Planta **232:** 37-49

Pais SM, Gonzalez MA, Tellez-Inon MT, Capiati DA (2009a) Characterization of potato (Solanum tuberosum) and tomato (Solanum lycopersicum) protein phosphatases type 2A catalytic subunits and their involvement in stress responses. Planta **230:** 13-25

Pais SM, Tellez-Inon MT, Capiati DA (2009b) Serine/threonine protein phosphatases type 2A and their roles in stress signaling. Plant Signal Behav **4:** 1013-1015

Peach C, Velten J (1991) Transgene expression variability (position effect) of CAT and GUS reporter genes driven by linked divergent T-DNA promoters. Plant Mol Biol **17:** 49-60

Peret B, De Rybel B, Casimiro I, Benkova E, Swarup R, Laplaze L, Beeckman T, Bennett MJ (2009) Arabidopsis lateral root development: an emerging story. Trends Plant Sci **14:** 399-408

Perez-Callejon E, Casamayor A, Pujol G, Camps M, Ferrer A, Arino J (1998) Molecular cloning and characterization of two phosphatase 2A catalytic subunit genes from Arabidopsis thaliana. Gene **209:** 105-112

Perez-Callejon E, Casamayor A, Pujol G, Clua E, Ferrer A, Arino J (1993) Identification and molecular cloning of two homologues of protein phosphatase X from Arabidopsis thaliana. Plant Mol Biol **23:** 1177-1185

Pernas M, Garcia-Casado G, Rojo E, Solano R, Sanchez-Serrano JJ (2007) A protein phosphatase 2A catalytic subunit is a negative regulator of abscisic acid signalling. Plant J **51:** 763-778

Pfaffl MW (2001) A new mathematical model for relative quantification in real-time RT-PCR. Nucl Acids Res **29:** 2002-2007

Pirck M, Pay A, Heberle-Bors E, Hirt H (1993) Isolation and characterization of a phosphoprotein phosphatase type 2A gene from alfalfa. Mol Gen Genet **240:** 126-131

Planchais S, Perennes C, Glab N, Mironov V, Inze D, Bergounioux C (2002) Characterization of cis-acting element involved in cell cycle phase-independent activation of Arath;CycB1;1 transcription and identification of putative regulatory proteins. Plant Mol Biol **50:** 111-127

Polit JT, Kazmierczak A (2007) Okadaic acid (1 μM) accelerates S phase and mitosis but inhibits heterochromatin replication and metaphase-anaphase transition in *Vicia faba* meristem cells. J Exp Bot **58:** 2785-2797

Pyke KA, Marrison JL, Leech AM (1991) Temporal and spatial development of the cells of the expanding first leaf of *Arabidopsis thaliana* (L.) Heynh. J Exp Bot **42:** 1407-1416

Ramirez-Parra E, Frundt C, Gutierrez C (2003) A genome-wide identification of E2F-regulated genes in Arabidopsis. Plant J **33:** 801-811

Rashotte AM, Brady SR, Reed RC, Ante SJ, Muday GK (2000) Basipetal auxin transport is required for gravitropism in roots of Arabidopsis. Plant Physiol **122:** 481-490

Reddy VS, Reddy AS (2004) Proteomics of calcium-signaling components in plants. Phytochemistry **65:** 1745-1776

Riechmann JL (2009) Transcriptional regulation: a genomic overview. *In* The Arabidopsis Book. The American Society of Plant Biologists

Röbbelen G (1957) Über Heterophyllie bei *Arabidopsis thaliana* (L.) Heynh. Ber Dtsch Bot Ges **70:** 39–44

Roeder AHK, Yanofsky MF (2009) Fruit development in Arabidopsis. *In* The Arabidopsis Book. The American Society of Plant Biologists

Ronne H, Carlberg M, Hu GZ, Nehlin JO (1991) Protein phosphatase 2A in *Saccharomyces cerevisiae*: effects on cell growth and bud morphogenesis. Mol Cell Biol **11:** 4876-4884

Rutherford R, Masson PH (1996) Arabidopsis thaliana *sku* mutant seedlings show exaggerated surface-dependent alteration in root growth vector. Plant Physiol **111:** 987-998

Sakai H, Aoyama T, Oka A (2000) Arabidopsis ARR1 and ARR2 response regulators operate as transcriptional activators. Plant J **24:** 703-711

Samuels L, Kunst L, Jetter R (2008) Sealing plant surfaces: cuticular wax formation by epidermal cells. Annu Rev Plant Biol **59:** 683-707

Scheres B, Benfey P, Dolan L (2009) Root development. *In* The Arabidopsis Book. The American Society of Plant Biologists

Scheres B, Wolkenfelt H, Willemsen V, Terlouw M, Lawson E, Dean C, Weisbeek P (1994) Embryonic origin of the Arabidopsis primary root and root meristem initials. Development **120:** 2475-2487

Schiefelbein J, Kwak SH, Wieckowski Y, Barron C, Bruex A (2009) The gene regulatory network for root epidermal cell-type pattern formation in Arabidopsis. J Exp Bot **60:** 1515-1521

Schubert D, Lechtenberg B, Forsbach A, Gils M, Bahadur S, Schmidt R (2004) Silencing in Arabidopsis T-DNA transformants: the predominant role of a gene-specific RNA sensing mechanism versus position effects. Plant Cell **16:** 2561-2572

Sieburth LE (1999) Auxin is required for leaf vein pattern in Arabidopsis. Plant Physiol **121:** 1179-1190

Simpson SD, Nakashima K, Narusaka Y, Seki M, Shinozaki K, Yamaguchi-Shinozaki K (2003) Two different novel cis-acting elements of erd1, a clpA homologous Arabidopsis gene function in induction by dehydration stress and dark-induced senescence. Plant J **33:** 259-270

Smith RD, Walker JC (1996) Plant protein phosphatases. Annu Rev Plant Physiol Plant Mol Biol **47:** 101-125

Smyth DR, Bowman JL, Meyerowitz EM (1990) Early flower development in Arabidopsis. Plant Cell **2:** 755-767

Suh MC, Cho HS, Kim YS, Liu JR, Lee HS (1998) Multiple genes encoding serine/threonine protein phosphatases and their differential expression in Nicotiana tabacum. Plant Mol Biol **36:** 315-322

Sun F, Zhang W, Hu H, Li B, Wang Y, Zhao Y, Li K, Liu M, Li X (2008) Salt modulates gravity signaling pathway to regulate growth direction of primary roots in Arabidopsis. Plant Physiol **146:** 178-188

Swarbreck D, Wilks C, Lamesch P, Berardini TZ, Garcia-Hernandez M, Foerster H, Li D, Meyer T, Muller R, Ploetz L, Radenbaugh A, Singh S, Swing V, Tissier C, Zhang P, Huala E (2008) The Arabidopsis Information Resource (TAIR): gene structure and function annotation. Nucleic Acids Res **36:** D1009-1014

Szabados L, Kovacs I, Oberschall A, Abraham E, Kerekes I, Zsigmond L, Nagy R, Alvarado M, Krasovskaja I, Gal M, Berente A, Redei GP, Haim AB, Koncz C (2002) Distribution of 1000 sequenced T-DNA tags in the Arabidopsis genome. Plant J **32:** 233-242

Teakle GR, Manfield IW, Graham JF, Gilmartin PM (2002) Arabidopsis thaliana GATA factors: organisation, expression and DNA-binding characteristics. Plant Mol Biol **50:** 43-57

Telfer A, Bollman KM, Poethig RS (1997) Phase change and the regulation of trichome distribution in *Arabidopsis thaliana*. Development **124:** 645-654

Terol J, Bargues M, Carrasco P, Perez-Alonso M, Paricio N (2002) Molecular characterization and evolution of the protein phosphatase 2A B' regulatory subunit family in plants. Plant Physiol **129:** 808-822

Thakore CU, Livengood AJ, HendershotIii JD, Corum JW, LaTorre KA, Rundle SJ (1999) Characterization of the promoter region and expression pattern of three Arabidopsis protein phosphatase type 2A subunit genes. Plant Science **147:** 165-176

The Arabidopsis Genome Initiative (2000) Analysis of the genome sequence of the flowering plant *Arabidopsis thaliana*. Nature **408:** 796-815

Torres-Ruiz RA, Jurgens G (1994) Mutations in the FASS gene uncouple pattern formation and morphogenesis in Arabidopsis development. Development **120:** 2967-2978

Toth EC, Vissi E, Kovacs I, Szoke A, Arino J, Gergely P, Dudits D, Dombradi V (2000) Protein phosphatase 2A holoenzyme and its subunits from Medicago sativa. Plant Mol Biol **43:** 527-536

Tsuchisaka A, Theologis A (2004) Unique and overlapping expression patterns among the Arabidopsis 1-amino-cyclopropane-1-carboxylate synthase gene family members. Plant Physiol **136:** 2982-3000

Turner S, Sieburth L (2009) Vascular patterning. *In* The Arabidopsis Book. The American Society of Plant Biologists

Urao T, Yamaguchi-Shinozaki K, Urao S, Shinozaki K (1993) An Arabidopsis myb homolog is induced by dehydration stress and its gene product binds to the conserved MYB recognition sequence. Plant Cell **5:** 1529-1539

van den Berg C, Willemsen V, Hage W, Weisbeek P, Scheres B (1995) Cell fate in the Arabidopsis root meristem determined by directional signalling. Nature **378:** 62-65

Vandepoele K, Vlieghe K, Florquin K, Hennig L, Beemster GT, Gruissem W, Van de Peer Y, Inze D, De Veylder L (2005) Genome-wide identification of potential plant E2F target genes. Plant Physiol **139:** 316-328

Varshavsky A (1997) The N-end rule pathway of protein degradation. Genes Cells **2:** 13-28

Venter M, Botha FC (2004) Promoter analysis and transcription profiling: Integration of genetic data enhances understanding of gene expression. Physiol Plant **120:** 74-83

Wang E (2008) Identification and characterization of protein phosphatase 2A mutants in *Arabidopsis thaliana*. Dissertation. University of New Hampshire, Durham

Wang H, Chevalier D, Larue C, Ki Cho S, Walker John C (2009) The Protein Phosphatases and Protein Kinases of *Arabidopsis thaliana*. *In* The Arabidopsis Book. The American Society of Plant Biologists

Wenkel S, Turck F, Singer K, Gissot L, Le Gourrierec J, Samach A, Coupland G (2006) CONSTANS and the CCAAT box binding complex share a functionally important domain and interact to regulate flowering of Arabidopsis. Plant Cell **18:** 2971-2984

Wickens M, Bernstein DS, Kimble J, Parker R (2002) A PUF family portrait: 3'UTR regulation as a way of life. Trends Genet **18:** 150-157

Windels P, De Buck S, Van Bockstaele E, De Loose M, Depicker A (2003) T-DNA integration in Arabidopsis chromosomes. Presence and origin of filler DNA sequences. Plant Physiol **133:** 2061-2068

Wortman JR, Haas BJ, Hannick LI, Smith RK, Jr., Maiti R, Ronning CM, Chan AP, Yu C, Ayele M, Whitelaw CA, White OR, Town CD (2003) Annotation of the Arabidopsis genome. Plant Physiol **132:** 461-468

Yamamoto YY, Ichida H, Matsui M, Obokata J, Sakurai T, Satou M, Seki M, Shinozaki K, Abe T (2007) Identification of plant promoter constituents by analysis of local distribution of short sequences. BMC Genomics **8:** 67

Yang M, Song S, Liu G, Chen K, Tian X, Zhao Z, Hu S, Yu J (2010) A comprehensive analysis of protein phosphatases in rice and Arabidopsis. Plant Systemat Evol **289:** 111-126

Yang XJ (2005) Multisite protein modification and intramolecular signaling. Oncogene **24:** 1653-1662

Yu RM, Wong MM, Jack RW, Kong RY (2005) Structure, evolution and expression of a second subfamily of protein phosphatase 2A catalytic subunit genes in the rice plant (Oryza sativa L.). Planta **222:** 757-768

Yu RM, Zhou Y, Xu ZF, Chye ML, Kong RY (2003) Two genes encoding protein phosphatase 2A catalytic subunits are differentially expressed in rice. Plant Mol Biol **51:** 295-311

Zhang L, Zuo K, Zhang F, Cao Y, Wang J, Zhang Y, Sun X, Tang K (2006) Conservation of noncoding microsatellites in plants: implication for gene regulation. BMC Genomics **7:** 323

Zhong R, Taylor JJ, Ye Z-H (1999) Transformation of the collateral vascular bundles into amphivasal vascular bundles in an Arabidopsis mutant. Plant Physiol **120:** 53-64

Zhou H-W, Nussbaumer C, Chao Y, DeLong A (2004) Disparate roles for the regulatory A subunit isoforms in Arabidopsis protein phosphatase 2A. Plant Cell **16:** 709-722

Zhou J, Pham HT, Ruediger R, Walter G (2003) Characterization of the Aalpha and Abeta subunit isoforms of protein phosphatase 2A: differences in expression, subunit interaction, and evolution. Biochem J **369:** 387-398

Zhuo S, Clemens JC, Stone RL, Dixon JE (1994) Mutational analysis of a Ser/Thr phosphatase. Identification of residues important in phosphoesterase substrate binding and catalysis. J Biol Chem **269:** 26234-26238